THE UNIVERSITY *of* EDINBURGH

An exploration into the virulence mechanisms of *Listeria*

Magdalena Kamila Bielecka

A thesis submitted to the University of Edinburgh in accordance with the requirements of the degree of Doctor of Philosophy

The University of Edinburgh

The College of Medicine and Veterinary Medicine

School of Biomedical Sciences

October, 2010

ABSTRACT

Pathogenic *Listeria* are the causative agents of listeriosis, a severe food-borne infection. They are able to invade various non-phagocytic cell types including epithelial cells. The life cycle of these intracellular parasites involves penetrating into host cells, rupturing of the phagocytic vacuole, rapidly proliferating in the cytosol, and directly spreading cell to cell. Each step of the listerial intracellular infection involves activation of virulence factors dependent on PrfA, the master regulator of *Listeria* virulence. PrfA-mediated virulence gene activation occurs within host cells by mechanisms that remain unknown. This thesis explores several aspects of PrfA regulation and its impact in the host-pathogen interaction.

Methods for assessing PrfA-dependent gene expression were first developed and standardized, including a highly sensitive and accurate quantitative reverse-transcription real-time PCR (RT-QPCR), as well as procedures to investigate the correlation with virulence using cell culture-based assays. These techniques were applied in an investigation into the structure-function of PrfA. We studied the role of a solvent-accessible pocket identified in the N-terminal domain of PrfA, homologous to the cyclic nucleotide-binding (CNB) domain of Crp and other cAMP-regulated proteins, in intracellular virulence gene activation. Site-directed PrfA mutants were constructed. Our data support the notion that PrfA activity is allosterically regulated and are consistent with a role for the pocket as putative binding site for the PrfA-activating allosteric effector. The characterization of spontaneously occurring PrfA mutations that identified in our laboratory as PrfA*-suppressor or attenuator mutations, A129T, E173G and C229Y, allowed us to gain additional insight into PrfA structure-function. The role of the C229Y in sugar-mediated repression was investigated and found to explain the anomalous phenotype of strain NCTC 7973, a *prfA** (G145S) mutant that carries this second mutation and is repressed by cellobiose but not glucose.

We also carried out experiments to address the intriguing activation of PrfA-dependent virulence genes upon addition of an adsorbent to the culture medium, the so-called "charcoal effect". Using a chemically defined culture medium and resin, Amberlite™ XAD-4, we provided evidence that the virulence gene activation may involve the sequestration of a medium component rather than a bacteria-derived autorepressor, as initially thought.

We also explored the role of PrfA and the sigma factor σ^B in *L. monocytogenes* entry into host cells. Δ*sigB* mutants in different *prfA* regulation backgrounds were constructed. We showed that σ^B has no major effect on host cell invasion, and that *L. monocytogenes* invasiveness is a strictly PrfA-dependent trait. Our results also demonstrate a differential role of σ^B in *L. monocytogenes* serotypes. σ^B apparently plays no role in stress tolerance in serotype 4b, whereas it is important in serotype 1/2a for maintenance of bacterial fitness in stress conditions.

Finally, we investigated the occurrence of apoptosis in *Listeria*-infected cells and developed normalized methods to accurately determine and quantify this cellular response in infected cell monolayers.

ACKNOWLEDGEMENTS

I would primarily like to acknowledge the help and guidance given to me by both of my research supervisors, Professor J. A. Vázquez-Boland and Dr. M. Scortti.

I would also like to express my deep and sincere gratitude to Dr. C. Deshayes for her contribution to the work on structure-function analysis of PrfA and for providing valuable comments on parts of my thesis manuscript.

I also wish to express my warm and sincere thanks to our collaborators Professor B. Luisi, Dr. R. Núñez Miguel and Z. Pietras for their help in the structure-function analysis of PrfA.

I would also like to thank Dr. N. Savill for the apoptosis index mathematical model.

A special thank you to Dr. D. Rodríguez-Lázaro and Dr. C. Helps for help and advice on RT-QPCR.

I also wish to thank Professor W. Goebel for providing the *E.coli* pLSV101Δ*sigB* strain.

I extend my thanks to Dr. M. Waterfall and Professor M. Bailey for advice and help with flow cytofluorometry.

I would also like to thank E. Boyle and the staff of the Media and Wash up Services at the University of Edinburgh, and H. Lea-Wilson and the staff of the Central Laboratory Services at the University of Bristol for their help.

I also thank the College of Medicine and Veterinary Medicine of the University of Edinburgh for supporting my tuition fees after transferring from the University of Bristol.

I warmly thank my many colleagues and my friends for the enthusiasm, camaraderie and caring they provided.

Lastly, and most importantly, I owe my loving thanks to my parents and my sister for their unconditional support, understanding and encouragement throughout my PhD studies. To them I dedicate this thesis.

Moim Rodzicom i mojej Siostrze ...

AUTHOR'S DECLARATION

I declare that the work included in this thesis was carried out in accordance with the Regulations of the University of Edinburgh. The work is original, except where indicated by special reference in the text, and no part of the thesis has been submitted for any other academic award.

Any views expressed in the thesis are those of the author.

The thesis has not been presented to any other University for examination either in the United Kingdom or overseas.

SIGNED: ……..

DATE: ……..

TABLE OF CONTENTS

LIST OF FIGURES

LIST OF TABLES

LIST OF COMMON ABBREVIATIONS

ASA	accessible surface areas
BHI	Brain Heart Infusion
bp	base pair
Cap	catabolite gene activator protein
CCR	carbon catabolite repression
CFU	colony forming units
c(M)	molar mass distribution coefficient
CNB	cyclic nucleotide binding
cNMP	cyclic nucleotide
CNS	central nervous system
DAG	diacylglycerol
DMEM	Dulbecco's modified Eagle's medium
DPBS	Dulbecco's phosphate-buffered saline
EYA	egg yolk agar
FBS	foetal bovine serum
FITC	Fluorescein isothiocyanate
F-6-P	fructose-6-phosphate
G-1-P	glucose-1-phosphate
G-6-P	glucose -6-phosphate
HTH	helix-turn-helix
IGC	intracellular growth coefficient
IMM	Improved Minimal Medium
K_D	equilibrium dissociation constant
kDa	kiloDaltons
LB	Luria Bertani
MOI	multiplicity of infection
MW (Da)	mass weight in Daltons
M-6-P	mannose-6-phosphate
OD_{600}	optical density at 600 nm wavelength
o/n	overnight

PBC	phosphate binding cassette
PBS	phosphate buffered saline
PCR	polymerase chain reaction
PI	Propidium iodide
PTS	phosphoenolpyruvate-sugar phosphotransferase system
rpm	revolutions per minute
RT-QPCR	reverse transcription real-time quantitative PCR
SBA	sheep blood agar
SD	standard deviation
SDS	Sodium dodecyl sulphate
SE	standard error
sp.	species (singular form)
spp.	species (plural form)
sp. nov.	species *novum* (new species)
T_m	melting temperature
WT	wild-type

1 INTRODUCTION

1.1 *LISTERIA* AND LISTERIOSIS

Listeria bacteria are low G+C gram-positive rods closely related phylogenetically to the genera *Bacillus, Staphylococcus, Streptococcus, Enterococcus* and *Clostridium*. They are facultatively anaerobic, non-spore forming, catalase positive and motile at 30°C and below but not at 35-37°C (Collins *et al.*, 1991, Rocourt, 1999, Grundling *et al.*, 2004). Until very recently, the genus *Listeria* comprised six species: two of them, *L. monocytogenes* and *L. ivanovii*, are able to cause infection; the others, *L. seeligeri, L. innocua* and *L. welshimeri*, are considered non-pathogenic (Jones, 1991). In 2009, Graves *et al.* has proposed a new species named *Listeria marthii* sp. nov. to designate *Listeria*-like bacilli isolated from the natural environment of the Finger Lakes region in New York. Their close phylogenetic relatedness to *L. monocytogenes* and *L. innocua* was confirmed by 16S ribosomal RNA sequence analysis. Up to date, *L. marthii* has not been associated with any case of human or animal disease (Graves *et al.*, 2009). Also in 2009, a new species *Listeria rocourtiae* sp. nov. was identified and named in honour of Jocelyne Rocourt, French bacteriologist, whose work greatly contributed to clarifying the taxonomy of the genus *Listeria*. This strain, isolated from a pre-cut lettuce in Salzburg, Austria, was found to be avirulent as assessed by cell culture assays and inoculation of mice (Leclercq *et al.*, 2009).

Listeria are the causative agents of listeriosis, a severe food-borne infection. The first case of human listeriosis caused by *L. monocytogenes* was reported in 1929 in Denmark (Nyflet, 1929). However, it was not until late 1970's and early 1980's that this species started to emerge as a serious food-borne pathogen associated with several epidemic outbreaks. The average occurrence of listeriosis is approximately 2-10 cases per million people per year in European countries and in the United States (Ryser, 1999, Goulet *et al.*, 2001, Roberts & Wiedmann, 2003, Anonymous, 2005, de Valk *et al.*, 2005, Goulet *et al.*, 2008). Although listeriosis remains rare when compared to other food-borne infections, its high mortality rate (20 - 30%) places it

amongst the most deadly diseases transmitted by food. For example, in years 1983-2003, 359 and 408 cases of food-borne disease outbreaks of invasive listeriosis have been reported in France and the United States, with 108 and 96 deaths, respectively, *L. monocytogenes* serotype 4b was found to be involved in most of these cases. In the UK, an outbreak involving 366 cases was reported in years 1987-1989 due to contaminated pâté (Swaminathan & Gerner-Smidt, 2007). According to the report of the advisory committee on the microbiological safety of food (ACMSF), during the 1990s, the annual number of reported cases of listeriosis ranged from 90 to 128 in England and Wales, 6 to 17 in Scotland and 1 to 6 in Northern Ireland. Furthermore, 204 cases in England and Wales and 8 and 3 cases in Scotland and Northern Ireland, respectively, have been reported to Health Protection Agency's (HPA) Communicable Disease Surveillance Centre (CDSC) and Food Safety Microbiology Laboratory (FSML) in 2003 (Anonymous, 2003). *L. monocytogenes* accounts for up to 10% of community-acquired bacterial meningitis in humans and is the primary cause of central nervous system infection in domestic ruminants. Listeriosis has one of the highest hospitalization (90%) and mortality rates of all food-borne infections. For example, reports from United States show that *Listeria* is responsible for approximately 20 - 65% of deaths caused by food-borne infections (Lynch *et al.*, 2006, Bortolussi, 2008).

1.1.1 ECOLOGY AND DISTRIBUTION

Listeria organisms are widespread in the environment. Their primary habitat is soil rich in decomposing plant material but they can be isolated from many other sources, including silage, faeces, surface waters, sewage and many raw materials used in food production (Welshimer & Donker-Voet, 1971, Weis & Seeliger, 1975, Watkins & Sleath, 1981, Rocourt & Seeliger, 1985, McCarthy, 1990, Farber & Peterkin, 1991, Fenlon, 1999).

The ubiquitous distribution of *Listeria* in the environment and their capacity to grow in a wide variety of pH conditions (between pH = 4.3 and 9.6), temperatures

(1 - 45°C) and salt concentrations (exceeding 10%) has made them a major problem for the food industry and a potential risk to the safety of processed foods. Pathogenic *Listeria* are frequent contaminants of fresh and processed foods, where they are able to survive and multiply, resulting in food-borne disease upon consumption without previous heat treatment (Gravany, 1999, Ryser, 1999, Vazquez-Boland *et al.*, 2001a, Roberts & Wiedmann, 2003).

1.1.2 *L. MONOCYTOGENES* AND *L. IVANOVII* DIFFER IN NATURAL PATHOGENICITY

L. monocytogenes was first described in 1924 by Murray, Webb, and Swann in Cambridge, UK. (Murray *et al.*, 1926). The organism was found as the causative agent of a septicaemic disease that affected laboratory rabbits and guinea pigs. Since the infection was associated with an intense monocytosis, it was named *Bacterium monocytogenes.* A few years later a similar organism was isolated from the livers of sick gerbils by Pirie during studies of plague in Africa (Pirie, 1940). Pirie did not make a connection between the organism he isolated and that described by Murray *et al.* and, therefore, named it as if it were a new species, *Listerella hepatolytica* after the famous surgeon Joseph Lister. As a group of slime moulds had previously been called *Listerella*, and after taking notice that his organism was the same as that discovered by the Cambridge team, Pirie himself changed the name to the contemporary designation, "*Listeria monocytogenes*" (Pirie, 1940) .

The second pathogenic species of the genus, *L. ivanovii,* was first isolated in 1955 in Bulgaria by the veterinary surgeon Ivan Ivanov from cases of abortion and neonatal septicaemia in sheep. Due to its distinctive phenotypical features (strong bizonal haemolysis; see section 1.3.7), in 1962 Ivanov suggested it was a different species and proposed the non-official name "*Listeria bulgarica*". The organism remained, however, known as *L. monocytogenes* serovar 5 until detailed genotypic studies carried out in 1984 by J. Rocourt established it was an independent species,

which received the name *L. ivanovii* (Seeliger *et al.*, 1984, Seeliger & Jones, 1986). *L. ivanovii* contains two subspecies, subsp. *ivanovii* and subsp. *londoniensis* (Boerlin *et al.*, 1992).

Both *L. monocytogenes* and *L. ivanovii* are facultative intracellular parasites that use the host cell cytosol as replication niche. Although their intracellular infection cycle is very similar (see section 1.3), the two bacteria show clear differences in pathogenicity. *L. monocytogenes* can infect a wide range of animal species including humans and birds, whereas *L. ivanovii* appears to be only pathogenic for ruminants. *L. ivanovii* infections in humans have been recorded on extremely rare occasions (up to date, only 8 cases of human *L. ivanovii* infection reported) (Guillet *et al.*, 2010) (see Appendix I).

In addition, *L. monocytogenes* is often associated with central nervous system infections, whereas *L. ivanovii* is only isolated from foetomaternal septicaemic infections. This is highly relevant because meningoencephalitis is a hallmark of listeriosis in ruminants, meaning that *L. monocytogenes* and *L. ivanovii* clearly differ in terms of pathogenic tropism. These differences are also evident in the mouse model: here *L. monocytogenes* is more virulent and proliferates in both the liver and the spleen, whereas *L. ivanovii* mainly colonizes the liver and not the spleen (Gonzalez-Zorn *et al.*, 1999, Vazquez-Boland *et al.*, 2001a). Furthermore, differences in susceptibility of eukaryotic cell lines between *L. monocytogenes* and *L. ivanovii* have been reported (Guillet *et al.*, 2010).

1.2 PATHOPHYSIOLOGY OF LISTERIOSIS

Listeriosis can manifest perinatally and in adult patients. Pregnant women, neonates and elderly people are primarily affected by the disease. *Listeria* is more likely to cause severe illness and death in those with a compromised immune

response (*i.e.* people with AIDS, cancer patients or people affected with chronic, debilitating diseases such as diabetes, chronic heart condition, renal disease or cirrhosis) or in people with immature immune systems (*e.g.* foetuses and newborns) (Schwartz *et al.*, 1988, Vazquez-Boland *et al.*, 2001a).

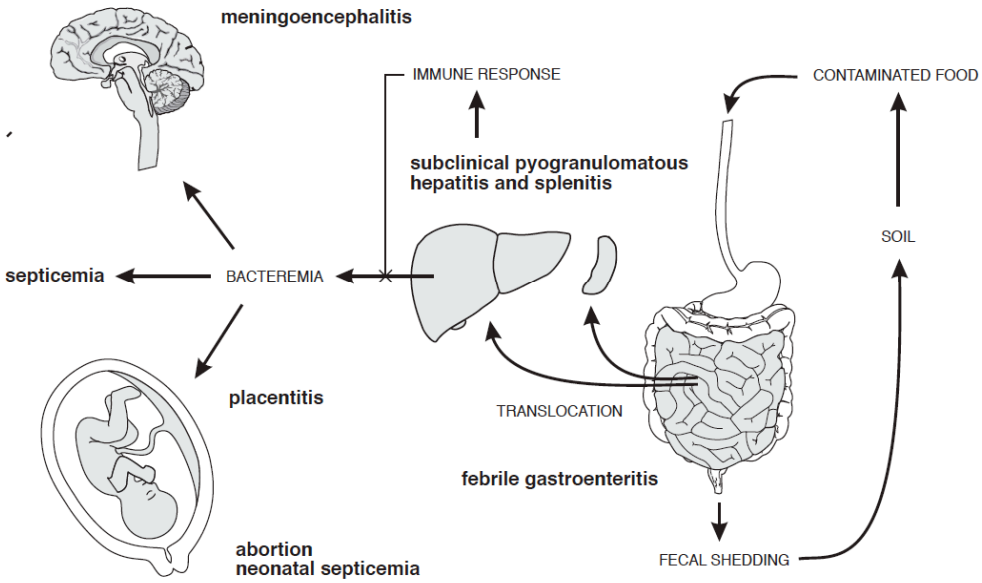

Figure 1.1: Schematic representation of the pathophysiology of *Listeria* infection.
Adapted from Vazquez-Boland *et al.* (2001a).

There are two forms of listeriosis: non-invasive, restricted to the gastrointestinal tract, and invasive, involving the entry and spread of the bacterium to different internal organs of the body. The non-invasive form has an incubation period of about 20 h and is characterized by febrile gastroenteritis. This form appears primarily in healthy adults upon consumption of heavily contaminated food (approximately 10^9 CFU / ml). Symptoms have a sudden onset and include fever, severe headache, vomiting and several flu-like manifestations. Invasive listeriosis has a much longer incubation period, up to 20 to 30 days, and is characterized by severe clinical conditions including meningoencephalitis, septicaemia or abortion.

This form occurs primarily in immuno-compromised individuals or pregnant women and newborns (Schuchat *et al.*, 1991, Ramaswamy *et al.*, 2007).

The main portal of entry of pathogenic *Listeria* is the intestine. During invasive infection, the bacteria cross the epithelial barrier and get translocated to the local lymph nods, and via lymphohaematogenous dissemination they gain access to the primary target-organs, *i.e.* the spleen and liver. At this stage the infection is normally controlled by the immune response in immunocompetent people. In immuno-compromised patients, however, the immune defences are overwhelmed by the pathogenic bacteria and these spread to secondary target organs, such as the brain or the placenta, causing meningoencephalitis or abortion and neonatal septicaemia (figure 1.1) (Vazquez-Boland *et al.*, 2001a, Lecuit, 2007).

1.3 PATHOGENESIS OF *LISTERIA* INFECTION AND ITS MOLECULAR DETERMINANTS

1.3.1 INTRACELLULAR INFECTION CYCLE

Listeria organisms are not only able to survive and multiply within macrophages but also to actively invade a wide variety of mammalian cells which are not normally phagocytic, like epithelial cells, fibroblasts, hepatocytes, endothelial cells and nerve cells. The intracellular life cycle of *Listeria* shares similar characteristic in all the above-mentioned cells (Kuhn & Goebel, 2000, Vazquez-Boland *et al.*, 2001a). First, the bacterium adheres to the eukaryotic cell surface and, then, gets internalized. Inside the host cell, the bacterium survives, proliferates and spreads from one cell to another without leaving the intracellular environment (Ireton & Cossart, 1997, Vazquez-Boland *et al.*, 2001a, Portnoy *et al.*, 2002) (figure 1.2).

Listeria interact with the surface of host cells through at least two eukaryotic receptors, E-cadherin present in epithelial cells, and the Met receptor for the hepatocyte growth factor (HGF), present in a wide variety of cell types (Cossart *et al.*, 2003). At the beginning, the pathogen becomes surrounded by pseudopods, which adhere firmly to the bacterial surface and fuse laterally forming a membrane, a process that progressively surrounds by a "zipper-like" mechanism the bacterial cell. The bacterium becomes completely engulfed within a phagocytic vacuole. The secretion by *Listeria* of membrane-damaging factors rapidly lyse the vacuole (within 30 minutes) and release the bacterium into the cytosol where it multiplies (Vazquez-Boland *et al.*, 2001a).

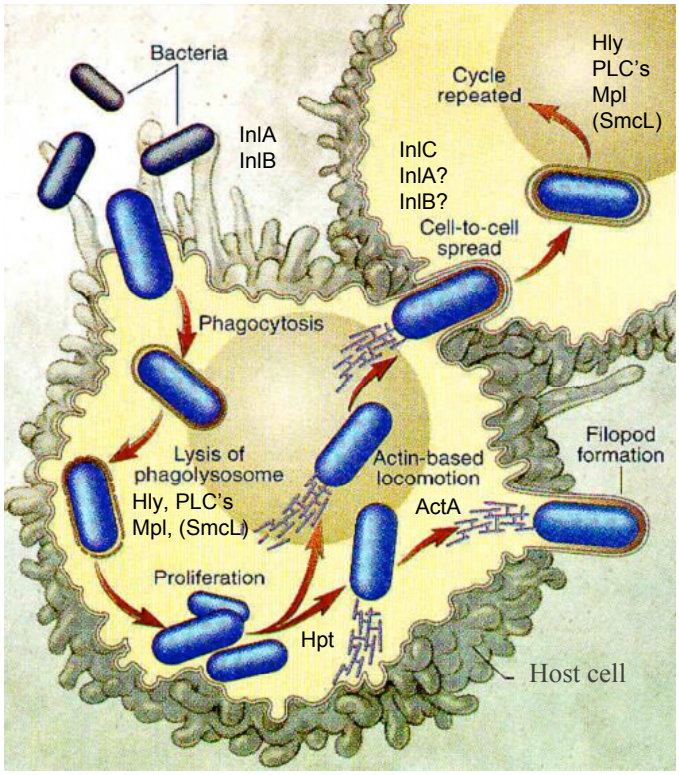

Figure 1.2: Intracellular life cycle of pathogenic *Listeria* spp.
The scheme includes virulence factors involved in each step of *L. monocytogenes* life cycle (apart from SmcL, which is produced only by *L. ivanovii*; see text for details). *L. ivanovii* possesses equivalent virulence factors similarly involved in the cycle. Adapted from Portnoy *et al.* (2002).

In parallel, *Listeria* induces the polymerization of actin filaments at one of its poles, resulting in the formation of an "actin tail". In this way, a motor force is generated which allows bacteria to propel themselves across the cytoplasm. Due to this actin-based motility mechanism, bacteria eventually reach the cell periphery, push the membrane outwards, and protrude in filopod-like structures with a bacterium at the tip. These structures penetrate into neighbouring cells where they are phagocytosed, resulting in the formation of a double-membrane vacuole (or "secondary phagosome") (figure 1.2). The vacuole becomes again disrupted, releasing the bacteria into the cytoplasm where they begin a new cycle of replication and actin-based motility. Thanks to this mechanism, the bacteria spread throughout host tissues sheltered from the humoral effectors of the immune system. Therefore, only a strong cytotoxic T-cell-mediated immune response, reflected in the formation of granuloma-like structures that physically contain the pathogen, can prevent the spread of listerial infectious foci in the affected organs (Tilney & Portnoy, 1989, Vazquez-Boland *et al.*, 2001a, Portnoy *et al.*, 2002, Cossart *et al.*, 2003, Dussurget *et al.*, 2004, Hamon *et al.*, 2006).

1.3.2 VIRULENCE FACTORS OF *LISTERIA*

Different virulence factors are involved in each step of the *Listeria* intracellular life cycle (figure 1.2). Internalization by host cells involves two bacterial surface proteins, InlA and InlB, which recognize host-cell surface receptors (E-cadherin and Met, respectively). This receptor-ligand interaction activates intracellular signalling pathways, under active investigation, ultimately leading to cortical actin cytoskeletal rearrangements and phagocytosis. InlA and InlB belong to a multigene family exclusive to *Listeria* and collectively known as internalins, which comprises additional members coding for either surface-attached or small-excreted proteins. The internalin proteins are characterized by the presence of a leucine-rich repeat (LRR) region, which provides a structural framework for protein-protein interactions. InlA and InlB interact with their specific receptors via the LRR domain

(Vazquez-Boland *et al.*, 2001a, Hamon *et al.*, 2006, Cossart & Toledo-Arana, 2008, Mostowy & Cossart, 2009).

In order to rupture the phagosome membranes, *Listeria* secretes a pore-forming toxin belonging to the family of thiol-activated or cholesterol-dependent cytolysins. This haemolysin is known as listeriolysin O (LLO) in case of *L. monocytogenes* and ivanolysin O (ILO) in case of *L. ivanovii* (Geoffroy *et al.*, 1987). Furthermore, studies showed that expression of the haemolysin gene of *L. monocytogenes* in *Bacillus subtilis* allowed this non-pathogenic bacterium to escape from the phagosome and proliferate intracellularly, confirming the important role of LLO in the listerial intracellular life cycle (Bielecki *et al.*, 1990).

Pathogenic *Listeria* produce other phagosome disrupting factors, such as the phospholipases C (PLC): the phosphatidylinositol-specific phospholipase C (PI-PLC) PlcA, and the phosphatidylcholine-preferring phospholipase C (PC-PLC), PlcB. These two enzymes are secreted by both *L. monocytogenes* and *L. ivanovii*, whereas the latter species produces an additional phospholipase C specific for sphingomyelin, SmcL, a sphingomyelinase (SMase). Activation of pro-PlcB and post-secretion processing of PlcB involves a metalloprotease (Mpl) (Leighton *et al.*, 1975, Vazquez-Boland *et al.*, 1989, Camilli *et al.*, 1991, Poyart *et al.*, 1993, Gonzalez-Zorn *et al.*, 1999, Ray *et al.*, 2009).

The replication phase in the cytoplasm is mediated by a hexose phosphate transporter, Hpt, a member of the organophosphate:inorganic antiporter (OPA) family, of the major facilitator superfamily (MFS) of permeases. Hpt transports glucose-6-phosphate (G-6-P) and other hexose monophosphates such as glucose-1-phosphate (G-1-P), fructose-6-phosphate (F-6-P), and mannose-6-phosphate (M-6-P). This transmembrane protein enables pathogenic *Listeria* to use sugar phosphates from the host cell to fuel rapid bacterial intracellular growth (Chico-Calero *et al.*, 2002). Actin-based motility is mediated by the listerial surface protein ActA. This protein induces actin polymerization via mimicry of the natural action of the Arp2/3 complex-activating protein WASP/Scar-1 (Cossart *et al.*, 2003, Hamon *et al.*, 2006).

Recent studies have shown that InlC, a secreted *L. monocytogenes* virulence protein, is also required in order to efficiently spread from cell-to-cell (Rajabian *et al.*, 2009).

A novel haemolytic/cytolytic factor named listeriolysin S (LLS) has been recently discovered in the lineage I *L. monocytogenes* (serotypes 1/2b and 4b), and was found to be associated with the majority of spontaneous and epidemic outbreaks of listeriosis. This second haemolysin of *Listeria* is only induced under oxidative stress conditions and contributes to murine virulence and survival in polymorphonuclear neutrophils (PMNs). The gene cluster encoding LLS has been named *Listeria* pathogenicity island 3 (LIPI-3), in order to distinguish it from LIPI-1 and LIPI-2 (see below section 1.3.3 and 1.3.7, respectively). LLS belongs to a family of modified virulence peptides such as Streptolysin S (SLS), produced by *Streptococccus pyogenes* (Cotter *et al.*, 2008).

1.3.3 GENETIC ORGANIZATION OF LISTERIAL VIRULENCE DETERMINANTS

Most of the key listerial virulence factors such as LLO/ILO, PlcA, PlcB, Mpl, ActA and the positive regulatory factor A (PrfA), required for intracellular survival and spread, are encoded in *Listeria* pathogenicity island 1 (LIPI-1), a 9-kb chromosomal locus (figure 1.3). In the non-pathogenic *Listeria* spp., LIPI-1 is absent (*L. innocua* and *L. welshimeri*) or present in non-functional form, as in *L. seeligeri*, in which an insertion disrupts the positive autoregulatory loop between *plcA* and *prfA*, essential for adequate PrfA-dependent virulence gene activation (Karunasagar *et al.*, 1997, Vazquez-Boland *et al.*, 2001a). LIPI-1 has the same genetic structure and is inserted at the same chromosomal position in *L. monocytogenes* and *L. ivanovii*, indicating that this central pathogenicity island was acquired by a *Listeria* ancestor before speciation. Consistent with this, the corresponding gene homologues share only 73-78% identity at the level of DNA sequence, a degree of divergence that is compatible with the genetic distance between the two species (Vazquez-

Boland *et al.*, 2001b). *actA* is the LIPI-1 gene that shows the greatest dissimilarity between the two pathogenic *Listeria* spp., even at the protein level (only 34% identity), although the two proteins are equally functional (Gouin *et al.*, 1995, Kreft *et al.*, 1995).

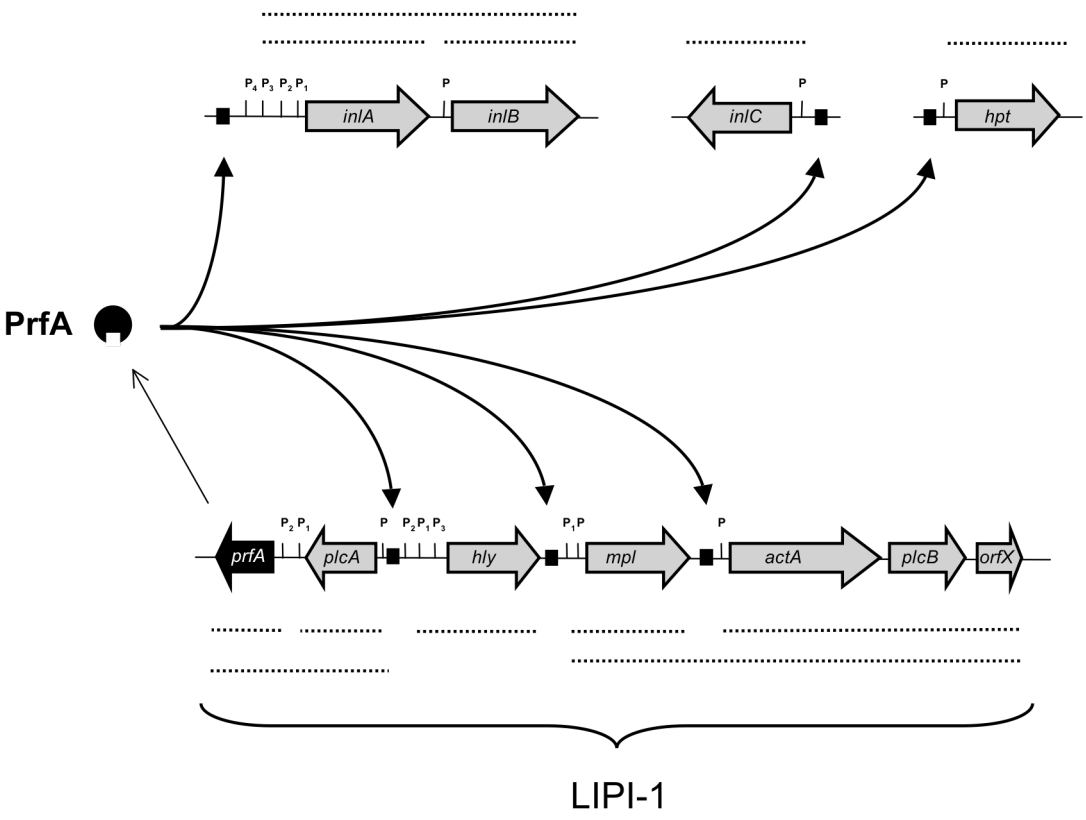

Figure 1.3: The PrfA virulon of *L. monocytogenes.*
The schematic representation includes the physical and transcriptional organization of *Listeria* pathogenicity island-1 (LIPI-1) genes and the three other PrfA-regulated loci: the *inlAB* operon, and the *inlC* and *hpt* monocistrons; right-pointing genes are on the positive strand of the genome. PrfA-boxes are indicated by black squares, known promoters and transcripts are indicated "P" and dotted lines, respectively. *inlC*, encoding an internalin homologue, is also regulated by PrfA (Engelbrecht *et al.*, 1998). LIPI-1 genes and *hpt* are present in both *L. monocytogenes* and *L. ivanovii*; however, the two species differ in their PrfA-dependent *inl* gene complement. Taken from Scortti *et al*. (2007).

The central position in LIPI-1 is occupied by the *hly* monocistron encoding LLO (in *L. monocytogenes*) or ILO (in *L. ivanovii*). Downstream from *hly* is the lecithinase operon with the *mpl, actA* and *plcB* genes. Upstream and divergent from

hly lies the *plcA-prfA* operon. The *prfA* gene encodes PrfA, a transcription activator of the Crp/Cap-Fnr family (Sheehan *et al.*, 1995, Bubert *et al.*, 1999, Goebel *et al.*, 2000, Vazquez-Boland *et al.*, 2001b, Gray *et al.*, 2006, Scortti *et al.*, 2007). PrfA is required for the transcription of all LIPI-1 genes and also coordinates the expression of other genes located elsewhere on the listerial chromosome and which also code for virulence factors involved in listerial intracellular parasitism. These are the *inlAB* operon, the *inlC* and the *hpt* monocistrons (Skoble *et al.*, 2001, Chico-Calero *et al.*, 2002). Collectively, all the PrfA-dependent genes are known as the PrfA regulon (figure 1.3).

1.3.4 THE CENTRAL VIRULENCE REGULATOR PRFA

PrfA is the major regulator of virulence in *Listeria*. This 237-residue protein of 27 kDa is structurally related to the *Escherichia coli* regulator, cAMP receptor protein (Crp), also called catabolite gene activator protein (Cap) (Goebel *et al.*, 2000, Kreft & Vazquez-Boland, 2001, Scortti *et al.*, 2007). The arrangement of subunits of both of these homodimers is similar (figure 1.4). The structure of PrfA and Crp consists of three regions. In the N-terminal domain there is a β(jelly)-roll and long α-helices that provide the majority of the monomer-monomer interface. The middle region is called the hinge or the inter-domain region. In the C-terminal domain there is the DNA-binding helix-turn-helix (HTH) motif. In the PrfA structure, the presence of a unique extension in the C-terminal stabilizes the HTH motif (Vega *et al.*, 2004, Eiting *et al.*, 2005). It has been shown that when the Crp protein is unliganded it remains inactive. However, if cAMP (cyclic adenosine 3', 5' -mono-phosphate) binds to the N-terminal domain of Crp, it adopts a conformation with a higher affinity for the target DNA (Kolb *et al.*, 1993, Green *et al.*, 2001). It has been suggested that due to the fact that PrfA is structurally similar to Crp (figure 1.5), it may also have a similar type of allosteric mechanism of activation (Scortti *et al.*, 2007).

There is evidence that PrfA can adopt two functional states: weakly active as in the native form of the protein, and highly active after a conformational change.

The latter state can be found in *L. monocytogenes prfA** mutants, in which PrfA-dependent genes are constantly overexpressed due to the presence of a hyperactive PrfA* protein variant (Ripio *et al.*, 1996, Ripio *et al.*, 1997a). The *prfA** bacteria carry a point mutation, which leads to a single amino acid substitution outside the HTH motif that renders the PrfA protein constitutively hyperactive, *i.e.* with a significantly increased specific DNA-binding activity (Vega *et al.*, 2004).

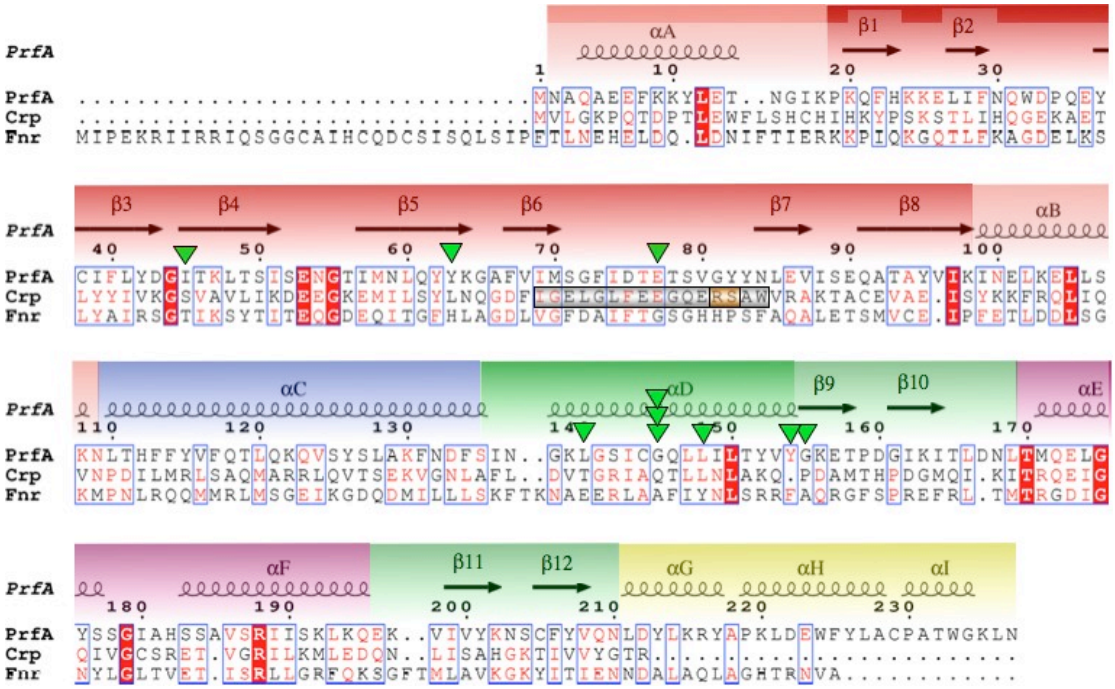

Figure 1.4: Alignment of amino-acid sequence of PrfA from *L. monocytogenes* and the related Crp and Fnr (fumerate and nitrate reductase regulator) transcription factors of *E. coli*.
Adapted from Scortti *et al.* (2007). The secondary structure elements of PrfA are presented above the sequence (spirals = α-helices; arrows = β-strands). Protein domains are boxed in colour: N-terminal domain: red = β(jelly)-roll, pink = flanking β-strands, blue = the α-helix that gives majority of monomer-monomer interface; inter-domain (hinge) region represented as a green section flanked by the αC-helix and the αD-helix, consists of: N-terminal domain: green = αD-helix, pale green = β-strands flanking the HTH motif, magenta = HTH motif, yellow = the PrfA "G" domain, which includes three C-terminal α-helices that form a wedge inserted into the inter-domain cleft and which stabilizes the HTH motif. The positions of ten PrfA* mutations described up to date (see text for details) are indicated by green triangles. The phosphate binding cassette signature motif involved in cAMP binding in Crp is indicated by the grey rectangle. Orange highlights indicate the critical residues interacting with the phosphate moiety of cAMP phosphoribose.

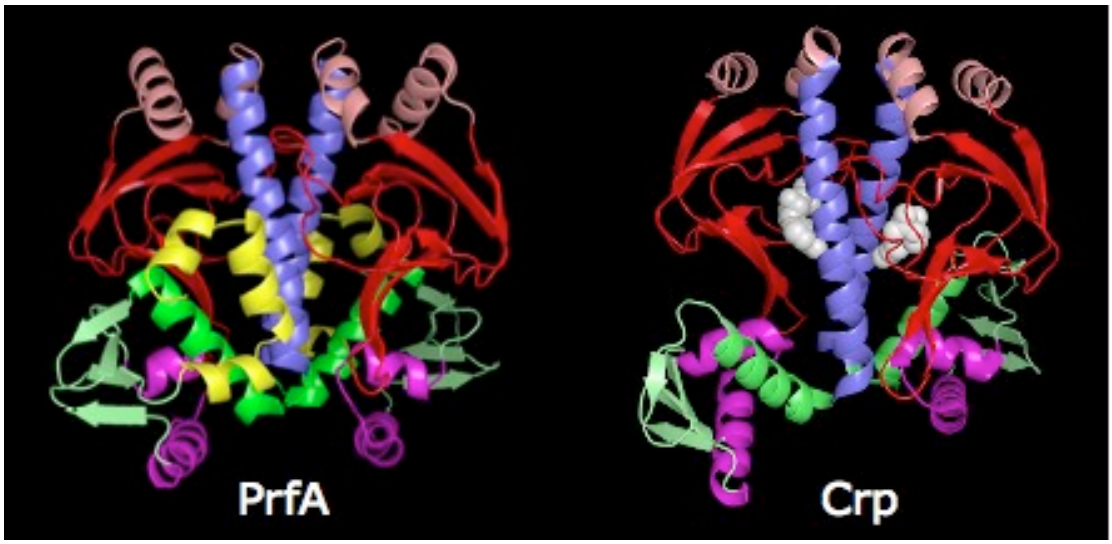

Figure 1.5: Comparison of the crystal structures of the PrfA and Crp dimers.
Colour code as in figure 1.4. In Crp structure, white spheres indicate the cAMP molecule inserted in each of the two β(jelly)-rolls of the dimer. Taken from Scortti *et al.* (2007).

Up to date, ten *prfA** mutations have been described: G145S, G145C, G145R, I45S, Y63C, E77K, L140F, L148T (in literature mistakenly named as A148T), Y154C and G155S (Ripio *et al.*, 1997a, Vega *et al.*, 2004, Monk *et al.*, 2008, Freitag *et al.*, 2009). These *prfA** mutations target PrfA regions or positions equivalent to those affected by Crp* mutations in Crp with the same functional consequences (Vega *et al.*, 1998, Vega *et al.*, 2004). Transcriptional activity levels of Crp* proteins have been found to be similarly high to the levels of Crp proteins complexed with cAMP, and, interestingly, this does not require the presence of the activating cofactor. It has been suggested that the Crp* mutations mimic the conformational changes caused by cAMP (Passner *et al.*, 2000). The structural and functional similarities between PrfA and Crp have led to the suggestion that the listerial regulator may also function through an allosteric transition mechanism, activation resulting from the interaction with a hypothetical small molecule or cofactor. The crystal structures of wild-type PrfA ($PrfA^{WT}$) and $PrfA^{*G145S}$ mutant proteins have been recently obtained and compared, and the analysis seem to confirm the hypothesis (Ripio *et al.*, 1997a, Vega *et al.*, 1998, Vega *et al.*, 2004, Scortti *et al.*, 2007).

The N-terminal β(jelly)-roll structure of PrfA and the cyclic nucleotide-binding domain of Crp are structurally very similar. In the PrfA protein, however, the majority of the residues responsible for cAMP binding in Crp are absent (Diller *et al.*, 2001). *In vitro* and *in vivo* studies from our group have shown that PrfA-dependent expression of the genes was not affected by the presence of cAMP (Vega *et al.*, 1998). It was, therefore, concluded that this nucleotide is not the PrfA-activating cofactor. Detailed analyses of the crystal structure of PrfA have indicated the presence of a tunnel, similar to the one found in Crp protein, located in the inter-domain cleft of the PrfA protein (figure 1.6). Additionally, in order to stabilize the protein, glycerol or DTT were used. Interestingly, these small molecules are lodged in the β-roll. Overall, all these observations are consistent with the notion that a small cofactor interacts with PrfA (Vega *et al.*, 2004, Eiting *et al.*, 2005).

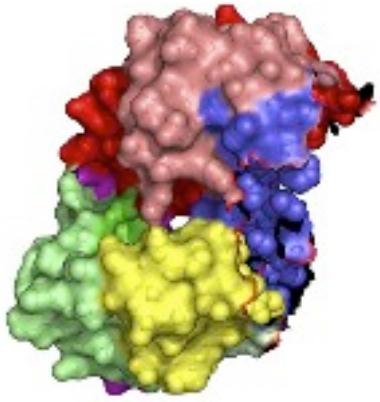

Figure 1.6: Representation of the PrfA monomer with combined surface and space-fill.
A solvent-accessible tunnel at the inter-domain cleft is visualized in the middle of the structure. In Crp protein, the cAMP–binding pocket is accessed through a similarly located tunnel (Eiting *et al.*, 2005). Broken red line indicates the dimeric interface; spheres represent buried atoms from the dimeric interface. Colour-code as in figure 1.4. The image has been prepared with MacPyMOL 0.99 and taken from Scortti *et al.* (2007).

Single residue substitutions in the PrfA protein may contribute to high transcriptional activity levels (as in case of *prfA** mutations), however, they can also have the opposite effect. Up to date, thirteen single-substitution mutations have been described, which lead to loss of function in PrfA (table 1.1). These mutations affect

the N-terminal β-roll, in the HTH motif and in the GHI α-helical extension (Sheehan *et al.*, 1996, Herler *et al.*, 2001, Vega *et al.*, 2004, Roche *et al.*, 2005, Monk *et al.*, 2008). Deletions or truncations in PrfA have also been found to be associated with the loss of function (Herler *et al.*, 2001, Vega *et al.*, 2004). Additionally, Sheehan *et al.* (1996) described a point mutation (a substitution of serine for alanine obtained by site-directed mutagenesis) in position 183 of PrfA, located in αF of the HTH motif, which had no major effect on PrfA function (Sheehan *et al.*, 1996). Collectively, these mutations confirmed the functional importance of the β-roll, HTH motif and C-terminal extension in PrfA.

Table 1.1: Single-substitution mutations and deletions (or truncations) associated with loss of PrfA function.

PrfA⁻ mutation	Location	Type	Activity (intracell. induction)	Comments	References
M58I	β-roll	*iap*-based positive selection in *Bacillus*	Unknown	Shows same binding as wild-type PrfA (CIII formation) to *hly* promoter but does not activate transcription.	Herler *et al*. (2001) Vega *et al*. (2004)
Y62C	β-roll	*iap*-based positive selection in *Bacillus*	Unknown	Reduced activity? Paper states reduced CI complex formation but this is unclear. CIII formation and *in vitro* transcription not tested.	Herler *et al*. (2001)
M70I^	β-roll	Spontaneous suppressor mutation of *prfA**G145S	Unknown	Total loss of function, however, mutation not checked with a complemented strain.	Vega Y. (2002) (unpublished data)
S71C	β-roll	Site-directed	Unknown	Limited data: only a slight increase in haemolysis on BHI agar containing sheep blood (5%) with sphingomyelinase, however, no halo observed on 4% lecithin agar, suggesting no secretion of PlcA or PlcB.	Monk *et al.* (2008)
Y83S	β-roll	*iap*-based positive selection in *Bacillus*	Unknown	Reduced activity? Paper states reduced CI complex formation but this is unclear. CIII formation and *in vitro* transcription not tested.	Herler *et al*. (2001) Vega *et al*. (2004)
A94T	β-roll	Site-directed	Unknown	Limited data: only a slight increase in haemolysis on BHI agar containing sheep blood (5%) with sphingomyelinase, however, no halo observed on 4% lecithin agar, suggesting no secretion of PlcA or PlcB, similar to S71C.	Monk *et al.* (2008)
D133Y	End of αC	*iap*-based positive selection in *Bacillus*	Unknown	No CI complex detected. CIII formation and *in vitro* transcription not tested.	Herler *et al*. (2001) Vega *et al*. (2004)
K139T	αD near αC (hinge region)	*iap*-based positive selection in *Bacillus*	Unknown	No CI complex detected. CIII formation and *in vitro* transcription not tested.	Herler *et al*. (2001) Vega *et al*. (2004)
E173G^	αE, HTH motif	Spontaneous suppressor mutation of *prfA**G145S	Unknown	Total loss of function.	Vega *et al*. (2004)
S184A	αF, HTH motif	Site-directed	Unknown	Significant reduction of DNA-binding, PrfA-dependent gene expression and virulence.	Sheehan *et al*. (1996)
R188I	αF, HTH motif	*iap*-based positive selection in *Bacillus*	Unknown	Strongly impairs, abolishes CIII and CI complex formation.	Herler *et al*. (2001) Vega *et al*. (2004)
K220T	αH (C-terminal extension	Spontaneous	Unknown	No PrfA-dependent expression and virulence. No effect on dimerization but DNA-binding (CIII) abolished.	Roche *et al*. (2005) Velge *et al*. (2007)
C229Y	αH (C-terminal extension)	Spontaneous suppressor mutation of *prfA**G145S	Unknown	Always found together with G145S in division II spontaneous *L. monocytogenes* PrfA* mutants.	Ripio *et al*. (1997) Vega *et al*. (2004)
ΔELK101-103	αB just after β-roll and before αC	*iap*-based positive selection in *Bacillus*	Unknown	No CI complex detected. CIII formation and *in vitro* transcription not tested.	Herler *et al*. (2001) Vega *et al*. (2004)
E173*	αE→αI	Spontaneous	Unknown	Total loss of function.	Roche *et al*. (2005)
L193*	αF→αI	*iap*-based positive selection in *Bacillus*	Unknown	No CI complex detected. CIII formation and *in vitro* transcription not tested.	Herler *et al*. (2001) Vega *et al*. (2004)
ΔFYV206-208	β12 just before αG	*iap*-based positive selection in *Bacillus*	Unknown	No CI complex detected. CIII formation and *in vitro* transcription not tested. Wrongly described by Herler *et al.* (2001) as ΔFYV207-209.	Herler *et al*. (2001) Vega *et al*. (2004)
APK218-220→PLN* (ΔL221-N237)	αG-αH, C-terminal extension	*iap*-based positive selection in *Bacillus*	Unknown	No CI and CIII complex formation.	Herler *et al*. (2001) Vega *et al*. (2004)

^ - Spontaneous mutations found in *L. monocytogenes* belonging to phylogenetic divison II (which includes serovars such as 1/2a, 1/2c and 3a). In such strains PrfA* activity is always associated with the presence of two point mutations $PrfA^{G145S}$ and $PrfA^{C229Y}$ (Ripio *et al.* [1997b]).

1.3.5 REGULATION MECHANISMS OF PRFA

The PrfA concentration, the promoter configuration and the above-mentioned changes in PrfA activity are believed to be the three key mechanisms that contribute to the modulation of PrfA-dependent gene transcription.

During extracellular growth, *e.g. in vitro* growth in bacteriological culture media, the genes of the PrfA regulon are normally very weakly or even not expressed (Chakraborty *et al.*, 1992, Ripio *et al.*, 1996, Ripio *et al.*, 1997a). The weakly active, native PrfA protein binds with low affinity to the PrfA box in the target promoters (Vega *et al.*, 1998, Vega *et al.*, 2004). However, PrfA-dependent genes are maximally induced after the invasion of host cells, especially when the pathogenic organisms reach the cytosolic compartment (Moors *et al.*, 1999, Shetron-Rama *et al.*, 2002). It is believed that this extra / intracellular differential expression operates through changes in PrfA activity by a cofactor-mediated allosteric shift. It has been suggested that this positive control pathway is involved in the strong induction of PrfA-dependent expression occurring during intracellular growth. Data suggest that *Listeria* mutants carrying a *prfA** allele reach a similar level of induction, *e.g.* up to 300-fold for the *actA* gene, when cultured in broth media (Ripio *et al.*, 1997a; Shetron-Rama *et al.*, 2003; Vega *et al.*, 1998 and other unpublished data from our laboratory). These observations support the hypothesis that during infection, the master regulator of *Listeria* adopts a conformation similar to that of the PrfA* mutant protein (Ripio *et al.*, 1997a, Vega *et al.*, 2004). *L. monocytogenes* wild-type and the *prfA** mutant strains have been shown to significantly differ in their PrfA-dependent gene expression levels *in vitro*. Apart from this, both microorganisms proved to be similar as far as their virulence is concerned, in line with the above-mentioned hypothesis (Ripio *et al.*, 1996; Shetron-Rama *et al.*, 2003 and our unpublished observations).

Apart from the PrfA-activating pathway, two negative regulatory pathways, which downregulate *Listeria* virulence genes, have been described. One of the repressor pathways involves the addition of activated charcoal to the *Listeria* culture

medium (Ermolaeva *et al.*, 2004). It has been proposed that the so-called "charcoal effect" is due to the adsorption of a diffusible autorepressor substance released to the supernatant during *Listeria* exponential growth. The nature of the autorepressor remains unknown but preliminary experimental evidence using different types of adsorptive resins suggests it is a small hydrophobic molecule (Ermolaeva *et al.*, 2004). In the *prfA** mutants, PrfA is locked in its fully active form, therefore, the regulator is not inhibited by this small hydrophobic molecule. These observations led to the conclusion that activated charcoal mediates the upregulation of PrfA-dependent genes *in vitro* by sequestering a diffusible autorepressor substance released by *L. monocytogenes* in the culture medium (Ermolaeva *et al.*, 2004).

Another virulence gene negative regulatory pathway manifests when *L. monocytogenes* bacteria grow on fermentable carbohydrates such as glucose, fructose, mannose or β-glucosides, *e.g.* cellobiose. Virulence genes are repressed only if there is enough amount of carbohydrate allowing bacteria to grow (Milenbachs *et al.*, 1997, Vega *et al.*, 1998, Brehm *et al.*, 1999, Kreft & Vazquez-Boland, 2001, Ermolaeva *et al.*, 2004, Vega *et al.*, 2004), indicating that the phenomenon is connected to sugar metabolism and possibly reflects an aspect of carbon catabolite repression (CCR). Indeed, only sugars that are transported by phosphoenolpyruvate-sugar phosphotransferase system (PTS) permeases trigger repression. Such repression is not observed with hexose phosphates, which are transported by the listerial non-PTS permease Hpt (Ripio *et al.*, 1997b, Chico-Calero *et al.*, 2002), although the same glycolytic intermediates *e.g.* fructose-1,6-bisphosphate are produced when these sugars are metabolized. This suggested that there may be a direct link between the transport of sugars through the PTS-system and CCR network. Further data supporting this observation showed that the repression caused by cellobiose was eliminated by inactivation of a β-glucoside-specific PTS permease system (*bvrABC*) (Brehm *et al.*, 1999). Although the major CCR mediator CcpA does not seem to be involved in the sugar-mediated virulence gene repression (Behari & Youngman, 1998a), there is evidence that the PTS protein, Hpr-Ser-P (histidine containing protein serine phosphorylated), is involved in the response by acting as a corepressor of PrfA (Herro *et al.*, 2005). Data showed

that the amount of PrfA protein present in bacterial cytosol did not decrease with repression, indicating that sugars modulate PrfA-dependent gene expression through changes in PrfA activity (Renzoni *et al.*, 1999, Ermolaeva *et al.*, 2004). It has been suggested that this negative regulatory pathway may play an important role in repressing virulence genes in the environmental habitat, where β-glucosides cellobiose and other plant-derived sugars are presumably abundant (Park & Kroll, 1993, Ripio *et al.*, 1997b). Until today, however, the exact connection between sugar-mediated repression and CCR and the underlying mechanism remains unsolved.

The amount of PrfA protein available also plays an important role in the expression of PrfA-dependent genes. Two types of promoters direct the transcription of *prfA*: P1*prfA* and P2*prfA,* located in the intergenic region upstream from the *prfA* gene, generate a monocistronic transcript (figure 1.3), whereas P*plcA*, upstream from the *plcA* gene, generates a bicistronic *plcA-prfA* transcript (figure 1.7) (Mengaud *et al.*, 1991, Camilli *et al.*, 1993, Freitag *et al.*, 1993, Freitag & Portnoy, 1994). During extracellular bacterial growth at temperatures below 30°C, low-level *prfA* mRNAs is synthesized due to the direct contribution of the sigma A (σ^A)-dependent P1*prfA* promoter. The PrfA regulon is induced, however, when the environmental temperature is 37°C (as on entry into a warm-blooded animal host). This thermoregulation is mediated by a secondary structure present in the 5' non-coding region of the *prfA* mRNA and which prevents ribosome binding unless it melts when the temperature reaches 35 - 37ºC, enabling translation (Johansson *et al.*, 2002). Located downstream from P1*prfA*, the P2*prfA* promoter is controlled by σ^A and additionally by σ^B (sigma B), which is a stress-responsive alternative sigma factor (see section 1.3.6) (Nadon *et al.*, 2002, Rauch *et al.*, 2005, Schwab *et al.*, 2005). In order to ensure that a minimum amount of PrfA protein is always present in the bacterial cytosol, both, P1*prfA* and P2*prfA* promoters are responsible for supplying basal levels of *prfA* transcripts (Freitag *et al.*, 1993, Freitag & Portnoy, 1994).

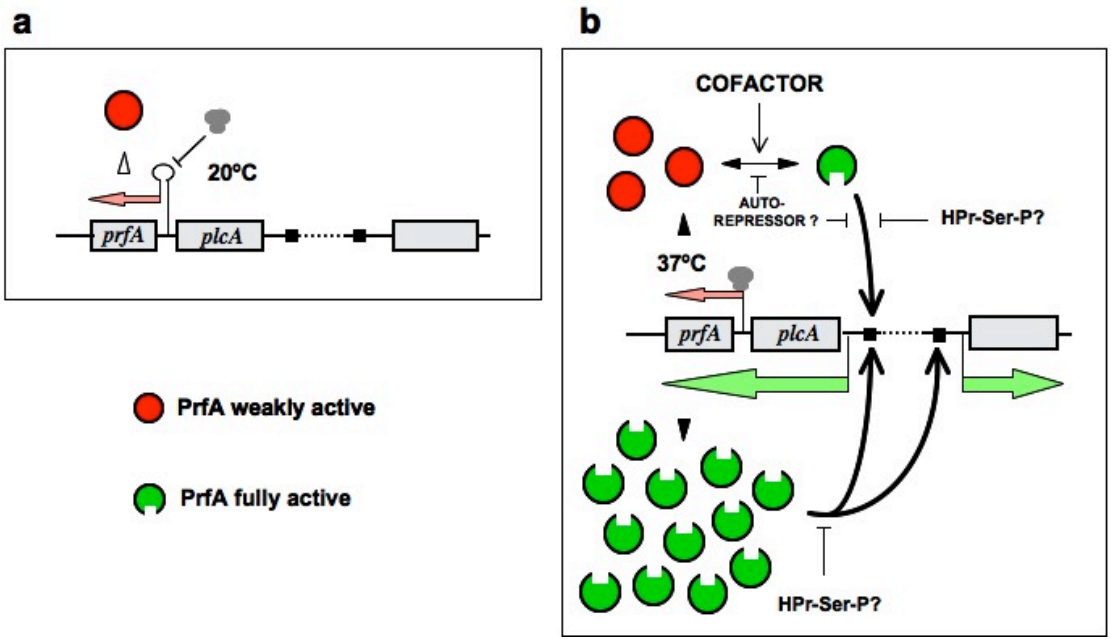

Figure 1.7: Schematic representation of PrfA regulation.
See text for details: a) Resting state of PrfA system: during growth at low temperatures, in the absence of PrfA-activating cofactor, very small amount of PrfA is generated. Synthesis of PrfA in a native weakly active conformation involves monocistronic *prfA* mRNAs, which are produced from P1*prfA* and P2*prfA* promoters (pink arrow). Inefficient translation from these growth-phase regulated promoters is due to the presence of a secondary structure, which forbids the ribosome (represented by grey mushroom-like structure) to access to its binding site. b) Active state of PrfA system: Efficient translation (represented by filled arrowhead) is possible due to the break down of the *prfA* mRNA secondary structure, as a result of an increase in temperature to 37°C (mimicking the entry into a warm-blooded animal host). In the cytosolic compartment of the host cell, a putative low-molecular weight cofactor binds to PrfA. As a consequence, the affinity of the regulatory protein for its target sequence (indicated by black squares) increases. The highly active form of PrfA contributes to the synthesis of more PrfA. The PrfA regulon is fully induced in the environmental temperature of 37°C, in the presence of the cofactor and the absence of repressor signals that could potentially act on the system. Taken from Scortti *et al*. (2007).

The P*plcA* promoter, on the other hand, is strictly PrfA-dependent. Through positive feedback, PrfA is able to stimulate its own synthesis via the *plcA-prfA* bicistronic transcript (Mengaud *et al.*, 1991, Chakraborty *et al.*, 1992). This loop is activated when the PrfA concentration increases *e.g.* when *prfA* message translation is de-inhibited at 37ºC, and / or when PrfA protein activity increases, presumably by allosteric change, as above discussed. Due to the presence of this autoregulatory loop, any change in PrfA activity is immediately amplified at the transcriptional

level. In order for *Listeria* to infect successfully its host cells, the bacteria need to synthesize sufficiently large amount of PrfA protein through activation of the autoregulatory loop (Mengaud *et al.*, 1991, Camilli *et al.*, 1993, Vega *et al.*, 2004).

The third mechanism contributing to the regulation of PrfA-dependent gene expression depends on the architecture of the promoters. PrfA-dependent promoters stimulated by PrfA respond in different ways. These promoters bear a 14-bp "box" of dyad symmetry with the consensus sequence TTAACANNTGTTAA. The PrfA dimer uses this sequence as a binding site (Vega *et al.*, 1998, Goebel *et al.*, 2000, Kreft & Vazquez-Boland, 2001, Scortti *et al.*, 2007). Depending on the number of mismatches in the target sequence the binding affinity of PrfA is affected. The more the sequence differs from the perfect inverted repeat the weaker the binding is. Promoters such as P*plcA* or P*hly* with perfectly symmetrical PrfA boxes respond with greater sensitivity to PrfA. In contrast, promoters such as P*actA*, P*mpl*, P*hpt* and P*inlC*, carrying a nucleotide mismatch, or P*inlA* having two nucleotide mismatches, require greater amounts of the regulatory protein in order to get fully activated. As a consequence, these promoters have a less linear response to the PrfA input (Vega *et al.*, 2004, Scortti *et al.*, 2007).

1.3.6 σ^B IN STRESS AND VIRULENCE OF *LISTERIA*

1.3.6.1 σ^B and the stress response of *Listeria*

Listeria monocytogenes is able to respond rapidly to changing environmental conditions. Bacterial survival depends on several regulatory mechanisms, which can function at various levels, including the transcriptional level, the post-transcriptional level and the post-translational level (Chaturongakul *et al.*, 2008).

Exposure to environmental stress conditions can lead to significant changes in the gene expression of bacteria due to the presence of alternative sigma (σ)

factors. Sigma factors are proteins, which form essential dissociable subunits of prokaryotic RNA polymerase. These factors contribute to transcriptional level regulation in *L. monocytogenes*. Under specific environmental conditions alternative σ factors have the ability to associate with the core RNA polymerase. They recognize a specific DNA sequence that is a promoter region for a certain gene and initiate the transcription at that promoter site. Two structurally unrelated families of sigma factors have been described: the σ^{70} and the σ^{54} families (Kazmierczak *et al.*, 2005).

One of the first bacterial alternative σ factors described is the alternative sigma B (σ^B) factor, belonging to the σ^{70} family, and encoded by the *sigB* gene. Specific anti-sigma-factor protein keeps σ^B factor in an inactive state until the bacterium finds itself in the environmental conditions requiring gene expression recognized by the σ^B factor (Haldenwang & Losick, 1979, 1980, Kazmierczak *et al.*, 2005). *Staphylococcus aureus* was the first pathogen in which σ^B (originally known as σ^{37}) was found. Apart from *L. monocytogenes*, it has been also identified in other Gram-positive bacteria such as *Bacillus subtilis*, *Bacillus anthracis*, *Bacillus cereus*, *Bacillus licheniformis* and *Staphylococcus epidermidis* (Brody & Price, 1998, Kazmierczak *et al.*, 2005). The σ^B regulon of *L. monocytogenes* has been found to have a similar size to that of *B. subtilis* and *S. aureus*, which contain 125-150 genes and 198 genes, respectively (Petersohn *et al.*, 2001, Bischoff *et al.*, 2004, Senn *et al.*, 2005, van Schaik *et al.*, 2005, Hecker *et al.*, 2007). In *L. monocytogenes*, the *sigB* gene is located in seventh position in an operon consisting of eight genes (*rsbR, rsbS, rsbT, rsbU, rsbV, rsbW, sigB* and *rsbX*), which contribute to the regulation of σ^B. The presence of a housekeeping sigma factor (σ^A)-dependent promoter P_A upstream from the *rsbR* gene enables the co-transcription of all of these genes. Additionally, there is a second promoter (P_B), situated upstream of *rsbV* gene. This σ^B-dependent promoter contributes to the increased levels of transcription of the four genes located downstream in the *sigB* operon (figure 1.8) under conditions, in which σ^B is activated (Becker *et al.*, 1998, Kazmierczak *et al.*, 2005, Severino *et al.*, 2007).

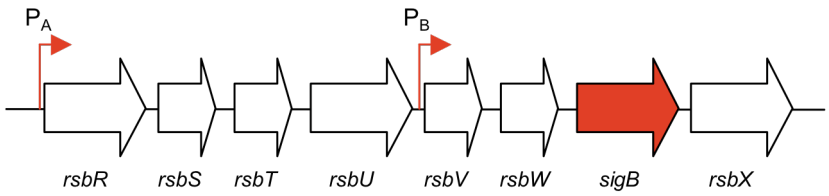

Figure 1.8: Schematic representation of *sigB* operon structure in *L. monocytogenes.*
Adapted from Kazmierczak *et al.* (2005). Arrows represent promoter sites. P_A is a housekeeping σ^A-dependent promoter, which is transcribed with RNAP-σ^A. P_B is σ^B-dependent promoter, which is transcribed with RNAP-σ^B.

The *L. monocytogenes sigB* operon structure is identical to that of *B. subtilis*, however, the signal transduction pathway is different in both bacteria. Unlike in *B. subtilis*, environmental and energy stresses are transmitted to σ^B through a single pathway in *Listeria*. The single pathway consists of RsbT, RsbU, RsbV and RsbW proteins (Becker *et al.*, 1998, Wiedmann *et al.*, 1998, Chaturongakul & Boor, 2004, Kazmierczak *et al.*, 2005).

Apart from two specific heat-shock responses such as HrcA regulated class I response and the CtsR regulated class III response, which are activated in the presence of increased temperatures or other stresses such as cold-shock, high salt concentrations and acid-shock, *L. monocytogenes* possesses also the class II stress response mechanism, which is regulated by the σ^B. In *L. monocytogenes*, σ^B has been shown to contribute to the ability of this bacteria to survive a variety of stress conditions, including acid stress, osmotic stress, cold stress, oxidative stress, nutritional stress and also intracellular survival (Duche *et al.*, 2002, Liu *et al.*, 2002, Kazmierczak *et al.*, 2003, Gray *et al.*, 2006, Abram *et al.*, 2008a, Abram *et al.*, 2008b).

There is evidence that the transcription of genes responsible for acid tolerance is regulated by σ^B. Some of these genes encode proteins involved in the glutamate decarboxylase (GAD) system, which consists of glutamate decarboxylase

enzyme and glutamate-γ-aminobutyrate (GABA) antiporter, contributing to the reduction of the acidification within the bacterial cell cytoplasm (Kazmierczak *et al.*, 2003, Wemekamp-Kamphuis *et al.*, 2004, Cotter *et al.*, 2005, Kazmierczak *et al.*, 2006, Raengpradub *et al.*, 2008). Studies have shown that the ability of a *L. monocytogenes* EGDe Δ*sigB* mutant to survive low acidic conditions (*e.g.* pH = 2.5) was significantly decreased compared to the wild-type (Chaturongakul & Boor, 2004, Wemekamp-Kamphuis *et al.*, 2004).

L. monocytogenes resistance to osmotic stress is also mediated by σ^B. The *sigB* gene showed higher activation levels with increased osmolarity of the medium (Becker *et al.*, 1998, Sue *et al.*, 2003). *L. monocytogenes* is able to survive under high osmolarity conditions due to the presence of transport systems such as OpuC, Gbu and BetL, which enable osmolyte compounds such as carnitine and glycine-betaine to penetrate through the bacterial membrane from the environment to ensure a proper osmotic balance. σ^B regulates the transcription of these compatible solute transporters (Fraser & O'Byrne, 2002, O'Byrne & Booth, 2002, Fraser *et al.*, 2003, Cetin *et al.*, 2004). Additionally, carnitine enables *L. monocytogenes* to survive in acidic environment in the gastrointestinal tract of a mammalian host (Sleator *et al.*, 2001, Gahan & Hill, 2005). Studies carried out with *L. monocytogenes* 10403S and L61, both serotype 1/2a, and corresponding Δ*sigB* mutants showed that the latter are unable to utilise these osmoprotectants. However, a Δ*sigB* mutant of *L. monocytogenes* L99, serotype 4c, did not manifest the same phenotype. It was suggested that the resistance to osmotic stress and uptake of osmolytes in this strain is independent of the *sigB* gene (Becker *et al.*, 1998, Moorhead & Dykes, 2003). Using a Δ*sigB* mutant, reverse transcription real-time quantitative PCR (RT-QPCR) and proteomic techniques it was found that in the presence of 0.5 M NaCl, a number of genes and proteins are expressed in a σ^B-dependent manner. Microarray experiments showed that σ^B regulates several transporters and transport systems in *L. monocytogenes* 10403S when logarithmic phase cells are exposed to 0.5 M KCl or 0.3 M NaCl (Kazmierczak *et al.*, 2003, Raengpradub *et al.*, 2008, Abram *et al.*, 2008b). Moreover, during cold-shock, σ^B contributes to adaptation in a growth phase

dependent-manner and is necessary for efficient accumulation of betaine and carnitine as cryoprotectants (Becker *et al.*, 2000).

A transcriptional profiling of the σ^B regulon was carried out under oxidative stress and several genes, including *lmo0669* and *lmo1433* (encoding an oxidoreductase and a glutathione reductase, respectively), are possibly involved in the oxidative stress regulation and several genes were identified as σ^B-dependent in these conditions (Kazmierczak *et al.*, 2003, Hain *et al.*, 2008, Raengpradub *et al.*, 2008). Studies carried out with stationary-phase *L. monocytogenes* 10403S (serotype 1/2a) and isogenic Δ*sigB* mutant demonstrated that σ^B is required for survival during exposure to 13 mM cumene hydroperoxide (CHP). It appears that the contribution of σ^B to protection of *L. monocytogenes* against oxidative stress is variable and strain-specific. Indeed, studies involving another strain of *L. monocytogenes*, L99, serotype 4c, showed that Δ*sigB* mutant was more resistant than the wild-type strain when exposed to CHP for 15 minutes. A different observation, however, was made with another listerial strain, L61, serotype 1/2a, according to which the Δ*sigB* mutant responded similarly to such stress conditions as the wild-type strain (Ferreira *et al.*, 2001, Moorhead & Dykes, 2003, Chaturongakul & Boor, 2004).

Whole-genome transcriptional profiling of *L. monocytogenes* enabled to identify σ^B-dependent genes upregulated during stationary phase. This suggested that σ^B plays a major role in survival under environmental stresses related to nutrient limitation (Hain *et al.*, 2008, Raengpradub *et al.*, 2008). There is also evidence that σ^B regulates carbohydrate metabolism. *lmo0398-lmo0400* and *lmo0784-lmo0781*, encoding fructose- and mannose-specific PTS systems, respectively, are σ^B-dependent operons involved in carbohydrate metabolism (Raengpradub *et al.*, 2008). σ^B was also found to be directly involved in the regulation of glycolysis and gluconeogenesis. A putative σ^B-dependent promoter, situated upstream of *lmo2460*, encodes a transcriptional regulator, CggR (central glycolytic genes regulator), which was involved in these metabolic processes (Raengpradub *et al.*, 2008). Studies carried out by Abram *et al.* (2008a) revealed that σ^B is involved in glycerol metabolism (Abram *et al.*, 2008a). The wild-type and the Δ*sigB* mutant strains of *L.*

monocytogenes 10403S were checked for the ability to utilize glycerol. It turned out that Δ*sigB* mutant grew slower in a chemically defined growth medium using glycerol as the only carbon source in comparison to the wild-type strain. Additionally, the mutant showed a much prolonged lag phase.

It has also been shown that σ^B contributes to energy-stress survival in *L. monocytogenes*. The evidence was obtained using the strain 10403S and its isogenic Δ*sigB* mutant grown in BHI supplemmented with CCCP (protonophore carbonyl cyanide 3-chloropenylhydrazone), which inhibits ATP synthesis. The Δ*sigB* strain survived less effectively in comparison to the parental strain when incubated at 37°C for 36 h (Chaturongakul & Boor, 2004). In addition, RT-QPCR analyses showed that *opuCA* transcription was activated only in the presence of σ^B after 5-minute exposure to CCCP (Chaturongakul & Boor, 2006). Studies involving other strains of *L. monocytogenes,* such as L61 of serotype 1/2a and L99 of serotype 4c, however, showed no effect of σ^B on the survival in stresses related to energy and carbon limitation, indicating that the role of this σ factor is strain dependent (Ferreira *et al.*, 2001, Moorhead & Dykes, 2003).

Other stresses against which a protective role of σ^B has been demonstrated includes resistance to detergents and surface-active agents, as observed with benzalkoniumchloride (BC), cetylpyridinium chloride (CPC) and sodium dodecyl sulphate (SDS) (Ryan *et al.*, 2008).

1.3.6.2 PrfA-σ^B crosstalk

Alternative sigma factors like σ^B are involved in complex regulatory networks, which allow the controlled genes to be expressed in a variety of changing environmental conditions and situations, like for example those involved in the different stages of *Listeria* pathogenesis and transmission cycle. For example, *L. monocytogenes* needs to survive nutrient-limiting conditions in the environment, the acidity of the stomache after ingestion, and oxidative damage in the host cell

phagosome, and this is likely to require the coordinated expression of specific virulence factors and stress resistance mediators (Kazmierczak *et al.*, 2005, Freitag *et al.*, 2009).

Such coordinated expression appears to exist in *L. monocytogenes* between the *prfA* gene, encoding the major gene regulator PrfA, and *sigB* (Nadon *et al.*, 2002, Chaturongakul *et al.*, 2008). Studies have shown that σ^B together with PrfA co-regulate important virulence genes, such as *inlA* and *inlB*, both involved in host cell invasion (figure 1.9), indicating that regulatory interactions between σ^B and PrfA are important for the transit from a non-host to host environment (Dussurget *et al.*, 2002, Kazmierczak *et al.*, 2003, Kim *et al.*, 2004, Sleator *et al.*, 2005, McGann *et al.*, 2007, McGann *et al.*, 2008). Studies carried out by Kim *et al.,* (2005) have shown that σ^B contributes to *L. monocytogenes* invasion mainly through direct control of *inlA* and *inlB* expression rather than indirectly via PrfA. It has also been demonstrated using RT-QPCR that σ^B contributes to *inlA* and *inlB* expression in mainly stationary-phase (Kim *et al.*, 2005). Evidence provided by Garner *et al.,* (2006) confirmed that σ^B contributes to *L. monocytogenes* invasion partially, by direct effects on *inlA* transcription rather than on *prfA* transcription. These authors showed the important role of σ^B during the gastrointestinal stage of listeriosis in guinea pigs, which have the InlA-susceptible isoform of the E-cadherin receptor (Lecuit *et al.*, 2001), but its dispensability for the later phases of invasive infection, *i.e.* systemic spread (Garner *et al.*, 2006). It is unclear whether the role of σ^B in the gastrointestinal tract reflects its role in *inlAB* operon regulation or that *L. monocytogenes* confronts a set of stress conditions that are not found in internal host tissues.

Additionally, *L. monocytogenes* σ^B may contribute to intestinal colonization by mediating resistance to bile through transcriptional regulation of *bilE,* encoding a bile-exclusion system, and the *bsh* gene, which encodes a bile-salt hydrolase (Dussurget *et al.*, 2002, Sleator *et al.*, 2005). It is unclear whether these genes, together with the *opuC* operon, all involved in gastrointestinal stages of *Listeria* infection, are also directly or indirectly regulated by PrfA. In the transcriptomic study of the PrfA regulon of Milohanic *et al.* (2003) these bile resistance genes were

classifed as group III genes, characterized by apparent PrfA regulation but lacking a *bona fide* PrfA-box and being expressed from a σ^B-dependent promoter (Milohanic *et al.*, 2003, Sleator *et al.*, 2005, Kazmierczak *et al.*, 2006). Corrupted PrfA boxes are present in front of *opuCD* and *bsh* (Milohanic *et al.*, 2003, Scortti *et al.*, 2007) but *in vitro* transcription studies and RT-QPCR analyses gave no evidence for direct PrfA-dependent activation of these genes (Rauch *et al.*, 2005, Ollinger *et al.*, 2008). Genes classified as group III genes by Milohanic *et al.* (2003) are in fact weakly or inconsistently regulated by PrfA (Scortti *et al.*, 2007), and the observed effects of PrfA on their regulation is most probably indirect.

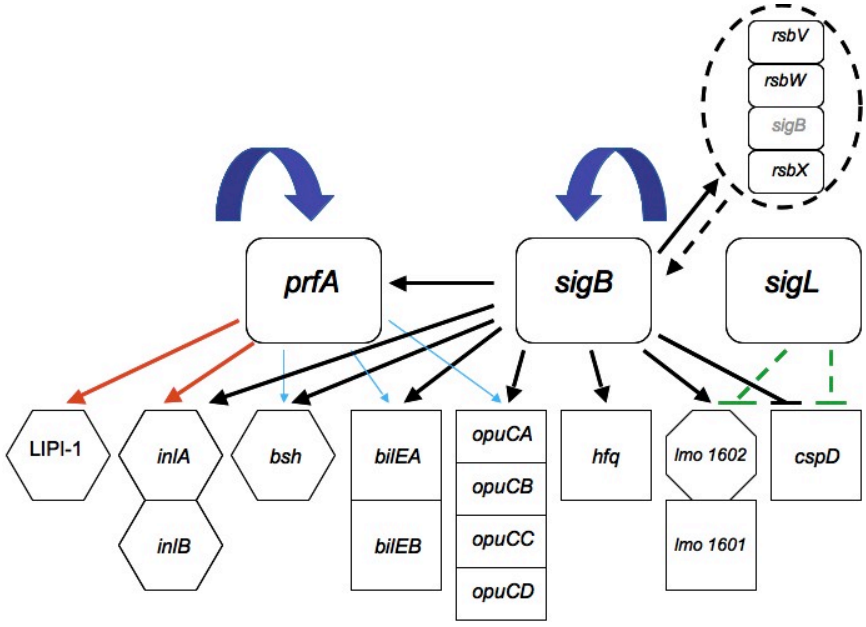

Figure 1.9: Hypothetical model of the regulation network of PrfA, σ^B and σ^L in *L. monocytogenes*. Adapted from Kazmierczak *et al.* (2005, 2006), Scortti *et al.* (2007) and Chaturongakul *et al.* (2008). Colour-coded arrows indicate genes regulated by PrfA (red and blue), σ^B (black) and σ^L (green). Direct regulation of a gene by a certain regulator (determined by the presence of either PrfA box or σ^B promoter or σ^L promoter) is indicated by thick, solid lines; indirect regulation is indicated by thick, broken lines. Thin, blue arrows indicate weak or inconsistent regulation of a gene by a given regulator. Positive regulation by a given regulator is indicated by a target arrow (↓), whereas negative regulation by a given regulator is represented by a target stop (⊥). Navy blue arrows forming loops indicate auto-regulation. Large rounded rectangles indicate transcriptional regulators, small rounded rectangles indicate genes that regulate a transcriptional regulator. Virulence genes (including *Listeria* pathogenicity island [LIPI-1] virulence genes such as *hly, plcA, plcB, mpl,* and *actA*) are indicated by hexagons. A gene encoding a protein of unknown function is represented by an octagon. Stress-response genes are indicated by squares and rectangles. Operons are indicated by genes arranged in vertical columns. The thick, black, broken-lined circle and arrow targeting σ^B indicate post-translational regulation of σ^B by Rsb proteins (encoded by *rsbV, rsbW* and *rsbX*, respectively), (see figure 1.8).

Studies have shown that genes regulated by σ^B are also expressed after the entry into various host cells (both: phagocytic and non-phagocytic). It is unclear whether this activation is solely due to σ^B or reflects some kind of interaction or co-regulation with PrfA (Sleator *et al.*, 2005, Chatterjee *et al.*, 2006, Joseph *et al.*, 2006, Raengpradub *et al.*, 2008). It has been proposed that σ^B regulates specifically the expression of genes important for *L. monocytogenes* adaptation to the intestinal environment, whereas PrfA and the virulence gene cluster contribute to survival and replication in the blood (Toledo-Arana *et al.*, 2009).

As mentioned above in section 1.3.5, σ^B directly contributes to the expression of PrfA in *Listeria*. This is achieved through direct regulation of the P2*prfA* promoter located upstream from *prfA* in the *plcA-prfA* intergenic region (figure 1.3). As P2*prfA* is also σ^A-dependent promoter, the transcription of the monocistronic *prfA* mRNA involves overlapping σ^A- and σ^B-dependent promoters (Freitag & Portnoy, 1994, Nadon *et al.*, 2002, Lemon *et al.*, 2010). In contrast to P1*prfA* transcript translation (activated at temperatures higher than 30°C), translation from P2*prfA* promoter transcripts is temperature independent. Therefore, σ^B-dependent *prfA* expression can occur outside the mammalian host (Johansson *et al.*, 2002, Chaturongakul *et al.*, 2008). The contribution of this σ^B-dependent *prfA* gene activation pathway to virulence is, however, unclear since a deletion mutant in P2*prfA* promoter was similarly virulent to the wild-type after intragastric inoculation (Garner *et al.*, 2006). Additionally, cell-to-cell spread of these mutants was not affected in several mammalian cell lines (Freitag & Portnoy, 1994, Chaturongakul *et al.*, 2008). It has been suggested that the presence of σ^B is required to allow the transcription of *prfA*, only in undetermined, specific stages of infection. It appears that P2*prfA* directed expression of the *prfA* gene is growth phase-dependent and particularly relevant in stationary phase (Schwab *et al.*, 2005, Abram *et al.*, 2008a).

σ^B is known to influence the expression of a major virulence gene regulator not only in *L. monocytogenes* but also in other bacteria. For example, σ^B regulates at the transcriptional level the *S. aureus sar* gene, which in turn controls the expression

of the global regulatory gene, *agr*. The synthesis of wide range of virulence-related extracellular and cell-surface proteins is controlled by these two genes and, therefore, they are regarded as prime regulatory factors in *S. aureus* pathogenesis (Arvidson & Tegmark, 2001, Bischoff *et al.*, 2001, Bischoff *et al.*, 2004).

It has been also found that σ^B together with another alternative sigma factor, σ^L, co-regulates the expression of some genes, such as a general-stress protein, *lmo1601,* and a cold-shock protein, *cspD*, required for overcoming metabolic and physiological stresses in *L. monocytogenes* (Arous *et al.*, 2004, Raengpradub *et al.*, 2008). σ^L, also called σ^N or RpoN, is encoded by the *sigL* gene of *L. monocytogenes* and belongs to the σ^{54} family of sigma factors (Robichon *et al.*, 1997, Kazmierczak *et al.*, 2005, Chaturongakul *et al.*, 2008). Studies have shown that different growth phases and temperatures influence the expression of *sigL* (Liu *et al.*, 2002, Chan *et al.*, 2007a). Among the 77 σ^L-dependent genes described in *L. monocytogenes*, several are involved in the amino acid and carbohydrate metabolisms. Twenty-four of these genes showed differential expression depending on the environmental conditions, particularly during *in vitro* growth in BHI vs intracellular conditions. In macrophages, for example, an oligopeptide transporter gene and *clpP* (stress-related serine protease) were activated, whereas, genes involving cell division or encoding thioredoxin and pyruvate dehydrogenase were repressed. Other findings indicated that SigL facilitates survival to osmotic stress (Chatterjee *et al.*, 2006, Okada *et al.*, 2006), and confirms resistance to mesentericin Y105, a bacteriocin bactericidal agent against *L. monocytogenes* (Robichon *et al.*, 1997). Additionally, it has been shown that both σ^B and σ^L contribute to the *L. monocytogenes* response to antimicrobial peptides such as nisin, produced by the lactic acid bacterium *Lactococcus lactis,* and SdpC (sporulation delaying protein C), produced by some strains of *B. subtilis* (Gonzalez-Pastor *et al.*, 2003, Butcher & Helmann, 2006, Palmer *et al.*, 2009).

Regulation of stress response and virulence genes can be also obtained through controlling directly or indirectly the transcription of small RNAs (sRNAs) by alternative σ factors (Chaturongakul *et al.*, 2008). In the latter case, σ factors regulate the expression of RNA-binding proteins and chaperones such as Hfq. It has

been shown that in stress conditions caused by the presence of salt or ethanol, Hfq is involved in the stress response and it is σ^B controlled in *L. monocytogenes*. This muliple stress resistance protein also plays a role in virulence in mice, however, in tissue culture models it has not been found to contribute to virulence. Regulation of sRNAs and Hfq is an example of post-transcriptional control by alternative σ factors (Christiansen *et al.*, 2004, Chaturongakul *et al.*, 2008).

1.3.7 LISTERIAL PATHOGENIC TROPISM AND ITS MOLECULAR DETERMINANTS

Up to date, not much is known about the molecular basis of *Listeria* pathogenic tropism, despite evidence that strains / species of these pathogens differ in infectivity, host range and clinical presentation. Indeed, there is proof for differences in pathogenic potential of *L. monocytogenes* strains depending on the phylogenetic lineage of the bacteria. *L. monocytogenes* has three genetic lineages: lineage I contains serovars 1/2b, 3b, 4b, 4d and 4e; lineage II includes serovars 1/2a, 1/2c, 3a and 3c; and lineage III consists of serovars 4a and 4c. The lineage status of serovar 7 remains unclear (Piffaretti *et al.*, 1989, Wiedmann *et al.*, 1997, Doumith *et al.*, 2004, Liu, 2006a, Liu *et al.*, 2006b). It has been observed that most of the human listeriosis cases are caused by just three serotypes (*i.e*. 1/2a, 1/2b and 4b). Data from the literature show, however, that serovar 4b *Listeria* are responsible for the majority of food-borne listeriosis outbreaks, whereas *L. monocytogenes* serovar 1/2a and 1/2b appear to be associated with sporadic cases (McLauchlin, 1987, Farber & Peterkin, 1991, Buncic *et al.*, 2001, Jeffers *et al.*, 2001, Gray *et al.*, 2004). It has been also shown that the majority of *L. monocytogenes* food isolates belong to serogroup 1, which include serovar 1/2a (Rocourt, 1989, Gilot *et al.*, 1996, Ojeniyi *et al.*, 1996, Autio *et al.*, 1999). Despite that *Listeria* serotypes 4a and 4c (lineage III) are frequently isolated from animal, food or environmental sources, they are found to be rarely responsible for human infections (Wiedmann *et al.*, 1997, Liu, 2006a).

To date, the only well-characterized molecular mechanism involved in listerial pathogenic tropism is the internalization process mediated by InlA and InlB. Both proteins appear to differ in target cell specificities (Vazquez-Boland *et al.*, 2001a): whereas InlB was found to mediate entry into a wide range of cell types, InlA has been reported to specifically facilitate invasion of epithelial cells bearing a specific isotype (human) of the E-cadherin receptor. This "InlA-susceptible" isotype is present in guinea pig but not in mice, explaining why the murine model is not satisfactory to reproduce the epithelial (intestinal) phase of infection, in contrast to the guinea pig model (Dramsi *et al.*, 1995, Drevets *et al.*, 1995, Parida *et al.*, 1998, Lecuit *et al.*, 1999).

In *Listeria*, the most striking difference in pathogenicity is observed between *L. monocytogenes* and *L. ivanovii* (see above section 1.3.3). Thanks to its differential pathogenic properties, *L. ivanovii* offers a unique comparative model to study the molecular mechanisms involved in bacterial host and tissue tropism. In a search for species-specific factors that could explain the differences in pathogenicity between these two bacteria, our group identified "*Listeria* pathogenicity island 2" (LIPI-2) (Dominguez-Bernal *et al.*, 2006) (figure 1.10). LIPI-2 is a large (22 kb) chromosomal locus specifically present in *L. ivanovii* within the genus *Listeria*. LIPI-2 is the largest of the known internalin islands. Most of the *inl* genes in this island are PrfA-dependent and encode small-secreted internalins (Dominguez-Bernal *et al.*, 2006). As internalin proteins have been shown to be involved in host cell tropism (Hamon *et al.*, 2006), it is likely that this new large internalin island plays a role in the specific pathogenic properties of *L. ivanovii* and, possibly, its marked specificity for ruminants.

LIPI-2 also contains the *smcL* gene encoding the *L. ivanovii*-specific SMase. In contrast to the surrounding *inl* genes, *smcL* is expressed independently of PrfA and is transcribed in the opposite orientation (Gonzalez-Zorn *et al.*, 1999) (figure 1.10). The *smcL* product, SmcL, is responsible for the distinctive phenotype of *L. ivanovii* on sheep blood agar, characterized by a strong bizonal haemolysis and a typical synergistic haemolytic effect in the presence of *Rhodococcus equi* cholesterol

oxidase (the so called "CAMP-like" reaction) (figure 1.11). Our group also determined that SmcL is a phagosome-disrupting factor, the loss of which attenuates *L. ivanovii* virulence in the mouse and impairs intracellular proliferation in Madin-Darby Bovine Kidney (MDBK) cells. Interestingly, SmcL is only lytic on sheep erythrocyte membranes, which are rich in sphingomyelin (51% of total phospholipids), but not in horse erythrocytes, which are poor in sphingomyelin (13.5% of total phospholipids), suggesting that this enzyme may play a role in host tropism (Vazquez-Boland *et al.*, 2001a).

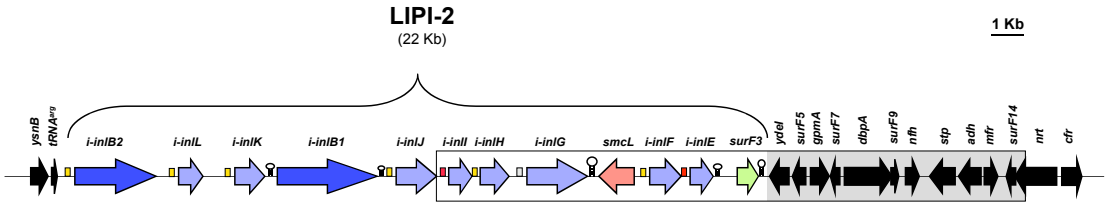

Figure 1.10: Genetic organization of LIPI-2 and the right flanking chromosomal region.
LIPI-2 genes such as the *smcL* and *inl* genes are in pink and blue, respectively. Black-coloured genes belong to the housekeeping core genome. Small rectangles in front of the genes indicate PrfA-boxes: in red these with no or one mismatch respect to the perfect consensus palindrome, in yellow these with two mismatches and in grey these with three mismatches. Hairpins represent transcription terminators. LIPI-2 is inserted into a tRNA gene and, yet perfectly conserved in all *L. ivanovii* isolates, is genetically unstable *in vitro*, a large section of it undergoing site-specific spontaneous deletion together with a portion of the flanking core listerial genome at approximately 10^{-4} frequency. The spontaneously deletable fragment is boxed. Taken from Dominguez-Bernal *et al.* (2006).

SmcL is not only similar to the bacterial SMases C from *S. aureus* (ß-toxin), *B. cereus* or *Leptospira interrogans* (Gonzalez-Zorn *et al.*, 1999, Gonzalez-Zorn *et al.*, 2000) but also exhibits extensive sequence similarity with the mammalian neutral SMases (Openshaw *et al.*, 2005). These endogenous membrane-associated SMases are thought to play a critical role in the sphingomyelin-ceramide signalling pathway. Ceramide is primarily generated in mammalian cells by the degradation of sphingomyelin by SMases and this lipid metabolite is believed to be a key second messenger in important eukaryotic cell processes, such as cell proliferation, differentiation and survival, and cell cycle arrest (Kolesnick & Kronke, 1998, Goni & Alonso, 2002, Clarke & Hannun, 2006). Therefore, in addition to its "mechanical"

function in a phagosome disruption, SmcL may also play a subtler role in pathogenesis by directly interfering with the SM-ceramide host cell-signalling pathway. Studies carried out by Zhang *et al*. (2008), have shown that Sph2, a sphingomyelinase haemolysin from *L. interrogans* strain Lai, possibly induces apoptosis in human liver L-02 cells (Zhang *et al.*, 2008).

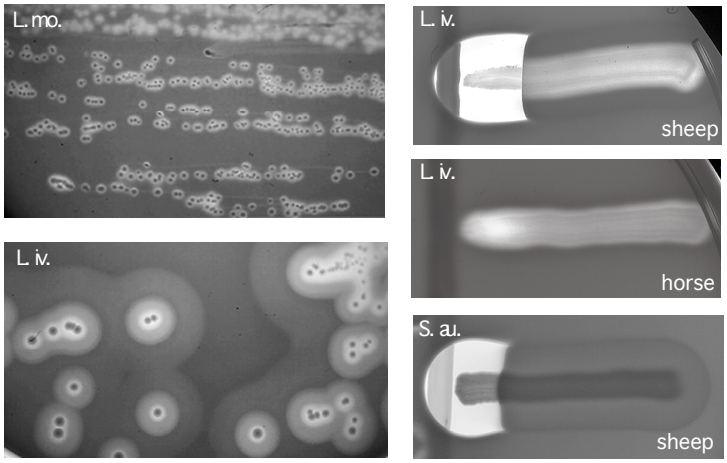

Figure 1.11: *Listeria* haemolytic activity and CAMP-like reaction.
Left panels indicate haemolytic activities of *L. monocytogenes* (L. mo.) and *L. ivanovii* (L. iv.) on sheep blood agar. Note the strong multizonal lytic activity of *L. ivanovii* due to the production of the SMase, SmcL. Right panels show synergistic (CAMP-like) haemolysis of *L. ivanovii* and *S. aureus* (S. au.) producing ß-toxin (SMase) with vertically streaked *R. equi*; identical shovel-shaped patches of synergistic haemolysis were obtained for *L. ivanovii* and *S. aureus,* showing that sphingomyelinases C of these two bacteria are functionally related. The SMase completely lyses the erythrocytes exposed to *R. equi* cholesterol oxidase resulting in a shovel-shaped lytic phenomenon, bizonal haemolysis (Ripio *et al.*, 1995, Gonzalez-Zorn *et al.*, 1999). As shown in the two upper right panels, the *L. ivanovii* SMase is active on sheep erythrocytes but not on horse erythrocytes. Bacteria were cultured at 37°C for 24 h (taken from Vazquez-Boland *et al*., [2001a]).

According to preliminary experiments carried out in collaboration with Prof. T. Levade, University of Toulouse, *L. ivanovii* induces a potent ceramide response during intracellular infection in MDBK cells. SmcL appears to contribute to this response as ceramide generation was much less intense in cells infected with an isogenic *smcL* mutant (unpublished data from our laboratory). A wealth of circumstantial evidence suggests that ceramide is a major regulator/mediator of the apoptotic response triggered by some cytokines, such as TNF-α and Fas ligand, or a variety of stresses including irradiation, heat shock and toxic drugs (Hannun &

Luberto, 2000, Andrieu-Abadie & Levade, 2002, Hannun & Obeid, 2002, Levade *et al.*, 2002, Luberto *et al.*, 2002, Pettus *et al.*, 2002, Cossart *et al.*, 2003, Gulbins, 2003, Lin *et al.*, 2006). Consistent with a possible role of SmcL in ceramide generation and apoptosis, data from our laboratory indicate that *L. ivanovii* causes apoptosis in MDBK cells suggesting that SmcL may contribute to this apoptotic response as an *smcL* mutant showed a reduced apoptogenic activity compared to wild-type bacteria (Domínguez-Bernal *et al.*, 2006 and other unpublished observations).

Apoptosis induction by pathogens has been shown to contribute to limiting the spread of infection because of enhancing antigen presentation and the immune response (Gao & Abu Kwaik, 2000). Invasion of the central nervous system by *L. monocytogenes* requires a prolonged exposure of the blood-brain barrier to bacteria that are continually released into the bloodstream from active infectious foci in the primary target organs (reviewed in Vazquez-Boland *et al.*, [2001a]). It is, therefore, tempting to speculate that the apoptogenic activity of *L. ivanovii* may account for the inability of this species to cause meningoencephalitis.

1.4 APOPTOSIS IN BACTERIAL INFECTIONS

Apoptosis, or programmed cell death, is an essential and tightly regulated process important for development and tissue homeostasis. Apoptosis is a Greek word meaning “falling off “, which was first introduced in 1972 by Kerr, Wyllie and Currie (Kerr *et al.*, 1972) to designate a mammalian cell death process accompanied by various morphological and biochemical changes, including chromatin aggregation, nuclear and cytoplasmic condensation resulting in cell shrinkage, membrane blebbing, DNA fragmentation and the emergence of “apoptotic” bodies, which contain ribosomes, morphologically intact mitochondria and nuclear material (Wyllie *et al.*, 1981, Pallardy *et al.*, 1997, Raffray & Cohen, 1997, Maria *et al.*, 2000,

Lecoeur, 2002, Weiss & Zychlinsky, 2002, Vallender & Lahn, 2006). In contrast to necrosis (also known as "accidental" cell death, which is due to exposure to a serious physical or chemical damage), apoptosis is an active process with well-organized, regulated biochemical events, involving cell signalling and ordered enzyme cascades (Bortner *et al.*, 1995, Raffray & Cohen, 1997, Gulbins *et al.*, 2000, Castedo *et al.*, 2002, Chowdhury *et al.*, 2006).

Eukaryotic cells can undergo apoptosis dependently or independently of caspases, which are a group of cellular proteases. The caspase-dependent pathway can be either mediated by mitochondria or by surface receptors and is, then, called the intrinsic or extrinsic pathway, respectively. Both, the intrinsic and extrinsic pathways, involve a cascade of caspases ultimately leading to activation of caspase-3 or -6, which directly results in apoptotic cell death. The extrinsic pathway begins with the activation of caspase-8 by receptors. The intrinsic pathway is more likely to involve activation of caspase-9 by cytochrome c (cyt-c) through Apaf-1 (apoptotic protease activating factor 1). The caspase-independent pathway involves the activation of calpains, which are Ca^{2+}-dependent cysteine proteases (figure 1.12) (Li *et al.*, 1997, Scorrano & Korsmeyer, 2003, Chowdhury *et al.*, 2006, Fettucciari *et al.*, 2006).

Substrates involved in apoptotic cell death may interact with each other resulting in a variety of pathways. For example, calpains and caspases may both activate other caspases or proteins such as Bax and Bid. These pro-apoptotic Bcl-2 family members may contribute to the release of proteins from mitochondria. As a consequence, other factors, either caspase-dependent such as cyt-c, second mitochondria derived activator of caspase (Smac/Diablo), or caspase-independent, such as apoptosis inducing factor (AIF) or endonuclease G (EndoG), may be activated leading to apoptotic cell death (Kohler *et al.*, 2002, Scorrano & Korsmeyer, 2003, Fettucciari *et al.*, 2006).

Many pathogens modulate the death pathways of host cells in order to manipulate host defences to their benefit. Bacteria induce apoptosis either through:

(i) activation of pro-apoptotic factors such as caspases, Bim, Bax, Bad, Bid and Bak; (ii) inhibition of anti-apoptotic factors such as NF-κB (Nuclear Factor κB), MAP-kinases (Mitogen Activated Protein kinases), IAPs (Inhibitors of Apoptosis Proteins) or Bcl-2 and Bcl-x_L; (iii) interference with upstream endogenous receptor-ligand systems exposed to the cell surface. Bacteria often use host cell apoptosis to gain easier access to target organs (Chen & Zychlinsky, 1994, Behnia *et al.*, 2000, Dockrell, 2001, Hasnain *et al.*, 2003, Scorrano & Korsmeyer, 2003). The ability of bacteria to modulate phagocyte apoptosis has shown to be an important mechanism of pathogenesis. 56 bacterial strains have been found to modulate cell death in phagocytic leukocytes (*e.g*. macrophages, neutrophils, dendritic cells, monocytes) (DeLeo, 2004). Inducing apoptosis in macrophages is especially important for bacteria as these cells play a pivotal role in phagocytosis and antigen presentation. Induction of apoptosis in epithelial or endothelial cells may also allow bacteria to optimize their colonization capacity and invade deeper tissues (Grassme *et al.*, 2001).

However, as apoptotic cells are rapidly removed by phagocytic/antigen–presenting cells, apoptosis of infected cells may also favour the development of a specific immune response without inducing inflammation and tissue destruction. Therefore, in some instances, rather than promoting colonization, apoptosis may have opposite effects, limiting the virulence and the spread of the pathogen (which paradoxically may in turn maximize the pathogen's within-host survival and transmission). This has been suggested to occur with the intracellular pathogens *Mycobacterium tuberculosis* and *Coxiella burnetii* (Weinrauch & Zychlinsky, 1999, Gao & Abu Kwaik, 2000, Danelishvili *et al.*, 2003, Dao *et al.*, 2004, Winau *et al.*, 2004).

Infection of macrophages by *M. tuberculosis* causes down-regulation of expression of the anti-apoptotic protein Bcl-2 and production of TNF-α, promoting apoptosis in a caspase-1 dependent manner; this proapoptotic effect is modulated by the secretion of soluble tumour necrosis factor receptor 2 (sTNFR2), which neutralizes the pro-apoptotic activity of TNF-α. It has been also reported that presence of high numbers of intracellular *M. tuberculosis* bacilli triggers a

macrophage caspase-independent apoptotic pathway (Gao & Abu Kwaik, 2000, Lee *et al.*, 2006).

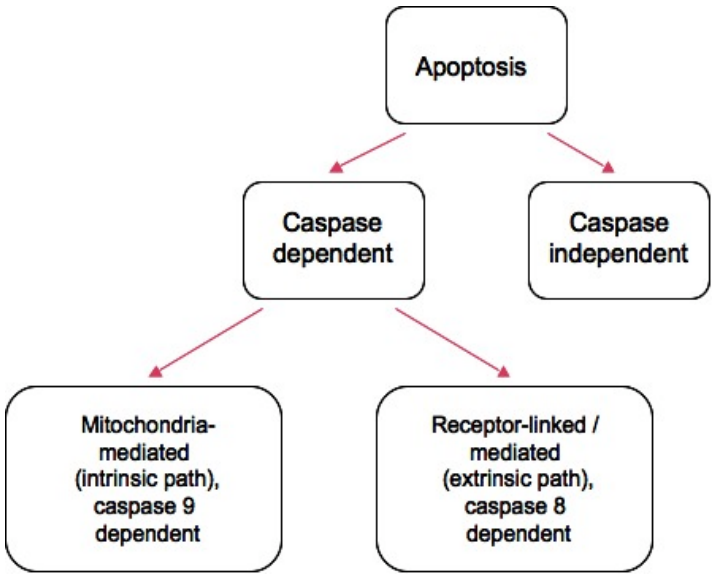

Figure 1.12: A schematic representation of the types of apoptosis.
Based on morphological and biochemical studies (adapted from Chowdhury *et al.* [2006]).

There is strong evidence that Group B Streptococci (GBS), such as *Streptococcus agalactiae,* trigger apoptosis in macrophages and monocytes (Fettucciari *et al.*, 2000, Ulett *et al.*, 2003). GBS have been reported to induce macrophage apoptosis by calpain activation involving either caspase-dependent or -independent pathways (Fettucciari *et al.*, 2006).

Pneumolysin, a pore-forming exotoxin of *Streptococcus pneumoniae*, has been found to have a direct proapoptotic activity on macrophages and neuronal cells (Braun *et al.*, 2002, Bifrare *et al.*, 2003, Marriott *et al.*, 2004). H_2O_2 is another exotoxin produced by this bacterium contributing to stimulation of apoptosis (Braun *et al.*, 2002). Apart from macrophages and neurons, *S. pneumoniae* has been shown to cause the programmed cell death in many other cell types including dendritic cells, neutrophils and human alveolar and bronchial epithelial cells (Ulett & Adderson, 2006). Interestingly, in these epithelial cells, Pneumococcus-induced apoptosis was

independent of pneumolysin and H_2O_2. The programmed cell death occurred through caspase-6 and non-caspase proteases but independently of caspase-3, which seemed to be unique in bacterial infections (Schmeck *et al.*, 2004).

Streptococcus pyogenes produces exotoxin B, which has been found to induce apoptosis in epithelial cells and macrophages (Kuo *et al.*, 1999, Tsai *et al.*, 1999). It has been demonstrated that this virulence factor activates eukaryotic matrix metalloproteinases, which contribute to the release of TNF-α and FASL, resulting in the induction of the programmed cell death process (Tamura *et al.*, 2004). Other studies have shown that infection with *S. pyogenes* of epithelial cells triggers the intrinsic pathway of apoptosis through activation of caspase-9 (Nakagawa *et al.*, 2004). *Helicobacter pylori* induces apoptosis in macrophages through a caspase-dependent mitochondrial pathway (Menaker *et al.*, 2004). Upon host cell invasion, *Legionella pneumophila* activates caspase-3 in macrophages, monocytes and alveolar epithelial cells (Gao & Abu Kwaik, 2000, Dockrell, 2001, Abu-Zant *et al.*, 2005). *Salmonella, Shigella* and *Yersinia* spp. inject directly into host macrophages type III secretion system effector proteins (SipB, IpaB and YopP/J, respectively) that cause apoptosis; *Salmonella* and *Shigella* induce caspase-1, whereas *Yersinia* inhibits survival pathways mediated by nuclear factor κB (NF-κB) and mitogen-activated protein kinase (MAPK) and, in parallel, appears to induce unknown caspases (Zychlinsky *et al.*, 1992, Ruckdeschel *et al.*, 1997, Navarre & Zychlinsky, 2000, Dockrell, 2001, Grassme *et al.*, 2001, Hueffer & Galan, 2004, Zhang *et al.*, 2005, Ogawa & Sasakawa, 2006).

Staphylococcus aureus has been found to induce apoptosis in various eukaryotic cells such as neutrophils, monocytes, chondrocytes, keratinocytes, endothelial cells, epithelial cells and osteoblasts (DeLeo, 2004, Ulett & Adderson, 2006). *S. aureus* produces several exotoxigenic virulence factors, two of which are the superantigen enterotoxin B and the haemolysin: α-toxin; both involved in the induction of apoptosis. Enterotoxin B-induced apoptosis is carried out through the extrinsic pathway involving TCR (T-cell receptor) engagement and FASL-CD95 signal transduction (Ulett & Adderson, 2006). On the contrary, α-toxin induces the

programmed cell death through caspase activation via the intrinsic pathway, which involves the release of mitochondrial cyt-c and the regulation of BCL-2 (Bantel *et al.*, 2001, Esen *et al.*, 2001, Haslinger *et al.*, 2003). Additionally, α-toxin has been also found to contribute to pore formation resulting in apoptosis in endothelial cells (Menzies & Kourteva, 2000). Furthermore, it has been shown that strongly haemolytic and invasive *S. aureus*, but not non-invasive staphylococcal strains, induce caspase-dependent, Fas-independent apoptosis in endothelial cells (*e.g.* HUVEC [human umbilical vein endothelial cells] or HBMEC [human brain microvascular endothelial cells]); heterologous expression of α-toxin in a non-haemolytic strain partially restored apoptosis induction, suggesting a role of this pore-forming haemolysin as an apoptosis trigger factor (Haslinger-Loffler *et al.*, 2005).

The opportunistic pathogen *Pseudomonas aeruginosa* activates the endogenous Fas (CD95)/FasL (CD95 ligand) system, inducing caspases and mitochondrial changes. *P. aeruginosa* infection also triggers activation of the acid sphingomyelinase and the release of ceramide in sphingolipid-rich rafts in epithelial cells, leading to raft reorganization into larger membrane platforms which are required for bacterial internalization, apoptosis in infected cells and regulation of cytokine responses (Grassme *et al.*, 2001, Grassme *et al.*, 2003).

Clostridium difficile encodes virulence factors such as exotoxins A and B, which have been shown to cause apoptosis in several epithelial and endothelial cell types (reviewed in Ulett and Adderson, 2006). A common mechanism by which *Clostridia spp*. trigger apoptosis in host cells has emerged. Studies have shown that exotoxins produced by these bacteria contribute to the intrinsic pathway of inducing programmed cell death, which involves mitochondrial dysfunction and inactivation of Rho protein function (Fiorentini *et al.*, 2003).

Pro-apoptotic activity has been demonstrated for a lethal toxin of *Bacillius anthracis* in murine macrophages. Studies have shown that the induction of apoptosis in these cell lines involved FASL binding and activation of caspases -1, -3, -4, and -8

(Popov *et al.*, 2002a, Popov *et al.*, 2002b). Additionally, it has been shown that in order to trigger macrophage apoptosis by the lethal toxin, the presence of the protein kinase PKR is essential after activation of Toll-like receptor 4 (Hsu *et al.*, 2004).

Interestingly, it has been found that *L. monocytogenes* has the ability to either induce or inhibit apoptosis in the host cell, depending on the type of the cell infected. However, the information is limited and sometimes contradictory. *L. monocytogenes* develops several strategies to evade or modulate host immune responses in order to obtain a more favourable environment, ensuring its survival and pathogenesis. One of them is the ability to induce apoptosis in immune effector cells (Corr & O'Neill, 2009). The potential benefit of this effect on immune cells is that the inflammatory response is limited. Thus, experiments demonstrated that the presence of apoptotic lymphocytes suppressed early innate immunity, allowing *Listeria* bacteria to grow in the host environment (Carrero *et al.*, 2006, Carrero & Unanue, 2006). Lymphocyte apoptosis caused by *L. monocytogenes* is apparently mediated by LLO, which is released during the early growth phase of this bacterium (Carrero *et al.*, 2004a, 2004b, Carrero *et al.*, 2009). LLO-induced apoptosis can occur through two pathways: a fast one, which is caspase-dependent and a slow one, which is caspase-independent (Carrero *et al.*, 2008, Cervantes *et al.*, 2008). LLO-induced programmed cell death in T lymphocytes has been found to be associated with the activation of caspase-9 and -3 and loss of mitochondrial membrane potential, pointing to the intrinsic apoptotic pathway (Carrero *et al.*, 2004a). Granzymes appear to be also involved in the rapid apoptosis induced by LLO on T-cells. The lack of granzymes results in a dramatic reduction in all apoptotic parameters, such as caspase activation, phosphatidylserine exposure, mitochondrial depolarization and DNA fragmentation (Carrero *et al.*, 2008).

Host cell apoptosis induction by *Listeria* has been reported to also occur in murine-splenic dendritic cells (Guzman *et al.*, 1996) and lymphocytes (Mannering *et al.*, 2002, Carrero *et al.*, 2004a), as well as in human neutrophils (Kobayashi *et al.*, 2003). This may result in lower levels of antigen presentation and downregulation of the immune response, thereby favouring the spread of the pathogen.

There are also reports showing that *L. monocytogenes* causes apoptosis in murine hepatocytes (Rogers *et al.*, 1996) and Caco-2 human colonic cells (Valenti *et al.*, 1999) but these observations have not been independently confirmed. In this case apoptosis would have an opposite effect, inhibiting the spread of *L. monocytogenes* to neighbouring cells and making the pathogen accessible to effector cells. It has been also shown that *Listeria* induces apoptosis in murine neuroblastoma Neuro-2a cells (Parra *et al.*, 2008) and this effect may contribute to listerial neuropathogenesis during invasion of the central nervous system (CNS).

Other studies, in contrast, show that *L. monocytogenes* inhibits apoptosis. This has been observed in infected murine bone marrow macrophages (Barsig & Kaufmann, 1997). In the human promyelocytic cell line THP1 this appears to be mediated through induction of host cell apoptosis-inhibiting products, including members of the Bcl-2-family. These anti-apoptotic proteins may promote host cell survival despite the infection, therefore, preserving the integrity of the intracellular replication niche and allowing bacteria to proliferate and spread to neighbouring cells. Due to this mechanism *L. monocytogenes* would remain inaccessible to effector cells such as neutrophils, which eliminate infected and apoptotic cells *in vivo* (Cohen *et al.*, 2000, Carrero *et al.*, 2004a).

2 JUSTIFICATION AND AIMS

Pathogenic microorganisms are becoming increasingly resistant to current antimicrobial agents, posing a serious risk to public health that is continually increasing. In the last decade, multiresistant clones have emerged and are spreading, particularly in hospital wards, and people are already dying from non-tractable infections. New infectious diseases and pathogenic variants are also continually emerging, and old pathogens, such as *M. tuberculosis* are re-emerging, significantly contributing to the infectious morbidity and mortality worldwide. The development of new antibiotics, antimicrobial drugs and vaccines has become, therefore, a priority. The pharmaceutical industry has traditionally relied on empirical drug discovery and vaccine development, but the new threats require innovative approaches. Knowing in its intimate details the biology of pathogens and the mechanism of host-pathogen interactions, as well as an advanced understanding of molecular and cellular immunology, provides a rational framework to guide translational research for novel, better tools to combat infection. A paradigmatic example is provided by recent advances in vaccine and biological drug delivery vector development based on the exploitation of fundamental knowledge in intracellular pathogen biology.

Perhaps one of the most investigated and best-understood intracellular pathogens is *L. monocytogenes*. Its unique intracellular infection cycle, the sophisticated strategies that it deploys to subvert host cellular functions and signalling pathways to survive and proliferate within host cells, and its immunobiological characteristics, have established this pathogen as a classical research model in microbial pathogenesis and cell biology.

Despite the very significant advances in our understanding of the infection mechanisms of pathogenic *Listeria*, many aspects still remain obscure. Clearly, the pathogen-host cell interface remains an unexplored field of active interest at the forefront of contemporary research in microbial pathogenesis. There are also areas in *Listeria* research that, although extensively investigated, require further and continued work in order to be fully understood. One of these is the regulation of

virulence and the major role played by the transcription factor PrfA in the control of key steps of listerial intracellular parasitism.

Although the importance of PrfA in *L. monocytogenes* virulence has been long established, the mechanisms governing its regulatory activity, in particular those leading to the activation of the virulence regulon within host cells, remain poorly characterized or unknown. This subject has been a main focus of attention for our group in the last years. The currently accepted model for PrfA regulation is based on key findings from our laboratory. Central to this model is the ability of PrfA to undergo allosteric activation, presumably produced by the binding of a hypothetical small molecule or cofactor.

Besides being intrinsically important from a fundamental point of view, the investigations on the regulatory mechanism of PrfA have a clear translational interest. Since PrfA function is essential for pathogenicity, gaining a detailed molecular and structural understanding of the mechanisms underlying PrfA allostery may lead to the development of specific inhibitors of potential therapeutic use.

This thesis is a continuation of the work on *Listeria* pathogenesis being carried out by our laboratory, with a particular focus on PrfA.

Our primary goal was to gain a better understanding of the allosteric nature of the listerial regulator. We undertook a detailed structure-function analysis by site-directed mutagenesis of the N-terminal domain of the protein. Our aim was to test experimentally the prediction that this domain accommodates the signalling module where the hypothetical allosteric effector binds, triggering the critical conformational changes that lead to the intracellular activation of PrfA.

This work was complemented by structure-function studies on several spontaneous loss-of-function mutations in the PrfA protein that were identified in the laboratory.

Another important aim was to optimize the techniques used in the laboratory for the precise quantification of PrfA-dependent gene expression. The availability of such methods was capital for our work on PrfA and *Listeria* virulence gene regulation.

As secondary aims within the general theme of virulence gene regulation, we developed experiments to address existing gaps in specific aspects under investigation in the laboratory. One is the "charcoal effect", *i.e.* the activation of PrfA-dependent genes observed when the growth medium is supplemented with the adsorbent, activated charcoal. This effect was hypothesized to be caused by the sequestration by charcoal of a soluble virulence gene autorepressor released during exponential growth by *L. monocytogenes*. In this thesis, we moved to a more reductionist, better-defined experimental setup that would facilitate the isolation and characterization of the repressor molecule(s). We replaced the complex medium in which the previous data were obtained (Brain Heart Infusion) by a chemically-defined medium, and the natural compound, activated charcoal, by a synthetic resin with similar adsorptive characteristics, Amberlite^{TM} XAD-4. We, then, developed experiments aimed at validating the previous findings and the hypothesis of the *Listeria*-derived diffusible autorepressor.

The other experiments described in this thesis pertaining to virulence gene regulation were aimed at further exploring the role of PrfA in host cell invasion and the possible involvement of and/or crosstalk with the stress-related alternative sigma factor σ^B. Whilst previous findings from our laboratory indicated that *L. monocytogenes* invasiveness is strictly dependent on PrfA, other groups consider that σ^B plays a key role, particularly during entry through the intestine. Therefore, it was important to precisely determine the relative contributions of these two transcription factors in host cell invasion, the first step of *Listeria* intracellular pathogenesis.

In a final chapter of the thesis, our focus shifts to the cellular responses triggered by *Listeria* during intracellular infection. Our interest is centred on the apoptotic response, about which there are conflicting data in the literature. Upon

examination of the apoptosis bibliography we came to the conclusion that much of the discrepancies among studies may be due to technical issues, particularly related to the way the occurrence of apoptosis in infected cell monolayers is quantified.

As a first step in our investigations on apoptosis and *Listeria* infection, in this thesis we aimed at setting up all the assays for determining this response in *Listeria*-infected cells, and to establish the optimal experimental conditions for these determinations. It was also important to ascertain the factors that may influence the occurrence of apoptosis in *Listeria*-infected cells, and establish a mathematical model with a simple equation to precisely quantify the apoptogenic capacity of different strains and mutants.

3 RESULTS AND DISCUSSION

3.1 REGULATION OF VIRULENCE

3.1.1 PRFA REGULATION

3.1.1.1 Optimization of RT-QPCR analysis of PrfA-dependent gene expression

Throughout this study, we used the RT-QPCR technique to quantify gene expression levels. Thanks to its exquisite sensitivity, accuracy and precision this technique has become the method of choice for the analysis of the regulation of the gene expression in both eukaryotic and prokaryotic systems (Bustin, 2000, Bustin & Nolan, 2004). In contrast to conventional PCR, RT-QPCR permits to exactly quantitate the number of copies of certain target DNA sequence in a sample (Gibson *et al.*, 1996, Heid *et al.*, 1996). The quantitative determination of transcriptional levels of specific genes is obtained by measuring the mRNA levels. Since RNA cannot serve as a template for PCR, in order to quantitatively determine the amount of specific mRNA, the initial step of RT-QPCR involves the reverse transcription of the RNA template into cDNA, which is, then, exponentially amplified in a PCR reaction. Quantitation is achieved through the detection of the fluorescence emitted by a reporter dye each time a new amplicon molecule is generated during PCR. In this way, the number of PCR cycles needed for a target amplicon to obtain a pre-established threshold of fluorescence is determined. This is the so-called Ct value, *i.e.* the number of PCR cycles needed to obtain this threshold, which is inversely proportional to the initial copy number of the target DNA sequence. This parameter is calculated by plotting the experimental Ct on a standard curve of known DNA concentrations against corresponding reference Ct values (Bustin, 2000).

Housekeeping genes are generally used as internal standards in RT-QPCR for normalization of expression data across experiments. Suitable reference

housekeeping genes should be transcribed at relatively constant levels and their expression be stable under the experimental conditions. Constitutively expressed housekeeping genes are generally involved in basic functions needed for the maintenance of the cells and their viability. Reference genes are amplified from the same cDNA samples used for target gene determinations to permit comparison between RT-QPCR results (Karge *et al.*, 1998, Bustin, 2000, Bustin & Nolan, 2004, Radonic *et al.*, 2004, Huggett *et al.*, 2005). Normalization to a reference gene serves as an internal control for possible technical errors in the RT-QPCR. The application of this type of control allows knowing the bias introduced during the transcription analysis process by differences in the starting material, RNA preparation, RNA quality and cDNA synthesis (Bustin & Nolan, 2004, Huggett *et al.*, 2005).

The suitability of several *L. monocytogenes* housekeeping genes for incorporation as normalization controls in RT-QPCR-based analyses of PrfA-dependent regulation was previously investigated. Two genes in particular were selected, *rpoB* encoding the β subunit of RNA polymerase, and *ldh* encoding lactate dehydrogenase, an enzyme that mediates the anaerobic energetic metabolism of glucose (Ripio *et al.*, 1997b). The former gene has been extensively used as a housekeeping reference in many gene expression studies (Milohanic *et al.*, 2003, Sue *et al.*, 2003, Kim *et al.*, 2004, Sue *et al.*, 2004, Kim *et al.*, 2005, Roberts *et al.*, 2005, Schwab *et al.*, 2005, Stritzker *et al.*, 2005, Chaturongakul & Boor, 2006, Joseph *et al.*, 2006, Kazmierczak *et al.*, 2006, Marr *et al.*, 2006, Tasara & Stephan, 2007); *ldh*, however, was never employed before for gene expression analysis in *L. monocytogenes*.

The stability of *rpoB* and *ldh* expression was tested in experimental conditions relevant to PrfA-dependent gene expression analysis such as growth *in vitro* in extracellular conditions (Brain Heart Infusion broth, BHI) and during intracellular infection in HeLa cells (D. Rodriguez-Lazaro *et al*., unpublished data). As part of these experiments, three different isogenic *prfA* backgrounds were assessed: wild-type ($prfA^{WT}$), *prfA** (*prfA* mutant allele encoding a PrfA* protein with a G145S substitution that leads to the constitutive overexpression of PrfA-

dependent genes), and Δ*prfA* (an in-frame deletion mutant of the *prfA** strain). The expression stability of the two reference genes was determined by comparing the absolute number of transcripts for each of them with the number of bacterial CFU in the sample. When grown in BHI broth, the three listerial strains showed a constant number of *rpoB* and *ldh* transcripts at different OD_{600} measurements (0.4, 0.8, 1.2 and 2.4) (figure 3.1.1, upper panel). When grown intracellularly, the wild-type and the *prfA** bacteria produced very similar, constant levels of *rpoB* and *ldh* transcripts at different time points of infection (0, 3, 6 and 12 h) (figure 3.1.1, lower panel). Intriguingly, the Δ*prfA* strain had slightly higher levels of *rpoB* and *ldh* transcript production in comparison with the other two strains. This difference was not observed when calculating the number of genome equivalents by RT-QPCR, indicating that a fraction of the intracellular bacterial population of the Δ*prfA* strain had either died or was present in a non-culturable state (D. Rodriguez-Lazaro *et al*., unpublished data). This observation may be explained by the fact that *L. monocytogenes* bacteria lacking *prfA* do not express the PrfA-dependent genes required for intracellular survival (*hly*, *plcA* and *plcB*). These bacteria remain trapped within the harmful environment of the phagosome, and the stressed bacteria may be unable to resume growth on agar plates, or be simply dead.

Building on these data, in this study, the stability of the *rpoB* and *ldh* genes was tested to confirm their specific suitability for use with the bacteria constructed in section 3.1.1.3 for the structure-function analysis of PrfA (Δ*prfA* complemented with $prfA^{WT}$, *prfA** and the empty vector alone) (figure 3.1.2); and in sections 3.1.1.2 and 3.1.2.2 for investigating the role of the stress tolerance mediator σ^B involved in *L. monocytogenes prfA* regulation and invasiveness (Δ*sigB* mutant background in serotypes 4b [strain P14 background] and 1/2a [EGDe background]) (figure 3.1.3). The same analyses were applied to ensure that the chemically defined medium used in this study (IMM with different treatment conditions with the adsorbent Amberlite™ XAD-4; see 3.1.1.2) did not alter the expression of the reference genes.

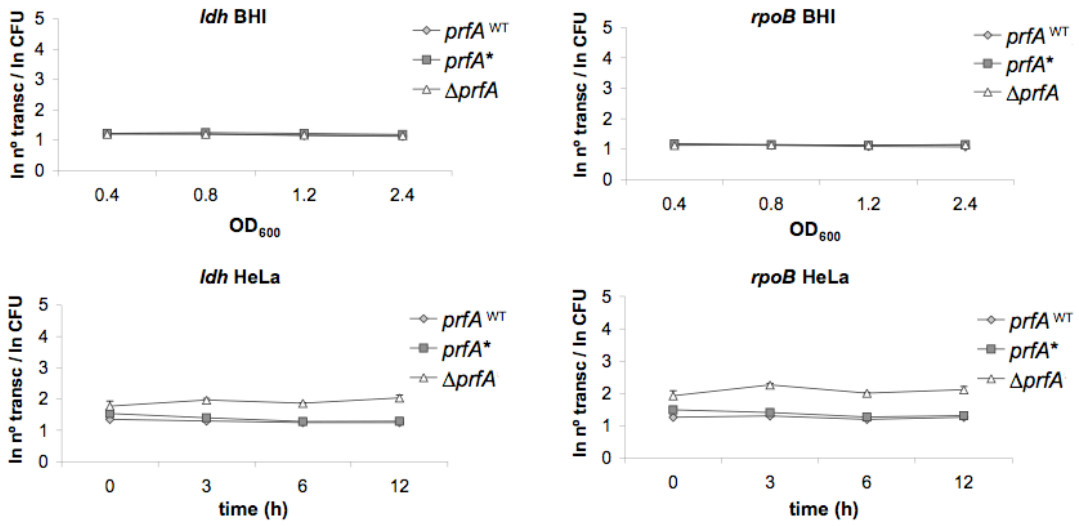

Figure 3.1.1: Comparison of the two housekeeping genes *ldh* and *rpoB*, and their assessment for normalization of virulence gene expression during extracellular growth of *L. monocytogenes* in BHI and intracellular infection of HeLa cell line using RT-QPCR.
Top two graphs show the ratio between transcripts and number of bacteria (CFU), both expressed as natural logarithm, plotted against optical densities at 600 nm (OD_{600}) of *L. monocytogenes* culture in BHI (indicating different stages of the bacterial growth: initial exponential phase -OD 0.4-, middle exponential phase -OD 0.8 and 1.2- and late exponential phase -OD 2.4-) for *rpoB* and *ldh* genes, respectively. Bottom two graphs represent the ratio between transcripts and number of bacteria (CFU), both expressed as natural logarithm, plotted against different time points of intracellular infection in human epithelial cells (HeLa) for *rpoB* and *ldh* genes, respectively. Mean of three independent experiments ± standard error (SE). Source: D. Rodriguez-Lazaro *et al*., unpublished data.

For the assays in extracelullar conditions, we chose a single optical density (OD_{600} = 0.3 or 1.0, depending on the study), at which the samples of broth-grown bacteria were taken for analysis. Similarly for the intracellular studies, we chose a single time point (6 h post-infection), at which the samples were collected for analysis. The absolute number of transcripts for each gene was compared with the CFU in these conditions, as described above. The results are summarized in figures 3.1.2 and 3.1.3.

Our data demonstrate that the reference housekeeping genes are stably expressed in the relevant test conditions. Again, the data obtained in HeLa cells show the same behaviour for the strain lacking *prfA* (Δ*prfA* complemented with empty vector), confirming that intracellular bacterial viability is compromised in the absence of PrfA-dependent expression.

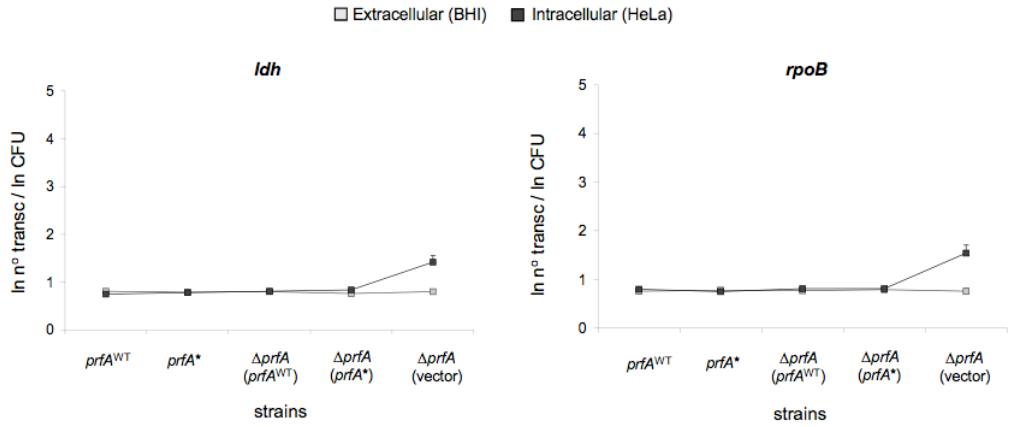

Figure 3.1.2: Stability assessment of the two housekeeping genes *rpoB* and *ldh* during extracellular and intracellular listerial growth using RT-QPCR.

Graphs show the ratio between transcripts and number of bacteria (CFU), both expressed as natural logarithm, plotted against optical density (OD_{600}) of a *L. monocytogenes* culture in BHI. See text for details. Mean of at least three independent experiments ± SE.

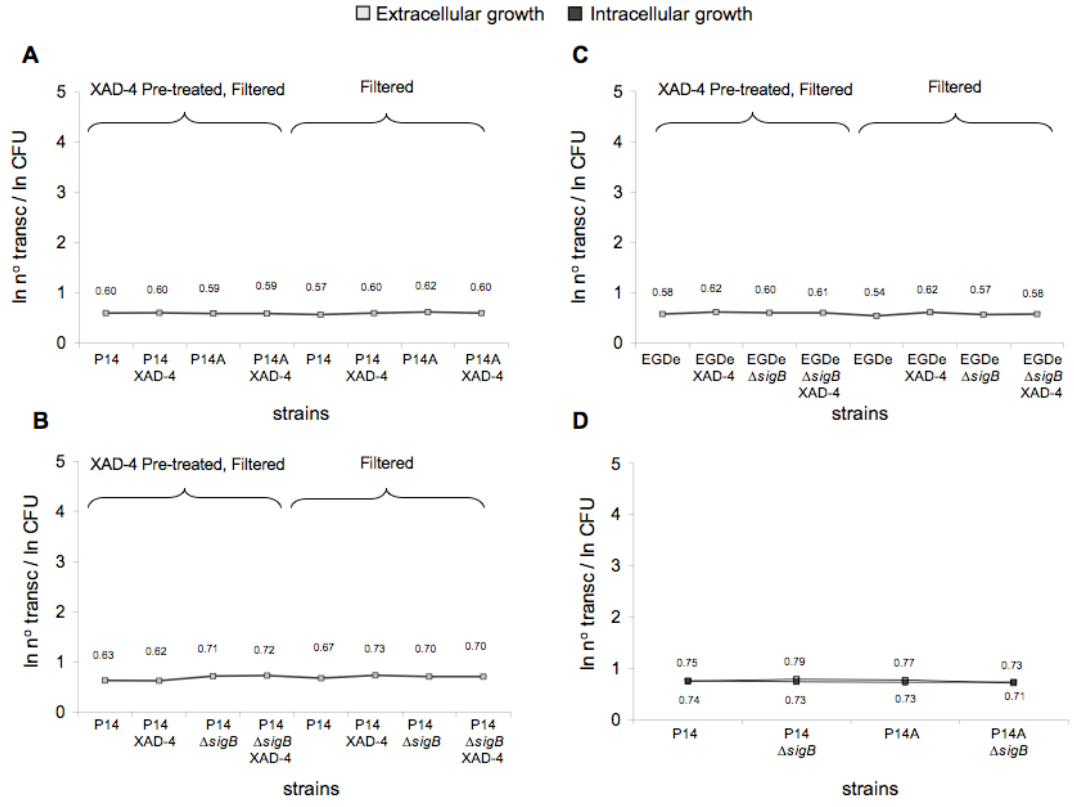

Figure 3.1.3: Stability assessment of the housekeeping reference gene, *ldh*, in different experimental conditions.

"XAD-4" is IMM supplemented with 1% Amberlite™ XAD-4; "XAD-4 Pre-treated, Filtered" is a medium treated with Amberlite™ XAD-4 for 24 h at 37°C and from which the resin was then removed by filtration prior to bacterial growth; "Filtered" is the medium that has been filtered prior to bacterial growth: A. *ldh* stability assessment of the wild-type *L. monocytogenes* (P14) and the *prfA** mutant (P14A) in the IMM alone or supplemented with Amberlite™ XAD-4. Mean of at least three

independent experiments ± SE; B. *ldh* stability assessment of the P14 and its isogenic mutant P14Δ*sigB* in IMM alone or supplemented with Amberlite™ XAD-4. Mean of two independent experiments ± SE; C. *ldh* stability assessment of the wild-type *L. monocytogenes* EGDe and its isogenic mutant EGDeΔ*sigB* in IMM alone or supplemented with Amberlite™ XAD-4. Mean of three independent experiments ± SE; D. *ldh* stability assessment of the P14 and P14A and their isogenic mutants P14Δ*sigB* and P14AΔ*sigB*, respectively, extracellularly (in BHI) and intracellularly (in HeLa cells). Similar stability data were obtained with the *rpoB* gene (data not shown).

According to the data shown in figures 3.1.1, 3.1.2 and 3.1.3, it is obvious that both housekeeping genes are equally valid for use as a reference gene for *L. monocytogenes* transcription analysis. However, the use of geNorm software for selection of control genes (http://medgen.ugent.be/~jvdesomp/genorm/) showed that, in the tested conditions, *ldh* had marginally better overall stability (data not shown). Therefore, we used *ldh* as routine reference gene for our RT-QPCR transcritption analyses throughout the study.

3.1.1.2 Further characterization of the "charcoal effect"

3.1.1.2.1 Background

L. monocytogenes is capable of modulating the expression of its virulence genes to adapt to the specific needs of its dual saprophytic and parasitic lifestyle. To achieve this, *Listeria* bacteria recognize physical signals from the medium, like temperature. This physical cue is transduced down to PrfA via a thermosensor mechanism in the *prfA* mRNA that regulates its translation regulation (Kreft & Vazquez-Boland, 2001). Thanks to this mechanism, *L. monocytogenes* bacteria activate PrfA-dependent expression on sensing an environmental temperature of 37ºC, which signals the entry into a warm-blooded host. Temperature, however, is not sufficient for full PrfA regulon activation, as demonstrates the fact that virulence genes are only very weakly expressed at 37°C in standard culture medium. A strong activation is observed at 37ºC when the bacteria are within host cells, indicating that additional signals, probably chemical components from the intracelullar medium, are

sensed by *L. monocytogenes*. The most clear evidence for a role of chemical signals in the regulation of PrfA-expression comes from the so-called "charcoal effect" (Moors *et al.*, 1999, Shetron-Rama *et al.*, 2002, Ermolaeva *et al.*, 2004).

The "charcoal effect" refers to the observation that listerial virulence gene expression is significantly induced when bacteria are cultured at 37°C in a medium supplemented with the adsorbent, activated charcoal (Ripio *et al.*, 1996). These authors showed that the supplementation of BHI with 0.2% charcoal did not affect the bacterial growth or change the pH of the culture medium. This indicated that the underlying mechanism of PrfA activation in such conditions was probably not due to sequestration by charcoal of essential nutrients or to charcoal-mediated changes in pH of the medium. Experiments were carried out in which the medium (BHI) was pre-treated for 24 h with 0.2% charcoal, after which the adsorbent was completely removed by centrifugation and filtration prior to culturing the bacteria. No activation of PrfA-dependent genes was observed unless the charcoal-pre-treated medium was supplemented again with 0.2% charcoal. It was concluded that (i) the "charcoal effect" was not due to the sequestration of a component from the medium composition acting as a PrfA-repressing signal; and that (ii) activated charcoal needs to be present in the culture medium while bacteria are growing. Transwell experiments, in which *L. monocytogenes* was grown, separated from activated charcoal particles by a microporous membrane, suggested that the effect was mediated by a diffusible molecule. Experiments in BHI conditioned with spent media indicated that a charcoal-sequestrable repressor molecule accumulated in the growth medium. Using a *L. monocytogenes* strain in which *prfA* was expressed only in monocistronic transcript form (*i.e.* PrfA-independently, no autoregulatory loop) demonstrated that charcoal induced PrfA-dependent expression without concomitant changes in the amounts of PrfA protein. Collectively, these data were interpreted as that *L. monocytogenes* releases into the medium an "autorepressor" molecule that inhibits PrfA activity. The fact that *prfA** mutant bacteria, in which PrfA is locked in active conformation, did not exhibit the charcoal effect, seemed to indicate that the autorepressor somehow interferes with the allosteric activation mechanism of PrfA (Ermolaeva *et al.*, 2004). It was suggested that this "negative quorum sensing"

mechanism could be important to prevent the expression of virulence genes in *L. monocytogenes* microcolonies in the environment at elevated ambient temperature, or as a way to dampen down PrfA-dependent gene activation when the intracellular bacterial population reaches a certain threshold, to avoid damaging the host cells (Ermolaeva *et al.*, 2004).

The above conclusions were reached using BHI, a complex medium of undetermined chemical composition, and activated vegetable charcoal, a natural adsorbent substance. In this chapter we explored the "charcoal effect" and sought to obtain confirmatory evidence of the existence of the hypothetical *Listeria*-derived autorepressor molecule. We used a chemically defined medium, Improved Minimal Medium (IMM; Phan-Thanh and Gormon, 1997), and a synthetic resin, Amberlite^{TM} XAD-4, of similar adsorptive profile to charcoal but with defined chemical composition and properties (Held *et al.*, 1999).

3.1.1.2.2 Results

Preliminary experiments in BHI supplemented with 1% Amberlite^{TM} XAD-4 showed that this triggered an activation of the PrfA-dependent gene *plcB* similar to that observed with charcoal (Ermolaeva *et al.*, 2004). In these experiments, gene activation was monitored by measuring the activity of the *plcB* gene product, the PlcB phospholipase, in the culture medium. This natural reporter system provides an estimation of PrfA-dependent gene expression but does not allow to accurately measure the levels of gene transcriptional activation. We repeated these experiments in IMM to move to a more reductionist and amenable experimental system for investigating the nature of the charcoal-sequestrable autorepressor. Gene expression was measured by quantification of the specific transcripts of the *actA* gene by RT-QPCR using *ldh* as the normalizing reference gene. The *actA* gene is co-transcribed in the same operon with the previously used *plcB* gene reporter system and is expressed from the strictly PrfA-dependent promoter P*actA* (Vega *et al.*, 2004).

L. monocytogenes P14 (*prfA*^{WT} genotype, *i.e*. charcoal-activable) and P14A (*prfA** genotype, *i.e*. charcoal-insensitive since PrfA system already fully activated) were used to test the effect of the resin in IMM. Two types of conditions were used: (i) medium with and without Amberlite^{TM} XAD-4 supplementation; and (ii) medium that was pre-treated with the same concentration of adsorbent for 24 h at 37ºC, then filtered to remove the resin particles, and used with and without 1% Amberlite^{TM} XAD-4 supplementation. To ensure that the experimental parameters were as similar as possible in all conditions, the preparation of IMM for condition (i) included filtration through the same type of microporous membrane. After inoculation, the cultures were grown until an OD_{600} = 0.3 and RNA was extracted for RT-QPCR transcription analysis. This optical density was chosen because PrfA-dependent expression is highest in the early exponential phase (Mengaud *et al.*, 1991 and our own unpublished observations). The IMM medium contained 10 mM glucose, *i.e*. excess carbon source conditions for exponentially growing *L. monocytogenes*.

The data confirmed that the presence of an adsorbent in the medium significantly activates (26.3 times) PrfA-dependent gene expression in wild-type *L. monocytogenes*, as determined by measuring transcription from the P*actA* promoter (figure 3.1.4). As previously observed with activated charcoal, supplementation with Amberlite^{TM} XAD-4 did not alter significantly the already elevated levels of P*actA*-driven expression in the constitutively activated *prfA** mutant background.

Similar results were obtained with the Amberlite^{TM} XAD-4-pre-treated IMM, with one interesting exception: in this case, a significant induction (23.3-fold, P = 0.002) in the expression of the *actA* gene was observed for wild-type *L. monocytogenes* in comparison with normal filtered IMM medium. This induction is of the same magnitude as that observed when the bacteria are cultured with the adsorbent resin present in the medium (9.3 ±1.2 vs 10.5 ±3.0, P = 0.766) (figure 3.1.4). The addition of fresh Amberlite^{TM} XAD-4 to the pre-treated medium produced a further increase in the expression levels (14.2 ±4.2 vs 9.3 ±1.2), although the difference was not significant (P = 0.155). Again, there were no significant differences in the (high) expression levels of the *prfA** bacteria in the two conditions.

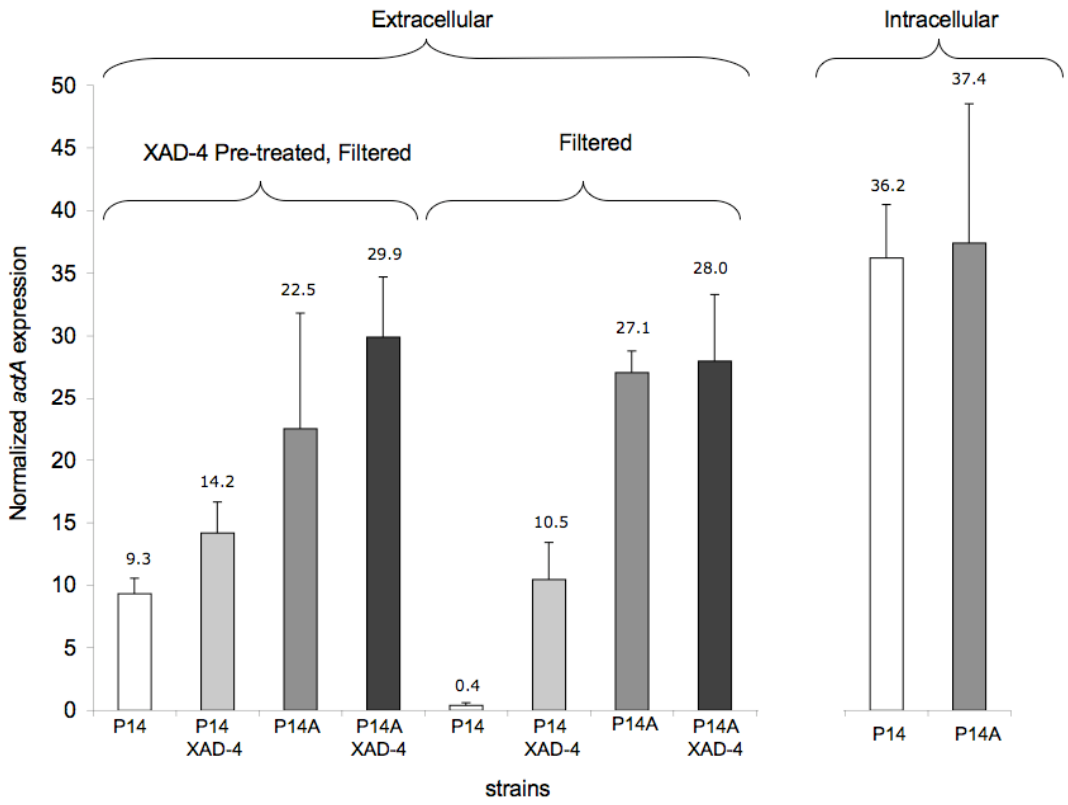

Figure 3.1.4: *actA* gene expression of wild-type *L. monocytogenes* (P14) and the *prfA**^{G145S} isogenic mutant (P14A), grown extracellularly in differently treated IMM medium and intracellularly in HeLa cells.
See text for details. "XAD-4" corresponds to IMM supplemented with 1% Amberlite^{TM} XAD-4. Intracellular values for both bacteria were taken from experiments carried out in section 3.1.2.2.3. Mean of at least three independent experiments ± SE.

These data are different from those observed with charcoal and clearly suggest that there is a repressor signal in the (IMM) medium composition that is removed by the resin treatment, leading to significant activation of PrfA-dependent expression in wild-type *L. monocytogenes*.

It is known that stresses enhance PrfA-dependent expression (see section 1.3.6). It has been shown, in particular, that transfer of logarithmically growing *L. monocytogenes* bacteria to a medium that does not support growth, like cell culture Minimal Essential Medium (MEM), possibly creating a nutritional stress, leads to substantial induction of PrfA-regulated genes (Bohne *et al.*, 1996). In order to exclude that the effect of Amberlite^{TM} XAD-4 is due to the removal of a critical

nutrient from the medium, we monitored the growth of *L. monocytogenes* in IMM and in resin-supplemented or -pre-treated IMM. As shown in figure 3.1.5, the growth kinetics was the same in the three test conditions. This excludes that PrfA activation results from a major nutritional stress response associated with significant growth inhibition.

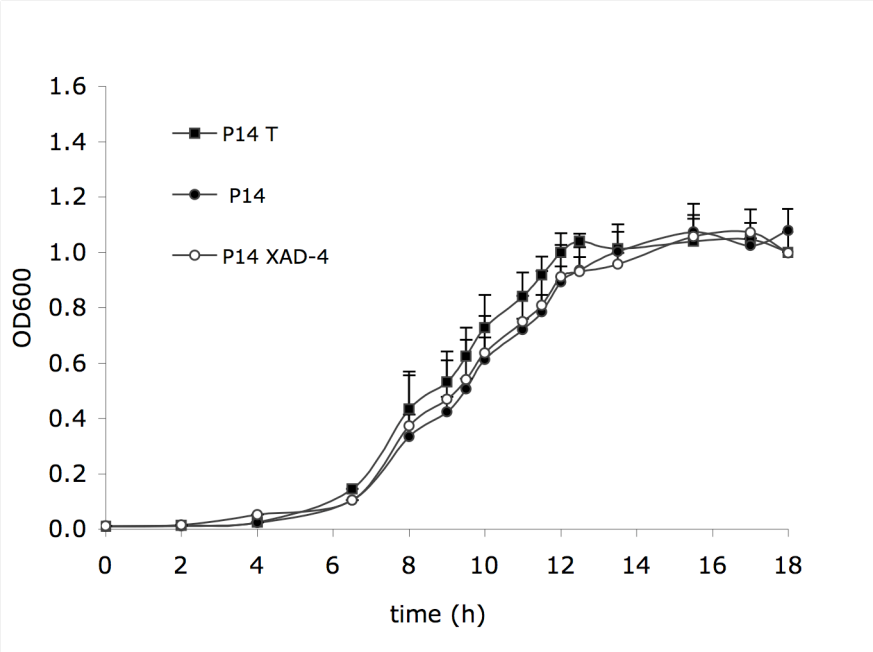

Figure 3.1.5: Comparison of the growth of wild-type *L. monocytogenes* (P14) in IMM medium pre-treated with Amberlite™ XAD-4 (T) (see text for details) and in IMM medium in the presence (XAD-4) or absence of the resin.
Mean of two independent experiments ± SE.

In order to further exclude the involvement of a stress response in the observed effects, we repeated the experiments using a Δ*sigB* mutant. As previously explained in section 1.3.6.2, the alternative σ^B, a major stress response mediator in *Listeria*, regulates the expression of *prfA* via P2*prfA* (Kazmierczak *et al.*, 2005). Even if there is no apparent growth defect associated with the use of Amberlite™ XAD-4, there might still be a low-level nutritional stress response that passes unnoticed because the loss of fitness is compensated for by σ^B. We, therefore, tested the effect of σ^B in the *prfA*^{WT} regulation context using a Δ*sigB* mutant in two different *L. monocytogenes* genetic backgrounds, serotypes 4b (strain P14) and 1/2a (strain EGDe). A precise description of these two mutants and how they were constructed can be found in section 3.1.2.2.

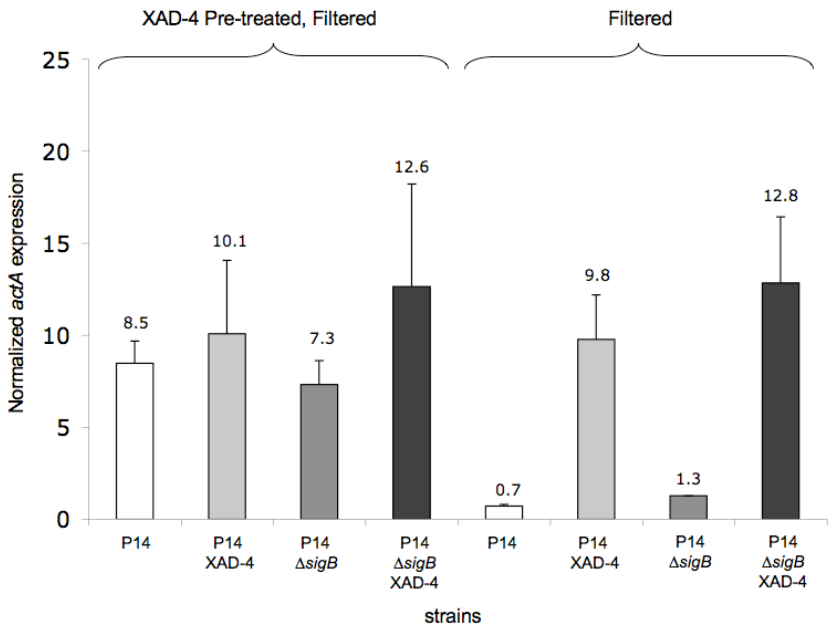

Figure 3.1.6: *actA* gene expression of *L. monocytogenes* P14 (wild-type) and its isogenic mutant P14Δ*sigB*, grown in differently treated IMM media until OD_{600} = 0.3.
See text for details. "XAD-4" is IMM supplemented with 1% Amberlite™ XAD-4. Mean of two independent experiments ± SE.

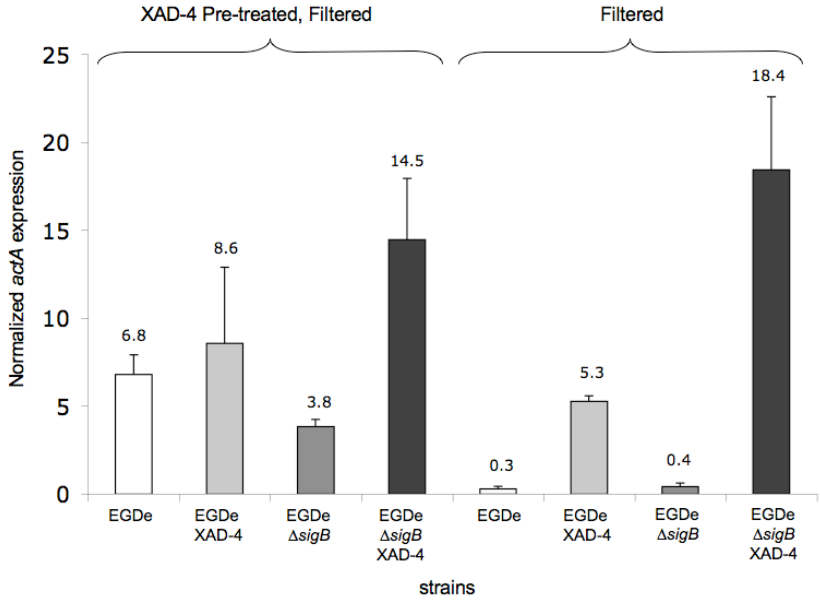

Figure 3.1.7: *actA* gene expression of *L. monocytogenes* EGDe (wild-type) and its isogenic mutant EGDeΔ*sigB*, grown in differently treated IMM media until OD_{600} = 0.3.
See text for details. "XAD-4" is IMM supplemented with 1% Amberlite™ XAD-4. Mean of three independent experiments ± SE.

Figure 3.1.6 shows that the removal of *sigB* does not have a significant effect on PrfA-dependent gene expression in *L. monocytogenes* P14 both in non-treated IMM and in response to the treatments with the adsorbent resin (P = 0.55 to 0.75). Similar results were observed in *L. monocytogenes* EGDe, except that in IMM supplemented with Amberlite^{TM} XAD-4, the Δ*sigB* mutant showed a significantly enhanced *actA* expression (figure 3.1.7). These data indicate that σ^B has no role in the Amberlite^{TM} XAD-4-mediated virulence gene activation (and even may have an inhibitory effect in EGDe).

3.1.1.2.3 Discussion

In this section of the thesis we revisited the "charcoal effect" and carried out experiments using both a culture medium and adsorbent resin with defined chemical composition. The aim was to set up an experimental system more suitable for the identification of the small molecule(s) involved.

In the Amberlite^{TM} XAD-4 pre-treated medium, the gene expression levels were significantly induced in wild-type *L. monocytogenes*, even in the absence of the resin. This clearly shows that Amberlite^{TM} XAD-4 does not need to be present in the culture medium while the bacteria are growing, in order to exert its effect. The resin seems, therefore, to mediate its effect by sequestering some component of the IMM medium that could act as a PrfA-repressing signal. These observations, however, are not in agreement with the hypothesis previously formulated for the "charcoal effect" according to which the autorepressor substance comes from the bacteria and not the medium (Ermolaeva *et al.*, 2004).

The treatment with Amberlite^{TM} XAD-4 did not affect the bacterial growth, and the σ^B stress response regulator was not involved in the effect. Therefore, the resin-mediated virulence gene activation most probably reflects an interference with a repressor chemical signalling mechanism, rather than the outcome of a general physiological response to stress, indirectly affecting PrfA.

L. monocytogenes bacteria with a *prfA**^{G145S} allele, expressing high levels of PrfA-dependent virulence factors (Ripio *et al.*, 1997a, Vega *et al.*, 2004), remained unaffected by the Amberlite^{TM} XAD-4 treatments *i.e.* the high levels of PrfA-dependent expression were not further enhanced. This is similar to what was previously observed with activated charcoal (Ermolaeva *et al.*, 2004). Thus, the *prfA**^{G145S} mutation over-rides the repression caused by the resin-adsorbed repressor signal(s) from the medium, consistent with the notion that the PrfA* mutant proteins are locked in a constitutively hyperactive conformation.

To date, the only other known situation in which PrfA-dependent genes are strongly activated at a given temperature (*e.g.* 37ºC) is when the bacteria are growing intracellularly. This is also likely to involve chemical signals from the surrounding medium (the cytosol in this case) and is probably effected through an allosteric shift of the PrfA protein (Vega *et al.*, 1998, Vega *et al.*, 2004, Scortti *et al.*, 2007). If the levels of activation achieved by wild-type *L. monocytogenes* in IMM with Amberlite^{TM} XAD-4 and intracellularly are compared, the former remain clearly below (26.3-fold vs 90.5 in HeLa cells, *i.e.* a difference of 3.5 times). This indicates that the intracellular activation pathway does not only involve the removal of a repression on PrfA, as observed when an adsorbent is added to the culture medium, but some other activation pathway, most likely the allosteric activation mechanism suggested for PrfA, presumably mediated by the binding of a small ligand or cofactor (Scortti *et al.*, 2007, Vega *et al.*, 1998, Vega *et al.*, 2004; see below section 3.1.1.3 for more details).

The constitutively active PrfA* mutant protein is thought to mimic the conformation adopted by PrfA intracellularly (Vega *et al.*, 1998, Vega *et al.*, 2004, Scortti *et al.*, 2007). Concordant to this, the values obtained with the *prfA** bacteria in IMM were also significantly higher than those of wild-type *L. monocytogenes* with Amberlite^{TM} XAD-4 treatments.

While our new findings indicate that the treatment with the resin removes a repressor component from the medium that is not bacteria-derived, they do not formally exclude the existence of an autorepressor molecule released by *Listeria*. Indeed, the addition of Amberlite^{TM} XAD-4 to the resin-pretreated medium tended to further enhance the activation of PrfA-dependent gene expression. This was very evident, for example, with the EGDeΔ*sigB* strain (figure 3.1.7). Although despite the extensive pre-treatment some amount of a repressor component may have remained in the medium, requiring the addition of more adsorbent during bacterial growth for complete removal, these data also support the notion that *Listeria* release an autorepressor molecule during growth.

Amberlite^{TM} XAD-4 is a polymeric non-polar adsorbent, which has been used instead of activated charcoal in order to remove small organic substances from aqueous solutions. This synthetic resin has a small pore size, high exchange area and an aromatic surface. Amberlite^{TM} XAD-4, therefore, is especially effective for the adsorption of low-molecular-weight hydrophobic, aromatic substances (Held *et al.*, 1999, Ermolaeva *et al.*, 2004). Our future experimental work will focus on eluting and fractionating the adsorbed material from the resin to isolate and identify the PrfA-repressor molecule(s) and characterize their chemical nature.

3.1.1.3 Structure-function analysis of the N-terminal PrfA domain

3.1.1.3.1 Background

PrfA is critical in *Listeria* pathogenesis through its role as central regulator of virulence. While a number of significant details concerning its general mode of regulation and target promoter activation have been elucidated in recent years, the intimate mechanism underlying PrfA activation, particularly in response to the cytosolic environment, remains unknown. PrfA^{-} mutants are totally avirulent despite

all other listerial virulence genes being present (Vega *et al.*, 2004), highlighting the key importance of this regulator in *Listeria* infection. Understanding in structural detail the mechanism of PrfA activation and the interactions with the effector molecules involved will be an important achievement in terms of our fundamental knowledge on *Listeria* pathogenesis, and for the development of specific inhibitory drugs to treat listeriosis.

As mentioned in section 1.3.4, the structure-function similarities between PrfA and the enterobacterial regulator Crp (Cap), a paradigm in small molecule-mediated allostery (Popovych *et al.*, 2009), have led to the assumption that the listerial regulator is allosterically activated (Ripio *et al.*, 1997a, Vega *et al.*, 1998, Vega *et al.*, 2004, Eiting *et al.*, 2005, Scortti *et al.*, 2007). Besides the overall similarities in structural arrangement between the two proteins (Eiting *et al.*, 2005), the characterization of *prfA** mutants, targeting the same protein regions and even residues to those affected by *crp** mutations, with identical functional consequences, is the most clear evidence that the two proteins share a similar type of mechanism for regulating their activity (Vega *et al.*, 2004).

The recent crystallization and structural comparison of $PrfA^{WT}$ and the constitutively hyperactive PrfA* (G145S) mutant protein, likely mimicking the in *vivo* (activated) PrfA state, has provided some insight into the kind of structural rearrangements associated with the PrfA allosteric shift. The $PrfA^{*G145S}$ mutation was first described by Ripio *et al.* (1996) in our group. It was found in a hyperhaemolytic derivative of strain P14 that overexpressed all PrfA-dependent factors. The G145S substitution is the most commonly found among spontaneous *prfA** mutants (Ripio *et al.*, 1997a, Vega *et al.*, 2004). The constitutively active mutant $prfA^{*G145S}$ is functionally analogous to crp^{*A144T}, encoding a mutant form of Crp with a substitution, A144T, targeting the very same position on αD helix in the aligned proteins (figure 1.4). Both mutations result in a very significantly increased DNA-binding activity, in the case of (apo) Crp* to levels equivalent to those observed in the cAMP-complexed (activated) wild-type protein (Weber *et al.*, 1987a, Vega *et al.*, 2004). The crystal structure of PrfA revealed that the G145 position in

αD establishes multiple contacts with residues from αG (A218) and αH (L221) that are part of the C-terminal extension of PrfA. The PrfA*^{G145S} mutation was predicted to introduce steric clashes, placing a larger residue into a compact hydrophobic pocket, repulsing αD away from αGH, indirectly repositioning the neighbouring HTH motif for optimal interaction with the target DNA (Vega *et al.*, 2004). This was essentially confirmed by Eiting *et al.* (2005), who also showed that the αE-αF loop was disordered in both monomers of PrfA^{WT} in contrast to PrfA*^{G145S}. The detailed structural studies by these authors revealed that while the general conformation of both PrfA^{WT} and PrfA*^{G145S} is similar, significant differences exist in the C-terminal (DNA-binding) domain. However, the structural differences were not only confined to the C-terminal domain. A lateral movement of β4-β5 from the β-barrel of the N-terminal domain towards αE was observed, resulting in altered interactions with the C-terminal domain across the interdomain cleft (figure 3.1.8).

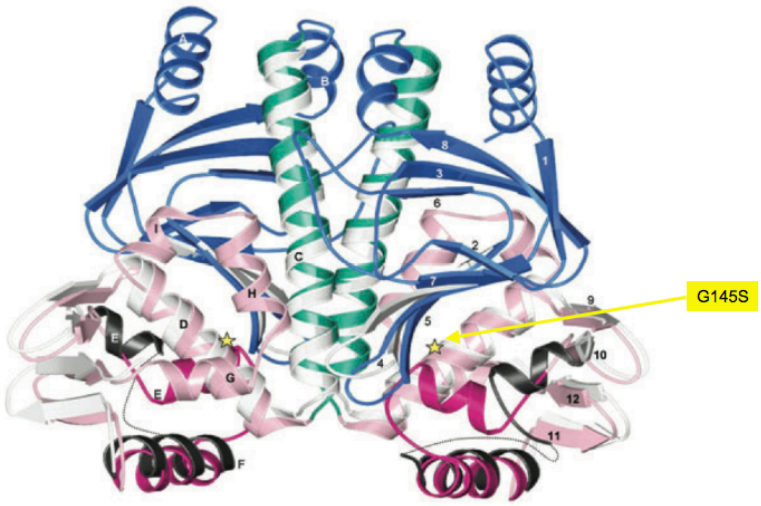

Figure 3.1.8: Superposition of PrfA^{WT} and PrfA*^{G145S}.
Taken from Eiting *et al.* (2005). Light grey represents PrfA^{WT}. For clarity, structurally conserved regions (N-terminal domain, α-helices αG, αH, αI of the C-terminal domain) are omitted for PrfA^{WT}. PrfA*^{G145S} is shown in the following domain colours: N-terminal domain is blue, dimerization-helix (αC) in green and C-terminal domain in pink. Yellow asterisk indicates the position of the mutation G145S. Magenta colour shows the helix-turn-helix (HTH) motif in PrfA*^{G145S} and dark grey in PrfA^{WT}. The disordered loop αE-αF is indicated by a dotted magenta line. The α-helices are sequentially marked by letters (left-hand monomer), β-strands by numbers (right-hand monomer).

These structural effects were the consequence of critical rearrangements between helices αD and αC, which also resulted in the straightening of the latter helix (that provides most of the monomer-monomer interface) by ~11° in PrfA*^{G145S} in comparison to PrfA^{WT} (figure 3.1.9). These structural studies concluded that, whereas PrfA^{WT} structurally resembles Crp in the absence of cAMP, PrfA*^{G145S} adopts a conformation in which the C-terminal domains, and especially the HTH motif, are very similarly arranged to cAMP-Crp, further supporting the hypothesis that PrfA*^{G145S} mimics the activated state of a liganded PrfA (Eiting *et al.*, 2005).

In this section of the thesis we explored the hypothetical allosteric nature of PrfA by focussing on the N-terminal domain of the protein, a jelly-roll β-barrel, which in Crp forms the cAMP-binding site. The PrfA β-barrel is homologous to the cyclic nucleotide-binding (CNB) domain generally present in cAMP-regulated proteins. We tested the hypothesis that this structure could serve as binding site for a PrfA-activating ligand by structure-guided site-directed mutagenesis and functional analysis.

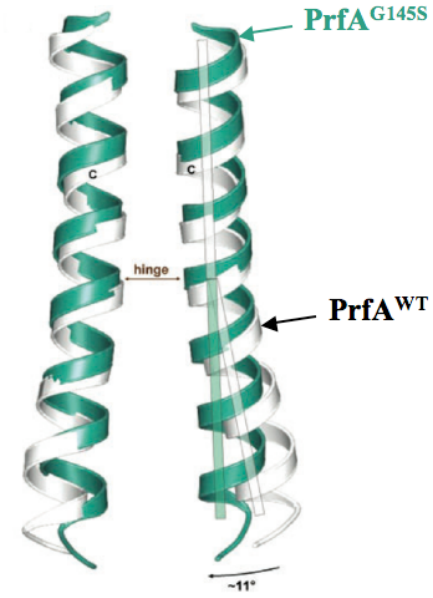

Figure 3.1.9: Conformational changes induced by the mutation G145S.
Taken from Eiting *et al*. (2005). Light grey colour represents PrfA^{WT} and green indicates PrfA*^{G145S}. The mutation induces helix αC to straighten in PrfA^{G145S} by ~11°, in comparison to the PrfA^{WT}.

3.1.1.3.2 Results

A major structural component of the CNB domain is the jelly-roll β-barrel. This ~120-residue signalling module is conserved across biology in functionally diverse cAMP/cGMP-regulated proteins including eukaryotic regulators such as protein kinases A and G or guanine nucleotide exchange factor Epac, eukaryotic and prokaryotic ion channels, and a variety of bacterial transcription factors (Berman *et al.*, 2005, Kannan *et al.*, 2007, Rehmann *et al.*, 2007, Kornev *et al.*, 2008). The CNB domain is conserved in PrfA except for the phosphate binding cassette (PBC), a signature sequence located between β-sheets 6 and 7 of the β-barrel that includes key residues involved in the docking of the cyclic nucleotide (cNMP) via its phosphoribose moiety (Diller *et al.*, 2001, Berman *et al.*, 2005, Kannan *et al.*, 2007, Rehmann *et al.*, 2007) (figure 3.1.10A). A phylogenetic analysis of the region flanked by β-sheets 6 and 7 in CNB domains from proteins known to be regulated by cNMPs or by various unrelated effector molecules showed that the PrfA sequence clusters with the latter in a distinct clade characterized by the absence of conserved PBC features (figure 3.1.10B). These data exclude cNMPs as PrfA-activating ligands, consistent with the reported lack of effect of cAMP and cGMP on PrfA activity (Vega *et al.*, 1998). However, they also suggest that the N-terminal domain of the listerial virulence regulator may contain a binding site for an unknown signalling molecule.

3.1.1.3.2.1 Structural analysis of the N-terminal solvent-exposed pocket of PrfA

In order to determine whether an allosteric effector could be accommodated in the CNB domain identified in PrfA, the cAMP molecule from the cAMP-Crp complex (Protein Data Bank [PDB] accession no. 1G6N) (Passner *et al.*, 2000) was fitted into the three-dimensional (3D) structure of the wild-type PrfA ($PrfA^{WT}$) (PDB 2BEO) (Eiting *et al.*, 2005) through coordinate superposition. This *in silico* work was carried out in collaboration with Prof. Ben Luisi and Dr. Ricardo Núñez Miguel, Biochemistry Department, University of Cambridge. A fairly large void space within

the PrfA β-barrel at about the same position as the Crp cAMP-binding pocket was observed. Residues lining this internal cavity that could interact with a ligand were also identified (figure 3.1.10C). The same putative functional sites were independently recognized using the Functional Protein Sequence Pattern (FPSP) programme (Miguel, 2004), designed to predict solvent-accessible regions in proteins with a high probability of establishing functional interactions (patterns 62-YYKGAFVI-69 and 69-IMSGFIDTETSVGYY-83, from a total of nine FPSP patterns).

Further *in silico* work, carried out in our laboratory by Dr. Caroline Deshayes, was aimed at mapping the β-roll pocket of $PrfA^{WT}$ using residues from the internal part of the cavity with CAVER (Petrek *et al.*, 2006). This programme calculates pathways leading from buried pockets to outside solvent in protein structures. The Caver output of the putative cofactor-binding site of $PrfA^{WT}$ was visualized using MacPyMOL programme (figure 3.1.11).

The PrfA pocket forms an elongated, irregular channel that varies in width. It extends from the protein surface deep into the β-barrel. The average inner width of the channel is approximately 4.5Å (figures 3.1.11, 3.1.12 and 3.1.13). However, the pocket becomes wider in its distal part (approximately 4.5Å × 7Å × 10Å). It ends between the two αC helices of the PrfA dimer (αC and αC' from the opposite monomer), halfway their length where the αC/αC' axes cross each other (figures 3.1.11 and 3.1.13). Both αC and αC' contribute residues to form the walls of a monomer's distal chamber (figure 3.1.13). These αC helices form most of the monomer-monomer interface and are possibly critical for dimerization. They are known to rotate about this point by roughly 11º in the $PrfA^{G145S}$ mutant (Eiting *et al.*, 2005). Their realignment upon cofactor binding is thought to play a key role in the allosteric transition (activation) of PrfA (Eiting *et al.*, 2005). The pocket was formed from residues of both protomers of the dimeric PrfA. Therefore, we believe that the filling of the cavity with the putative ligand may directly alter the relative orientation of the two αC helices in a sort of "scissor-type" movement.

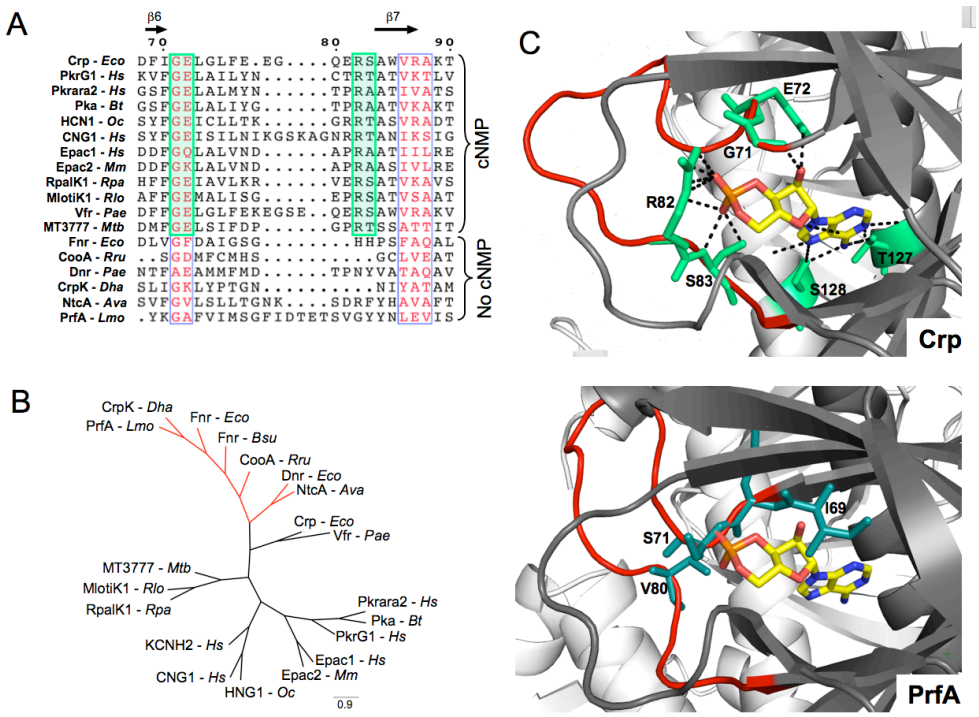

Figure 3.1.10: CNB domains in cyclic nucleotide (cNMP)-regulated and non-regulated proteins and identification of the putative ligand-binding site in the PrfA β-barrel.

(A) Amino-acid sequence alignment of the β6-β7 region encompassing the PBC motif in a selection of bacterial and eukaryotic CNB domain-containing proteins (cNMP = cNMP-regulated; No-cNMP = cNMP-non-regulated). Conserved blocks of sequence in red case, residues known to interact with the cNMP molecule in cNMP-regulated proteins are shaded green. Numbering above the sequences corresponds to Crp coordinates and the position of β-sheets 6 and 7 of the β-barrel is indicated by arrows. Alignment constructed with ClustalW2 (EMBL, http://www.ebi.ac.uk/Tools/clustalw2/) and visualized with ESPript (Gouet *et al.*, 1999), (http://espript.ibcp.fr/). Protein sequences used (EMBL accession nos.): Crp/Cap (P0ACK0), PrkG1 (Q13976), Prkar2A (P13861), Pka (P00514), KCNH2 (Q12809), HCN1 (Q9MZS1), CNG1 (P29973), Epac1 (O95398), Epac2 (Q9EQZ6), RpalK1 (Q02006), MlotiK1 (Q98GN8), Vfr (P55222), MT3777 (O69644), Fnr (P0A9E5), CooA (P72322), Dnr (Q51441), CprK (B8FW11), NtcA (P0A4U7), PrfA (P22262). Source species: *Eco, Escherichia coli; Hs, Homo sapiens*; *Bt*, *Bos taurus*; *Oc, Oryctolagus cuniculus; Mm*, *Mus musculus*; *Rpa, Rhodopseudomonas palustris*; *Rlo, Rhizobium loti*; *Pae*, *Pseudomonas aeruginosa; Mtb, Mycobacterium tuberculosis; Bsu*, *Bacillus subtilis*; *Rru, Rhodospirillum rubrum*; *Dha, Desulfitobacterium hafniense*; *Ava, Anabaena variabilis; Lmo, Listeria monocytogenes*. See Figure 1.4 for reference.

(B) Unrooted phylogenetic tree of PBC sequences used for the alignment shown in (A). Constructed with Phylip 3.69 (http://evolution.genetics.washington.edu/phylip.html) and visualized using FigTree (http://tree.bio.ed.ac.uk/software/figtree/). Distinct evolutionary branch with cNMP-non-regulated CNB-containing proteins is represented in red.

(C) Upper panel, crystal structure of holo-Crp (1G6N) showing polar contacts (black dashed line) between the cAMP molecule and residues in its binding pocket; lower panel, equivalent image of $PrfA^{WT}$ (2BEO) with cAMP positioned in the β-barrel according to a structural alignment with the Crp-cAMP complex. The superimposed cAMP molecule lodges in a cavity in PrfA's CNB domain at a similar position that in Crp. In the two panels, a monomer is coloured light grey and the other dark grey and the PBC loop (or corresponding region in PrfA) is represented in red. Residues that interact (Crp) or clash (PrfA) with cAMP are represented in sticks (modified from an analysis carried out by our collaborator R. Núñez Miguel).

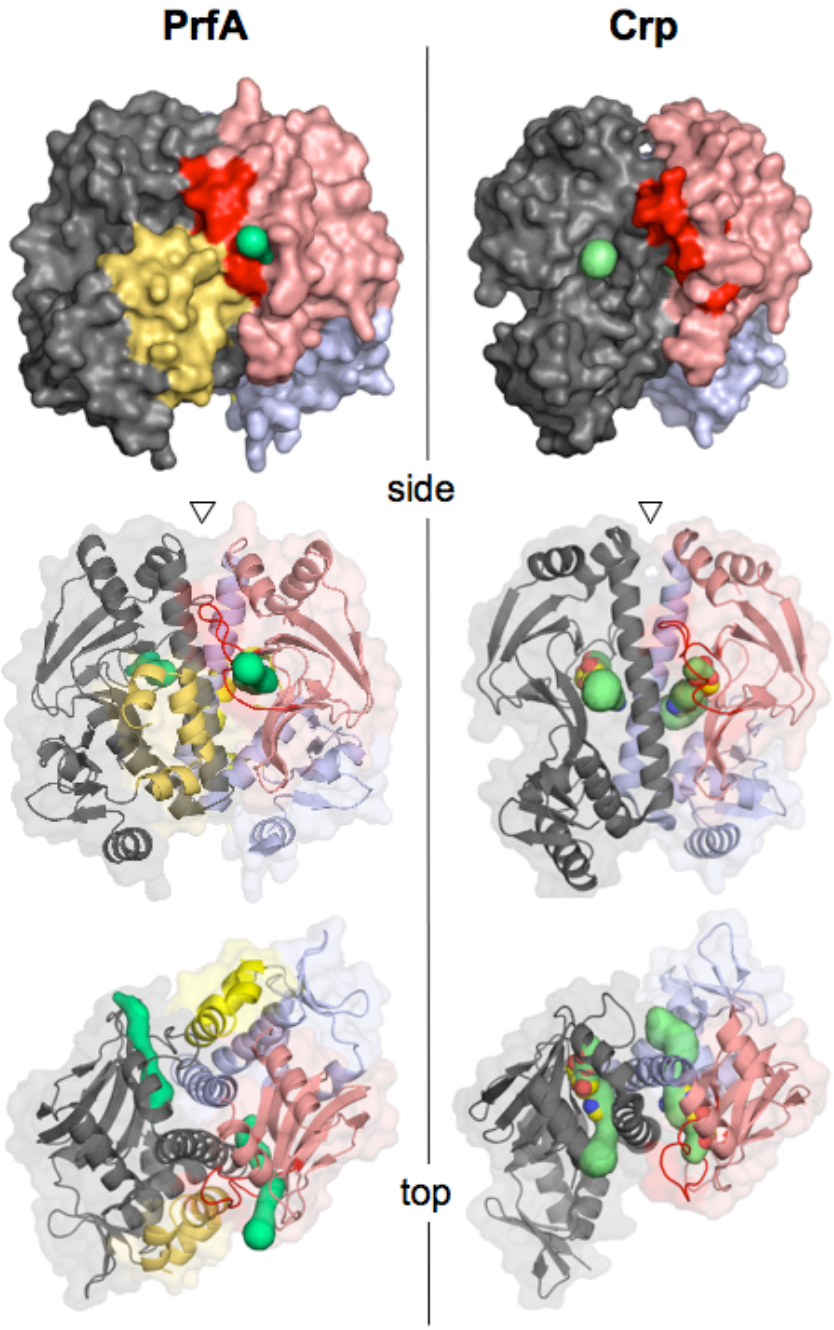

Figure 3.1.11: Structure of PrfA and the cAMP-Crp complex showing the position of their surface-exposed pockets and corresponding entrances with surface and ribbon representation.
("side" and "top" views; top view is 90º x-axial rotation of side view with arrowhead area towards the foreground). In both structures, one monomer is coloured light blue with N-terminal domain in pink and the other monomer is in grey. The PBC loop (or corresponding region in PrfA) is represented in red. The additional C-terminal GHI helical bundles of PrfA are in yellow. In Crp, the cAMP molecule is in sphere representation with atoms coloured by element (C, yellow; O, red; N, blue). Trajectories of the N-terminal pocket of PrfA and the cAMP-binding pocket as determined by CAVER are shown in green (see also figure 3.1.15B). Figure constructed with MacPyMOL. See figure 1.4 for secondary structure features; the N-terminal domain, αC and the "G wedge" domain (C-terminal αGHI bundle) are similarly colour coded.

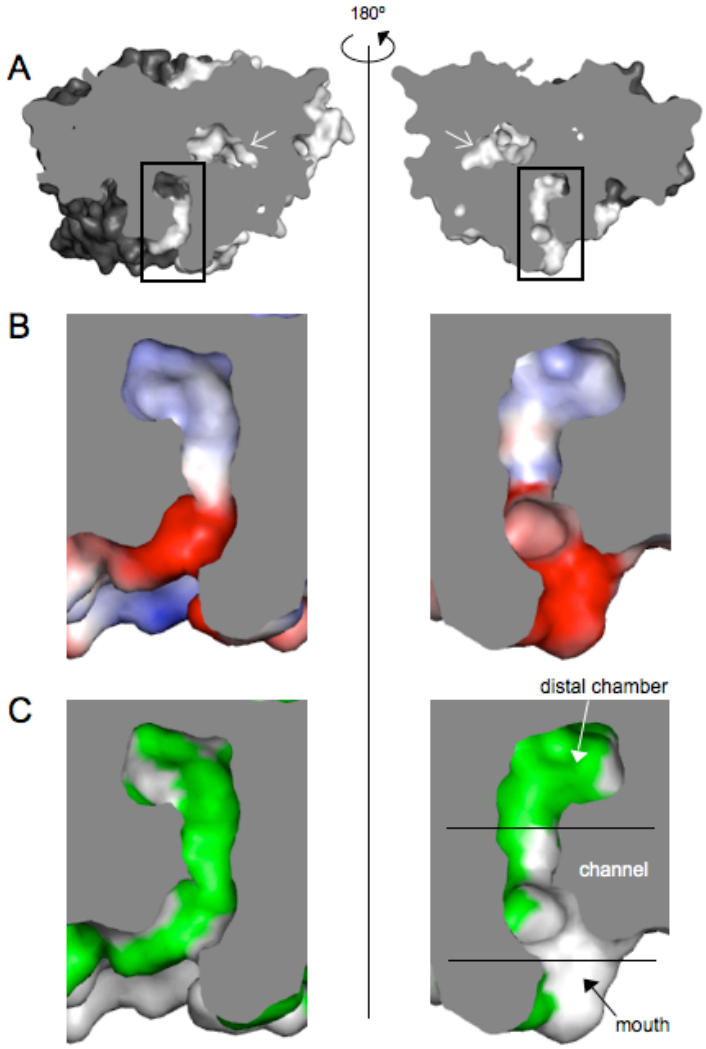

Figure 3.1.12: PrfA pocket topology and surface properties.
(A) Stereo cutaway surface representation of the PrfA dimer (top view, see figure 3.1.11). PrfA pocket is framed in black. Arrows indicate the inter-domain tunnel (see figure 3.1.14). Surfaces of one monomer are light grey, those of the other monomer in dark grey. Cutaway plane in flat grey.
(B) Enlargement of framed areas in (A) showing qualitative surface electrostatics of the PrfA pocket, as determined with the built-in vacuum electrostatics MacPyMOL function. Electronegative charge surfaces in red, electropositive ones in blue.
(C) Enlargement of framed areas in (A) showing the solvent-exposed hydrophobic surface area of the PrfA pocket. Hydrophobic residues (Val, Ile, Leu, Met, Phe, Tyr and Trp) are shown in green.
The three panels have been constructed with MacPyMOL.

The walls of the pocket have been found to be mostly non-polar except at the mouth and proximal section of the channel tract, where there is an electronegative patch, and in portions of the distal chamber where the polar constituents of the side

chains of Q121, Q123 and Y63 line the surface of the cavity (figures 3.1.12 and 3.1.13).

Similar analyses of the cAMP-Crp complex using CAVER revealed interesting differences in topology and trajectory between the PrfA pocket and the Crp cAMP-binding site. While the latter traverses the β-barrel side to side, with a small second opening at the bottom end close to the PBC where the cAMP polar head lodges, that from PrfA is shorter and ends at the monomer-monomer interface. Moreover, the mouth of the PrfA pocket opens at the opposite side of the β-barrel, between the loop that forms the PBC in Crp and an adjacent loop between β-sheets 2 and 3 (see figure 1.4 for secondary structure features of PrfA). The region that corresponds to the entrance of the pocket in Crp is blocked up in PrfA by the additional C-terminal GHI α-helical bundle wedged between the protomer domains (figure 3.1.11).

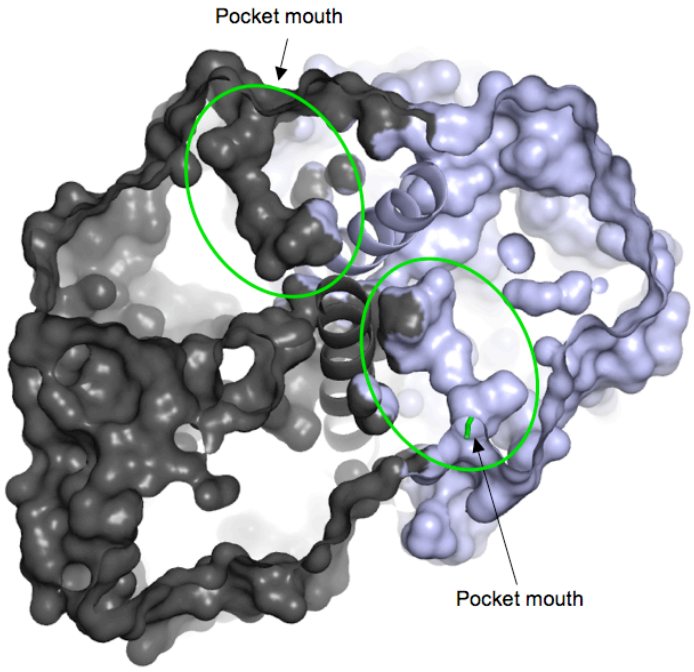

Figure 3.1.13: Surface representation of the PrfA dimer (top view) with front and back planes clipped off to allow visualization of the internal contour of the PrfA pocket (encircled in green).
One monomer is coloured light blue and the other in dark grey. The two αC-helices are shown in cartoon representation. The entrance of the pocket from each monomer is indicated by an arrow. Figure constructed with MacPyMOL.

Interestingly, the pocket identified in the N-terminal domain using CAVER is different from the cavity described previously by Eiting *et al.* (2005) as possible cofactor binding site. According to our analysis, the cavity identified by Eiting *et al.* corresponds to the large inter-domain cleft, a hollow space left between the N- and C-terminal domains of PrfA and which in surface representation appears as a large tunnel or channel. The "inter-domain tunnel" has two entries and traverses the molecule from side to side. In contrast to the inter-domain tunnel, the putative binding site cavity has only one external entrance and ends deep into the PrfA molecule at the interface of the two monomers, between the two αC helices. The inter-domain tunnel and the N-terminal pocket within the β-barrel are two independent internal cavities in PrfA, which are not interconnected (figure 3.1.14).

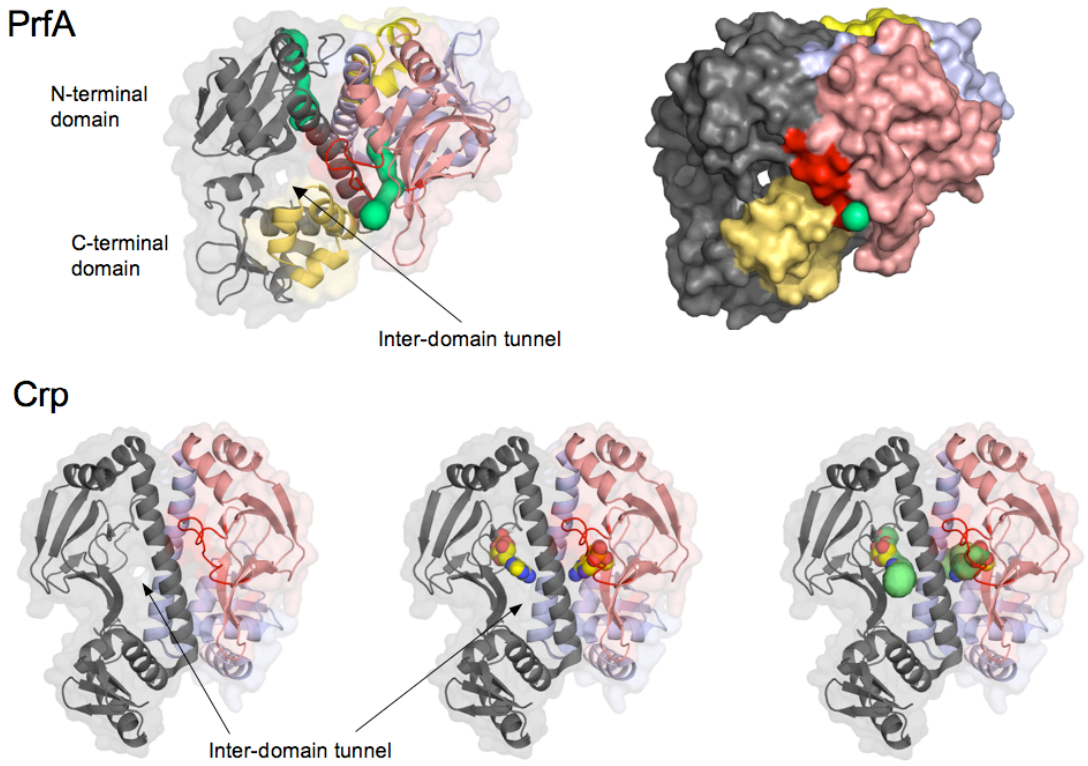

Figure 3.1.14: PrfA (upper panels) and cAMP-Crp complex (lower panels) dimer structures from figure 3.1.11 appropriately rotated to expose the inter-domain tunnel.
The N-terminal β-barrel pocket trajectories (CAVER output) are represented in green. Note that, whereas in Crp the entrance of the cAMP-binding pocket is through the inter-domain tunnel, in PrfA the pocket mouth opens at the opposite side of the β-barrel and does not coincide with the inter-domain tunnel. See text for details.

3.1.1.3.2.2 Mutant design and construction

In order to explore the function of the PrfA pocket, we chose in collaboration with our Cambridge colleagues a number of residues lining the cavity, with solvent-exposed side chains, for site-directed mutagenesis (figure 3.1.15). The mutations were selected, so that the newly introduced side chain altered internal surface properties with minimal secondary structure consequences. In some cases, the substitution was predicted to accommodate an infrequently observed rotameric state that would protrude into the pocket to avoid steric clashes with neighbouring residues.

If the function of the pocket is to accommodate an activating ligand, a mutation specifically interfering with this interaction is expected to confer a phenotype characterized by wild-type levels of basal, "intrinsic" PrfA activity but severely impaired intracellular activation of PrfA-dependent genes. The effect on phenotype was evaluated with a model infection system. To ensure that the mutations had little secondary effects, we explored the impact on protein stability, DNA binding capacity and dimerization.

Five mutations were designed to introduce changes in the topology of the pocket without altering the local hydrophobicity. These included substitutions affecting hydrophobic residues at the mouth (F29M) and the distal portion (I69W, V80L, and L48F) of the channel, in which the new side chains were likely to protrude into the cavity, and at the end of the pocket (L120V), with the mutation predicted to displace further inwards the wall of the cul-de-sac against αC. Two mutations targeted residues in the middle (S71L) and distal (Y63W) sections of the channel, which, in addition to altering the structure of the pocket, removed hydroxyl groups that could potentially be involved in the docking of a ligand via hydrogen bonding. Finally, two other substitutions targeted the negatively charged patch at the pocket entrance (E36Q, E36R) (figures 3.1.12, 3.1.15 and 3.1.16).

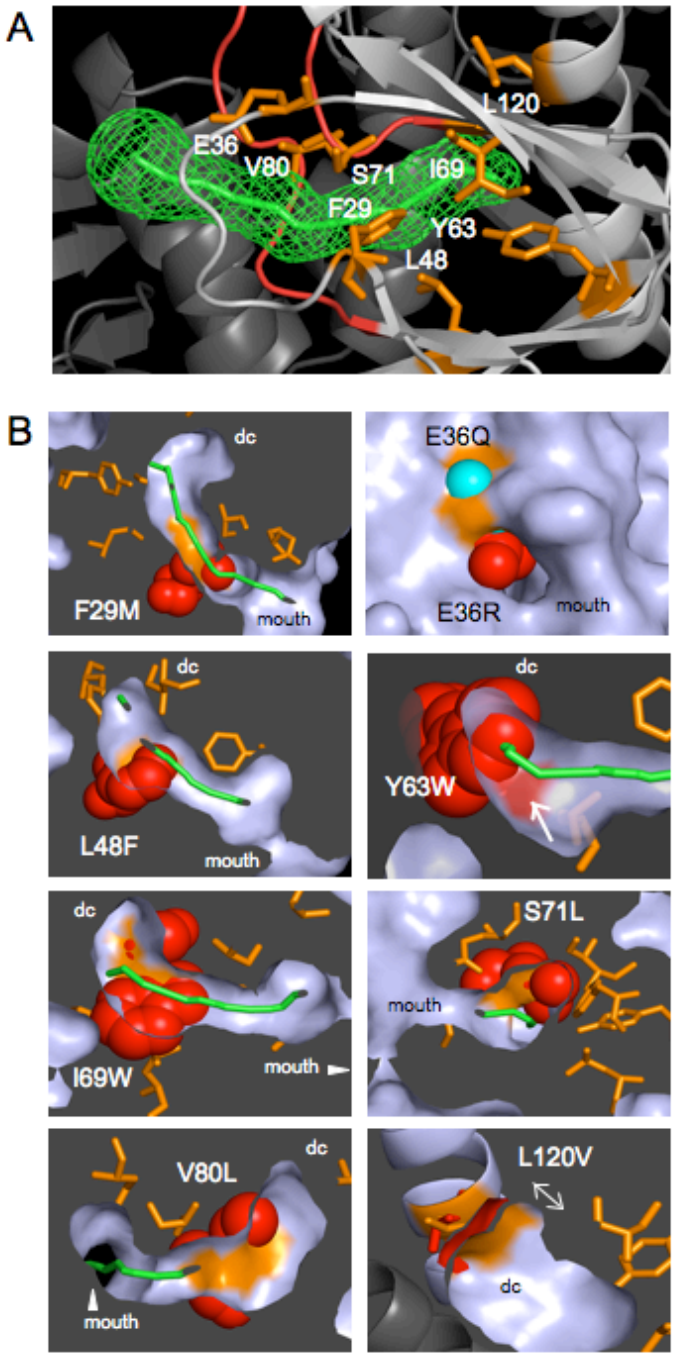

Figure 3.1.15: Site-directed mutagenesis of the N-terminal PrfA pocket.
(A) Close-up view of the PrfA β-barrel cavity with the CAVER-determined solvent-exposed trajectory in green mesh representation. In the cartoon structure, the eight residues lining the internal cavity that were mutated in this study are shown in orange stick representation (see also figure 3.1.16). A monomer is coloured light grey and the other dark grey. The loop between β-sheets 6 and 7, that corresponds to the PBC in Crp and which forms the mouth of the pocket in PrfA, is shown in red (see figure 3.1.11). (B) Modelling of the pocket mutations in a surface representation of PrfA. To illustrate the predicted local structural alterations introduced by the mutant residue, a cutaway section of an appropriately positioned PrfA structure exposes the relevant portion of the internal cavity when

necessary; the clipping plane is in flat dark grey. See figure 3.1.16 for additional spatial reference. In each panel, the atoms of the mutant residue/side chain are shown in space-fill representation as red spheres (except for Q36, shown as blue spheres, and V120 represented as red sticks with corresponding surface also in red); all other visible residues targeted in this study are shown as orange sticks. The wild-type surface of the original residue is shown in orange. The centerline of the access route of the pocket as determined by CAVER is represented in green. In the Y63W panel, the arrow indicates the position of the hydroxyl group of the Y63 side chain, which is directly exposed to the pocket surface (semitransparent red patch) and may establish polar interactions with a putative ligand (see text). The double arrow in the L120V panel illustrates the predicted inward displacement of the distal end of the pocket as a result of the shorter valine residue. See figure 3.1.16 for additional spatial reference.

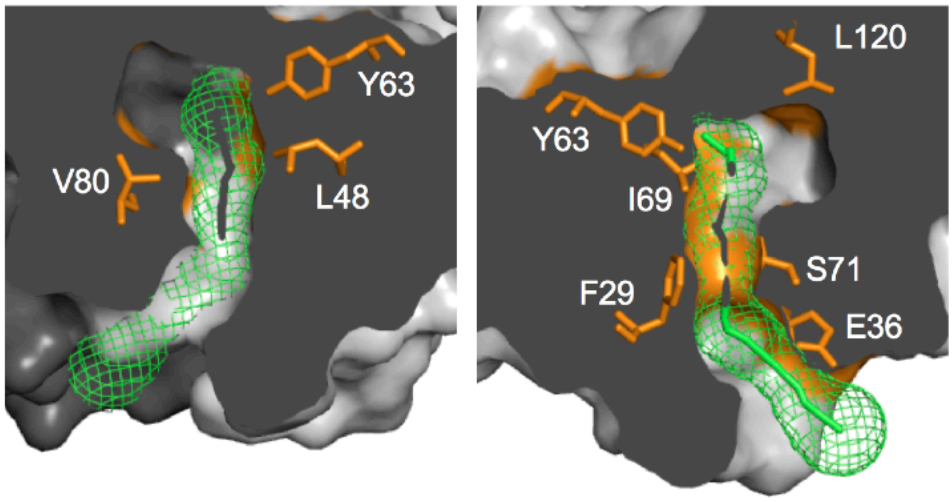

Figure 3.1.16: Same stereo cutaway surface view of the N-terminal PrfA pocket as in figure 3.1.12 showing the mutagenized residues represented as orange sticks.
The green volume in mesh representation is the pocket contour determined by CAVER. Note that the CAVER graphical output represents the solvent access path and does not fill the entire volume of the distal chamber cavity.

All nine site-directed mutations were constructed by overlap extension using the wild-type *prfA* gene as a template. The mutant alleles (with indigenous wild-type promoters P1*prfA* and P2*prfA*; see section 1.3.5) were inserted in monocopy into the chromosome of *Listeria prfA* deletion mutant (Δ*prfA**) using the integrative plasmid pPL2 (see Materials and Methods for details).

For each experiment performed throughout the study included in this section of the thesis, $PrfA^{WT}$, $PrfA^{*}$ (G145S), vector and Δ*prfA* bacteria complemented with

a totally inactive *prfA**^{supE173G} allele (Vega *et al.*, 2004) (designated in this section as E173G* for simplicity), which carries a mutation in the HTH motif that prevents binding to the target DNA, were used as controls.

We confirmed by western immunoblotting of bacterial whole cell extracts that all *prfA*-complemented Δ*prfA* bacteria produced equivalent amounts of PrfA protein (data not shown).

3.1.1.3.2.3 Functional analysis of the PrfA pocket mutants

The behaviour of the mutant PrfA proteins was tested in the complemented Δ*prfA* bacteria grown extracellularly at 37°C in BHI, in which PrfA-dependent expression is weak (basal levels) (Ripio *et al.*, 1997a, Vega *et al.*, 2004), and intracellularly in infected HeLa cells, where PrfA is believed to shift to its "on" conformation. Samples were taken for the analysis either after reaching an OD_{600} = 0.3 (early exponential phase) or after 6 h post-infection, respectively.

PrfA activity was analyzed by determining the transcription of the strictly PrfA-dependent genes *plcA* and *actA* (Lalic-Multhaler *et al.*, 2001, Vega *et al.*, 2004) using RT-QPCR. The *plcA* promoter (P*plcA*) has a “perfect” PrfA box and is, thus, very sensitive, and responds linearly, to PrfA. By contrast, the *actA* promoter (P*actA*) has a mismatch in the symmetrical palindrome and, therefore, it requires larger amounts of PrfA input for full activation, resulting in “all or nothing” response pattern (Sheehan *et al.*, 1995, Williams *et al.*, 2000, Vega *et al.*, 2004), which has been described in sections 3.1.1.2.2 and 1.3.5. The number of transcripts determined was normalized with the number of transcripts of the constitutive housekeeping reference gene *ldh* (see section 3.1.1.1).

The mutants fell in three categories according to their intracellular activability (figure 3.1.17). F29M and V80L showed no significant differences with respect to *prfA*^{WT} for the two promoters. A second group of mutants showed significantly reduced activability, particularly with the stringent P*actA* promoter. In

three of these, E36Q, E36R and I69W, the reduction was modest to intermediate (P*plcA* 7.3 - 40.6%, mean: 23.1%; P*actA*: 36.2% - 51.0%, mean 43.2%); in the other two, S71L and L120V, intracellular gene activation was substantially impaired (mean reduction: P*plcA* 69.9%, P*actA* 83.7%). Finally, in mutants L48F and Y63W the intracellular activation of PrfA-dependent expression was virtually abolished (mean reduction: P*plcA* 88.5%, P*actA* 94.1%) (figure 3.1.17).

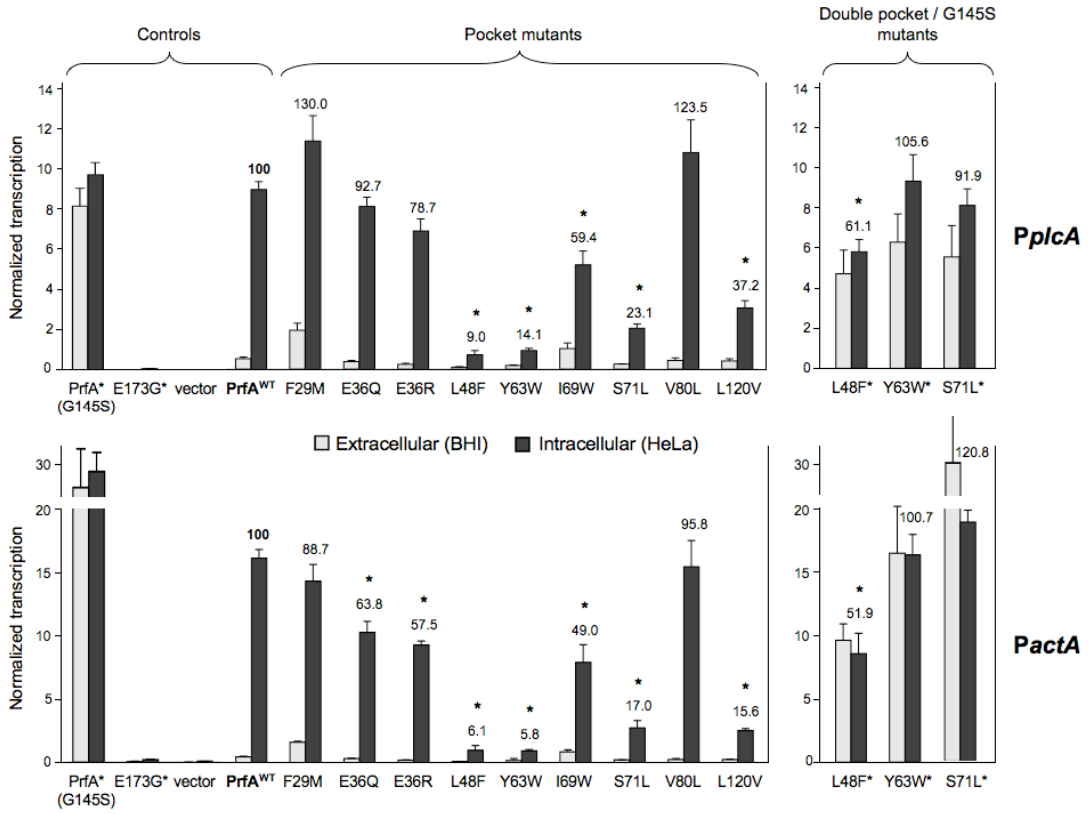

Figure 3.1.17: Transcriptional analysis of the PrfA pocket mutants.
The transcription of *plcA* (upper panel) and *actA* (bottom panel) genes has been checked by RT-QPCR in extracellular (OD_{600} = 0.3 in BHI broth) and intracellular (infection of human HeLa epithelial cells for 6 h post-infection) conditions. The percentages of the intracellular activation compared to the wild-type are indicated by numbers. Error bars indicate SE of at least three independent experiments. Statistical analyses were performed with Student's *t* test. *, $P \leq 0.01$. See text for details.

The negative controls behaved as expected, *i.e.* no detectable PrfA-dependent gene expression both extra- and intracellularly. The *prfA**^{G145S}-complemented bacteria showed in the two conditions the same high expression levels as intracellular *prfA*^{WT}-complemented bacteria, indicating that the PrfA*^{G145S} mutant possibly

mimics the hyperactive state adopted by the listerial virulence regulator within host cells (Ripio *et al.*, 1996, Ripio *et al.*, 1997a, Vega *et al.*, 2004, Scortti *et al.*, 2007).

Mutants F29M and I69W showed increased levels of basal (BHI) PrfA-dependent expression (mean increment relative to $prfA^{WT}$, respectively: P*plcA*, 270.9% and 140.0%; P*actA*, 312.5% and 145.1%).

In order to characterize the phenotype of the pocket mutants, a semiquantitative assessment of the intrinsic activity (*i.e.* extracellular growth in BHI medium) of the mutant PrfAs was carried out. The assay tests PrfA-dependent *actA* promoter expression using the *plcB* gene as a reporter; *plcB* is expressed from the strictly PrfA-dependent *actA* promoter and encodes a phospholipase whose activity can be revealed very easily via an opacity reaction on egg yolk BHI agar (EYA) (Vazquez-Boland *et al.*, 1992). Simultaneously, we performed another semiquantitative assessment of the intrinsic activity of the mutant PrfAs involving *hly* promoter expression using the *hly* gene as a reporter. The *hly* promoter, similarly to the *plcA* promoter, has a symmetrical PrfA box and is, therefore, very sensitive and responds linearly to PrfA (which has been also explained in sections 1.3.5). *hly* gene encodes the haemolysin LLO the activity of which can be revealed very easily via lysis of erythrocytes on sheep blood agar (SBA). The mutant bacteria were, therefore, streaked on both types of plates. After 3-day incubation at 37°C, the plates were examined for dark halo or lysis of erythrocytes around the streaked bacteria, respectively.

Consistent with RT-QPCR data, F29M and I69W displayed a PrfA* phenotype on EYA and SBA plates, indicating an increased intrinsic activity in the corresponding mutant PrfA proteins. This increase is only moderate compared to $PrfA^{*G145S}$, as judged from the noticeably less intense precipitation halos in EYA and less lysis of erythrocytes around streaked bacteria in SBA, respectively, in F29M and I69W. Although S71L did not show detectable differences in basal PrfA-dependent expression compared to the wild-type as determined by RT-QPCR, it also displayed

a partial PrfA* phenotype on EYA and SBA plates, respectively, suggesting a more elevated basal activity for $PrfA^{S71L}$ than $PrfA^{WT}$ (figure 3.1.18).

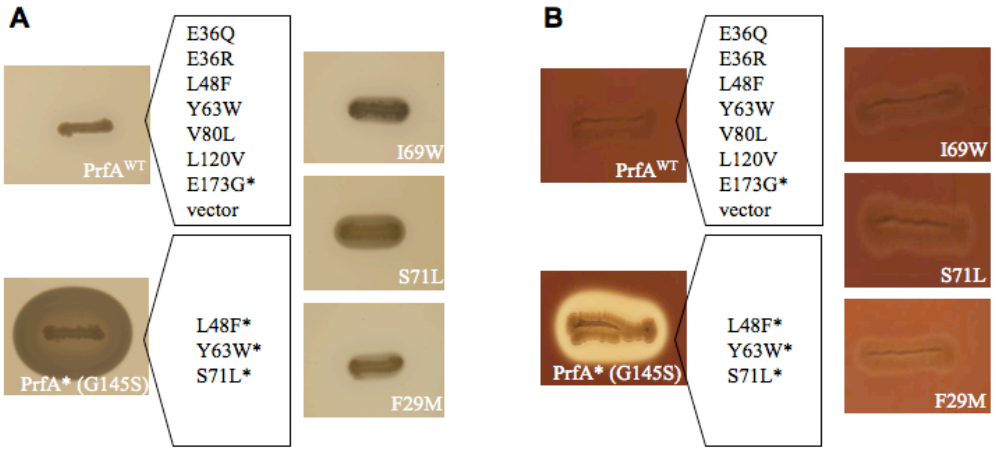

Figure 3.1.18: Phenotype characterization of the pocket mutants.
Pictures taken from representative agar plates incubated at 37°C for 72 h. (A) PlcB phenotype of the PrfA pocket mutants grown on BHI EYA plates; note that the I69W, S71L and F29M strains show a partial PrfA* phenotype; (B) Hly phenotype of the PrfA pocket mutants grown on SBA plates; note that the I69W, S71L and F29M strains show a slight PrfA* phenotype; (see text for details).

3.1.1.3.2.4 Virulence

We decided to investigate the effect of the mutations in virulence as PrfA is vital for *L. monocytogenes* pathogenesis. Some intracellular infection-related phenotypes only require some amount of PrfA activity (*e.g.* phagosomal escape/intracellular growth, which depend on "sensitive" promoters as found in front of the *plcA* and *hly* genes). Others, in contrast, require a high input of PrfA as provided by a fully activated regulator. This is the case of cell-to-cell spread, which primarily depends on the activity of the actin polymerizing protein ActA and the PlcB phospholipase, the synthesis of which is driven by the stringent PrfA-dependent P*actA* promoter (Freitag & Portnoy, 1994). Cell-to-cell spread was determined through the ability of the bacteria to form plaques in monolayers of L929 fibroblasts. L929 cells have been previously used for *L. monocytogenes* plaque assays and

reported to give better results than other cells, with more neat and wider plaques (Sun *et al.* [1990], Chatterjee *et al.* [2006] and our unpublished observations). The size of the plaques is an output variable of a complex phenotype to which several input variables contribute, including the efficiency of phagosome escape and cytosolic multiplication in addition to cell-to-cell spread and invasion of neighbouring cells. An isogenic deletion mutant in the *actA* gene, encoding the actin-polymerizing protein essential for cell-to-cell spread (Kocks *et al.*, 1992), was included as a negative control (see table 5.1 in Materials and Methods). In order to obtain a good distribution of individual plaques for counting purposes, the multiplicity of infection (MOI) was carefully adjusted (ranging from 0.005:1 to 2:1) according to the invasiveness of the tested strain.

The plaque assay results were completely consistent with the expression data (figures 3.1.19 and 3.1.20). As expected, negative controls showed a total lack of cell-to-cell spread capacity.

Mutants F29M and V80L, with no defect in PrfA function, and E36Q, which only showed a very minor intracellular activation defect (figure 3.1.17), were indistinguishable from the wild type (P = 0.61, 0.66 and 0.93, respectively).

Moreover, the activation-deficient E36R, I69W, S71L and L120V mutants showed cell-to-cell spread defects that were generally concordant to the observed reduction in intracellular activability.

The activation-null mutants L48F and Y63W did not form plaques, similarly to the spread-negative control Δ*actA* bacteria. Thus, the intracellular activation defects of the PrfA mutant proteins translated directly into commensurate deficiencies in infectivity. Again, despite the marked differences in extracellular (BHI) PrfA-depedendent expression levels between the $prfA^{WT}$- and $prfA^{*G145S}$-complemented bacteria, both exhibited the same (maximal) levels of spread, further reinforcing the notion that the $PrfA^{*G145S}$ mutant protein mimics the "on" (intracellular) conformation of PrfA.

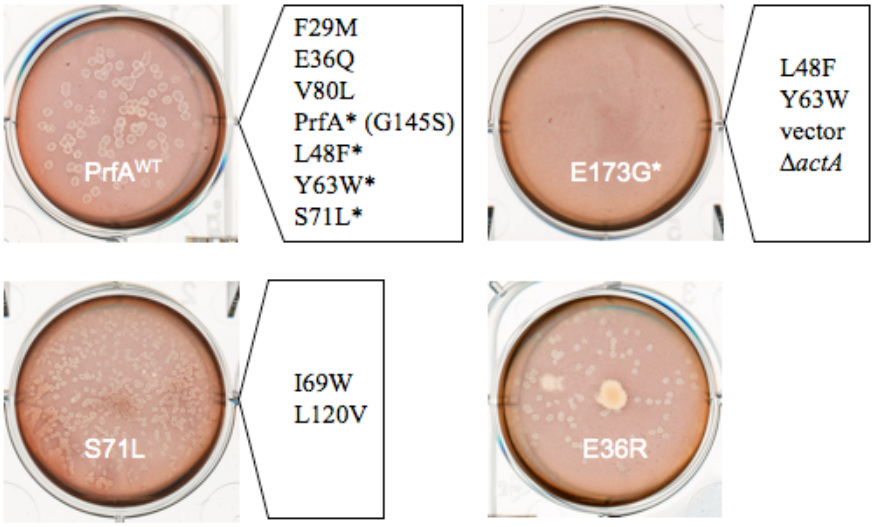

Figure 3.1.19: Visualization of the plaques of the PrfA pocket mutants.

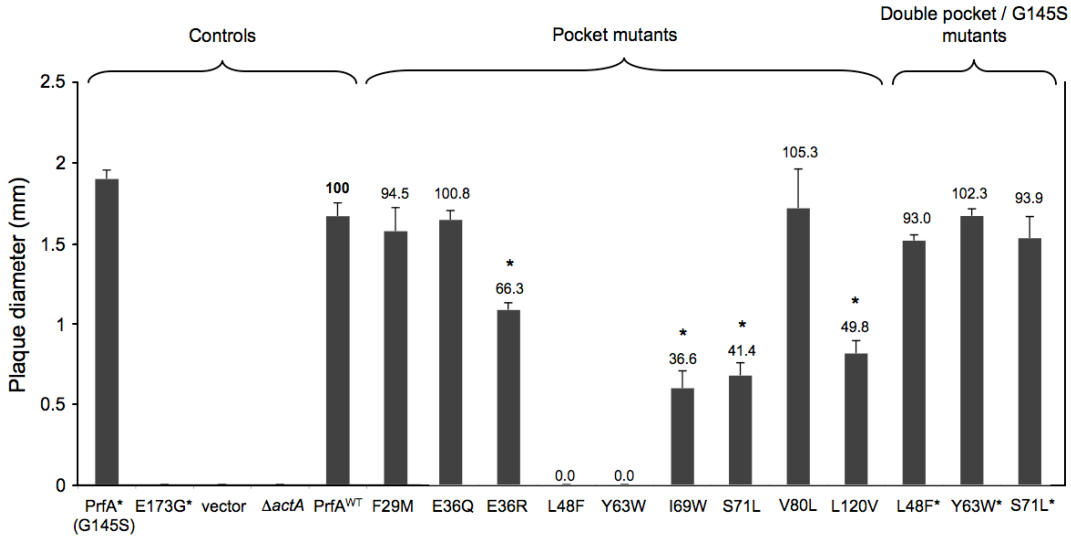

Figure 3.1.20: Cell-to-cell spread of the PrfA pocket mutants in murine L929 fibroblasts after 4-day incubation at 37ºC, represented by plaque size in mm.
Numbers above bars indicate the percentages of cell-to-cell spread in relation to the wild-type strain (which is 100%). Mean ± SE of at least two independent experiments. Statistical analyses were performed with Student's *t* test. *, $P \leq 0.01$.

3.1.1.3.2.5 Biochemical characterization

The hypothesis that the N-terminal pocket may serve as binding site for an activating ligand would be supported if the intracellular activation defects caused by the mutations were associated with minimal structural changes, not if they caused major perturbations in PrfA, resulting in global loss of function. To discriminate between these two situations, we expressed the mutant and control *prfA* alleles in *E. coli* and subjected the purified recombinant PrfA proteins to biochemical characterization (table 3.1). These experiments were coordinated by C. Deshayes and performed in part using our in-house protein biochemistry facilities (protein expression and purification in our laboratory, DNA-binding assays in the Biophysical Characterization Facility, Centre for Translational and Chemical Biology) and in the Department of Biochemistry of the University of Cambridge.

Analytical ultracentrifugation (AUC) was used to assess the dimeric state of PrfA, vital for transcriptional function. This separation technique gives an accurate estimation of the size of a protein in solution (Lebowitz *et al.*, 2002). The calculated molecular mass coincided for all proteins with the theoretical value of the PrfA dimer (54.56 kDa), indicating the mutations did not affect inter-protomer association (figure 3.1.21 and table 3.1). A PrfA mutant unable to form dimers, used here as a control, is described in section 3.1.1.4 (figure 3.1.29 and table 3.2).

The effect of the mutations on overall PrfA stability was assessed by a fluorescence-based thermal shift assay (TSA), in which the emission of the Sypro Orange fluorophore, quenched in aqueous solution, sharply increases in the nonpolar environment of the hydrophobic protein sites exposed upon thermally induced unfolding (Pantoliano *et al.*, 2001, Lo *et al.*, 2004, Ericsson *et al.*, 2006). Shifts in the temperature midpoint for protein unfolding (melting temperature, T_m) reflect differences in stability associated with mutation-induced conformational changes.

The T_m value for PrfA*^{G145S} was 7.2ºC lower than that of PrfA^{WT}, indicating that the structural changes associated with the G145S mutation (Eiting *et al.*, 2005)

make the hyperactive mutant protein slightly less stable. According to the TSA data, most of the mutations had no significant ($P > 0.01$) effect on PrfA stability (F29M, V80L, L120V, Y63W) or even caused a slight increase in the T_m (E36Q, E36R). I69W and S71L caused minor reductions in the T_m (4.25 and 7.4ºC below wild-type) but the values remained within the range of a functional PrfA protein (considering the T_m of PrfA*^{G145S}). Only the activation-null L48F mutation and the control null PrfA E173G* mutation affected more substantially protein stability (T_m 10.4 and 9.7 ºC lower than for PrfA^{WT}, respectively), but the T_m values still approximated those of PrfA*^{G145S} (table 3.1, table 3.2 in section 3.1.1.4).

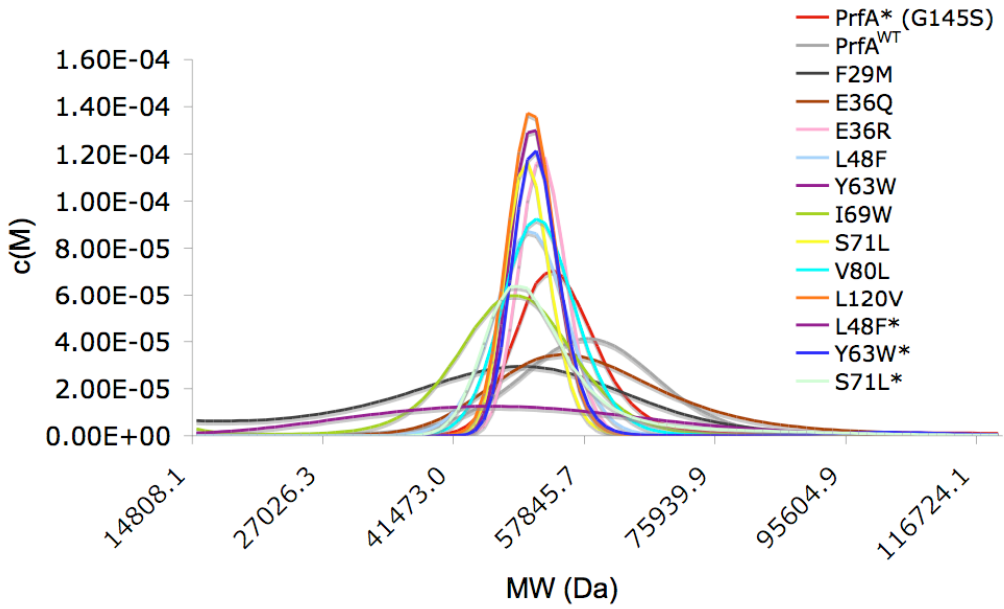

Figure 3.1.21: Dimerization assay by Analytical Ultracentrifugation (AUC) - targeted pocket mutants. MW = molecular weight in Daltons; c(M) = molar mass distribution coefficient. See also figure 3.1.29.

Finally, the surface plasmon resonance (SPR) technique enabled us to determine the specific DNA-binding activity using double-stranded DNA fragments containing the 14-bp PrfA boxes of P*plcA* and P*actA*. In order to assess the effect of the different mutations on the intrinsic ("off" or extracellular state) activity of the PrfA protein, the binding affinity of PrfA^{WT} served as a reference. If the mutation does not introduce major structural changes in PrfA, it is expected that this activity remains close to wild-type levels.

The calculated equilibrium dissociation constant (K_D) of $PrfA^{WT}$ for the P*plcA* promoter, 10.95 ±0.49 × 10^{-7} M, was very similar to that previously determined by Eiting *et al*. by SPR using the *hly* promoter (9.00 ±1.00 × 10^{-7} M) (Eiting *et al.*, 2005), which shares the same PrfA box with P*plcA*. The K_D value was also similar for P*actA* (13.63 ±0.24 × 10^{-7} M). Overall, our data show a good correspondence between the expression levels in BHI (figure 3.1.17) and the DNA binding activity of the respective PrfA proteins (table 3.1). $PrfA^{F29M}$ and $PrfA^{I69W}$, for example, had an intrinsic activity between three and five times greater than $PrfA^{WT}$, consistent with the elevated levels of basal PrfA-dependent expression in BHI and the partial PrfA* phenotype displayed by the bacteria expressing the corresponding alleles. $PrfA^{S71L}$, which caused partial PrfA* phenotype on agar plates, also showed a slightly increased DNA-binding activity for both target sequences. Of the two activation-null mutations, L48F associated with significantly reduced intrinsic DNA-binding activity (between 79 and 93%) whereas this parameter remained unaffected for Y63W (table 3.1).

Thus, with the possible exception of L48F, which associated with a significantly impaired intrinsic DNA-binding activity and somewhat reduced thermal stability, the PrfA pocket mutations did not seem to significantly affect basic structure-function properties of PrfA, apart from the observed defects in intracellular activability.

3.1.1.3.2.6 Double N-terminal pocket-C-terminal α-D G145S* mutant bacteria

In order to find out whether the intracellular activation-deficient mutations act mainly locally in the surroundings of the β-barrel or affect more generally the PrfA structure, we decided to analyze their effects in a $PrfA^{*G145S}$ protein. The

Table 3.1: Biochemical analysis of the PrfA pocket mutants.
For the dimerization assay, the apparent molecular weight (MW) of the proteins has been taken from the ordinate maximum of the c(M) distribution (see figure 3.1.21). Thermal denaturation midpoint temperature (T_m) was determined by a thermal shift assay, monitoring the fluorescence enhancement of the hydrophobic reporter dye SYPRO Orange. The equilibrium dissociation constants (K_D) for each purified PrfA protein was determined in a Biacore apparatus using as target the PrfA boxes of the P*plcA* and P*actA* promoters; relative binding affinities with respect to PrfA^{WT} are indicated in percentage. See Materials and Methods for details. Values are mean of three replicates (± standard deviation [SD] where relevant). Data for the "non-binding" control PrfA*^{E173G} mutant are in table 3.2. No precise K_D values are given for the constitutively hyperactive PrfA*^{G145S} mutant; likely due to the avidity for its target sequence, its dissociation rate was below the detection limit and could not be reliably quantified with the Biacore instrument. The same problem was previously reported for PrfA*^{G145S} (Mauder *et al.*, 2006); nd = not determined.

				Specific DNA-binding affinity			
	Dimerization		Thermal stability	P*plcA* box		P*actA* box	
	MW (Da)	% peak integration	T_m (ºC)	K_D (nM)	% PrfA^{WT}	K_D (nM)	% PrfA^{WT}
PrfA^{WT}	58300.18	95.49	61.75 ±1.30	1095.96 ±49.58	**100**	1363.18 ±24.10	**100**
F29M	48971.47	96.04	59.83 ±0.29	287.51 ±4.47	381	267.15 ±15.00	510
V80L	51961.09	92.57	62.00 ±0.00	1785.43 ±47.30	61	1404.14 ±54.05	97
E36Q	59365.22	85.33	65.50 ±0.50	1356.25 ±11.40	81	801.02 ±6.74	170
E36R	52037.49	86.78	66.50 ±0.50	1445.11 ±12.62	76	1078.95 ±10.31	126
I69W	49035.53	92.85	57.50 ±0.00	346.94 ±4.28	316	392.13 ±7.65	348
S71L	50300.96	83.30	54.33 ±0.29	695.14 ±4.24	158	740.52 ±5.93	184
L120V	50667.43	92.28	60.17 ±0.29	3122.77 ±36.67	35	1586.28 ±16.74	86
L48F	50440.53	90.87	51.33 ±0.29	5264.91 ±100.87	21	20841.58 ±262.12	7
Y63W	50955.16	84.35	59.33 ±2.02	1158.36 ±8.61	95	1660.02 ±14.28	82
S71L*	51354.84	72.88	nd	74.81 ±1.14	1465	66.87 ±11.96	2039
L48F*	49801.70	93.27	nd	14.89 ±0.5	7362	238.79 ±6.03	571
Y63W*	51318.86	83.03	nd	9.43 ±0.33	11617	28.68 ±0.28	4754
PrfA*^{G145S}	54352.46	83.93	54.50 ±1.00	≤ 1	-	≤ 1	-

G145S mutation lies in αD in the C-terminal domain and results in a constitutively activated PrfA form not by allostery but through local structural rearrangements that lead to a realignment of the adjacent DNA-binding α-helices of the HTH motif (figure 3.1.8; also schematized in figure 3.1.22) (Vega *et al.*, 2004, Eiting *et al.*, 2005). This approach assumes that the changes introduced by the PrfA*^{G145S} mutation remain mainly local, confined to the C-terminal DNA-binding domain, but (inevitably in such a compact molecule) there are some "retrograde" effects at the level of the inter-domain region and the N-terminal domain (figure 3.1.22), mainly realignment of a few degrees of the long inter-subunit αC (Eiting *et al.*, 2005).

Nevertheless, such double mutant approach should allow determining whether it is possible to dissociate the effects of the pocket mutations in the N-terminal domain from those of the G145S mutation in the C-terminal DNA-binding domain. If dissociation is possible and the pocket mutants do not abolish (or even better, alter significantly) the DNA-binding activity of the PrfA*^{G145S}, it would be an indication that the non-activability associated with the binding site mutations is mainly due to local blockage of the pocket. If dissociation is not possible, we would not be able at this stage to say anything more definite regarding the mechanism of the pocket mutations.

For the analysis, three mutants were chosen: S71L, in which the point mutation strongly affects PrfA's intracellular activability, and L48F and Y63W, in which the single substitutions almost completely abolish it.

The double mutants S71L*, L48F* and Y63W* showed a strong PrfA* phenotype on agar plates (figure 3.1.18). They also showed elevated basal (BHI) PrfA-dependent expression levels (figure 3.1.17) and the same levels of cell-to-cell spread of *prfA**^{G145S} (figures 3.1.19 and 3.1.20). The corresponding PrfA proteins bound 17 to 81 times more tightly than PrfA^{WT} to the target DNA (table 3.1).

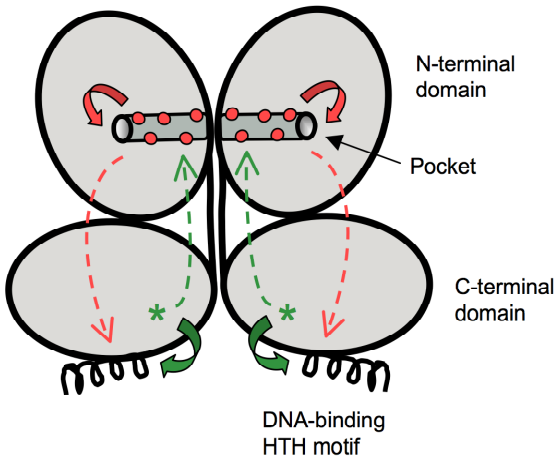

Figure 3.1.22: Schematic representation of the PrfA dimer with indication of the relevant structures, mutations and issues involved in the "pocket-PrfA*^{G145S} double mutant strategy.
Binding pocket mutations are represented as red dots, the PrfA*^{G145S} mutation as a green asterisk. Direct effects of the mutations are represented as solid red arrows, possible indirect or "retrograde" effects exerted on more distant parts of the molecule as broken arrows (originating from the pocket mutations in red, from the G145S mutation in αD in green). See text for details.

These data are consistent with the intracellular activation-deficient phenotype caused by the pocket mutations being mainly associated with local structural changes confined to the β-barrel environment.

3.1.1.3.3 Discussion

3.1.1.3.3.1 Activation negative mutations L48F and Y63W

The activation of PrfA-dependent genes in infected HeLa cells was almost completely abolished due to the L48F and Y63W substitutions (mean intracellular expression < 10% of wild-type levels). This correlated with total loss of cell-to-cell spread capacity, a strictly PrfA-dependent virulence trait (Freitag *et al.*, 1993, Scortti *et al.*, 2007) (see figures 3.1.19 and 3.1.20). Both substitutions are predicted to partially occlude the entrance of the distal chamber of the pocket (figure 3.1.15), suggesting that steric access to the cavity is important for mediating the activation response.

In L48F, the new phenylalanine is predicted to make close hydrophobic contacts with Y83 (2.9Å) and F29 (3.8Å) from the same monomer, and L128 (3.3Å) in the other monomer, which represent steric clashes since the distances are smaller than the summed van der Waals radii (3.4Å in the case of two carbon atoms). This implies that the accommodation of the L48F substitution involves substantial adjustments in the PrfA structure and, likely also, in the relative position of the two monomers. Indeed, modelling calculations carried by our collaborator R. Núñez Miguel showed that, while the accessible surface area (ASA) remains unchanged, the gap volume at the dimer interface is increased in $PrfA^{L48F}$ compared to $PrfA^{WT}$ (data not shown), suggesting that the mutation moves the two monomers slightly apart. Consistent with this, $PrfA^{L48F}$ shows a significantly impaired intrinsic DNA-binding activity (> 80% reduction) and decreased thermal stability compared to $PrfA^{WT}$ (table 3.1). Dimerization is, however, not affected and the stability, albeit reduced, is still comparable to that of the constitutively hyperactive PrfA* protein. Moreover, the double $PrfA^{L48F*G145S}$ mutant protein retains much of the PrfA* activity caused by the G145S mutation. Thus, although introducing substantial perturbations, the L48F mutation appears to preserve the basic structural integrity of PrfA, supporting the notion that the activation-negative phenotype of $PrfA^{L48F}$ may be related, at least in part, to the incapacity of an allosteric effector molecule to productively interact with the mutant pocket.

Residue Y63 lies in the proximal end of the distal chamber with its hydroxyl group directly exposed at the surface of the cavity, where it may contribute to stabilizing the interaction with a putative ligand via polar contacts. In addition, the indole ring in the rotameric state of the newly introduced tryptophan that formed less steric clashes with the surrounding residues is predicted to partially penetrate into the distal chamber (figure 3.1.15). Besides not abolishing the PrfA* phenotype of $PrfA^{*G145S}$, Y63W, in contrast to L48F, did not affect any of the protein biochemical parameters analyzed (dimerization, intrinsic DNA-binding activity, thermal stability). This suggests that the overall structural and functional integrity of PrfA is

not significantly altered, consistent with Y63W being a true binding pocket mutation specifically affecting the intracellular activability of the listerial regulator.

3.1.1.3.3.2 Activation deficient mutations I69W, S71L and L120V

Three mutations caused a significant but incomplete impairment of intracellular activability of PrfA-dependent genes (~ 23 to 60%) of wild-type mRNA levels in average) and a similar reduction in cell-to-cell spread efficiency (37 to 50%). None of these mutations significantly affected the structural parameters of the protein. In I69W and S71L the new larger side chains are predicted to partially obstruct the internal cavity, at the entrance of the distal chamber and access channel, respectively (figure 3.1.15), suggesting that a fully accessible pocket is required for PrfA intracellular activation. Interestingly, compared to $PrfA^{WT}$, $PrfA^{I69W}$ shows a significantly increased intrinsic transcriptional activity (~ 140%) and DNA-binding affinity (332%) (table 3.1) as well as partial PrfA* phenotype on EYA and SBA plates (figure 3.1.18). In I69W, the penetration of the bulky flat aromatic face of the tryptophan into the pocket and the clashes and/or new hydrophobic interactions with neighbouring residues (figure 3.1.15) may trigger structural changes that partially mimic the allosteric effects associated with the accommodation of a ligand. A similar interpretation can be given to the increased DNA-binding activity (~ 171%) and partial PrfA* phenotype associated with the S71L mutation. In this case these effects are not reflected in the RT-QPCR data, possibly because weaker than with I69W. Transcription analyses only capture steady-state mRNA levels at a specific time point, and the slightly increased DNA-binding affinity of $PrfA^{S71L}$ may only give a detectable phenotype in bacterial colonies by cumulative effect.

L120 is on αC at the monomer-monomer interface and forms part of the hydrophobic surface of the distal chamber (figure 3.1.15). Valine has a β-branched side chain with restricted rotamer choice on a helix and substitution to this shorter residue was expected to affect the shape of the pocket without altering the position of the helix. Consistent with this, dimerization was not affected in $PrfA^{L120V}$ and can be excluded as the origin of the phenotype. The loss of function is not due either to

PrfA^{L120V} instability, since it has the same thermal denaturation profile as PrfA^{WT}. If a wild-type distal end of pocket is required for the correct positioning of a ligand, in the deeper L120V mutant pocket the small molecule may penetrate further inside and "push" the central αC helices apart (figure 3.1.15), disrupting in the liganded conformation the correct protomer alignment and positioning of the C-terminal HTH motif.

3.1.1.3.3.3 Electronegative patch mutations E36Q/R

A portion of the pocket entrance is strongly electronegative (figure 3.1.12) and the charge may influence the delivery of a small molecule into the cavity, or form stabilizing interactions with a putative ligand once bound. To test this possibility, we substituted the negatively charged residue E36 at the mouth of the pocket with a neutral but polar amide (glutamine) or with a positively charged side chain (arginine). The E36Q substitution had little or no effect, but E36R resulted in a ~ 20% (P*plcA*) to ~ 40% (P*actA*) reduction in intracellular activation respect to PrfA^{WT}, similarly reflected at the level of cell-to-cell spread (~ 34% reduction), with no significant effects on intrinsic DNA-binding activity or protein stability (figure 3.1.17, 3.1.19, 3.1.20, table 3.1). We conclude that the electronegative patch at the entrance of the pocket may play some role in PrfA intracellular activation but is unlikely to be critical. Besides altering the charge, a rotameric state of the new arginine also introduces a bulkier side chain that partially occludes the entrance (figure 3.1.15).

3.1.1.3.3.4 Neutral F29M and V80L mutations

F29M was anticipated to change the shape of the wall of the pocket at a constriction in the middle of the channel (figure 3.1.15, 3.1.16). Our data indicate that the flexible methionine side chain replacing the bulky and more rigid phenylalanine is conformationally accommodated in the active (intracellular) PrfA form. They also suggest that interactions with a hypothetical ligand are unlikely to be dominated by aromatic stacking interactions on the surface of the phenylalanine.

$PrfA^{F29M}$ bound 3.8 to 5.1 times more tightly to the PrfA box, had about three times the intrinsic transcriptional activity of $PrfA^{WT}$ and exhibited PrfA* phenotype on agar plates (figure 3.1.17, 3.1.19, 3.1.20, table 3.1), indicating that like for the I69W and S71L substitutions, the structural changes introduced by the new methionine may partially mimic those affiliated with PrfA activation.

V80, on the other hand, occupies a dominating part of the hydrophobic surface of the distal chamber. Leucine was chosen to satisfy the criteria that the substitution produces little perturbation of the local structure while still being capable of modifying the pocket topology. The absolute neutrality of the mutant suggests that the V80L substitution is perfectly accommodated both in the off (apo) and on (liganded) PrfA conformations.

3.1.1.3.3.5 Concluding remarks

Two of the nine structure-guided, site-directed mutations analyzed (figures 3.1.15 and 3.1.16), L48F and Y63W, exhibited a phenotype consistent with the PrfA pocket serving as binding site for an activating ligand. Y63W satisfied all the criteria for a *bona fide* allosteric activation-negative mutation, *i.e.* abolition of intracellular activability with no other detectable structure-function alterations in PrfA that could explain the functional loss by reasons other than local structural changes in the pocket.

L48F and Y63W target residues in the distal section of the pocket, which forms an enlarged chamber leaning against the two central C-helices that provide most of the monomer interface and connect the protomer's N-terminal and C-terminal (DNA-binding) domains (figures 3.1.11, 3.1.13, 3.1.15 and 3.1.16). Another mutation at the distal end of the chamber, L120V on αC, and two other mutations near the distal chamber's entrance, S71L and I69W, also significantly impaired intracellular virulence gene activability without causing major overall structural alterations in the protein (figure 3.1.17), further suggesting a specific role for the inner section of the solvent-exposed pocket in PrfA allosteric activation.

The distal chamber contacts the αC helices near where they tilt by 11º and straighten in the activated PrfA* (G145S) form. This brings the C-terminal ends of the C-helices towards each other, "tightening" the dimer, a movement likely to play a key role in the conformational readjustments of the C-terminal DNA-binding domain involved in PrfA activation (Eiting *et al.*, 2005). Indeed, the αC helices at the C-terminus of the CNB domain are critically involved in the transmission of the allosteric signal to the effector domains in cAMP-regulated proteins. This involves a movement towards the cAMP-liganded pocket in the case of the shorter αC "lid" of the mammalian CNB domains (Rehmann *et al.*, 2007), or the packing of the liganded β-barrel against the elongated interdimeric αC helices in the enterobacterial and mycobacterial Crp transcription factors (Popovych *et al.*, 2009, Reddy *et al.*, 2009). Conceivably, penetration of a ligand in the distal chamber may directly affect the relative alignment of the monomers by altering the spatial relationships at the point where the two central C-helices lie closer to each other (figure 3.1.13). Attraction of a flap formed by the β4-β5 antiparallel hairpin of the β-barrel towards the liganded pocket, as observed in the cAMP-Crp complex (Popovych *et al.*, 2009), may also contribute to monomer realignment via contacts between the flap and the C-terminal end of αC' from the opposite monomer (figure 3.1.23).

The observed elevation in the basal (extracellular) activity with the F29M, I69W and S71L mutations also supports a role for the N-terminal pocket in PrfA allostery. The activity increase is modest compared to that caused by the G145S (and L140F) PrfA* mutation in αD (Vega *et al.*, 2004), which acts locally on the adjacent HTH motif in the C-terminal domain (Eiting *et al.*, 2005). A weaker intrinsic activity compared to PrfA*^{G145S} has been previously observed for other PrfA* mutations in the β-roll, such as I45S (Vega *et al.*, 2004) or Y63C (Miner *et al.*, 2008b). We interpret that the partial PrfA* phenotype of F29M, I69W and S71L may arise from conformational adjustments in the pocket that partially mimic the ligand-bound state.

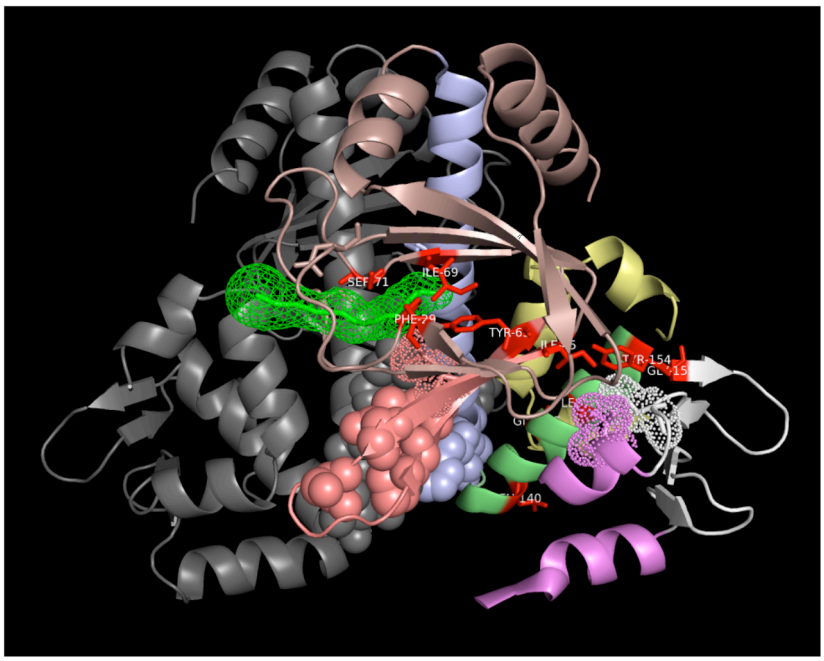

Figure 3.1.23: Allosteric "transmission chain" of PrfA and possible main contacts involved.
Cartoon representation of the crystal structure of PrfA with the CAVER output represented in green mesh indicating the position of the pocket within the N-terminal β-barrel. One monomer is coloured in grey, the other monomer is coloured according to structural features: β-barrel plus αA and αB in dark salmon, αC in light blue, αD helix in green, HTH in magenta, C-terminal GHI α-helical bundle in yellow, rest of monomer in white. Residues in which PrfA* mutations have been characterized (including those described in this study), *i.e.* F29, I45, Y63, I69, S71 and L140, G145, L148, Y154 and G155, are represented as red sticks. The β4-β5 "flap" of the β-barrel is highlighted in deep salmon. Residues of the flap that establish contacts with residues from αC and αC' are in sphere representation. The atomic volumes of the residues from the C-terminal domain in direct contact with the "allosteric transmission chain" (see text for details) are in dot representation. Constructed using MacPyMOL.

Mapping all the PrfA* mutations characterized to date in the PrfA 3D structure reveals a possible allosteric "transmission chain" between the pocket and the C-terminal domain via two key residues at the base of the β4-β5 flap, I45 and Y63 (figure 3.1.23). This allosteric signal path may contribute, alongside the repositioning of the C-helices, to the coordinated set of structural motions required for the correct alignment of the HTH binding helices in the active PrfA conformation.

Our data provide strong experimental support to the notion that PrfA is allosterically activated via a putative ligand-binding pocket in its N-terminal domain.

The shape and physicochemical characteristics of the pocket suggest that it could bind a relatively hydrophobic, elongated molecule with an aromatic head and aliphatic tail. The identification of the putative PrfA-activating ligand may lead to the development of inactive analogues that could serve as potent *Listeria* anti-infectives.

3.1.1.4 Analysis of spontaneously occurring *prfA* mutations

3.1.1.4.1 Background

NCTC 7973 is a well-known collection strain of serovar 1/2a, widely used in research laboratories worldwide and proposed as the type strain of *L. monocytogenes* in replacement of SLCC 53^T (ATCC 15313) (Jones & Seeliger, 1983, Seeliger & Jones, 1986). The latter is non-haemolytic and displays a multiple deficiency in virulence-associated phenotypes. This is due to a spontaneous deletion in the *prfA* gene (Mengaud *et al.*, 1991), therefore, it is not a good representative of the species (Kathariou & Pine, 1991, Ripio *et al.*, 1996). NCTC 7973 was chosen because, in contrast to the official type strain, it was strongly haemolytic and virulent. Early work from our group established, however, that NCTC 7973 was also a spontaneous mutant and did not display the true wild-type phenotype of *L. monocytogenes*. It was not weakly haemolytic, as is typical for wild-type *L. monocytogenes*, but hyperhaemolytic, and also overexpressed other virulence-associated factors, such as PlcB, giving a wide halo of lecithinase activity on EYA (Ripio *et al.*, 1996). The strain was found in fact to be a spontaneous *prfA** mutant carrying the G145S mutation (Ripio *et al.*, 1997a).

NCTC 7973 also carried a second mutation in *prfA*, C229Y, located in the loop between αH and αI helices of the C-terminal α-helical extension. Interestingly, this second mutation was always found in spontaneous *prfA** mutants from serovars

1/2a, 3a and 1/2c, *i.e*. belonging to *L. monocytogenes* phylogenetic division II. This was in contrast to *prfA** spontaneous mutants of phylogenetic division I, *e.g*. serovar 4b, which only carried a single residue substitution, typically G145S. On trans-complementation of a Δ*prfA* strain with a multicopy plasmid, both *prfA** alleles, *i.e*. *prfA**^{G145S} and *prfA**$^{G145S/C229Y}$ conferred a strong PrfA* phenotype in standard EYA and SBA. The intensities of the reactions tended, however, to be somewhat weaker with the strains carrying the natural *prfA**$^{G145S/C229Y}$, like NCTC 7973 (unpublished observations from our laboratory). The reason and functional impact of the second C229Y mutation in *prfA**^{G145S} mutant alleles of division II *L. monocytogenes* bacteria remains unknown.

Strain NCTC 7973 was used by Park and Kroll (1993) in the study that first showed that cellobiose represses PrfA-dependent expression. These authors found that *hly* and *plcA* gene expression was strongly downregulated when the bacteria were grown in the presence of this β-glucoside sugar, but not with other fermentable carbohydrates, such as glucose. This same effect was observed with another β-glucoside, arbutin (Park, 1994). On the basis of these observations it was concluded that β-glucosides, plant derived sugars presumably abundant in soil rich in decaying vegetation, are used by *L. monocytogenes* as signalling molecules to identify its presence in the natural environment, *i.e*. outside a host where virulence factors are not needed (Park & Kroll, 1993). It has to be emphasized that at the time these experiments were carried out, it was not known that NCTC 7973 was a *prfA** mutant nor that it carried a specific subtype of *prfA** allele with a second mutation.

Later work from our laboratory, carried out using a wide collection of truly wild-type *L. monocytogenes* strains, plus the *prfA** mutants P14A (single substitution G145S) and NCTC 7973 (double G145S/C229Y substitution), demonstrated that the latter in fact responded anomalously to sugars (see figure 3.1.24). Wild-type strains (*e.g*. EGD, the strain used by the European *Listeria* Genome Consortium for sequencing) were repressed not only by β-glucosides but also by glucose and all other fermentable sugars tested. As wild-type *L. monocytogenes* expresses virulence genes very weakly at 37ºC *in vitro*, to observe the repressor effect of sugars in its

true dimension, it was necessary to grow the bacteria in the presence of activated charcoal (Ripio *et al.*, 1997b, Brehm *et al.*, 1999). This adsorbent, as explained in section 3.1.1.2, activates PrfA-dependent expression (Ermolaeva *et al.*, 2004). Strain P14A, producing a constitutively hyperactive PrfA* protein, was found to be insensitive to sugar-mediated repression, including cellobiose (Ripio *et al.*, 1997b). This observation was extended to other *prfA** mutants with single amino acid substitutions (Vega *et al.*, 2004).

Interestingly, the repressor effect of sugars was not observed with hexose phosphates, which are taken up by *L. monocytogenes* via Hpt, a non-PTS permease (Ripio *et al.*, 1997b). This supported the notion that sugar-mediated repression of *L. monocytogenes* virulence genes may represent an aspect of the global catabolite repression response with collateral regulatory effects on the PrfA system (Milenbachs *et al.*, 1997). It was, therefore, speculated that the abnormal behaviour of NCTC 7973, in which only cellobiose and arbutin, not other PTS-transported sugars, repress *L. monocytogenes* virulence genes, could be due to a specific mutation in a specific mechanism(s) responding to β-glucosides (Behari & Youngman, 1998b, Brehm *et al.*, 1999, Milenbachs Lukowiak *et al.*, 2004).

In this study, we investigated the functional consequences of the C229Y mutation in PrfA. We also tested the hypothesis that the differential response to sugars of NCTC 7973 could be solely due to the presence of the second C229Y mutation in its *prfA**$^{G145S/C229Y}$ allele, with no involvement of other unidentified mutations.

As part of our ongoing investigations into PrfA structure-function, in this chapter we also functionally and biochemically characterized two additional spontaneous mutations identified in our laboratory as *prfA** suppressor (*prfA**^{sup}) mutations, A129T in the C-terminal third of αC, and E173G at the beginning of αE of the DNA-binding HTH motif.

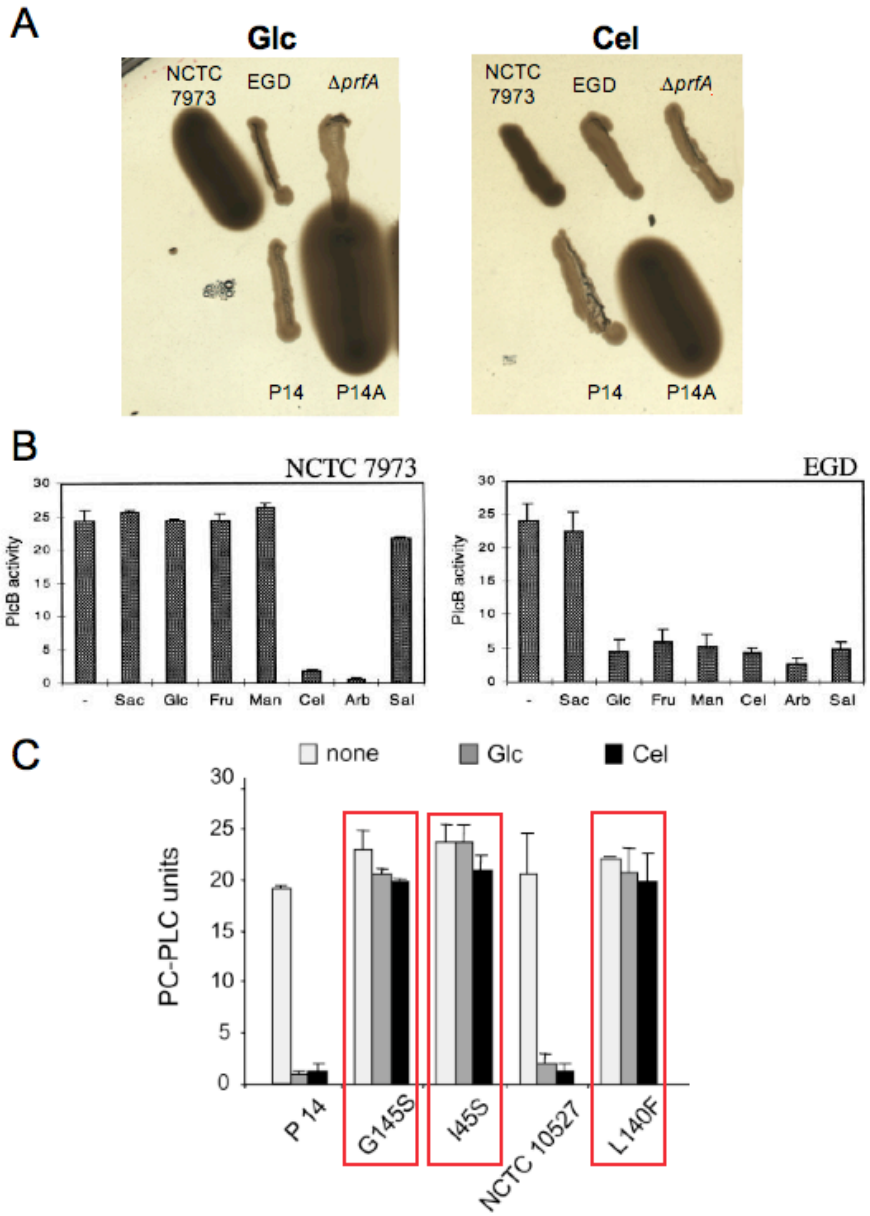

Figure 3.1.24: Differential response of NCTC 7973 virulence genes to sugars.
(A) *L. monocytogenes* strains streaked on Luria Bertani (LB) agar with 10% egg yolk and Tris 0.5 M (pH = 7.2) supplemented with 25 mM sugar: left panel, glucose (Glc); right panel, cellobiose (Cel). Strains shown: NCTC 7973 (*prfA*$^{*G145S/C229Y}$), EGD and P14 (*prfA*^{WT}), P14A (*prfA*^{*G145S}), Δ*prfA* (*prfA* deletion mutant of P14, negative control). Unpublished data from our laboratory: plates prepared by Katherine Norrby.
(B) Patterns of *plcB* repression in response to sugars in *L. monocytogenes* NCTC 7973 and EGD (Sac, saccharose; Glc, glucose; Fru, fructose; Man, mannose; Cel, cellobiose; Arb, arbutin, Sal, salicin; -, no sugar; Cel, Arb and Sal are β-glucosides). Taken from Brehm *et al.* (1999).
(C) Refractory effect of *prfA** mutations (G145S, I45S, L140F; indicated by red rectangles) to PrfA regulon repression by sugars, as determined using the *plcB* natural reporter system. The wild-type strains P14 and NCTC 10527 are strongly repressed by fermentable sugars such as glucose (Glc) and cellobiose (Cel), whereas the *prfA** mutants (boxed in red) are not repressed. PC-PLC units indicate the activity of the *plcB* gene product used as a reporter to measure PrfA-dependent expression. Taken from Vega *et al.* (2004).

3.1.1.4.2 Results and Discussion

3.1.1.4.2.1 General strategy

We followed here the same mutant characterization approach as used in the previous section for the targeted mutants in the N-terminal PrfA pocket. This included the construction of monocistronic *prfA* alleles carrying the natural mutant genotype in the *prfA**^{G145S} context (*i.e*. double mutants), or the investigated mutation alone (*i.e*. single mutants) in a *prfA*^{WT} context (table 5.1). Each of the alleles was integrated in single copy in the chromosome of a *prfA* deletion mutant (Δ*prfA*) to analyze the functional consequences *in vitro* in culture medium and during intracellular infection in HeLa cells. PrfA activity was monitored by RT-QPCR (figure 3.1.25) and also *in vitro* on EYA and SBA using the *plcB* and *hly* genes as natural reporters (figure 3.1.26). The impact of the mutations on virulence was measured using a plaque assay (figures 3.1.27 and 3.1.28). Western immunoblotting with an anti-PrfA antibody was used to verify that the complemented strains produced equivalent amounts of PrfA proteins (data not shown).

All the alleles were also expressed in *E. coli* and the mutant proteins purified and functionally and biochemically characterized (DNA-binding activity, dimerization, structural stability; table 3.2, figure 3.1.29).

In addition, we investigated the growth kinetics of the mutants in broth medium (figure 3.1.30). We carried out these experiments because we noticed that a PrfA* genotype/phenotype associates with growth defects, which are reversed to wild-type growth upon deletion of the *prfA** allele and its replacement by *prfA*^{WT} (unpublished observations from our laboratory).

Finally, for C229Y, specific experiments were conducted to investigate the effect on sugar-mediated PrfA-dependent gene repression (figure 3.1.32). These are described in detail in the following section.

Figure 3.1.31 shows the localization of the spontaneous mutations in the PrfA structure.

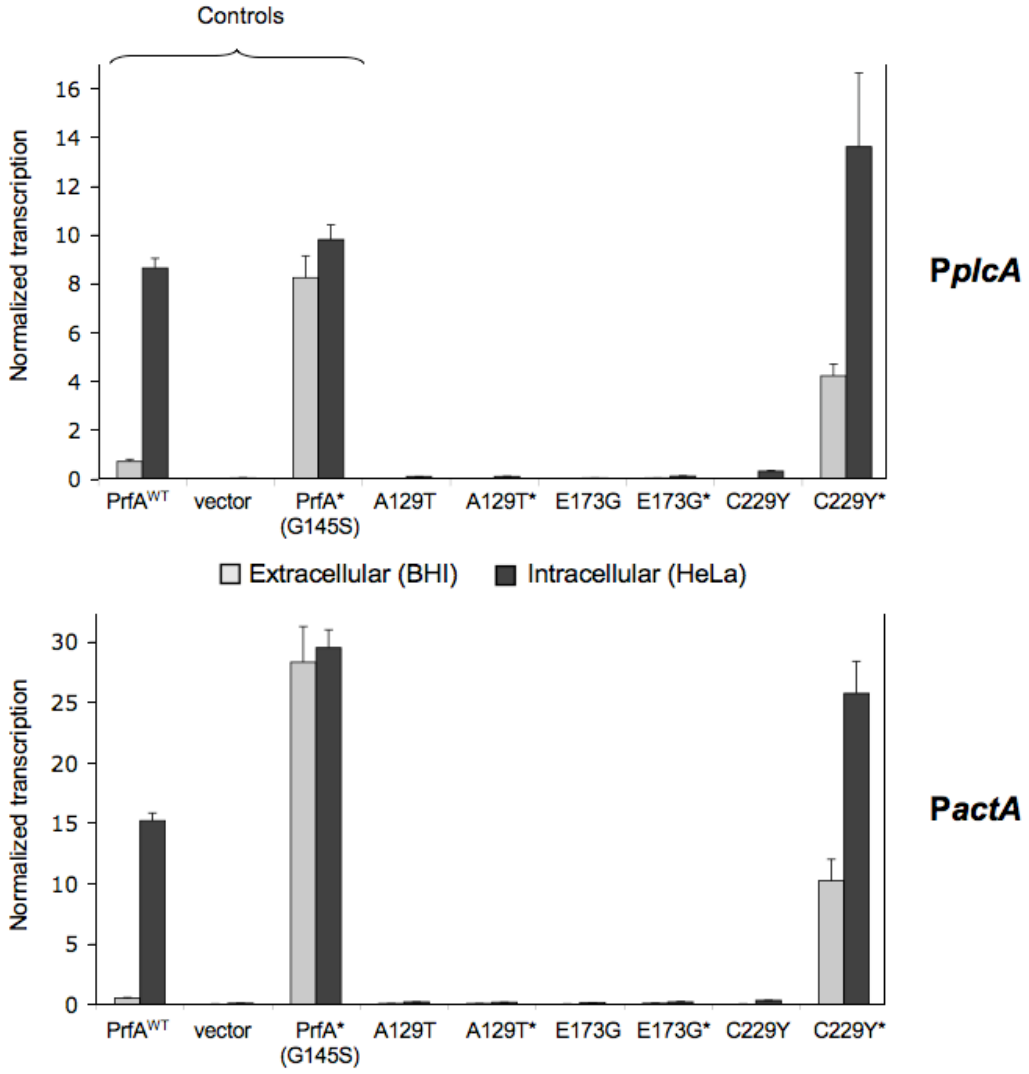

Figure 3.1.25: Transcriptional analysis of the PrfA mutants.
The transcription of *plcA* (upper panel) and *actA* (bottom panel) genes has been quantified by RT-QPCR in extracellular conditions (OD_{600} = 0.3 in BHI broth) and intracellular conditions (infection of human HeLa epithelial cells for 6 h post-infection). The transcription levels have been normalized by the number of bacteria and the level of transcription of the *ldh* housekeeping gene. Error bars indicate ± SE of at least three independent experiments.

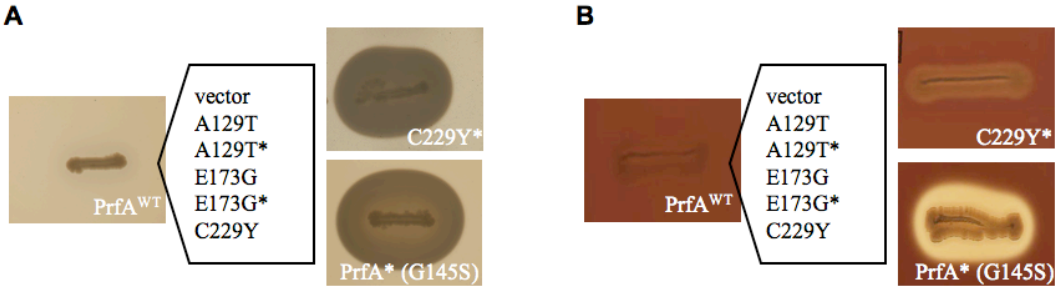

Figure 3.1.26: Phenotype conferred by the spontaneous PrfA mutations.
Pictures taken from representative agar plates incubated at 37ºC for 72 h. (A) PlcB phenotype of the PrfA mutants grown on BHI EYA plates; (B) Hly phenotype grown on SBA plates (see text for details).

3.1.1.4.2.2 Characterization of the C229Y mutation

To dissect the role of the C229Y mutation in PrfA, we constructed mutant *L. monocytogenes* strains expressing either the *prfA*$^{*G145S/C229Y}$ allele, as present in NCTC 7973, or the *prfA*^{C229Y} allele with no *prfA*^{*G145S} mutation. To simplify, the mutations or strains carrying these are designated hereafter C229Y* and C229Y, respectively. On agar plates, the former allele conferred, as expected, a clear PrfA* phenotype, albeit somewhat weaker in intensity compared to *prfA*^{*G145S} in both EYA and SBA (figure 3.1.26). Consistent with the phenotype on agar plates, the RT-QPCR data showed that the C229Y* allele associates with high extracellular expression levels (BHI, *i.e.* spontaneous activity) from both PrfA-dependent gene promoters, although not as high as with *prfA*^{*G145S} (respective fold-values relative to *prfA*^{WT}: P*plcA*, 6.01 and 11.76; P*actA*, 21.22 and 58.92) (figure 3.1.25).

Therefore, the second C229Y mutation appears to partially suppress the PrfA* phenotype conferred by the G145S mutation.

In intracellular (PrfA-activating) conditions, PrfA-dependent gene expression was significantly activated in the C229Y* mutant (3.23- and 2.52-fold for P*plcA* and P*actA*), up to levels comparable to those seen with the strains complemented with

prfA^{WT} and the constitutively activated *prfA**^{G145S} allele (figure 3.1.25). Interestingly, the single C229Y mutant showed no intracellular activability, suggesting that when this mutation is present alone it results in total loss of PrfA activity. Consistent with these observations, the double C229Y* mutant strain formed very visible plaques in the cell-to-cell spread assay, similar in size to those produced by the *prfA*^{WT} and the *prfA**^{G145S} bacteria (figures 3.1.27 and 3.1.28), whereas the single C229Y mutant did not.

The functional data correlated at the biochemical level with significantly increased (between 35.42- and 140.13-fold) and reduced (between 2.56- and 25.0-fold) DNA-binding activity for PrfA*$^{G145S/C229Y}$ and PrfA^{C229Y} compared to PrfA^{WT}, respectively. These results are entirely consistent with the RT-QPCR transcriptional data. No significant differences were observed for the two proteins in dimerization and thermal stability (table 3.2 and figure 3.1.29), suggesting that the C229Y mutation does not substantially alter the overall PrfA structure.

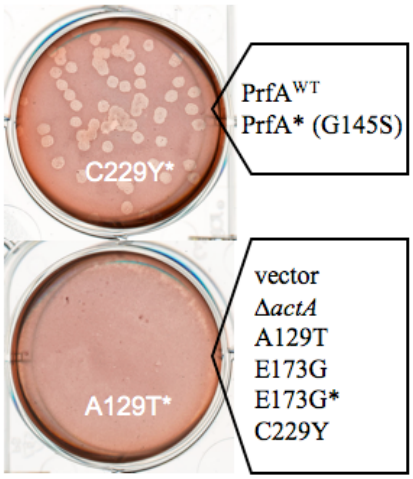

Figure 3.1.27: Visualization of the plaques of the PrfA mutants.
Note that C229Y behaves like the control cell-to-cell spread-negative bacteria Δ*prfA* complemented with an empty vector and Δ*actA*, indicating that PrfA^{C229Y} is inactive intracellularly. See also figure 3.1.28.

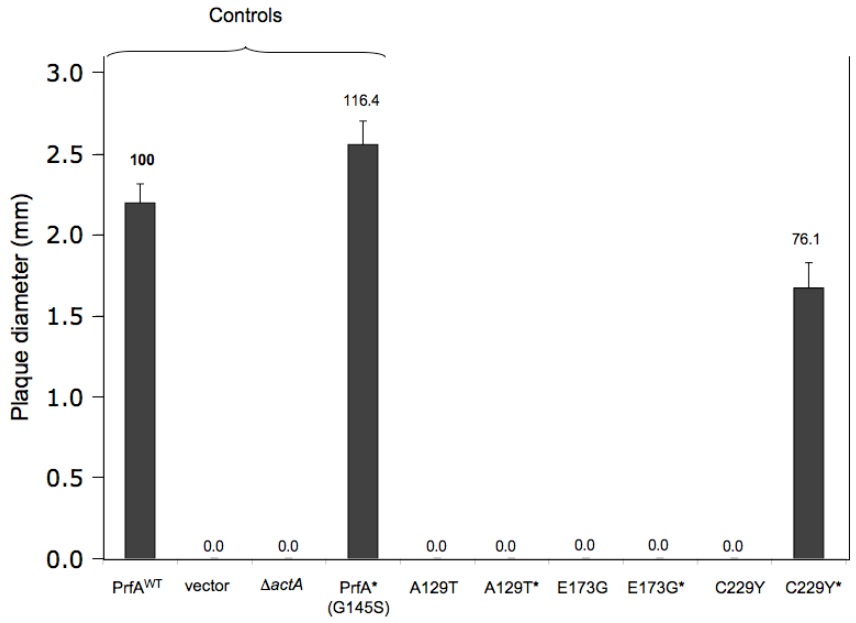

Figure 3.1.28: Cell-to-cell spread of the PrfA mutants in L929 fibroblasts after 5-day incubation at 37ºC, represented by plaque size in mm.
Numbers above bars indicate the percentages of cell-to-cell spread in relation to the wild-type strain (which is 100%). Mean ± SE of at least two independent experiments.

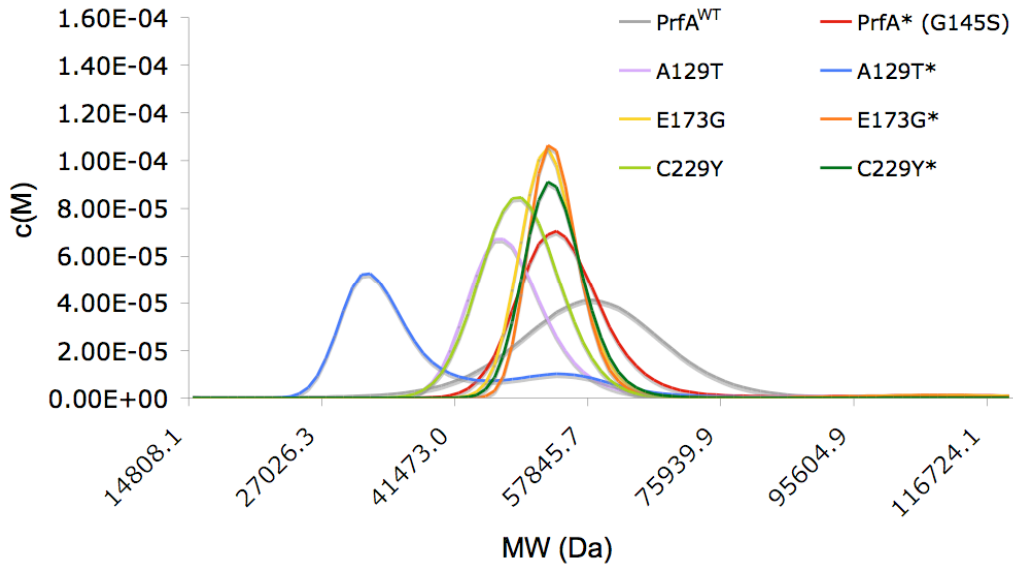

Figure 3.1.29: Dimerization assay by Analytical UltraCentrifugation (AUC) - spontaneous mutants. Graphs for PrfA^{WT} and PrfA* (G145S) have been extracted from the same experiment described in section 3.1.1.3.2.5. MW = molecular weight in Daltons; c(M) = molar mass distribution coefficient.

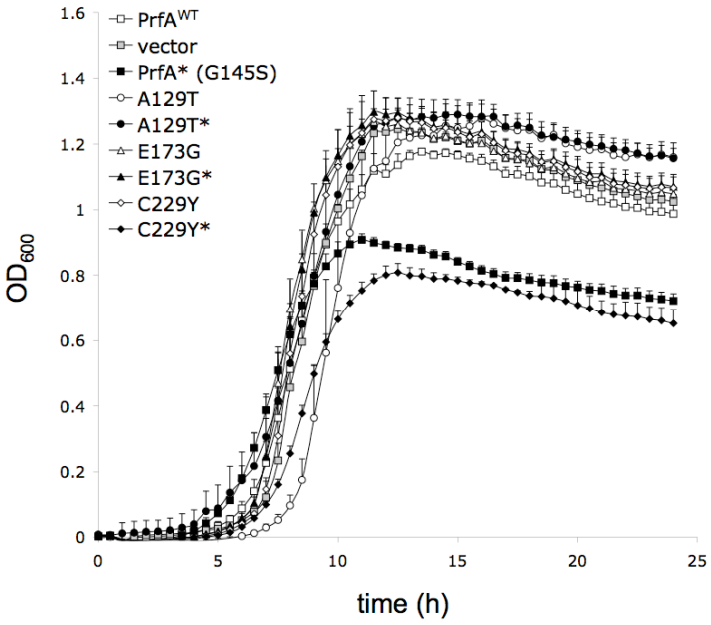

Figure 3.1.30: Growth kinetics of the spontaneous PrfA mutants in BHI broth at 37°C.
Probably because the constitutive overexpression of all genes of the PrfA regulon causes a substantial burden to the *L. monocytogenes* economy, *prfA** mutant bacteria consistently show a growth defect (unpublished observations from our laboratory). Note in the figure that despite the PrfA* phenotype being mitigated by the second C229Y mutation, the C229Y* mutant behaves similar to the reference *prfA*^{G145S} mutant. Mean of three experiments ± SD. Growth curves were obtained using a plate reader (see Materials and Methods).

Figure 3.1.31: Localization of the spontaneous mutation sites in PrfA^{WT} structure (PDB no. 2BEO).
PrfA^{WT} dimer shown in figure 3.1.23 (same colour codes for structural features) with the mutated residues highlighted in sphere representation: A129 in αC, marine blue; E173 in αE, hot pink; C229 in αH, orange. The Residue K25 in the loop between β1 and β2 of the N-terminal β-roll, which probably establishes an electrostatic interactions with E173, is also in sphere representation (dark salmon). The location of the G145S PrfA* mutation is indicated in red. Constructed with MacPyMOL.

Table 3.2: Biochemical analysis of the spontaneous PrfA mutants.
No dimerization defects were observed except for the PrfA*^{A129T} mutant protein, 47.9% of which was detected in monomeric form; the single-substituted PrfA^{A129T} was, however, a dimer. The E173G and C229Y mutant PrfA proteins, carrying also a G145S substitution, showed all a reduction in the thermal stability similar to that observed for PrfA*^{G145S} when compared to PrfA^{WT}. The least stable protein was the totally inactive PrfA*^{E173G} protein. For an unknown reason, the thermal stability of the A129T proteins could not be determined (indicated "nd"). Binding to the PrfA box was severely impaired in PrfA^{A129T}, PrfA*^{A129T}, and PrfA^{C229Y}; PrfA*^{E173G} strongly impaired binding, in contrast to the single-substituted PrfA^{E173G} mutant. See also legend to table 3.1.

	Dimerization		Thermal stability	Specific DNA-binding affinity			
				P*plcA* box		P*actA* box	
	MW (Da)	% peak integration	T_m (ºC)	K_D (nM)	% PrfA^{WT}	K_D (nM)	% PrfA^{WT}
PrfA^{WT}	58300.18	95.49	61.75 ±1.30	1095.96 ±49.58	**100**	1363.18 ±24.10	**100**
A129T	47814.09	71.92	nd	27162.75 ±419.36	4	37687.52816 ±744.77	4
A129T*	32257.30 53499.40	47.87 18.16	nd	32028.10 ±630.35	3	19039.13421 ±271.30	7
E173G	52763.20	81.93	58.17 ±0.29	1347.42 ±0.44	81	1695.308541 ±16.12	80
E173G*	53298.30	81.32	52.00 ±0.50	10518.48 ±317.49	10	32021.79 ±5274.58	4
C229Y	49111.50	99.99	62.50 ±0.00	28498.83 ±2665.95	4	3513.511196 ±67.54	39
C229Y*	53365.67	81.85	57.00 ±0.00	7.82 ±0.24	14013	38.48791547 ±0.420	3542
PrfA*^{G145S}	54352.46	83.93	54.50 ±1.00	≤ 1	-	≤ 1	-

We conclude that the C229Y mutation introduces minor structural changes that render the PrfA protein transcriptionally inactive, probably through local alterations in the C-terminal domain impacting on the stability of the DNA-binding HTH motif (figure 3.1.31). These alterations are overridden or compensated for by the PrfA* G145S mutation, through its direct effects on the conformation of the HTH motif (Eiting *et al.*, 2005).

3.1.1.4.2.3 Role of the C229Y mutation in the sugar-mediated repression phenotype of NCTC 7973

We next explored the impact of a second C229Y mutation in PrfA*^{G145S} on the response of the *L. monocytogenes* PrfA system to fermentable sugars. We investigated in particular whether this mutation had any role in the differential response to cellobiose and glucose displayed by the *prfA**$^{G145S/C229Y}$ strain NCTC 7973 (Park & Kroll, 1993, Behari & Youngman, 1998b, Brehm *et al.*, 1999). In addition to these two sugars, we checked gene expression upon growth on glucose-1-phosphate (G-1-P), which is taken up through the non-PTS permease Hpt and has been previously reported not to repress *L. monocytogenes* virulence genes (Ripio *et al.*, 1997b). For these analyses, we aimed to use experimental conditions maximizing the isolation of the potential effects of the test variable (presence of second C229Y in PrfA*^{G145S}) from other possible interfering factors.

First, we moved away from the genetic context of the *L. monocytogenes* phylogenetic division II, in which the C229Y substitution is naturally linked to the PrfA*^{G145S} mutation. This was also important because the anomalous response pattern of NCTC 7973 to cellobiose and glucose had been linked to unknown genetic defects in regulatory loci related to general catabolite repression and/or cellobiose-specific regulation (Behari & Youngman, 1998b, Brehm *et al.*, 1999, Milenbachs Lukowiak *et al.*, 2004). We achieved this by expressing the C229Y* allele in a serovar 4b (*i.e.* phylogenetic division I) Δ*prfA* mutant, after integration in single copy in the chromosome.

Second, as the culture medium composition may have a substantial effect on virulence gene expression (Ripio *et al.*, 1996, Behari & Youngman, 1998b), we used the chemically defined IMM (see section 3.1.1.2) for growing the bacteria. The IMM medium was modified by lowering the concentration of phosphates from 1,642 mM (used for pH buffering) to 25 mM and adding 3-(N-morpholino)propanesulfonic acid (MOPS) (see Materials and Methods). This was necessary to allow *L. monocytogenes* to grow on G-1-P via uptake by the Hpt hexose phosphate permease (growth of *L. monocytogenes* is strictly dependent on the presence of a utilizable sugar as a carbon source). Hpt is an organic:inorganic phosphate antiporter, *i.e.* the translocation of the sugar phosphate into the bacterial cell involves the simultaneous expulsion of an inorganic phosphate molecule to the extracellular medium (Kadner *et al.*, 1993, Huang *et al.*, 2003, Lemieux *et al.*, 2004). We noticed that the presence in the culture medium of a high concentration of phosphate buffer, as in IMM, prevents the uptake of hexose phosphates by *L. monocytogenes*, probably because the inorganic phosphate antiporting cannot proceed against gradient (our unpublished observations).

Third, instead of the natural adsorbent activated charcoal, we used the chemically defined synthetic resin Amberlite^{TM} XAD-4 to induce PrfA-dependent gene expression in the modified IMM (see section 3.1.1.2). Activation of PrfA regulation is necessary in these sugar repression experiments for two reasons. (i) Wild-type *L. monocytogenes* expresses very weak to undetectable levels of PrfA-regulated virulence genes *in vitro*, and it is questionable whether repressor effects observed in an already almost totally downregulated expression background are biologically relevant (Ripio *et al.*, 1997b). (ii) In addition, since the *hpt* gene is strictly PrfA-dependent, activation of the PrfA system is indispensable for *prfA*^{WT} bacteria to grow on G-1-P (Ripio *et al.*, 1997b, Chico-Calero *et al.*, 2002).

Finally, we used the highly sensitive and accurate RT-QPCR technique to quantify the effects of sugars on virulence gene expression. In previous studies from our laboratory PrfA-dependent expression was measured with the *plcB* natural

reporter system (Ripio *et al.*, 1997b, Brehm *et al.*, 1999, Vega *et al.*, 2004), which, although working well, is not sufficiently sensitive and has a restricted linear dynamic range (saturation of output units above a relatively low PrfA activation threshold; our unpublished observations).

The results obtained are summarized in figure 3.1.32.

The RT-QPCR transcription values obtained for P*plcA* and P*actA* in bacteria grown on G-1-P as the sole carbon source were significantly more elevated than those observed with glucose. This is consistent with the notion that this non-PTS sugar does not significantly repress PrfA-dependent expression (Ripio *et al.*, 1997b). If the transcription values obtained with G-1-P are taken as reference for non-repressed PrfA-dependent expression, the data in figure 3.1.32 show that glucose downregulates virulence genes in both the $prfA^{WT}$ and $prfA^{*G145S}$ genetic contexts, albeit more intensely in the former. Thus, contrary to what was initially thought (Vega *et al.*, 2004), the constitutively hyperactive PrfA*G145S mutant form is not totally "immune" to sugar-mediated repression.

This is particularly evident with cellobiose, which strongly repressed, in all conditions, PrfA-dependent expression. The reasons for these marked differences in the intensity of the repression in response to glucose and cellobiose are unknown. If this repression results from an interconnection between PrfA regulation and the carbon catabolite repression network (as suggested by the fact that only PTS-transported sugars seem to trigger the effect), the differential effect of the two sugars could be related to the relative number of PTS permeases involved in the transport of β-glucosides and glucose in *L. monocytogenes*. The former are much more abundant in the *L. monocytogenes* genome (n = 17 vs only *ptsG* for glucose; in addition, there is evidence that glucose can be transported through non-PTS permeases or membrane facilitators) (Glaser *et al.*, 2001) and can potentially generate a stronger catabolite "repressor wave". Further work is needed to examine the validity of this hypothesis.

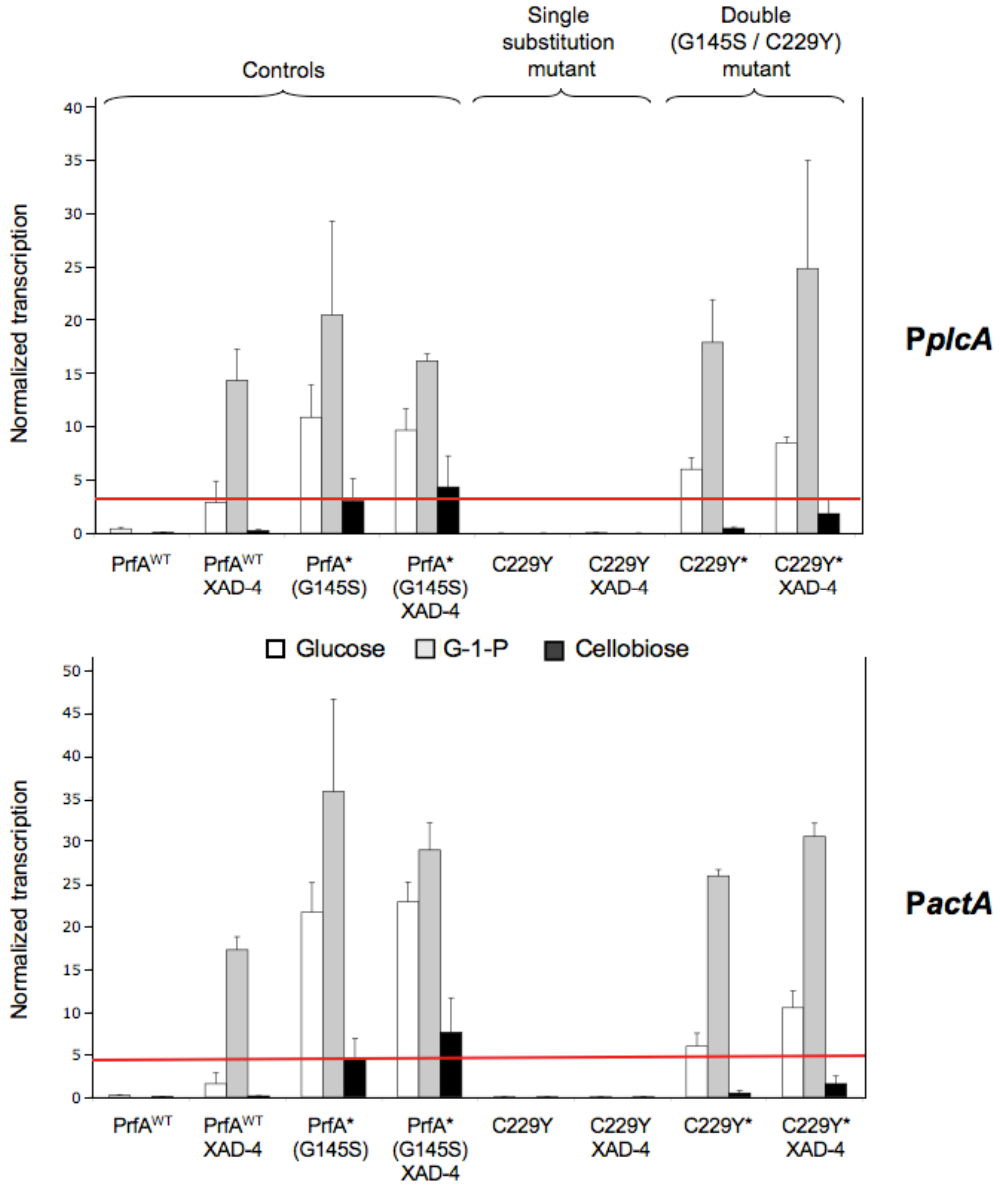

Figure 3.1.32: Transcriptional analysis of the C229Y mutants in the presence of different sugar sources.

The transcription of *plcA* (upper panel) and *actA* (bottom panel) genes has been determined by RT-QPCR in extracellular conditions at 37ºC in IMM (early exponential phase, OD_{600} = 0.2). IMM was supplemented with 20 mM of the indicated carbon source (excess conditions for exponentially growing bacteria). "XAD-4" means IMM supplemented with 1% Amberlite^{TM} XAD-4. For these experiments, normalization of transcription was carried out with *ldh* and a second reference gene, *rpoB*, since for an unknown reason, expression of *ldh* was on occasions slightly affected in bacteria grown on G-1-P. The red line represents a theoretical signal saturation threshold above which gene expression values are considered maximal. We set this threshold to the expression levels determined for *prfA*^{*G145S} in cellobiose, as in these conditions there is no detectable effect on PrfA-dependent expression using the *plcB* gene as reporter system (see figure 3.1.24). No expression values are detected for *prfA*^{WT} in normal medium (no Amberlite^{TM} XAD-4) with G-1-P because *L. monocytogenes* does not grow in these conditions (PrfA-dependent gene *hpt* not active; see text for details). The same applies to *prfA*^{C229Y} in IMM with or without Amberlite^{TM} XAD-4 supplementation, confirming that the PrfA^{C229Y} mutant protein encoded is inactive (see also figures 3.1.25, 3.1.27 and 3.1.28).

The above observations are important because they provide a simple explanation to the different response of NCTC 7973 to glucose and cellobiose. We suggest that the response of NCTC 7973 to sugars is no different from that exhibited by other *L. monocytogenes* strains, and that the difference seen between cellobiose and glucose are artifactual rather than biological. Our characterization work has shown that the second C229Y mutation partially suppresses the PrfA* phenotype conferred by the G145S mutation *in vitro*. This lower basal activity of PrfA*$^{G145S/C229Y}$ results in lower expression values (either with or without supplementation with Amberlite^{TM} XAD-4) in response to sugars than with PrfA*^{G145S} (figure 3.1.32). Reporter-based techniques, as those previously used for the analysis of NCTC 7973, have a narrower linear dynamic range than RT-QPCR. In these conditions, values below the signal saturation threshold are interpreted as repression whereas those slightly above are interpreted as maximal expression levels. This is illustrated in figure 3.1.32, in which a signal saturation threshold has been set to coincide with the expression levels of the *prfA*^{*G145S} with cellobiose. According to figure 3.1.24 and previous data from Brehm *et al*. (1999) (figure 3.1.24B) and Vega *et al*. (2004) (3.1.24C), these levels correspond to (or are above) the signal saturation threshold of the *plcB* reporter and, thus, no apparent repression is observed. Expression levels below this threshold, as observed with C229Y* grown on cellobiose but not on glucose (figure 3.1.32), are interpreted as repression.

3.1.1.4.2.4 Characterization of two PrfA*^{G145S} suppressor mutations

Two PrfA^{-} mutations were identified as *prfA*^{*G145S} suppressor mutations (*prfA*^{*sup}) while manipulating in our laboratory *prfA** mutant strains. The mutants are Hly and PlcB negative in SBA and EYA plates, do not utilize hexose phosphates, and are not charcoal or Amberlite^{TM} XAD-4-activable. To characterize these mutations, we used the same methodology as above, *i.e*. we expressed the *prfA*^{*sup} (double mutant) alleles plus the single mutated *prfA*^{WT} allele in a Δ*prfA* background, and analyzed the PrfA phenotype on plates and by RT-QPCR in broth-grown and

intracellular bacteria. We also recombinantly expressed the two (single and double mutant) alleles in *E. coli* and characterized biochemically the corresponding PrfA proteins.

A129T

The *prfA**^{sup} mutation A129T was accidentally identified during the construction of a Δ*sigB* mutant (section 3.1.2.2.1) by double crossover in our prototype *prfA**^{G145S} strain P14A. This procedure involves a selection step at 42ºC (for thermosensitive vector counterselection; see Materials and Methods), a high temperature that is dysgenesic to *L. monocytogenes* and favours the appearance of mutations (Vega *et al.*, 2004). The spontaneous *prfA**$^{G145S/A129T}$ mutant displayed all the phenotypic characteristics of a PrfA null mutant (*i.e.* no spontaneous PrfA-dependent gene expression and lack of activability by charcoal; see figure 3.1.2.2), as did the Δ*prfA* bacteria complemented with the corresponding allele (short name, A129T*) (figure 3.1.26). Neither the single A129T nor double A129T* mutated alleles showed any activity, even in intracellular conditions, *i.e*. they were non-activable, indicating that the PrfA was totally non-functional (figures 3.1.25, 3.1.27 and 3.1.28).

This spontaneous mutation appears to have a dramatic effect on PrfA following the reasoning used in section 3.1.1.3.2.6, since it was not overridden by the PrfA*^{G145S} mutation in the C-terminal domain. This is consistent with the major role of αC in the structure-function of the members of the Crp family of transcriptional regulators. αC is the "dorsal spine" that connects the N-and C-terminal domains of the regulator's monomer, establishes most of the protomer-protomer contacts important for dimerization, and is critically involved in the transmission of the allosteric activation signal, as recently demonstrated for Crp (Popovych *et al.*, 2009) and inferred from the comparison of the crystal structures of PrfA^{WT} and PrfA*^{G145S} (Eiting *et al.*, 2005) (see section 3.1.1.3 for additional details). Residue A129 is near the point where the αC helices tilt by 11º and straighten in the activated PrfA*^{G145S}

mutant form (figures 3.1.8 and 3.1.9), a movement that brings the C-terminal ends of these helices together, "tightening" the dimer (Eiting *et al.*, 2005).

Interestingly, the A129T mutation causes a significant defect in the dimerization of the PrfA*$^{G145S/A129T}$ double mutant protein, but not in the PrfA^{A129T} single mutant (figure 3.1.29, table 3.2), suggesting that this residue plays a key role in the monomer-monomer realignment and associated conformational readjustments of the C-terminal DNA-binding domain involved in PrfA activation.

Mutations at a similar position in Crp have been described, which also have a dramatic effect in protein function. Mutations in residues T127 and S128 (which align with S127 and L128 of PrfA; figure 1.4) of this region have been reported to alter Crp/cAMP interaction and interfere with cAMP-mediated changes in Crp structure (Lee *et al.*, 1994, Cheng *et al.*, 1995, Leu *et al.*, 1999). It has been also shown that amino acid substitutions that introduce hydrophobic amino acid side chain constituents at either position 127 or 128 decrease Crp discrimination of cAMP and cGMP (Lee *et al.*, 1994). In the Crp structure, S128 interacts with cAMP through hydrogen bonding. Additionally, it has been shown that amino acid substitutions at Crp positions 124 and 128 residues, which are one C-helix turn away from each other, affect both cAMP binding affinity and binding cooperativity (Tomlinson *et al.*, 2003). For example, Crp mutants including S128A and S128P showed inactive Crp phenotypes (Crp^{-}). Our PrfA^{A129T} mutant showed similar phenotype, as it was incapable of activating virulence gene expression intracellularly.

From the position of residue A129 in the PrfA structure, with the side chain facing the interior of the monomer towards αH of the C-terminal extension in both PrfA^{WT} (figure 3.1.31) and PrfA*^{G145S} (not shown), it is not totally clear how the A129T mutation may disrupt dimerization. It is probable that a larger side chain at PrfA position 129 introduces, primarily, major structural constraints in the normal interactions of the GHI α-helical bundle that "wedges" between the N- and C-terminal domains, which is critical for PrfA function (see below), leading to a totally

afunctional protein. In the PrfA*^{G145S} conformation, the changes obviously lead in addition to loss of critical monomer-monomer contacts involved in dimerization.

A similarly located substitution, D133Y only one helix turn away from A129T in αC, was identified by Herler *et al.* (2001) using a positive selection system for PrfA^{-}. In the PrfA three-dimensional structure, the Tyrosine 133 side chain also faces and pushes away αH of the C-terminal extension, suggesting a similar mechanism of mutational inactivation, through structural alteration of the αGHI interdomain wedge interactions and concomitant secondary destabilization of the C-terminal HTH DNA-binding motif.

E173G

This mutation was identified some time ago in the laboratory by Dr. Yolanda Vega (Vega *et al.*, 2004) as a spontaneous suppressor mutation in the *prfA** strain NCTC 7973. The PrfA protein of this mutant strain, designated *prfA**^{sup}^{E173G}, carries in total three mutations, E173G, G145S and C229Y. Here we isolated the E173G mutation and investigated its effect in the PrfA^{WT} (E173G mutant) and PrfA*^{G145S} (E173G* mutant) contexts.

As the data shown in figures 3.1.25, 3.1.26, 3.1.27 and 3.1.28 indicate, the E173G and E173G* PrfA proteins are totally inactive even intracellularly. This is easily explained by the fact that residue E173 forms part of αE, the first α-helix of the DNA-binding motif, suggesting that the functional defect specifically affects the binding to the target promoter sequence. This was confirmed by our biochemical characterization analyses, which show that the E173G mutation does not alter the general structural parameters of PrfA (dimerization, thermal stability). It does, however, results in an almost total loss of DNA-binding activity. Interestingly, this is only observable in PrfA*^{E173G}, not in PrfA^{E173G}. The explanation appears simple: in PrfA*^{G145S} the HTH motif is exposed and in the correct conformation for productive, specific interaction with the PrfA-box sequence, so that the effect of the mutation is readily observable; in PrfA^{WT}, by contrast, the HTH motif is inadequately arranged

and the mutation does not have a significant impact on specific DNA binding (the PrfA protein being in the "off", weakly active state).

Interestingly, the E173G mutation is identical to, and aligns to the very same protein position, as another mutation in Crp, Crp^{E171G}, identified in a suppressor mutant of a Crp^{*A144T} strain (Garges & Adhya, 1988), in turn homologous to our $PrfA^{*G145S}$. This coincidence highlights the significant structure-function similarities between PrfA and Crp.

Concluding remarks

Our observations show that the second C229Y mutation naturally present in all spontaneous *prfA*^{*G145S} mutants of *L. monocytogenes* phylogenetic division II (1/2a and related serovars) attenuates the PrfA* phenotype. The reason why this mutation is always associated with the G145S substitution is unknown. Clearly the two mutations are co-selected, and the attenuation in PrfA activity may provide a selective advantage because the bacteria do not express levels of PrfA-regulated genes and products as high as those associated with a *prfA*^{*G145S} genotype, thus, reducing the draw on vital resources. Clearly, this apparently does not entail any type of constraint in the phylogenetic division I genetic context, since the G145S mutation is found alone in these strains. The nature of the physiological constraints associated with a *prfA*^{*G145S} mutation in division II strains remains a mystery, since the C229Y mutation does not mitigate the effect on bacterial fitness exerted by the $PrfA^{*G145S}$ mutation on *L. monocytogenes*, as shown in figure 3.1.30.

Our data help to clarify several key aspects of carbon source regulation of *L. monocytogenes* virulence genes: (i) we confirm that hexose phosphates do not appear to repress PrfA-dependent gene expression, this only occurs with PTS-transported sugars; (ii) a PrfA* mutation does not render *L. monocytogenes* insensitive to sugar-mediated virulence gene regulation, as repression is still observable but with higher final output levels that are proportional to the intrinsic activity of the PrfA protein; (iii) the intensity of the repression varies depending on the sugar and may depend on

the number of potential PTS permeases involved in the uptake. Collectively, these observations suggest that there is a clear interconnection between the PrfA regulation and carbon catabolite repression systems in *L. monocytogenes*. Since the G145S mutation does not bypass the repressor effect of sugars, the carbon catabolite repression is probably exerted by a mechanism that is independent from, (or does not interfere with, *i.e.* it is superimposed to) the allosteric activation mechanism of PrfA.

Our data also provide a parsimonious explanation to the anomalous behaviour of strain NCTC 7973 in response to sugars. Earlier studies suggested that the differential response to glucose and cellobiose exhibited by this strain reflects the existence of at least two separate, semi-independent pathways of sugar-mediated repression, one related to general catabolite repression, which manifests when *L. monocytogenes* grows in the presence of glucose or fructose, and another responding specifically to β-glucosides. We demonstrate here that the point mutation C229Y is sufficient to confer differential response to glucose and cellobiose in quantitative terms, which depending on the gene expression analysis technique used and its corresponding signal saturation threshold, may lead to the conclusion that one sugar represses (cellobiose), whereas the other (glucose) not.

In essence, while it is certainly possible that independent sensing pathways exist for cellobiose or other sugars upstream of PrfA, we suggest that the underlying mechanism of PrfA repression is essentially the same but that it manifests with different intensities depending on the sugar transported. These different intensities may lead to artifactual interpretations related to the signal saturation threshold of the reporter systems used to measure gene expression.

Finally, our data also highlight the critical importance of the C-terminal αGHI extension, unique to PrfA among Crp-related transcription factors (Scortti *et al.*, 2007), for activity. Apart from C229Y in the loop between αH and αI, which entirely disables PrfA (no expression detected in PrfA-activating conditions, *i.e.* intracellularly or with Amberlite^{TM} XAD-4) if not accompanied by a second PrfA*^{G145S} substitution, there is another naturally occurring mutation in this region

that causes PrfA$^-$ phenotype. This is the L220T substitution identified by Roche *et al*. (2005) in avirulent food isolates of *L. monocytogenes*. Like C229Y, the L220T mutation (also in αH) results in total loss of PrfA-dependent gene expression and cell-to-cell spread capacity. The two mutations differ, however, in that L220T abolishes DNA-binding in native (non-active, apo-form) PrfA whereas C229Y, according to our data, apparently does not. However, it is difficult to judge whether this difference is biologically significant, given the low levels of intrinsic DNA binding activity of the non-activated PrfA form. Moreover, Roche *et al*. (2005) used an electrophoretic mobility shift assay (EMSA), much less sensitive than our Biacore assays, to measure DNA binding. In fact, previous data from our laboratory using EMSA show that PrfA^{WT} is unable to form detectable protein-DNA complexes.

A previous study, based on positive selection of PrfA$^-$ mutations using conditional lethality in *B. subtilis*, identified a number of mutations in the αGHI extension. The selection system involved co-transformation with a plasmid carrying the *L. monocytogenes iap* gene (encoding the P60 murein hydrolase, lethal for *B. subtilis*) under the control of the PrfA-dependent *hly* promoter, and a second plasmid encoding PrfA. Survival of *B. subtilis* was only possible if PrfA was inactivated by spontaneous mutations. The PrfA$^-$ mutations identified in this way mapped to the N-terminal β-barrel (n = 3), αC-hinge-αD (n = 2), the HTH motif (n = 1) and the αGHI extension (n = 3), highlighting the functional importance of these regions (table 1.1). The C-terminal extension mutants were unable to bind to the DNA (Herler *et al.*, 2001), consistent with the notion that the GHI α-helices are important for the stability of the HTH motif.

The GHI α-helical bundle packs against the inter-domain cleft, forming a wedge that is likely critical for the C-terminal domain to maintain some structural rigidity. This may explain why native (unliganded) PrfA is capable of specific binding to the target DNA sequence, albeit with low affinity, in contrast to Crp, which lacks this extension and only shows unspecific binding to the DNA (Harman, 2001). Indeed, the recently determined structure of (apo) Crp shows that the lower part of the αC helix is disordered in the absence of the allosteric activator cAMP,

resulting in inadequate intersubunit alignment and positioning of the HTH motif (Popovych *et al.*, 2009). Two other mutations in αC, A129T described in this thesis, and D133Y identified by Herler *et al.* (2001), affect residues that face αH in the PrfA structure (figure 3.1.31), further suggesting that any alteration in the conformation and interactions established by αGHI are critical for the activity of the listerial virulence regulator.

3.1.2 σ^B AND PRFA-DEPENDENT INVASIVENESS

3.1.2.1 Background

Some years ago it was observed in our laboratory that *L. monocytogenes prfA** mutants were hyperinvasive (Suarez *et al.*, 2001), suggesting an involvement of PrfA in the internalization process. Further work by Dr. Héctor Monzó *et al*. in our laboratory investigated in detail the role of PrfA in *L. monocytogenes* invasiveness. It was found that *prfA** mutants, which constitutively overexpress PrfA-regulated genes at high (~ intracellular) levels (see section 3.1.1.3), were up to 165 times more invasive than broth-grown wild-type *L. monocytogenes*. Deletion of the *prfA** allele reduced entry several orders of magnitude to the same levels observed with the non-invasive species *L. innocua* (typically 0.004 - 0.01% internalization vs 3% for *prfA** in HeLa cells). Re-complementation with *prfA**, but not $prfA^{WT}$, restored the hyperinvasive phenotype (figure 3.1.2.1). Using *inlAB* mutants, it was demonstrated that the internalins InlA and InlB were responsible for the PrfA-dependent invasiveness in HeLa cells and other non-phagocytic cells. Moreover, *inlAB* expression followed the typical pattern of PrfA-regulated loci: negligible in a Δ*prfA* mutant, weak during extracellular growth, and strong in *prfA** bacteria and within host cells (H. J. Monzó, M. K. Bielecka *et al*., manuscript in preparation). These observations were paradoxical as they showed that virulence determinants involved in cell invasion were induced after the bacteria had become internalized into host cells. They also were leaving unexplained how invasion of host

cells by extracellularly grown *L. monocytogenes* bacteria (*i.e*. PrfA regulon down, weakly invasive) can take place at the portal of entry during the epithelial phase of infection. In naturally susceptible hosts, this has been shown to involve the direct invasion of enterocytes via specific interactions of internalin proteins and host cell receptors, rather than the internalin-independent translocation of the intestinal barrier through the Peyer's patches (Racz *et al.*, 1972, Jensen *et al.*, 1998, Lecuit *et al.*, 2001, Corr *et al.*, 2006).

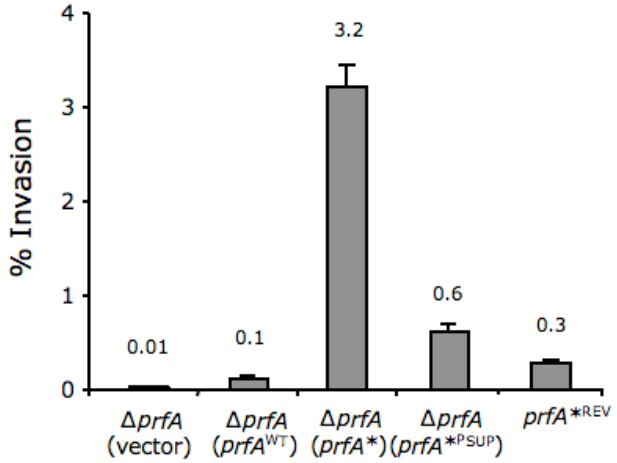

Figure 3.1.2.1: PrfA-dependence of *L. monocytogenes* invasiveness in HeLa cells.
Gene complementation experiments demonstrated that PrfA activity is essential for entry into host cells. Numbers above the bars are the mean % bacteria internalized. Trans-complementation of *L. monocytogenes* Δ*prfA* with multicopy plasmid constructs encoding PrfA proteins with different levels of intrinsic activity. *prfA*^{WT} = weakly active wild-type PrfA protein; *prfA** = constitutively hyperactive PrfA*^{G145S} mutant protein; *prfA**^{PSUP} = PrfA*$^{G145S/C229Y}$, a PrfA* protein with a second mutation C229Y that partially suppresses ("PSUP") the PrfA-activating effect of the G145S mutation (see section 3.1.1.4); vector = mock strain transformed with the trans-complementation shuttle vector (pHPS9) without insert. *prfA**^{REV} is a wild-type revertant of a natural *prfA**^{G145S} strain (P14A) obtained by replacing the *prfA** allele by a *prfA*^{WT} allele by double recombination. Taken from H. J. Monzó doctoral thesis, University of Bristol 2007.

Other groups maintain that the stress response mediator σ^B plays a major role in the invasion of the intestinal barrier by *L. monocytogenes* (Kim *et al.*, 2005, Garner *et al.*, 2006, Gray *et al.*, 2006). The rationale behind this notion is that the transit of *L. monocytogenes* through the intestine involves the exposure to environmental stresses, particularly to the acidic conditions of the stomach, the resistance against which has been shown to be σ^B mediated (Wiedmann *et al.*, 1998, Gahan & Hill, 2005, Freitag *et al.*, 2009). Indeed, the *inlAB* operon appears to be

subject to complex regulation involving both PrfA, through one of the six promoters identified in the locus, P3*inlA* controlled by an unconventional PrfA-box with two mistmatches, and σ^B through two other promoters, P4*inlA* and P2*inlB* (Lingnau *et al.*, 1995, Kazmierczak *et al.*, 2003).

Some studies suggest that *inlAB* is also controlled post-transcriptionally (Stritzker *et al.*, 2005), and others even report that the locus is poorly expressed within cells but substantially induced in broth medium (Bubert *et al.*, 1999), a pattern opposite to that expected for PrfA-regulated genes. Therefore, the *inlAB* locus is largely considered to be only partially regulated by PrfA and to have an expression pattern that does not conform to the PrfA regulon archetype. The fact that one of the monocistronic *prfA* promoters (P2*prfA*) is apparently controlled by σ^B (Nadon *et al.*, 2002, Rauch *et al.*, 2005, Schwab *et al.*, 2005) adds complexity to the situation. This raises questions about whether the reported effect of σ^B in *L. monocytogenes* invasiveness (Kim *et al.*, 2005, Garner *et al.*, 2006) is due to a direct (PrfA-independent) activation of *inlAB* expression, or is exerted indirectly via PrfA.

In this chapter of the thesis we have investigated, using isogenic deletion mutants, the relative importance of PrfA and σ^B in *L. monocytogenes* invasiveness, with the aim of clarifying the predominant regulatory pathway that controls this key step of listerial pathogenesis.

3.1.2.2 Results

3.1.2.2.1 Construction and characterization of Δ*sigB* mutants in *L. monocytogenes* serovar 4b

We constructed in-frame deletion mutants of the *sigB* gene in the genetic context of our model 4b strain to test the role of the σ^B stress mediator in *L. monocytogenes* invasiveness. Mutant bacteria were obtained in two *prfA*

backgrounds: the weakly invasive *prfA*^{WT} (strain P14), and the hyperinvasive *prfA**^{G145S} (isogenic derivative P14A). The P14Δ*sigB* and P14AΔ*sigB* mutants were produced by a homologous recombination technique as described in detail in Materials and Methods.

In order to characterize the phenotype of the Δ*sigB* mutants, we streaked them on EYA plates with or without 0.5% activated charcoal supplementation. This was important for ruling out any defect in PrfA activity, as according to our data, PrfA plays a critical role in the invasive phenotype of *L. monocytogenes*. A strong opacity reaction on EYA was observed for P14AΔ*sigB*, identical to that of P14A, indicating that both strains have similar PrfA-dependent gene expression. As expected, no opacity reaction was observed around the wild-type P14 strain, since in this regulation context the PrfA-dependent genes, including the phospholipase gene *plcB*, are weakly expressed *in vitro*. By contrast, in the presence of activated charcoal, which upregulates PrfA (Ermolaeva *et al.*, 2004), an opacity halo developed around the wild-type strain P14 and its Δ*sigB* derivative (figure 3.1.2.2).

The intensity of the PrfA-dependent *plcB* reporter activity in the two Δ*sigB* mutants was identical to that of their respective parental strains, indicating that σ^B does not seem to play a role in *prfA* expression, at least in the experimental conditions tested.

As controls, we carried out similar phenotypic analyses with a previously described Δ*sigB* mutant in the serovar 1/2a context of *L. monocytogenes* strain EGDe (Stritzker *et al.*, 2005). The behaviour of EGDe and EGDeΔ*sigB* was again similar, with no differences in the *plcB* reporter activity in charcoal-supplemented EYA.

In conclusion, no differences in terms of PrfA activity were observed between the serovar 4b and 1/2a strains and their counterpart strains lacking *sigB*, corroborating that σ^B is not apparently involved in *prfA*/PrfA-dependent gene activation.

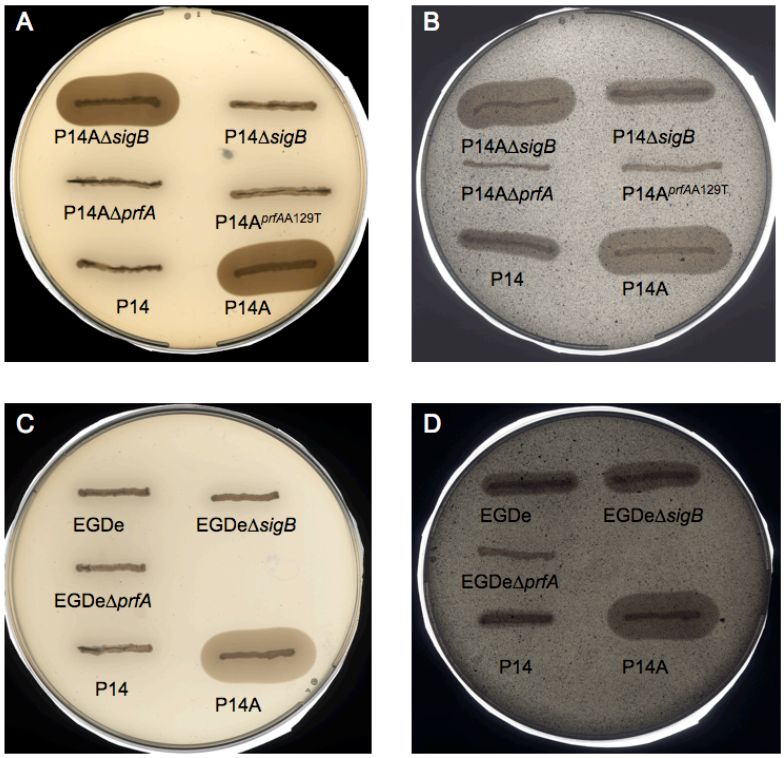

Figure 3.1.2.2: PrfA phenotype of the Δ*sigB* mutants.
Plates were incubated at 37°C for 48 h. (A and C) EYA medium; (B and D) EYA supplemented with 0.5% activated charcoal. (A and B) Δ*sigB* in *L. monocytogenes* serovar 4b. The plates also show the spontaneous PrfA^{-} mutant derivative of P14A, *prfA**$^{G145S/A129T}$ described in 3.1.1.4.2.4, which arose while selecting at 42ºC during Δ*sigB* mutant construction. (C and D) corresponding plates for Δ*sigB* in *L. monocytogenes* serovar 1/2a.

3.1.2.2.2 Effect of *sigB* on *L. monocytogenes* invasiveness

We next tested the Δ*sigB* mutants and corresponding parental bacteria in infection assays in HeLa cell monolayers, to determine the role of *L. monocytogenes* σ^B in host cell invasion. Inocula were initially prepared in BHI in standard conditions (pH = 7.4).

L. monocytogenes bacteria carrying a *prfA**^{G145S} allele showed a hyperinvasive phenotype compared to *in vitro*-grown wild-type bacteria (~ 10 times increment). Removal of PrfA in this background led to total loss of the ability to invade host cells (> 700-fold reduction in invasiveness). These assays, therefore,

confirmed previous observations from our laboratory that *L. monocytogenes* invasiveness is strictly dependent on PrfA.

In the *prfA*^{WT} background, in which basal PrfA-dependent expression levels are very low, the Δ*sigB* mutation associated with a detectable reduction in *L. monocytogenes* internalization (~ 6 times). This is consistent with previous observations by other groups (Kim *et al.*, 2005, Garner *et al.*, 2006, Gray *et al.*, 2006), which reported that σ^B plays a role in *L. monocytogenes* invasiveness.

However, we observed no effect of σ^B in *L. monocytogenes* with *prfA** background, which mimics the fully activated state that PrfA adopts *in vivo* during infection; see section 3.1.1.3) (figure 3.1.2.3).

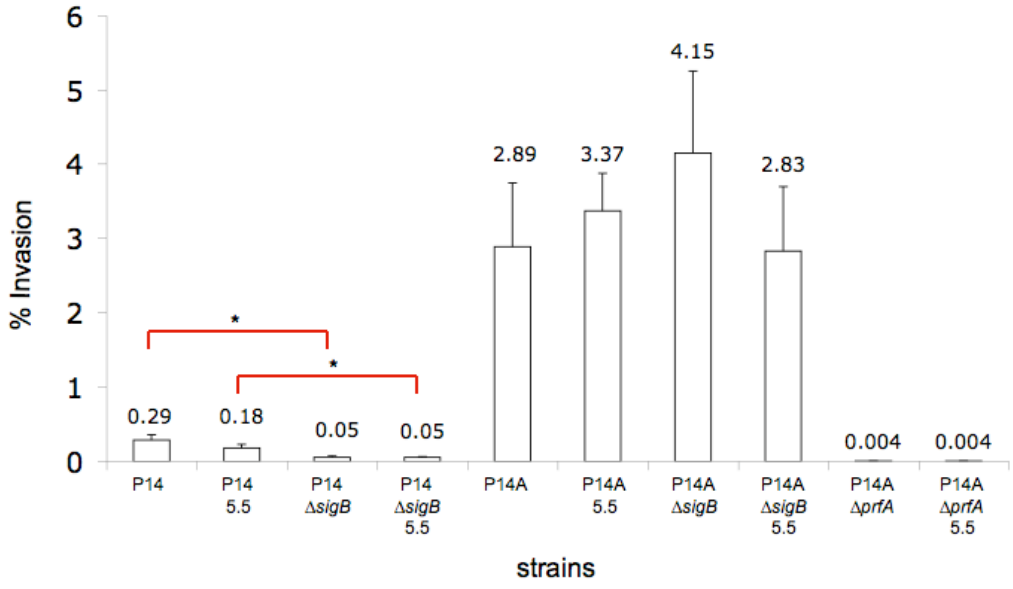

Figure 3.1.2.3: Effect of σ^B and acidic growth conditions on *L. monocytogenes* invasiveness.
"5.5" next to the name of the strain indicates the inoculum used was grown in acidic conditions (BHI, pH = 5.5), otherwise bacteria were grown in BHI with neutral pH (pH = 7.4). MOI used, 20:1. Mean of 4 independent duplicate experiments ± SE. Numbers above the bars are the mean percentage of bacteria internalized. * denotes statistically significant difference at $P \leq 0.05$ in the indicated comparisons (red). *L. monocytogenes* P14 serotype 4b has an intrinsically low invasion capacity because its PrfA system is not switched on in extracellular conditions.

In view of the apparent lack of effect of σ^B in bacteria cultured in standard, optimal growth conditions (rich medium at neutral pH), we repeated the experiments using bacterial inocula grown at pH = 5.5. This was to imitate the mildly acidic environment found by *L. monocytogenes* in the intestine, where the stress response is thought to be relevant for host colonization (Gahan & Hill, 2005, Kazmierczak *et al.*, 2005, Freitag *et al.*, 2009, Toledo-Arana *et al.*, 2009). No significant difference was observed in the internalization of the tested bacteria when grown in acidic conditions compared to neutral pH-grown inocula. Moreover, the acidic conditions did not affect the internalization rate of *L. monocytogenes* (figure 3.1.2.3).

Our results indicate (i) that σ^B does not seem to play a major role in the ability of *L. monocytogenes* to invade host cells in conditions relevant to infection, *i.e.* when the PrfA system is activated; and (ii) that mild acid conditions do not seem to trigger a stress response that activates *L. monocytogenes* invasiveness.

3.1.2.2.3 Effect of σ^B and PrfA activation status on *inlAB* expression

Given the above data, we sought to investigate in detail the effect of σ^B on the expression of the *inlAB* locus encoding the major listerial invasins, InlA and InlB (Hamon *et al.*, 2006). Since our invasion data suggested possible differential effects of σ^B on invasion depending on the activation status of PrfA (figure 3.1.2.3), we performed the expression analysis with the PrfA system downregulated (*prfA*^{WT} bacteria grown extracellularly in BHI) and activated (*prfA**^{G145S} bacteria, and intracellular conditions). For the RT-QPCR analyses we used specific probes for *inlA* and *inlB* as well as *actA*, which we used as strictly PrfA-dependent gene control.

The results of the transcription analyses are shown in figure 3.1.2.4. Overall, the expression patterns of *inlA* and *inlB* were similar to those of the strictly PrfA-dependent gene *actA*, except that the absolute transcription levels were about 10 times greater for the latter. In summary, our data show:

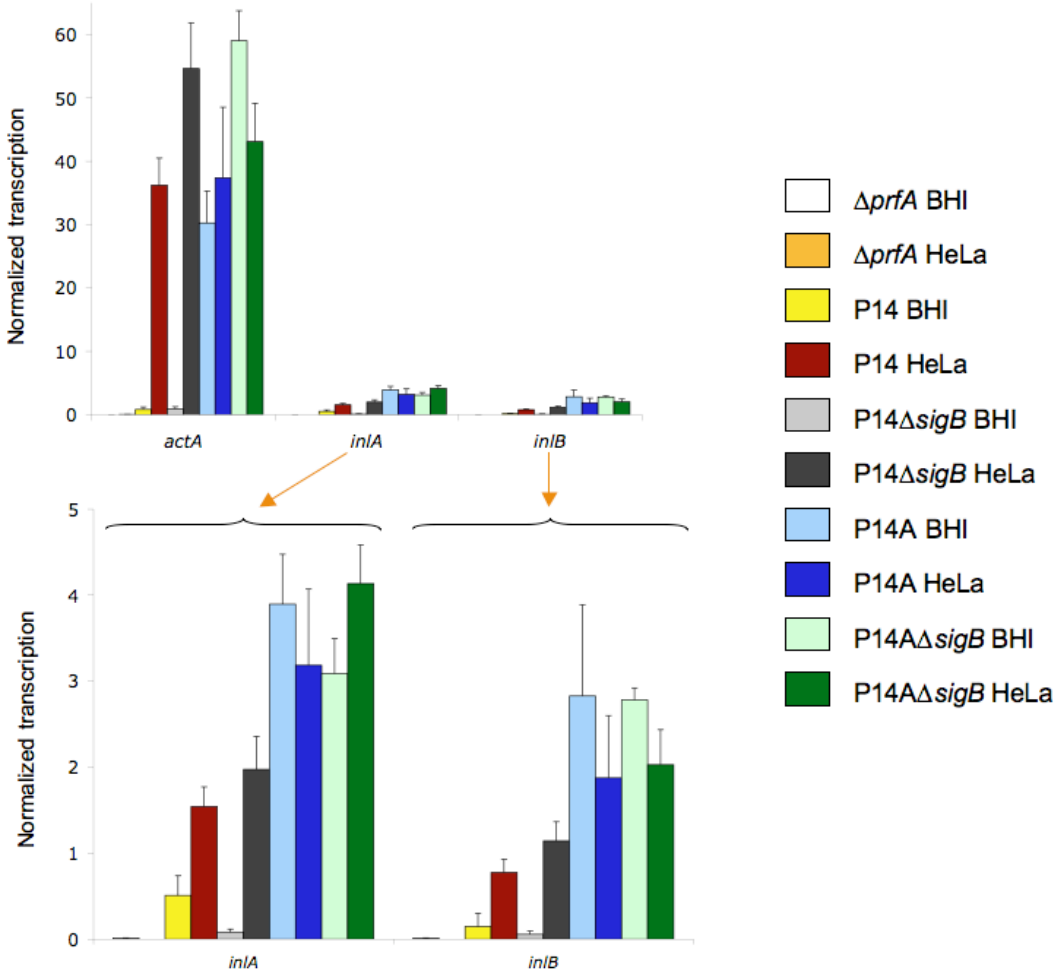

Figure 3.1.2.4: Transcription analysis of the *inlAB* locus: PrfA dependence and effect of a Δ*sigB* mutation in *L. monocytogenes* serovar 4b.

The transcription profiles were determined by RT-QPCR in wild-type *L. monocytogenes* (P14), the isogenic *prfA** strain (P14A), and isogenic *sigB* deletion mutants of strain P14 (P14Δ*sigB*) and P14A (P14AΔ*sigB*). As a control, transcription of the strictly PrfA-dependent *actA* gene was also determined in the same RNA samples. Expression analyses were carried out on bacteria grown until OD_{600} = 1 (mid-exponential phase in the conditions of the experiment, *i.e.* a BHI culture at 37ºC in a 100 ml flask with constant shaking at 200 rpm). Mean of at least two independent experiments ± SE. Note that *inlA/B* expression is undetectable for Δ*prfA* in HeLa cells. Confirming previous observations, there was no significant further activation of *inlAB* expression in *prfA**^{G145S} bacteria in intracellular vs extracellular (BHI) conditions. These findings are consistent with previous data indicating induction of the *inlAB* locus in conditions of PrfA activation (*prfA** background) (Ripio *et al.*, 1997a), and with recent genome-wide transcriptomic studies showing that PrfA stringently controls *inlA* and *inlB* (Milohanic *et al.*, 2003, Marr *et al.*, 2006) and is induced intracellularly (Chatterjee *et al.*, 2006, Joseph *et al.*, 2006).

(i) Similar to the control PrfA-regulated gene *actA*, *inlAB* expression is activated intracellularly (between ~ 3 and 5 times) and is insignificant in a Δ*prfA* mutant, extra or intracellularly. This is in perfect agreement with the observed loss of invasiveness upon removal of the *prfA* gene (figure 3.1.2.3), indicating that *inlAB* expression is strictly dependent on PrfA.

(ii) The Δ*sigB* mutations had no obvious influence on *inlAB* expression, except for a statistically insignificant decrease of ~ 3 to 6 times in transcript levels (for *inlB* and *inlA*, $P = 0.28$ and 0.13, respectively) in the $prfA^{WT}$ background in *in vitro* conditions (BHI). This effect is consistent with the reported presence of putative σ^B-regulated promoters in front of *inlA* (P4*inlA*) (Lingnau *et al.*, 1995) and *inlB* (Kazmierczak *et al.*, 2003) and the observed decrease in invasiveness associated with the Δ*sigB* mutant in the (weakly invasive) $prfA^{WT}$ background (figure 3.1.2.3).

(iii) There are no significant differences in *inlAB* expression associated with the presence/absence of σ^B in PrfA-activating conditions ($prfA^{WT}$ background intracellular; $prfA^{*G145S}$ background, extracellular and intracellular).

We conclude that σ^B does not play a major role in the control of *inlA* and *inlB* expression, and that these genes are tightly controlled by PrfA. Like other members of the PrfA regulon, *inlA* and *inlB* are expressed only weakly in extracellular conditions whilst they are strongly induced during intracellular infection, to levels similar to those observed in *prfA** bacteria.

3.1.2.2.4 Differential role of σ^B in *L. monocytogenes* serovars

Working with serovar 1/2a strains, other groups reported that a σ^B-mediated stress response does play a role in *L. monocytogenes* invasion. Our data with a 4b strain, however, do not support that σ^B is significantly involved in *L. monocytogenes* invasiveness. The only detectable effect was seen in broth-grown $prfA^{WT}$ bacteria, in which the internalization levels are intrinsically low, raising questions about the biological significance of the observation. Moreover, this effect was detectable

regardless of whether the bacteria were cultured at neutral pH, in which σ^B is not expected to play any significant role, or at an acidic pH, normally associated with the activation of a σ^B stress response in *L. monocytogenes* (Kazmierczak *et al.*, 2003, Wemekamp-Kamphuis *et al.*, 2004, Raengpradub *et al.*, 2008, Abram *et al.*, 2008a) (figure 3.1.2.3).

We, therefore, asked whether our conflicting findings could be explained by strain-specific differences in the role and function of σ^B in *L. monocytogenes* stress-related phenotypes. To address this, we compared the response of our serovar 4b bacteria and the serovar 1/2a EGDe strain, with and without the *sigB* gene, upon exposure to elevated temperature (42ºC) and oxidative stress. The effect on bacterial fitness was determined by monitoring the growth kinetics with an automated plate reader. The results are shown in figures 3.1.2.5 and 3.1.2.6.

Our data show a differential effect associated with the lack of *sigB* in our 4b bacteria and EGDe grown at 42ºC. The elevated temperature had a very clear effect on EGDeΔ*sigB* gene at the post-exponential phase, resulting in lower bacterial numbers in the stationary phase plateau than with wild-type EGDe. The effect of the lack of *sigB* was also observable at 37ºC, but less pronounced (figure 3.1.2.5A). By contrast, the serovar 4b Δ*sigB* mutant showed no fitness impairment with respect to its isogenic *sigB*-proficient parental strain. The elevated temperature had, in the wild-type 4b bacteria, a similar effect to that observed with EGDe. Thus, while *sigB* does not seem to play a role in protection against thermal stress in our serovar 4b strain, these bacteria seem to possess a mechanism to counteract the effects of high temperature.

Similar results were observed when testing, in the serovar 4b context, the effect of σ^B on thermal stress resistance in the *prfA**G145S and Δ*prfA* backgrounds (a Δ*sigB* was constructed in P14AΔ*prfA*; see table 5.1). Thus, the PrfA activation status does not seem to have any influence on the (lack of) effect of σ^B in serovar 4b bacteria.

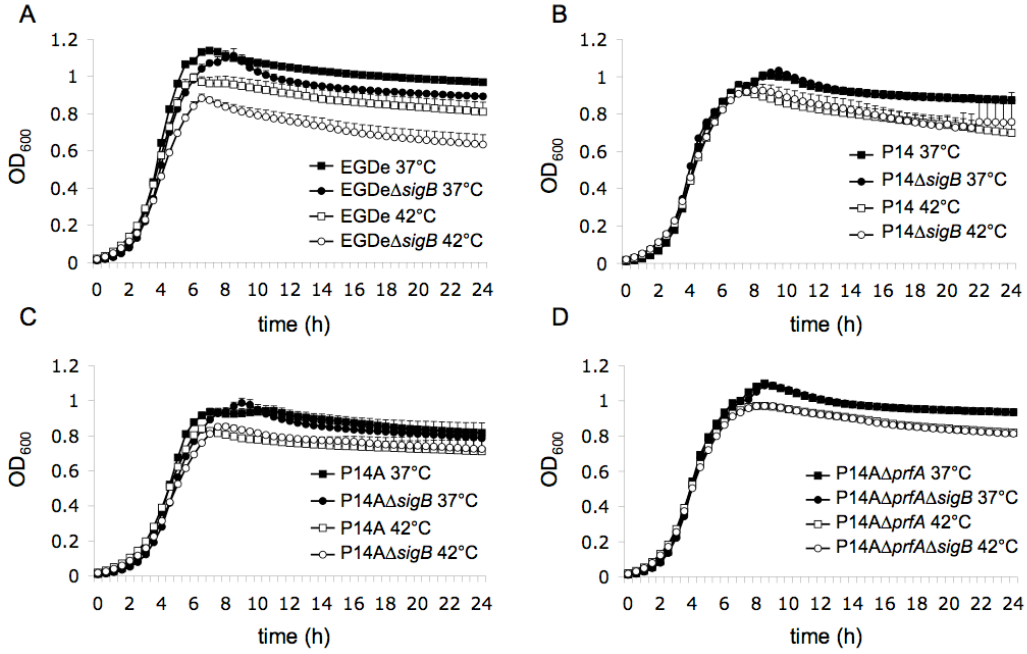

Figure 3.1.2.5: Growth kinetics of 4b and 1/2a mutant strains under thermal stress.
Bacteria were grown in BHI for 24 h at 37°C and 42°C. Comparisons of σ^B-proficient and isogenic Δ*sigB* bacteria: (A) EGDe and EGDeΔ*sigB* mutant; (B) P14 and isogenic P14Δ*sigB* mutant; (C) P14A and P14AΔ*sigB* mutant; (D) P14AΔ*prfA* and P14AΔ*prfA*Δ*sigB* double mutant. Mean of three experiments ± SD. Growth curves of each strain were obtained using an automated plate reader; note that the OD values differ from those obtained in standard flask cultures.

The same growth kinetics studies were also carried out under oxidative stress conditions (growth in the presence of 15 mM H_2O_2). A total lack of protective effect of σ^B was also observed here for the serovar 4b bacteria. In the *prfA*^{WT} background, even a marginal improvement in fitness was associated with the Δ*sigB* mutation. This was also observed by other authors with a Δ*sigB* mutant of a serovar 4c strain (L99) (Moorhead & Dykes, 2003). In our study, P14Δ*sigB* mutant (serotype 4b) seemed to behave similarly. In the experiments with EGDe, the same protective effect of σ^B was again observed at 37ºC (0 mM H_2O_2), combined with an extension in the lag phase and slight impairment in the growth rate in the presence of 15 mM H_2O_2.

The above results indicate that there are strain-specific differences regarding the protective role of σ^B in the tolerance of *L. monocytogenes* to environmental stresses.

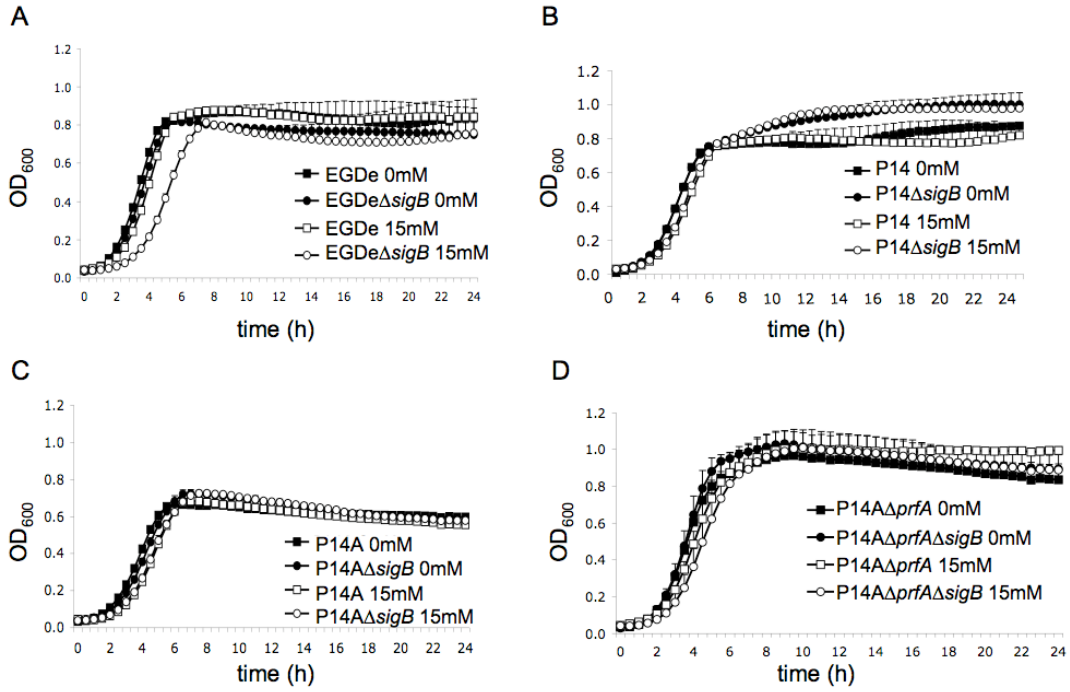

Figure 3.1.2.6: Growth kinetics of 4b and 1/2a mutant strains under oxidative stress.
Bacteria were grown in BHI for 24 h in the presence and absence of 15 mM H_2O_2 and OD_{600} values were taken every 30 min. with an automated plate reader. Similar strain comparisons as in figure 3.1.2.5. Note that EGDe responds differently to oxidative stress than to thermal stress, with a growth delay during the exponential phase. The differences seen in stationary phase are the same seen in figure 3.1.2.5 and are obviously the effect of the growth temperature.

3.1.2.3 Discussion

Contradicting previous reports by other groups, the data presented in this chapter do not support that the stress mediator σ^B plays a major role in host cell invasion by *L. monocytogenes*. We showed using in-frame deletion mutants that σ^B does not affect internalization when the PrfA system is activated, *i.e.* in a virulence gene regulatory context, in which the key *L. monocytogenes* invasion factors, InlA and InlB, are fully expressed and the bacteria are fully invasive. An effect of σ^B was

only observed when the PrfA system was downregulated, with extracellularly (BHI broth) grown bacteria of wild-type *prfA* genotype. This observation is in line with previous findings reported by others (who used *L. monocytogenes* with wild-type *prfA* genotype) that σ^B plays a role in *L. monocytogenes* invasion (Kim *et al.*, 2005, Garner *et al.*, 2006). However, in these conditions there is no significant expression of the *inlAB* operon and the bacteria are weakly invasive (figures 3.1.2.1, 3.1.2.3 and 3.1.2.4). We, therefore, question the biological significance of an effect that is only causing a reduction in internalization in an already much reduced invasive phenotype, and which corresponds to a PrfA activation status only seen *in vitro* and not *in vivo* during infection. It has been reported that the P4*inlA* and P2*inlB* promoters are σ^B-dependent (Lingnau *et al.*, 1995, Kazmierczak *et al.*, 2003) and this may explain the observed effect of the Δ*sigB* mutation in the absence of PrfA-mediated activation of *inlA/B* expression.

There is evidence suggesting that *L. monocytogenes* responds differently to various stress conditions in a serotype-dependent manner. Some studies found that food isolates of serotype 1/2a were less pathogenic and exhibited longer lag phases at 37ºC in comparison to clinical isolates of serovar 4b after being exposed to cold storage/starvation conditions (Avery & Buncic, 1997). Buncic *et al*. (2001) also observed some group differences between 1/2a and 4b strains in their response to stress factors associated with foods (such as mild heat treatment and bacteriocins from *Lactobacillus sake*) and in pathogenicity for chick embryos, although the data obtained were not entirely consistent. The authors did not investigate, however, the differences between the two serovars in respect to mutant strains lacking *sigB*. Other studies showed more specifically that the role of the *sigB* gene in the general stress response of *L. monocytogenes* differs between phylogenetic lineage II and III strains (Moorhead & Dykes, 2003, 2004). Thus, a serotype 1/2a strain, of food origin, was found to be more dependent on *sigB* for survival in stress conditions in comparison to a serotype 4c, of clinical origin. Also, in the *L. monocytogenes* serovar 1/2a strain, σ^B contributed to respond to osmotic stress (3% NaCl), lethal acid concentrations (pH = 2.5) and exposure to high temperatures (50ºC), whereas in the serovar 4c strain it did not.

Our data indicate that there are strain-dependent differences in the role of σ^B as stress response mediator in *L. monocytogenes*. In our serovar 4b bacteria, it does not seem to be important, whereas in the serovar 1/2a strain EGDe, a clear protective effect was observed against two stress-related conditions (growth at elevated temperature and exposure to hydrogen peroxide). This was surprising, because it is largely assumed that σ^B plays a major role in maintaining homeostasis during the *L. monocytogenes* stress response (Kazmierczak *et al.*, 2005, Gandhi & Chikindas, 2007, Freitag *et al.*, 2009). A possible explanation to the apparent lack of phenotype (both invasion- or stress tolerance-related) of the Δ*sigB* mutations in our model serovar 4b strain is that the gene could be non-functional due to non-expression or the presence of mutations in the coding sequence. Additionally, there could be alterations in the promoter sequences recognized by σ^B in the *prfA* and/or *inlAB* loci. We did not find any significant changes in the nucleotide sequence of the relevant promoters, but found a single amino acid substitution Y→F at position 216 of the protein. However, this mutation is conservative and is also present in all serovar 4b strains sequenced to date (figure 3.1.2.7), as well as in the phylogenetic division III serovar 4c (not shown), so it is unlikely to affect σ^B functionality. The *rsbV* and *rsbW* genes from the *sigB* operon, encoding proteins that regulate σ^B activity (Kazmierczak *et al.*, 2005), were also 100% conserved. Further research is needed to understand the reasons behind the apparent lack of functionality of σ^B in the stress response of our 4b strain.

Our results are in accordance with those of Moorhead and Dykes (2003), who also observed a clear involvement of the *sigB* gene in thermal stress tolerance in a serotype 1/2a strain, unlike a serotype 4c strain, in which it had no effect. However, other authors reported that heat stress responses were at least partially σ^B-independent in serotype 1/2a bacteria (Ferreira *et al.*, 2003), indicating that strain-specific differences may even occur within the same phylogenetic division.

```
F6854     MPKVSQPDKEAKEKVYIWIAAYQENGDQDAQYNLVVHYKNLVESIARKYSQGKSFHEDLV 60
10403S    MPKVSQPDKEAKEKVYIWIAAYQENGDQDAQYNLVVHYKNLVESIARKYSQGKSFHEDLV 60
EGDe      MPKVSQPDKEAKEKVYIWIAAYQENGDQDAQYNLVVHYKNLVESIARKYSQGKSFHEDLV 60
H7858     MPKVSQPDKEAKEKVYIWIAAYQENGDQDAQYNLVVHYKNLVESIARKYSQGKSFHEDLV 60
F2365     MPKVSQPDKEAKEKVYIWIAAYQENGDQDAQYNLVVHYKNLVESIARKYSQGKSFHEDLV 60
P14       MPKVSQPDKEAKEKVYIWIAAYQENGDQDAQYNLVVHYKNLVESIARKYSQGKSFHEDLV 60

F6854     QVGNIGLLGAIRRYDATFGKSFEAFAVPTIVGEIKRFLRDKTWSVHVPRRIKELGPKIKN 120
10403S    QVGNIGLLGAIRRYDATFGKSFEAFAVPTIVGEIKRFLRDKTWSVHVPRRIKELGPKIKN 120
EGDe      QVGNIGLLGAIRRYDATFGKSFEAFAVPTIVGEIKRFLRDKTWSVHVPRRIKELGPKIKN 120
H7858     QVGNIGLLGAIRRYDATFGKSFEAFAVPTIVGEIKRFLRDKTWSVHVPRRIKELGPKIKN 120
F2365     QVGNIGLLGAIRRYDATFGKSFEAFAVPTIVGEIKRFLRDKTWSVHVPRRIKELGPKIKN 120
P14       QVGNIGLLGAIRRYDATFGKSFEAFAVPTIVGEIKRFLRDKTWSVHVPRRIKELGPKIKN 120

F6854     AVEELTRELQSSPQISDIADFIGVTEEEVLEAMEMGKSYQALSVDHSIEADSDGSTITLL 180
10403S    AVEELTRELQSSPQISDIADFIGVTEEEVLEAMEMGKSYQALSVDHSIEADSDGSTITLL 180
EGDe      AVEELTRELQSSPQISDIADFIGVTEEEVLEAMEMGKSYQALSVDHSIEADSDGSTITLL 180
H7858     AVEELTRELQSSPQISDIADFIGVTEEEVLEAMEMGKSYQALSVDHSIEADSDGSTITLL 180
F2365     AVEELTRELQSSPQISDIADFIGVTEEEVLEAMEMGKSYQALSVDHSIEADSDGSTITLL 180
P14       AVEELTRELQSSPQISDIXDFIGVTEEEVLEAMEMGKSYQALSVDHSIEADSDGSTITLL 180

F6854     DVVGGTDDGFERVNQRMLLEKVLPVLDEREQKILQYTFIENRSQKETGELLDISQMHVSR 240
10403S    DVVGGTDDGFERVNQRMLLEKVLPVLDEREQKILQYTFIENRSQKETGELLDISQMHVSR 240
EGDe      DVVGGTDDGFERVNQRMLLEKVLPVLDEREQKILQYTFIENRSQKETGELLDISQMHVSR 240
H7858     DVVGGTDDGFERVNQRMLLEKVLPVLDEREQKILQFTFIENRSQKETGELLDISQMHVSR 240
F2365     DVVGGTDDGFERVNQRMLLEKVLPVLDEREQKILQFTFIENRSQKETGELLDISQMHVSR 240
P14       DVVGGTDDGFERVNQRMLLEKVLPVLDEREQKILQFTFIENRSQKETGELLDISQMHVSR 240

F6854     IQRQAIKKLREALQNEEVE 259
10403S    IQRQAIKKLREALQNEEVE 259
EGDe      IQRQAIKKLREALQNEEVE 259
H7858     IQRQAIKKLREALQNEEVE 259
F2365     IQRQAIKKLREALQNEEVE 259
P14       IQRQAIKKLREALQNEEVE 259
```

Figure 3.1.2.7: CLUSTAL W (1.83) multiple protein sequence alignment of σ^B from 1/2a (F6854 through EGDe) and 4b (H7858 through P14) serotype *L. monocytogenes*.
All 1/2a serotype strains checked contained tyrosine (Y) and all 4b strains a phenylalanine (F) at position 216 (indicated in colour). Genbank accession numbers of SigB sequence of strains F6854, 10403S, EGDe, H7858 and F2365 are as follows: AADQ00000000.1, AF032445.1, AL591824.1, AADR00000000.1 and AE017262.2, respectively, except for P14, which was sequenced in house (nucleotide sequence not yet deposited in public database).

Despite the lack of effect of the Δ*sigB* mutation in the serovar 4b strain, the two *sigB*-proficient 1/2a and 4b bacteria appeared to be equally resistant to the same stress conditions. This suggests that *L. monocytogenes* 4b possesses additional, σ^B-independent mechanisms for stress tolerance.

Others have reported that σ^B contributes to survival of stationary-phase *L. monocytogenes* 1/2a under oxidizing conditions (strain 10403S; Ferreira *et al.* [2003]). However, with EGDe under oxidative stress, we did not see any specific effect in stationary phase, only a significant delay of the Δ*sigB* mutant during exponential growth (figure 3.1.2.6). Thus, there seem also to exist strain-related qualitative differences in the σ^B-mediated response to stress.

There appear also to be qualitative differences in the protective role of σ^B within a same strain depending on the type of stress. This is shown by our EGDe data, in which the Δ*sigB*-related fitness defects associated with thermal and oxidative stress manifest, respectively, during the exponential phase, causing a growth delay, and the post-exponential phase, leading to a reduction of the stationary-phase bacterial population (figures 3.1.2.5 and 3.1.2.6).

Due to lack of time we could not prepare all necessary constructs needed to conduct comparative experiments in the EGDe context (particularly, *prfA*^{*G145S} genotype bacteria). Therefore, we could not test whether the observed role of σ^B in stress tolerance in EGDe associated with visible effects in invasion. Even if further work demonstrated that σ^B plays a significant role in the stress-induced modulation of EGDe invasiveness, we again question the biological significance of an observation that would be restricted to only one of the major serotypes involved in natural cases of listeriosis. Moreover, 1/2a strains are much less frequently isolated than 4b strains from human and animal clinical cases, and are not associated with major foodborne listeriosis outbreaks (Buncic *et al.*, 2001, Jeffers *et al.*, 2001, Vazquez-Boland *et al.*, 2001a, Gray *et al.*, 2004).

Although one of the monocistronic *prfA* gene promoters (P2*prfA*) has been reported to be regulated by σ^B (Nadon *et al.*, 2002, Rauch *et al.*, 2005, Schwab *et al.*, 2005), according to our data, σ^B does not appear to exert a major control on *prfA* gene expression (figure 3.1.2.2). This is consistent with the lack of any significant effect of the Δ*sigB* mutations on the transcription of the strictly PrfA-dependent gene *actA* (figure 3.1.2.4). It would be interesting to conduct additional experiments in

PrfA-downregulating and -activating conditions under different environmental stresses to determine the real importance of the σ^B-PrfA crosstalk in the fine regulation of *L. monocytogenes* virulence genes.

Finally, our data confirmed previous observations from our laboratory that *L. monocytogenes* invasiveness is strictly dependent on PrfA. We showed that PrfA is essential for the expression of the *L. monocytogenes* invasion locus *inlAB* and the ability of *L. monocytogenes* to invade host cells. Moreover, *inlAB* expression was activated intracellularly and in a *prfA*^{*G145S} context, in which PrfA is constitutively activated. This is consistent with recent genome-wide transcriptomic studies showing that *inlA* and *inlB* are stringently regulated by PrfA (Milohanic *et al.*, 2003, Marr *et al.*, 2006) and selectively induced intracellularly (Chatterjee *et al.*, 2006, Joseph *et al.*, 2006).

Interestingly, in contrast to what is normally seen with other PrfA-regulated genes, the intracellular activation of *inlAB* in the *prfA*^{WT} background did not reach the same high levels seen with *prfA*^{*G145S} (figure 3.1.2.4). The reason for this is unclear and may be related to the multiple promoters controlling *inlAB* expression (Lingnau *et al.*, 1995, Kazmierczak *et al.*, 2003). However, the low transcription levels of *inlAB* compared to *actA*, and the fact that only a single time point was sampled, makes it difficult to judge the biological significance of the differences observed. Since the deletion of the *sigB* gene did not affect the internalization of *prfA*^{*G145S} bacteria, which mimic the virulence gene regulatory context of *L. monocytogenes* during intracellular infection, we can rule out any significant intervention of σ^B during the invasion process *in vivo*.

The strict PrfA-dependent invasiveness suggests an infection model in which exposure to extracellular defences is minimized by the intracellular induction of invasins, facilitating bacterial re-entry into host cells and, eventually, efficient cell-to-cell spread. This model does not explain how the invasion occurs at the portal of entry, as this involves extracellularly grown bacteria that are likely to be weakly invasive as a consequence of the low PrfA-dependent expression levels.

It has been proposed that the exposure of *L. monocytogenes* to the gastrointestinal environment may result in the stress-mediated induction of *inlAB* via σ^B-dependent activation, directly or through σ^B-regulated expression of the *prfA* gene (Kim *et al.*, 2005, Gray *et al.*, 2006). As above explained, our data do not lend support to this hypothesis. A possibility is that the ability to attach to intestinal epithelial cells (via non-internalin adhesion proteins) may contribute to some level of PrfA activation (Renzoni *et al.*, 1999). Intestinal epithelial cells also tend to be more susceptible to InlA/B-mediated invasion, resulting in substantially more elevated levels of internalization compared to other cellular lineages (unpublished observations from our laboratory). The weak extracellular expression levels of the *inlAB* genes, eventually reinforced by the observed σ^B-dependent expression enhancement in these conditions, may trigger the uptake of sufficient numbers of *L. monocytogenes* bacteria to initiate a productive infection. Other initial mode of entry could be through the Peyer's patches, which have been confirmed to be involved in listerial crossing of the intestinal barrier (Jensen *et al.*, 1998). Indeed, it has been reported that transcytosis through microfold cells (M cells) does not require the presence of PrfA-dependent internalins or haemolysin (Pron *et al.*, 2001, Corr *et al.*, 2006). Further research is needed to clarify the impact and mechanisms involved in the traversal of the epithelial barrier at the portal of entry via the strictly PrfA-dependent *inlAB* invasion locus.

3.2 INVESTIGATION INTO *LISTERIA*-INDUCED APOPTOSIS IN INFECTED HOST CELLS

3.2.1 INTRODUCTION

There is increasing evidence that intracellular pathogens systematically subvert physiological pathways of the eukaryotic cell to survive and to proliferate within host cells. This subversion is quite often achieved via mimicry of host cell functions by the microbial virulence factors. Analysis of the *Listeria* model provides clear examples of how microbial adaptation to the intracellular habitat involves mimicry of eukaryotic structures and functions. The ActA protein, for example, induces actin polymerization by activating the Arp2/3 complex via mimicry of the natural function of the Cdc42 downstream effector WASP, to which sections of the N-terminal domain of ActA are structurally related (Cossart, 2000a, Zalevsky *et al.*, 2001, Vazquez-Boland *et al.*, 2001a, Cossart *et al.*, 2003). The Hpt transporter is another striking example. Hpt is a bacterial homologue of a key element of glucose homeostasis in mammals (Chico-Calero *et al.*, 2002), the G-6-P translocase (G-6-PT) that transports G-6-P from the cytosol into the endoplasmic reticulum in the final step of gluconeogenesis and glycogenolysis (Nordlie *et al.*, 1999). Via Hpt, *Listeria* adopt the same function as an eukaryotic organelle and eventually compete with it for capturing the central metabolite, G-6-P (Chico-Calero *et al.*, 2002).

In the general introduction we mentioned that *L. ivanovii* produces a neutral sphingomyelinase (nSMase), SmcL that shares sequence similarity with mammalian enzymes with the same function (see section 1.3.2). A major research interest in our group is to investigate the “mimicry” aspects of listerial intracellular parasitism, and our hypothesis is that SmcL may indeed act as a mimic of the mammalian nSMases. These enzymes are thought to play a key role in the sphingomyelin-ceramide

signalling pathway. Degradation of sphingomyelin by SMases generates ceramide, a lipid metabolite increasingly recognized as an important pro-apoptotic mediator (Hannun & Luberto, 2000, Birbes *et al.*, 2001, Andrieu-Abadie & Levade, 2002, Hannun & Obeid, 2002, Levade *et al.*, 2002, Luberto *et al.*, 2002, Pettus *et al.*, 2002, Lin *et al.*, 2006, Carpinteiro *et al.*, 2008). Despite intensive research in the past 15 years, the exact role of ceramide in apoptosis remains unclear, and aspects such as the source sphingomyelin pool attacked by the endogenous SMases, or whether a membrane-associated nSMase or a lysosomal acid SMase is primarily involved, remains to be established. Consequently, investigating the role of SmcL in ceramide generation and apoptosis may not only shed light onto the role of bacterial SMases in virulence; it may also provide key novel insight into the role played by ceramide in host cell physiology, with particular emphasis on the apoptotic response.

The work described in this chapter of the thesis is a first step in a broader project aimed at understanding the impact of the listerial SmcL enzyme in *L. ivanovii* virulence and pathogenic tropism, and in general on the role of SMases in the signalling of apoptosis. The first logical step in this research programme is to study in detail the phenomenon of apoptosis caused by *L. ivanovii* during intracellular infection, which we hypothesize may be linked to the intracellular release of the SmcL, neutral SMase.

3.2.2 RESULTS

3.2.2.1 Optimization of methodologies to monitor *Listeria*-induced apoptosis

3.2.2.1.1 Apoptosis detection by flow cytofluorometry

According to the literature, *Listeria* spp. either induce or inhibit apoptosis in different cell lines to promote their survival within the host environment (Rogers *et*

al., 1996, Barsig & Kaufmann, 1997, Carrero *et al.*, 2004a, Parra *et al.*, 2008). However, the exact mechanisms responsible for these contradictory behaviours remain unknown. In order to explore in detail the occurrence of apoptosis during *Listeria* infection, we first focussed on the experimental setup necessary for detection of the cell response in our model cell line for *L. ivanovii*, the bovine kidney epithelial cells MDBK. This cell line was chosen because we previously found that detectable apoptosis is induced in response to *L. ivanovii* infection (Dominguez-Bernal *et al.*, 2006).

For an objective and precise quantification of apoptotic cells, we used a flow cytofluorimetrical technique using infected cell in suspension (see Materials and Methods). The use of Annexin V-FITC staining allowed us to detect early apoptotic cells due to the ability of Annexin V to bind to phosphatidylserine. This phospholipid is translocated to the outer leaflet of the plasma membrane when the cells lose the symmetry of their membrane during the early stage of apoptosis (Koopman *et al.*, 1994, van Engeland *et al.*, 1998, Vermes *et al.*, 2000). This technique made also possible to discriminate those cells that were necrotic. This is achieved by using a second fluorescent dye, propidium iodide, which binds to double-stranded DNA after permeating through damaged cell membranes, indicative of cell death by necrosis (Nicoletti *et al.*, 1991, Vitale *et al.*, 1993, Vermes *et al.*, 2000).

We used MDBK cells grown in 6-well plates for 10 to 12 h until ~ 80% confluence. It was necessary to very carefully keep always the same conditions in order to obtain reproducible results, and also to ensure that cells were *Mycoplasma*-free with regular checks. In each set of experiments, we included non-infected cells as a negative control, to quantify the background spontaneous apoptosis during the experimental time. As a positive control, we used cell monolayers treated for 3 to 4 h with staurosporine (STS), a cell-permeable inhibitor of protein kinases that induces apoptosis (Chae *et al.*, 2000, Belmokhtar *et al.*, 2001, Zhang *et al.*, 2003).

We carried out intracellular proliferation assays using *L. ivanovii* ATCC 19119 and the wild-type *L. monocytogenes* serovar 4b strain P14. To infect the cells we used a multiplicity of infection (MOI) of 25:1 for *L. ivanovii* and 100:1 for *L. monocytogenes* P14.

After 12 h of intracellular proliferation we observed 14% more apoptosis in the cells infected with *L. ivanovii* compared to those infected with *L. monocytogenes* P14 (17.1 ±0.7% and 3.0 ±1.2%).

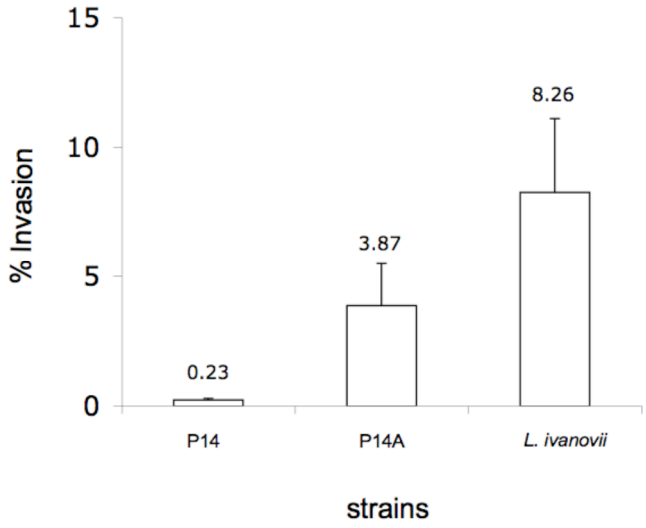

Figure 3.2.1: Percentage of internalization of *L. ivanovii* and *L. monocytogenes* (*prfA*^{WT} and *prfA**^{G145S} genotypes) in MDBK cells.
Mean ± SE of at least two independent experiments performed in duplicate.

We noticed that invasion of MDBK cells was substantially higher for *L. ivanovii* than *L. monocytogenes* P14 (8.3% vs 0.2%) (figure 3.2.1). We tried to adjust the MOI by either increasing it for *L. monocytogenes* or decreasing it for *L. ivanovii*. However, the changes of MOI did not markedly modify the percentage of invasion (data not shown). The two bacteria also exhibited marked differences in PrfA-dependent expression *in vitro*. Contrary to *L. monocytogenes* P14, *L. ivanovii* overexpresses constitutively all the virulence factors of the PrfA regulon (Mauder *et al.*, 2006). As the expression level of PrfA-dependent genes directly influences

invasiveness (section 3.1.2), we decided to carry out additional experiments using P14A, the isogenic *prfA**^{G145S} derivative of P14 (Ripio *et al.*, 1997a, Vega *et al.*, 1998). This mutant strain overexpresses *in vitro* all the PrfA-dependent genes to levels similar to *L. ivanovii* (our unpublished observations).

We observed that *L. monocytogenes prfA**^{G145S} was ~ 17 times more invasive than *L. monocytogenes prfA*^{WT}, reaching levels that were close to those of *L. ivanovii* (figure 3.2.1).

These data led us to perform new comparative apoptosis experiments between *L. ivanovii* and *L. monocytogenes* using P14A, readjusting the MOI for the latter to 50:1 to achieve, according to the observed internalization, similar initial intracellular numbers for both bacteria. In these experiments, we determined apoptosis at different time points and, in parallel, we carefully measured the amount of intracellular bacteria present in the cell monolayer (see Materials and Methods).

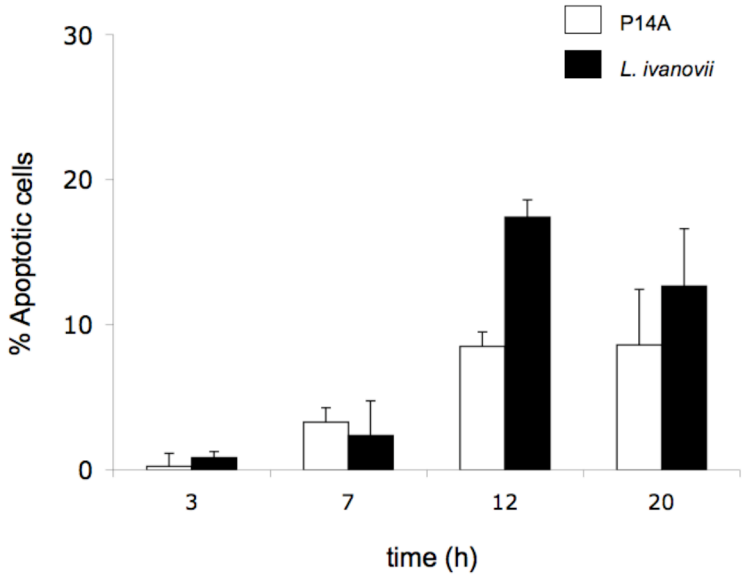

Figure 3.2.2: Percentage of apoptosis in *Listeria*-infected cells.
Data represent values in infected cells after the subtracting the background (spontaneous) apoptosis detected in the non-infected control cells. Data for controls: uninfected cells, 4.4 ±0.5; and STS-treated cells, 35.4 ±2.9. Mean ± SE of two independent experiments.

The percentage of apoptosis in infected cells is shown in figure 3.2.2. After 3 h of intracellular proliferation, the percentage of apoptosis was alike for both strains and similar to the one in untreated cells. At later time points, the level of apoptosis increased slightly, reaching the maximum at 12 h. At this time point the data were 17.1 ±1.2% for *L. ivanovii* and 8.5 ±1.0% for P14A; this difference was statistically significant (P = 0.02). At 20 h post-infection, we observed a similar percentage of apoptotic cells to that for P14A at 12 h, and a decrease in the percentage of apoptosis in the case of *L. ivanovii* (figure 3.2.2). There was substantial variability in the apoptosis data at this time point, which we attributed to the occurrence of cell damage and detachment of the monolayer from the bottom of the well in some of the samples.

The number of intracellular bacteria determined at each time point is presented in figure 3.2.3. There were only slight differences between the two strains at 3 and 7 h post-infection, but their amounts increased at later time points. At 12 h, *L. ivanovii* proliferated 3.3 times more than *L. monocytogenes* P14A (7.5 ±0.65 $\times 10^7$ and 2.3 ±0.61$\times 10^7$ CFU/well, respectively). At t = 20 h post-infection, however, the bacterial population declined in both cases. On microscopic examination of the infected cells, this effect coincided with very obvious cell destruction as indicated by the appearance of patches of monolayer detachment. Therefore, the observed reduction in the intracellular population at this late time-point was probably only paradoxical, likely due to the killing of the bacteria from the damaged cells by the gentamicin present in the extracellular medium (used to kill extracellular bacteria and prevent extracellular growth; see Materials and Methods).

We repeated the experiments using lower MOIs for *L. ivanovii*, in order to try to obtain similar numbers of intracellular bacteria for both strains during the proliferation phase. However, in these conditions we could not observe significant levels of apoptosis in the *L. ivanovii*-infected cells. We also tried to increase the MOI for P14A, but the MDBK monolayers were quickly damaged (data not shown).

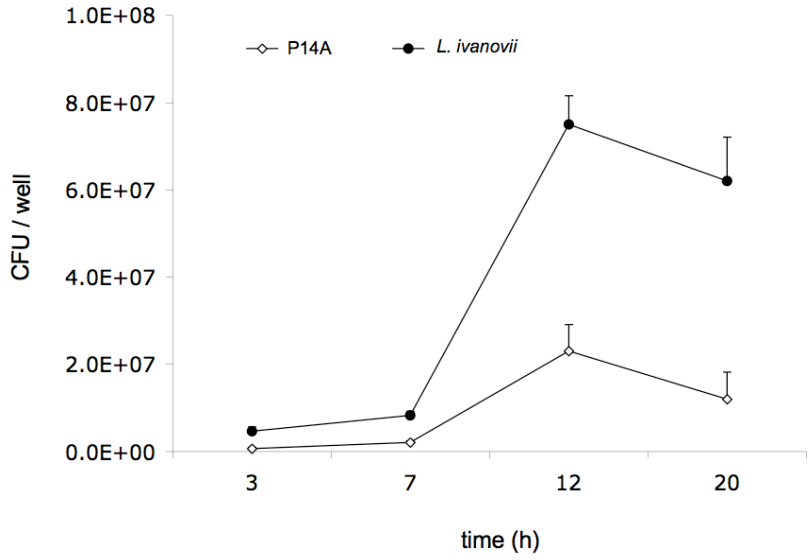

Figure 3.2.3: Intracellular proliferation of *L. ivanovii* and *L. monocytogenes* P14A in MDBK cells. The bacterial numbers were determined in the same samples as those used for apoptosis determination (figure 3.2.2). Mean ± SE of two independent experiments.

Thus, according to our results the optimum time to measure apoptosis in MDBK cells infected with *Listeria* spp. was around 12 h post-infection using MOIs ranging from 25:1 and 50:1 for *L. ivanovii* and *L. monocytogenes* P14A, respectively. At this time point, we observed the highest levels of apoptosis and maximum number of intracellular bacteria.

3.2.2.1.2 Normalization of apoptosis determinations

The above observations suggested that *L. ivanovii* was more apoptogenic than *L. monocytogenes*. However, if the bacteria are responsible for the increased apoptosis detected in an infected monolayer (over background levels), the values observed would be dependent on the number of intracellular bacteria present in the well. In cell-based infection assays it is difficult and impractical to try to adjust the conditions so that the exact number of the two bacteria that are being compared is always obtained at a given time point. One way of resolving this problem is to try to

normalize the apoptosis values by the total number of bacteria in the monolayer. We did this using the following simple formula:

$$NA = \frac{a}{b} \times 10^{n}$$

where *NA* is the normalized apoptosis, *a* is the percentage of infection-associated apoptotic cells (percentage of apoptotic cells in the sample minus the percentage of spontaneous apoptotic cells in the uninfected control), *b* is the total number of intracellular bacteria in the well, and *n* is a correction factor (common decimal exponent of the number of bacteria being compared).

When applying the *NA* formula to the values obtained in the above described experiments, the conclusion was that, despite the percentage of apoptosis being greater in *L. ivanovii*-infected monolayers, *L. monocytogenes* P14A bacteria would in fact be paradoxically more apoptogenic (37.04 ±2.8 and 22.8 ±1.2, respectively; $P = 0.001$) (figure 3.2.4).

However, the above calculations do not take into account another key factor with a direct influence on the outcome variable. Assuming there is a direct correlation between the presence of bacteria in the cell and the occurrence of apoptosis, it is obvious that the larger the percentage of infected cells in the monolayer, the greater the percentage of apoptosis is expected to be detected. Since the bacteria under comparison may differ in their capacity to invade and/or spread in the monolayer, it became apparent that it was also necessary to incorporate in the data normalization the number of infected cells. In summary, the number (or percentage) of apoptotic cells observed at a given time point *t* depends on how many cells are invaded, how quickly bacteria grow and spread, and how quickly they cause apoptosis.

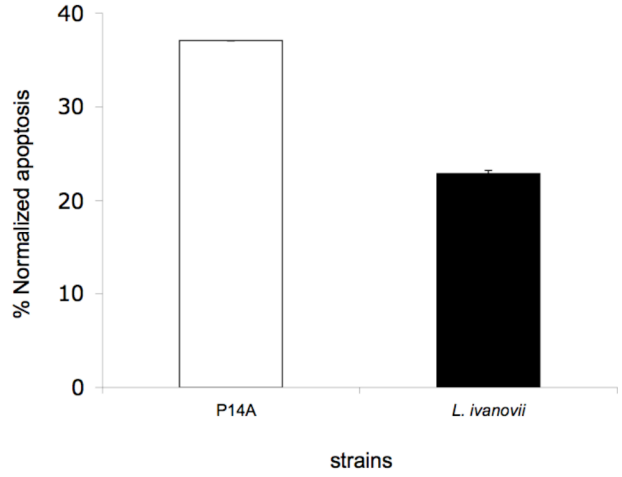

Figure 3.2.4: Normalized apoptosis in MDBK cells infected with *L. monocytogenes* P14A and *L. ivanovii* at t = 12 h post-infection.
Values were calculated with the formula $NA = a / b \times 10^n$ from data shown in figures 3.2.2 and 3.2.3 as indicated in the text. Mean ± SE of two independent experiments.

With the help of Dr. Nick Savill, an expert in mathematical modelling from the Centre for Infectious Diseases of the University of Edinburgh, an Apoptosis Index (*AI*) was derived taking into consideration these variables, as follows:

$$AI = \frac{a_t}{t b_t^{\beta} c_t^{1-\beta}}$$

where a is the net percentage of apoptotic cells (after subtraction of spontaneous apoptosis), b is the total number of intracellular bacteria, c is the percentage of infected cells, t is the time point, and β is a variable that determines how the number of bacteria in an infected cell (B) affects the apoptosis rate (a detailed description of the mathematical basis used in the derivation of the *AI* formula can be found in Appendix II).

3.2.2.1.3 Setting up and validation of microscopic apoptosis determination

To apply the above formula, we needed to determine accurately the percentage of infected cells. This had ideally to be in the very same cell monolayer in which we were determining apoptosis. To achieve this, we needed to use a microscopic technique, with visualization of intracellular bacteria by phase contrast and fluorescence microscopy for apoptosis. For the latter, we needed first to ensure that the apoptosis quantitative readouts were comparable to those obtained by the previously standardized Annexin V-FITC/PI flow cytometrical assay.

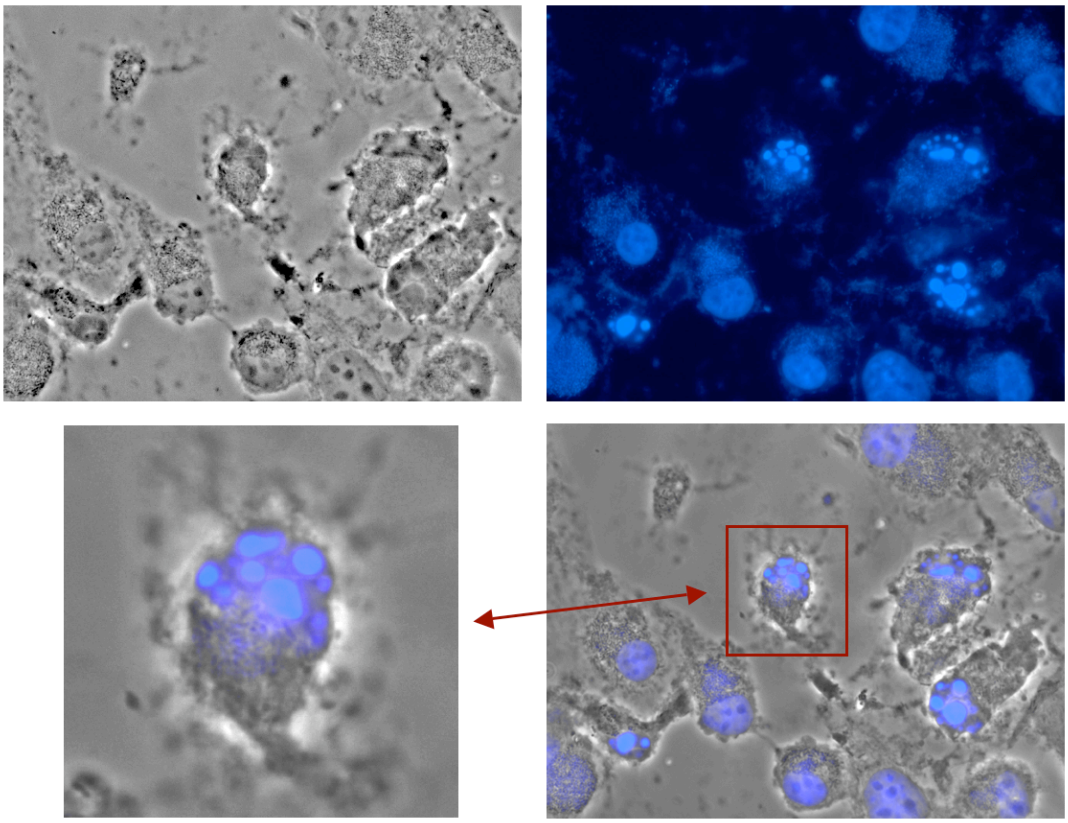

Figure 3.2.5: MDBK cells infected with *L. ivanovii* ATCC 19119 and stained with Hoechst 33258. Left top panel, phase contrast; right top panel, blue fluorescence with DAPI filter; right bottom panel, merge; left bottom panel, digital magnification of bright blue colour denoting chromatin condensation indicates apoptotic cells. Note the abundance of intracellular bacteria in the *L. ivanovii*-infected cells, seen in the left top panel as a granular material in the cytosol. Magnification: 630 ×

For the microscopic determinations, we used MDBK cell monolayers grown in glass-coverslips (see Materials and Methods). We compared two fluorescent stains, Annexin V-FITC used in the flow cytometry-based determinations, and a Hoechst dye, reported to provide a more simple and accurate method for visual apoptosis detection (Weiss & Zychlinsky, 2002). Hoechst dyes are cell permeable nuclear stains that emit blue fluorescence when bound to double-stranded DNA. They allow striking visualization of chromatin condensation, a hallmark in apoptotic cells (Vermes *et al.*, 2000, Chowdhury *et al.*, 2006).

Figure 3.2.5 shows MDBK cells infected with *L. ivanovii* ATCC 19119 and stained with Hoechst 33258, in which characteristic changes in chromatin are evident.

To compare the flow cytofluorometrical and visual detection of apoptosis using the above mentioned stains, we performed in parallel both techniques, incorporating cells treated/untreated with STS as controls. MDBK cells treated with STS showed 23.84% of apoptotic cells with flow cytofluorometry, and 28.04% and 27.31% of apoptotic cells in case of fluorescent microscopy when stained with Annexin V-FITC and Hoechst, respectively. The percentages of apoptosis in untreated cells were 7.23%, 2.44% and 7.77%, respectively (figures 3.2.6 and 3.2.7).

We concluded that the flow cytometrical and microscopic techniques gave essentially equivalent results. For the latter, we decided to use the Hoechst fluorophore because this reagent is less expensive than Annexin V-FITC and additionally it gives less background noise to the stained cell images. Moreover, the Annexin V-FITC stain was more prone to photobleaching.

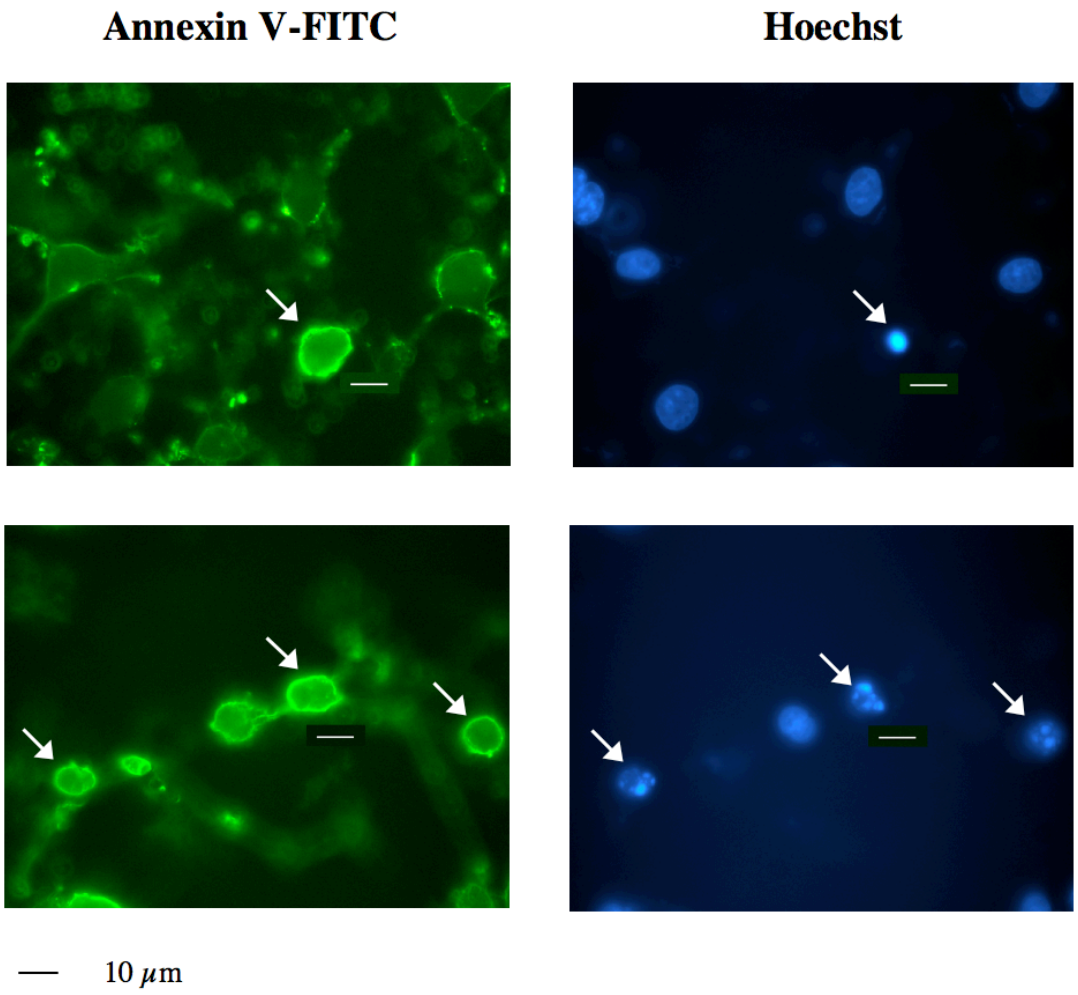

Figure 3.2.6: MDBK cells treated with STS and labelled with Annexin V-FITC (left panels) and Hoechst 33258 (right panels).
Same fields are shown for comparison. White arrows indicate some representative strongly positive cells. Note the surface decoration of Annexin V-FITC-positive cells, based on detection of surface translocation of phosphatidylserine. There was generally good correlation between Annexin V-FITC-positive signal and the presence of pyknotic, fragmented nuclei as observed with Hoechst 33258. Some Annexin V-FITC-positive cells did not show as apoptotic with the DNA stain, possibly because they were early apoptotic cells (the membrane translocation of phosphatidylserine is an early event during apoptosis that precedes nuclear condensation and fragmentation). However, overall, the two fluorescent dyes gave similar results (figure 3.2.7).

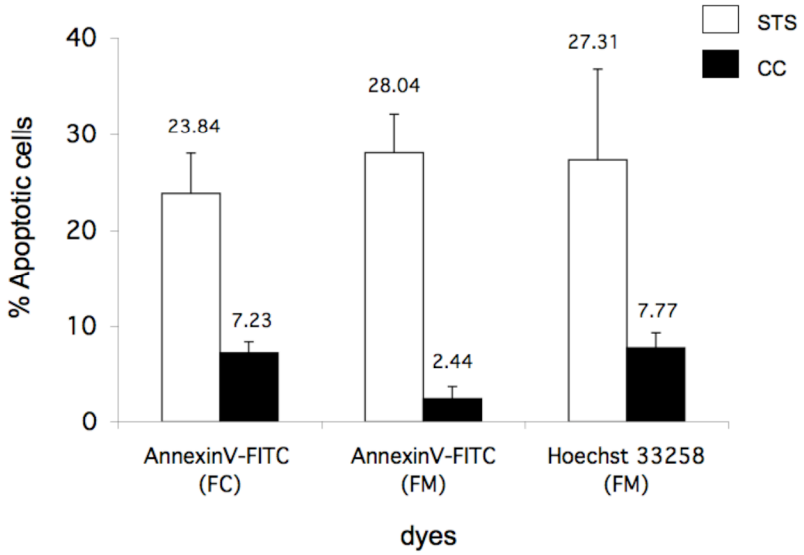

Figure 3.2.7: Apoptotic cells detected using flow cytofluorometry (FC) or fluorescent microscopy (FM) at 4 h after exposure to the pro-apoptotic drug, staurosporine (STS).
White bars represent percentage of apoptotic MDBK cells in samples treated with STS, black bars correspond to untreated control samples (CC). Mean ± SE of at least two independent experiments.

3.2.2.2 Comparative analysis of *L. ivanovii* and *L. monocytogenes* using the microscopic technique and Apoptosis Index (*AI*)

Once we set up the microscopical technique, we carried out infection assays with *L. ivanovii* and *L. monocytogenes* P14A in MDBK monolayers on coverslips and monitored for the presence of infected and apoptotic cells at t = 14 h. The fixed coverslips were stained with Hoechst 33258 and the number of infected and apoptotic cells was determined upon examination of a minimum population of 500 randomly selected cells, from random microscopical fields and at least two experiments. The results are shown in table 3.3 together with the corresponding *AI* calculations.

If we assume that there is a linear correlation between the number of bacteria and the apoptosis rate ($\beta = 1$), in the *AI* formula b_t^{β} becomes b_t^1 and $c_t^{1-\beta}$ becomes c_t^0

= 1, meaning that the apoptosis rate depends only on the number of bacteria. In this case, *L. ivanovii* and *L. monocytogenes* P14A would not significantly differ in apoptogenic activity ($P = 0.78$) (table 3.3B).

Table 3.3: Relevant data from *Listeria*-infected MDBK cells.
MOIs used: *L. ivanovii* 20:1, *L. monocytogenes* P14A 50:1, P14AΔ*actA* 75:1. Time point $t = 14$ h.
(A) Mean percentage of apoptosis and corresponding intracellular bacterial numbers per well and percentage of infected cells.
(B) Mean apoptosis index. This index was calculated independently for each experiment replicate. β is the variable that determines how the rate of apoptosis depends on the number of bacteria in an infected cell B. This parameter is not known and there are several possible scenarios, for example that the apoptosis rate (B^{β}) is independent on the number of bacteria, is linearly, quadratically, exponentially correlated, or even show a threshold, *etc*. For *AI* calculations, in this study we made the simpler assumptions that β was either independent ($\beta = 0$) or linearly correlated ($\beta = 1$) with bacterial numbers. See text and Appendix II for details.

A

	% apoptosis	CFU x 10^6	% infected cells
L. ivanovii	18.21 ±1.65	9.13 ±1.83	98.40 ±1.61
P14A	8.46 ±1.58	4.60 ±1.01	94.48 ±4.98
Δ*actA*	2.99 ±0.10	1.56 ±1.19	51.77 ±14.98

B

	AI $\beta=0$	*AI* $\beta=1$
L. ivanovii	0.013 ±0.001	0.142 ±0.013
P14A	0.006 ±0.001	0.154 ±0.039
Δ*actA*	0.004 ±0.001	0.340 ±0.264

However, if we assume that the apoptosis rate is independent from the number of intracellular bacteria ($\beta = 0$), then in the *AI* formula b_t^{β} becomes $b_t^0 = 1$ and $c_t^{1-\beta}$ becomes c_t^1, *i.e.* the apoptosis rate only depends on the percentage of infected cells. Here, *L. ivanovii* would be significantly more apoptogenic than *L. monocytogenes* P14A ($P = 0.008$) (table 3.3B).

Therefore, we clearly see that it is not really possible to estimate the relative apoptogenic potential of two different bacteria unless we know how the apoptosis rate of infected cells depends on the number of bacteria within these cells.

3.2.2.2.1 Relationship between apoptosis and presence of bacteria in MDBK cells

In order to approximate the above question, we applied the microscopic technique to investigate the relationship between the presence of bacteria and apoptosis in the MDBK monolayers infected with *L. ivanovii* and *L. monocytogenes* P14A. Two different time points were analyzed to monitor changes during the infection dynamics, early after inoculation (t = 4 h), and after the infection was well established in the monolayer (t = 14 h). To determine the percentage of infected cells, we inspected random microscopical fields under phase contrast and observed a minimum of 200 eukaryotic cells, again randomly. To provide a quantitative measure, these cells were classified in five different categories according to the number of associated bacteria: "0", "1-15", "16-30", "31-50" and " ≥ 51".

At t = 4 h, the percentage of infected cells was 62.7% for *L. monocytogenes* P14A and 95.2% for *L. ivanovii*, whereas at t = 14 h these percentages equalized (92.6% and 98.3%, respectively). Consistent with our previous observations at monolayer population level, the number of bacteria per infected cell was higher for *L. ivanovii* compared to *L. monocytogenes* P14A at both time points. At 4 h post-infection, most of the cells (50.5%) infected with P14A contained less than 16 bacteria, whereas most *L. ivanovii*-infected cells (52.2%) contained more than 16 bacteria and a significant percentage (30.4%) harboured between 16 and 30 bacteria. At 14 h, nearly half (46.6%) of *L. ivanovii*-infected cells were packed with bacteria (≥ 51 per cell), whereas only a few (7.8%) of P14A-infected cells contained more than 30 bacteria, and no cells contained ≥ 51 bacteria (figure 3.2.8). Thus, the bacterial load increased for both strains during the course of the infection, but the extent to which this happened was greater with *L. ivanovii* than *L. monocytogenes* P14A.

We next investigated the correlation between the presence of bacteria and the occurrence of apoptosis. To approach this, we compared the numbers of bacteria in apoptotic vs non-apoptotic cells.

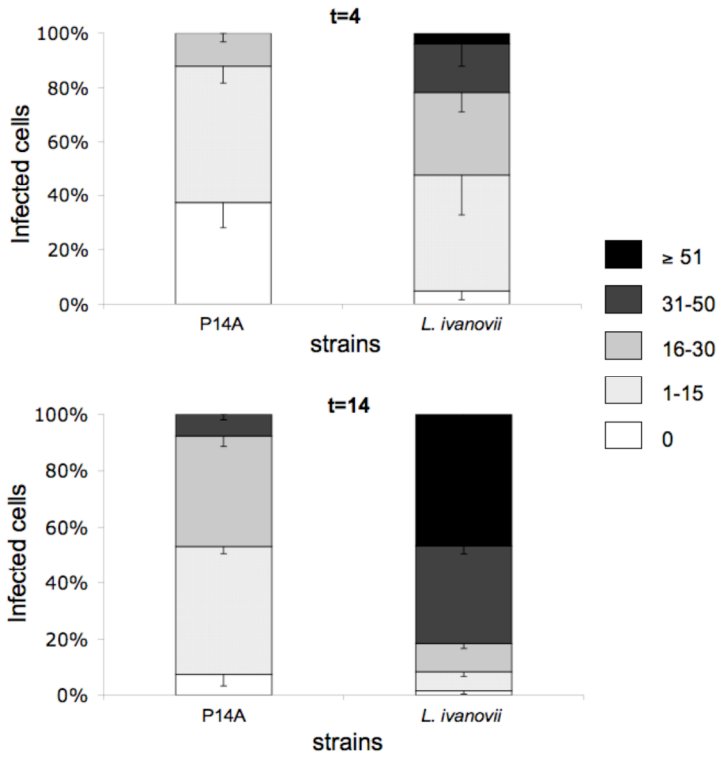

Figure 3.2.8: Percentage of infected cells and corresponding load of *L. ivanovii* and *L. monocytogenes* P14A bacteria per cell at 4 and 14 h of intracellular infection.
Mean ± SE of at least two independent experiments.

At 4 h post-infection, 42.7% of the apoptotic cells in the *L. ivanovii*-infected monolayer contained over 30 bacteria, whereas most apoptotic cells in the *L. monocytogenes* P14A-infected wells contained only few bacteria (≤ 15, 54.3%) or were not infected at all (35.3%). However, whilst at this time-point a significant number of positive cells (n = 150) could be identified in the *L. ivanovii*-infected monolayers, too few apoptotic cells were found with P14A (only 14), so the percentages with the latter should be interpreted with caution. Many of these few apoptotic cells, thus, clearly belonged to the spontaneously occurring population. At t = 14 h, the apoptotic cells were clearly more abundant and all were associated with intracellular bacteria. Most of the *L. ivanovii*-infected cells (64.2%) were packed with bacteria (≥ 51 per cell), whereas only 10.9% of P14A-infected cells contained more than 30 bacteria per cell; cells with ≥ 51 bacteria were not found with *L. monocytogenes* (figure 3.2.9).

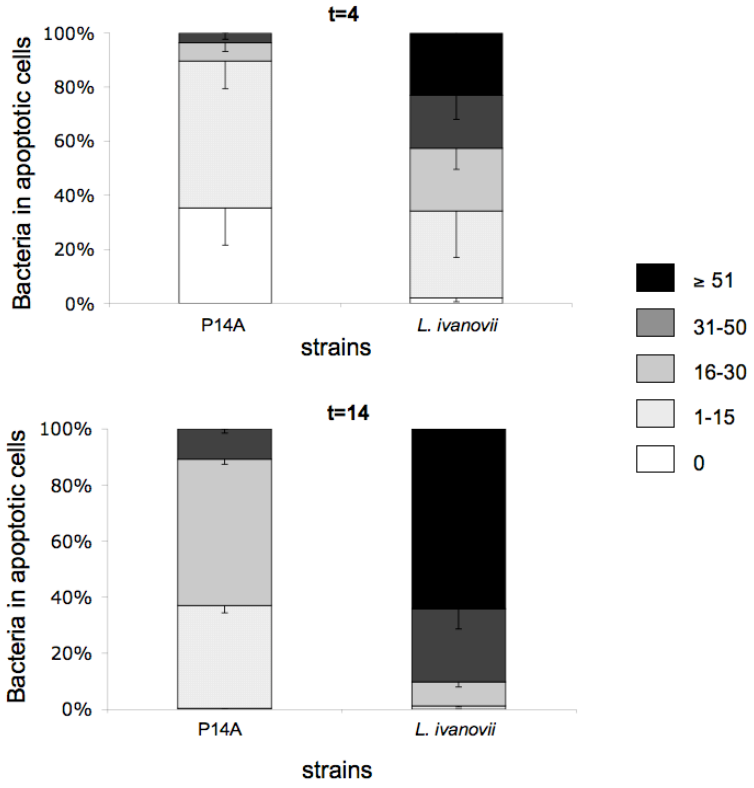

Figure 3.2.9: Distribution in percentage of the intracellular loads of *L. ivanovii* and *L. monocytogenes* P14A bacteria in apoptotic (Hoechst 33258-positive) cells at 4 and 14 h post-infection.
Mean ± SE of at least two independent experiments.

By contrast, in the non-apoptotic cells the number of bacteria found was generally lower at both time points for the two strains. In *L. ivanovii*-infected cells, for example, 1.8% and 35.1% contained ≥ 51 bacteria at t = 4 h and 14 h among the non-apoptotic population, whereas the corresponding percentages were 23.1 and 64.2 among the apoptotic cells. In addition, a number of non-apoptotic cells were bacteria-free (21.9 and 55.1% at t = 4 and 3.4 and 5.1% at t = 14 for *L. ivanovii* and P14A, respectively), whereas virtually all apoptotic cells contained bacteria (figures 3.2.9 and 3.2.10).

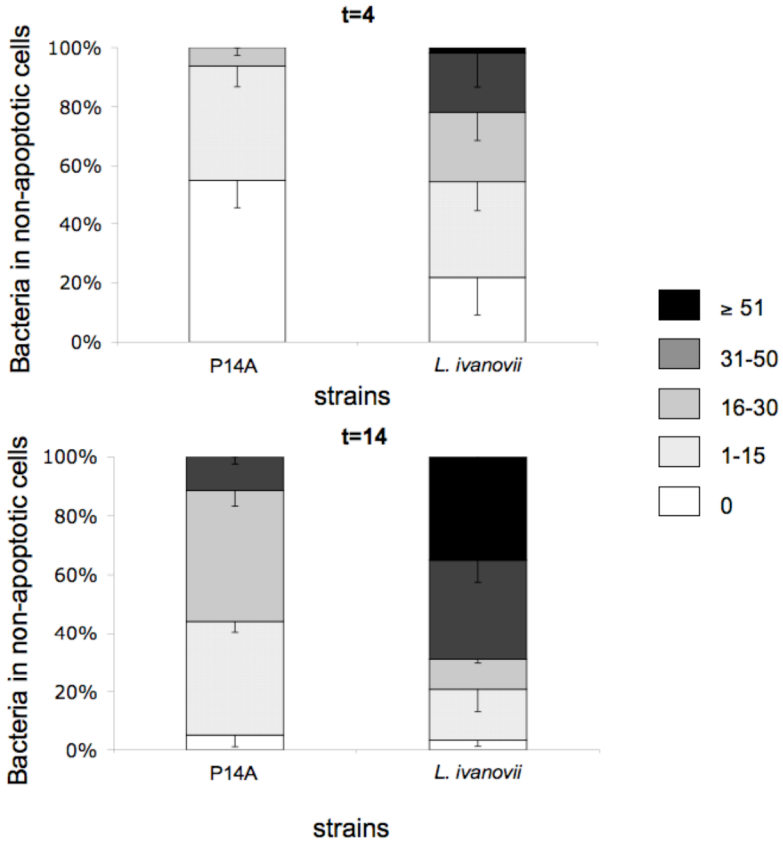

Figure 3.2.10: Distribution in percentage of the intracellular loads of *L. ivanovii* and *L. monocytogenes* P14A bacteria in non-apoptotic (Hoechst 33258 - negative) cells at 4 and 14 h post-infection.
Mean ± SE of at least two independent experiments.

Thus, (i) when an infection is established in the monolayer and there has been substantial bacterial proliferation, apoptotic cells are always associated with bacteria. This indicates that the apoptotic response is linked to listerial intracellular infection. In addition, (ii) a significant number of infected cells do not undergo apoptosis, although the number of bacteria within them tends to be lower than in apoptotic cells. This may indicate that the host cells belong to different subpopulations differing in their susceptibility to *Listeria*-induced apoptosis. It may also reflect that a minimum exposure time above a certain bacterial threshold could be also required to trigger host cell apoptosis.

In practical terms regarding our *AI* equation, our data exclude that there is a strict linear correlation between the number of bacteria in the monolayer and the percentage of apoptosis detected. Without further work clarifying the nature of the relationship between the presence of bacteria and the dynamics of appearance of the apoptotic response, we have, thus, to assume that $\beta = 0$, *i.e*. the apoptosis rate is not dependent on the total number of intracellular bacteria in the well but rather on the percentage of infected cells.

In these conditions, according to the data in table 3.3B, *L. ivanovii* would be at least twice as much apoptogenic as *L. monocytogenes* P14A.

3.2.2.2.2 Cell-to-cell spread and apoptosis

An element related to *Listeria* infection dynamics with a possible impact on apoptosis is the cell-to-cell spread phenomenon. Cell-to-cell spread may influence the apoptotic response by promoting the colonization of the cell monolayer as the infection progresses, leading to higher numbers of infected cells that may potentially undergo apoptosis. Also, if after internalization the bacteria do not move to neighbouring cells via actin-based motility, as in a Δ*actA* mutant, they accumulate in the infected cell as they replicate, forming compact micro-colonies near the nucleus (Domann *et al.*, 1992, Kocks *et al.*, 1992). This overcrowding and ensuing intracellular accumulation of secreted toxic PrfA-regulated virulence factors, such as the pro-apoptotic LLO toxin (Carrero *et al.*, 2008), may cause premature host cell death. The importance of bacterial overcrowding of the cytosol as an apoptosis trigger is suggested by our data, in which there seems to be an association between the more elevated percentage of apoptotic cells in *L. ivanovii* vs *L. monocytogenes* P14A and the greater numbers of bacteria found in the cells infected with the former species. In this scenario, the spreading of bacteria to adjacent cells after multiplication in the cytosol may be important to reduce the bacterial burden in the infected cell, favouring its survival, at least at short term. Incidentally, we observed that *L. ivanovii* spreads ~ 40% less efficiently than *L. monocytogenes* P14A in a

plaque assay (figures: 3.2.11 and 3.2.12), and this may contribute to explain the higher apoptosis levels seen in the cells infected with these bacteria. The reason for this cell-to-cell spread defect is unknown, although it may be related to the particularly divergent sequence of the ActA protein of *L. ivanovii* (the most dissimilar among all the listerial PrfA-regulated factors).

To examine the impact of cell-to-cell spread in apoptosis, we used the Δ*actA* mutant derivative of P14A (section 3.1.1.3) and compared its apoptogenic activity to that of its intercellular motility-proficient parent strain. Before carrying out the apoptosis assays, as ActA was previously shown to contribute to *L. monocytogenes* internalization (Suarez *et al.*, 2001), we carefully determined the invasiveness of the Δ*actA* mutant.

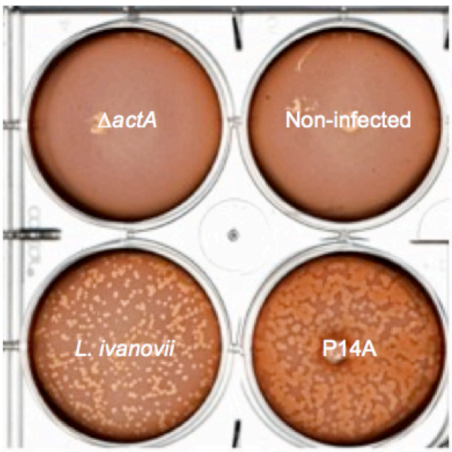

Figure 3.2.11: Plaque assay of *L. ivanovii* ATCC 19119, *L. monocytogenes* P14A and isogenic Δ*actA* derivative of P14A.
Infected monolayers were incubated at 37ºC for 72 h. Note the smaller size of the plaques formed by *L. ivanovii* relative to P14A.

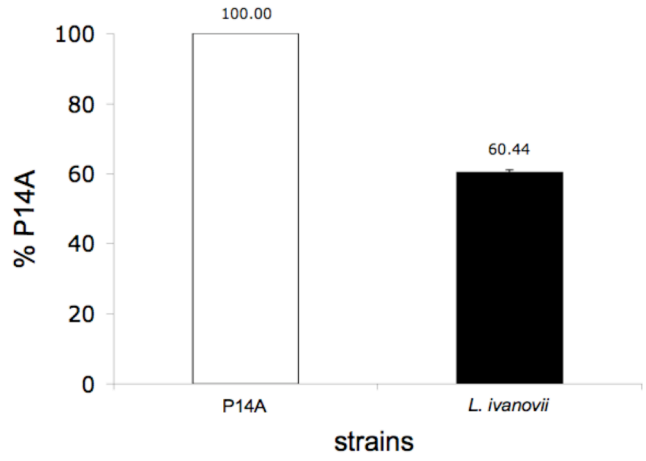

Figure 3.2.12: Quantification of cell-to-cell spread of *L. ivanovii* and *L. monocytogenes* P14A in L929 cells.
The diameter of the plaques shown in figure 3.2.11 was measured as in figure 3.1.20 but the data are presented in relative values (% of P14A). Mean ± SE of three experiments.

The *actA* gene deletion associated with a significant reduction in internalization into MDBK cells, from ~ 4% for P14A to 0.67%. We also found that the Δ*actA* mutant proliferated less efficiently than its parent strain (figure 3.2.13). Therefore, to obtain similar intracellular population numbers at the time point chosen for apoptosis determination, t = 14 h, we had to use a larger MOI for the Δ*actA* mutant (75:1 vs 50:1 for P14A).

The apoptosis experiments for the Δ*actA* mutant were carried out concomitantly with those for P14A and *L. ivanovii*, as described in section 3.2.2.2. The corresponding data are shown in table 3.3.

After 14 h of infection, the percentage of apoptotic cells in the monolayer was significantly lower for the Δ*actA* mutant than for P14A (2.99 ±0.1% and 8.5 ±1.6%, respectively, P = 0.03). The intracellular numbers and percentage of infected cells were also lower for Δ*actA*.

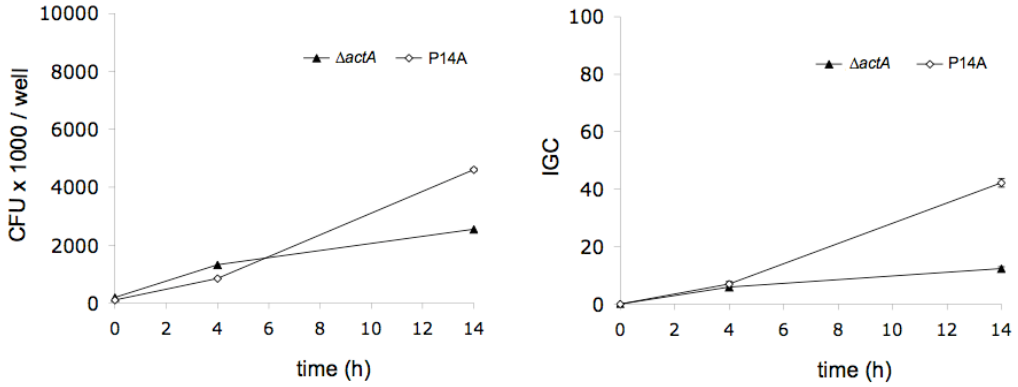

Figure 3.2.13: Intracellular proliferation of *L. monocytogenes* P14A and its isogenic Δ*actA* derivative in MDBK cells.
On the right panel the intracellular proliferation data were normalized to the initial bacteria counts at $t = 0$ using an intracellular growth coefficient (IGC = $[b_{t=n} - b_{t=0}] / b_{t=0}$, where $b_{t=n}$ and $b_{t=0}$ are the intracellular bacterial numbers at a specific time point, $t = n$, and $t = 0$, respectively). Positive IGC indicates proliferation, negative values reflect decrease in the intracellular bacterial population. Mean ± SE of at least two independent experiments.

When these data were applied to the *AI* formula, considering $\beta = 0$ (apoptosis rate assumed to be independent from the number of intracellular bacteria), no significantly different index values were obtained (0.004 ±0.001 and 0.006 ±0.001 for Δ*actA* and P14A, respectively; $P = 0.39$). The same conclusion was reached if taking $\beta = 1$ (apoptosis assumed to increase linearly with the number of bacteria; *AI* = 0.34 ±0.26 and 0.15 ±0.04, respectively, $P = 0.34$).

We also investigated the distribution of the Δ*actA* bacteria in infected cells, apoptotic cells and non-apoptotic cells. The data are shown in figures 3.2.14, 3.2.15, and 3.1.16. Whilst there were less infected cells in the monolayers, these contained more Δ*actA* bacteria. In addition, all apoptotic cells contained bacteria and were very heavily infected in comparison to apoptotic cells in the P14A-infected monolayers, whereas most non-apoptotic cells did not contain bacteria (~ 57.0%) or contained only a few bacteria (≤ 15, ~ 28.1%).

Thus, despite the significant differences in the numbers of intracellular bacteria in the infected cells, there seems not to be intrinsic differences in apoptogenic activity between *L. monocytogenes* P14A and its cell-to-cell spread-deficient Δ*actA* derivative. We also conclude that the presence of *L. monocytogenes* bacteria within the cells is associated with the occurrence of apoptosis.

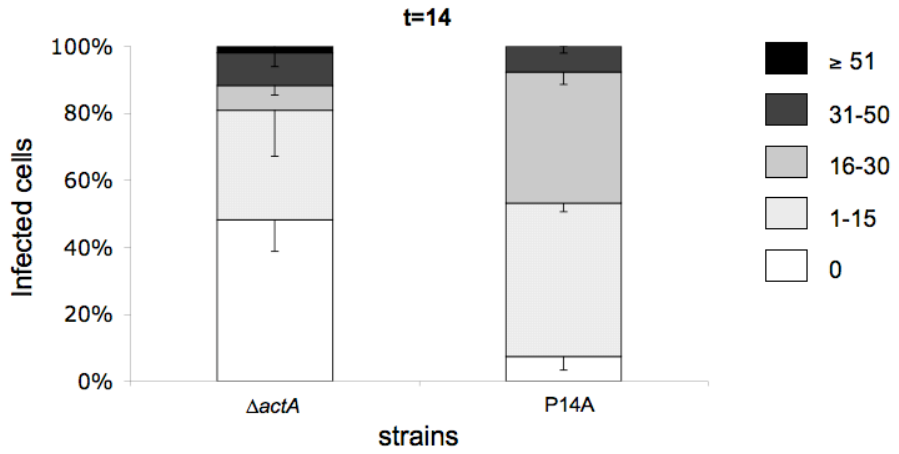

Figure 3.2.14: Distribution in percentage of *L. monocytogenes* P14AΔ*actA* bacteria and those of its parent strain in infected MDBK cells.
Data for P14A are the same as those shown in figure 3.2.8. Mean ± SE of at least two independent experiments.

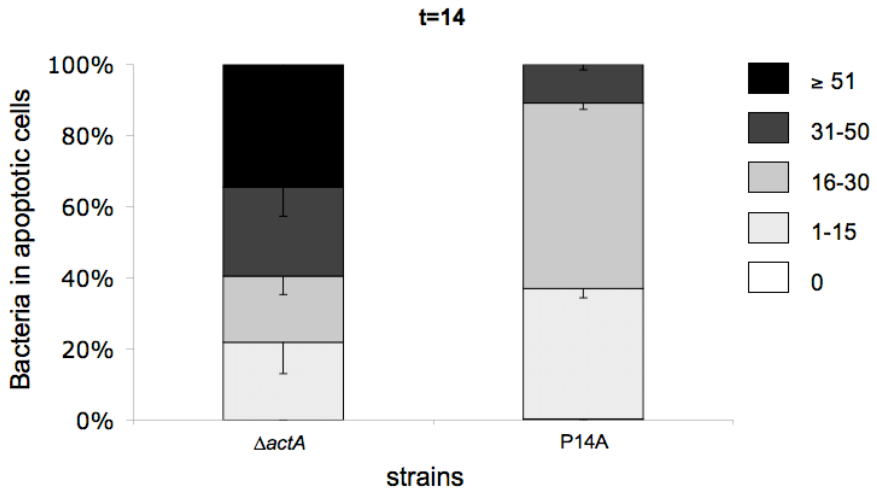

Figure 3.2.15: Distribution in percentage of *L. monocytogenes* P14AΔ*actA* bacteria and those of its parent strain in apoptotic (Hoechst 33258-positive) cells at 14 h post-infection.
Data for P14A are the same as those shown in figure 3.2.9. Mean ± SE of at least two independent experiments.

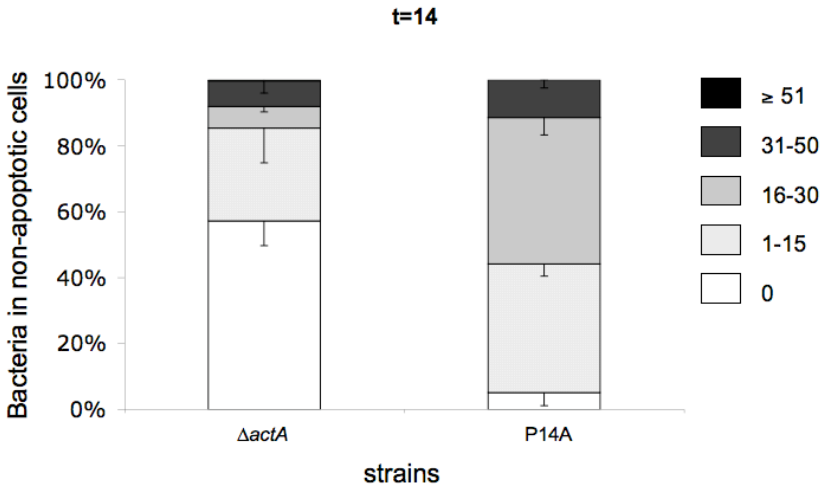

Figure 3.2.16: Distribution in percentage of *L. monocytogenes* P14AΔ*actA* bacteria and those of its parent strain in non-apoptotic (Hoechst 33258-negative) cells at 14 h post-infection.
Data for P14A are the same as those shown in figure 3.2.9. Mean ± SE of at least two independent experiments.

3.2.2.3 Investigating the role of *L. ivanovii* SMase (SmcL) in apoptosis – stable heterologous expression of *smcL* in Δ*plcAB L. monocytogenes*

In previous studies carried out in our laboratory, it was demonstrated that an *smcL* mutation in *L. ivanovii* has effects comparable to those reported for *plcA* and *plcB* mutations (Marquis *et al.*, 1995, Smith *et al.*, 1995). The *smcL* knock-out mutant showed moderate attenuation of virulence in mice and intracellular growth capacity in epithelial cells (*e.g.* MDBK cell line). Heterologous expression of the *smcL* gene in a *L. monocytogenes* background lacking all known phagosome-disrupting virulence factors, such as Hly, PlcA and PlcB, although with limited efficiency, enabled the release of the mutant bacteria to the cytosol and their intracellular proliferation. It was concluded that SmcL plays a role in virulence similar to that of PlcA and PlcB, as an accessory membrane-damaging factor acting alongside LLO and the other two phospholipases to faciliate bacterial escape from the phagocytic vacuole (Gonzalez-Zorn *et al.*, 1999).

The presence in *L. ivanovii* of an additional membrane-disrupting phospholipase, with redundant functions to PlcA and PlcB and partially overlapping substrate range with the PlcB enzyme, is intriguing. Since SmcL is encoded in the species-specific LIPI-2 pathogenicity island, we hypothesized that this SMase could play a role in the specific pathogenic properties of *L. ivanovii* (Dominguez-Bernal *et al.*, 2006) (see Introduction section 1.1.2).

Initial attempts were made in our laboratory to try to establish whether SmcL, in addition to its "mechanic" role in phagosome membrane disruption, could also modulate host cell responses via ceramide, the degradation product of sphingomyelin by a SMase. Preliminary experiments showed that infection of MDBK cells by *L. ivanovii* is accompanied by a strong ceramide generation response (6-fold relative to non-infected cells). The ceramide levels were very significantly reduced in cells infected with an isogenic *smcL* mutant (unpublished data). Using the same *smcL* bacteria, it was shown that the lack of SMase activity associates with significantly reduced apoptosis in MDBK cells (Dominguez-Bernal *et al.*, 2006), suggesting a connection between ceramide generation and cell death in *L. ivanovii*-infected cells.

It is known that ceramide can be generated also by the broad-substrate range phospholipase C, PlcB, which is active against many phospholipids, including sphingomyelin (Geoffroy *et al.*, 1991, Goldfine *et al.*, 1993). PlcB generates in addition diacylglycerol (DAG), a lipid second messenger that acts as a signalling molecule by binding directly to many different proteins. Depending on the target, DAG-induced cellular responses can be proliferative or apoptotic (Griner & Kazanietz, 2007). Moreover, the phosphatidyl-specific PlcA phospholipase can generate signalling phosphoinositides with important regulatory roles in eukaryotic cells. Therefore, to investigate the impact of SmcL in ceramide generation, apoptosis, and eventually other cell responses, it is essential to isolate its effects from those potentially associated with other listerial lipid second messenger-generating enzymes.

To achieve this, the *smcL* gene was expressed in a deletion mutant of *L. monocytogenes* EGD lacking the *plcA* and *plcB* genes. This mutant did express normally Hly, necessary for phagosomal escape (and ceramide generation by the SmcL nSMase; unpublished data). The heterologous expression in a different host bacterium had the additional advantage that the *smcL* gene was expressed outside *L. ivanovii*, thus, isolating SmcL from other bacterial products potentially involved in the apoptotic response caused by this species.

Previous attempts in our laboratory to express *smcL* in the EGDΔ*plcAB* mutant used the bifunctional *Bacillus* - *E. coli* shuttle vector pHPS9, that replicates in *L. monocytogenes* and, which we routinely use for *trans*-complementation experiments. We tested the pHPS9*smcL*-complemented Δ*plcAB* mutant in infection assays in MDBK cells but found that the vector carrying the *smcL* gene was lost at a high frequency (80 to 90% of plated colonies after 12 h of intracellular infection).

To overcome this problem, we used the pPL2 vector (Lauer *et al.*, 2002) to stably express *smcL* in *L. monocytogenes* bacteria. This vector integrates in single copy into the host chromosome and was successfully used for expressing our *prfA* mutant alleles in the work described in section 3.1.1.3. As a control, we constructed a mock-complemented Δ*plcAB* strain with the empty pPL2 vector integrated in the chromosome (figure 3.2.17).

We previously showed that *in vitro*-grown *L. monocytogenes* bacteria with $prfA^{WT}$ genotype, like EGD, are very weakly invasive due to down-regulation of the PrfA regulon (see section 3.1.2). In addition, we also earlier demonstrated that *L. monocytogenes* internalizes into MDBK cells much less efficiently than *L. ivanovii* (see figure 3.2.1 and Guillet *et al.*, 2010). Indeed, both the *smcL* and mock-vector EGD integrants showed very low invasivity in MDBK cells: 0.009% ±0.004 and 0.006% ±0.002 for EGDΔ*plcAB*(pPL2) and EGDΔ*plcAB*(pPL2*smcL*).

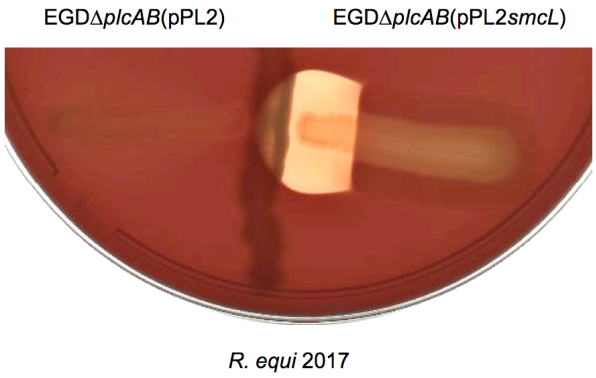

Figure 3.2.17: Stable expression of the *L. ivanovii* SMase gene *smcL* in single copy from the chromosome of a *L. monocytogenes* Δ*plcAB* mutant.
Blood agar plate in which the activity of the *smcL* product is detected through a CAMP-like (synergistic haemolytic reaction) with the *R. equi* cholesterol oxidase (Gonzalez-Zorn *et al.*, 1999, Navas *et al.*, 2001).

As a consequence, it was not possible to determine apoptosis, even using flow cytofluorometry, because there were too few bacteria inside the host cells to observe any detectable cell death response (only 10^4 CFU / well after 66 h post-infection). According to our data, to obtain workable levels of apoptosis with *Listeria*-infected cells it is necessary to reach an intracellular bacterial population in the monolayer between 10^6 and 10^7 CFU / well at 12-14 h post-infection (see figures 3.2.3 and 3.2.13).

To try to increase the invasion rate of the EGDΔ*plcAB* bacteria, we cultured them in BHI supplemented with 1% Amberlite^{TM} XAD-4 at 37ºC to activate the PrfA system (section 3.1.1.2) and the PrfA-regulated *inlAB* invasion locus (section 3.1.2.2.2). However, for an unknown reason, this approach did not result in any substantial increase in internalization. Prolonging the incubation time (from 40 min. to up to 2 h) after infection also did not result in significantly greater internalization. Due to these difficulties and time limitation for the completion of the PhD thesis work, it was not possible to try other possible strategies to increase the invasiveness of the strains. We plan, for example, to try in a first instance replacing the *prfA*^{WT} allele in EGDΔ*plcAB*(pPL2*smcL*) for the constitutively hyperactive *prfA**^{G145S} allele to ensure that a sustained high PrfA input drives the full activation of *inlAB*

expression. Alternatively, we may move to a macrophage infection model in which internalization is *inlAB*-independent and is significant (~ 5 - 10%), but we would need to explore first whether apoptosis is relevant to *Listeria*-infected macrophages. This work will be undertaken as part of the SmcL-ceramide-apoptosis research programme in a near future as a continuation of this thesis.

3.2.3 DISCUSSION

In this final chapter of the thesis we describe our initial approaches to the study of the apoptotic response caused in host cell by *Listeria* bacteria. This investigation was prompted by the observation that *L. ivanovii* causes significant levels of apoptosis in MDBK epithelial cells, in contrast to *L. monocytogenes*, which does not (Dominguez-Bernal *et al*., 2006; other unpublished observations from our laboratory). The information available about the apoptogenic activity of pathogenic *Listeria* is conflicting, so further research is clearly needed to clarify the role of this host cell response in listerial pathogenesis.

When researching the scientific literature about bacterial infections and apoptosis, we were surprised to see that on most occasions researchers just report crude percentage of apoptotic cells. When comparing two strains potentially differing in apoptotic activity, *e.g.* a mutant and its wild-type, usually the only normalization applied was based on the use of "similar" numbers of input bacteria in the system, with no consideration to possible differences in invasion, proliferation, survival, or even the actual numbers present at the time point where apoptosis is determined (Ojcius *et al.*, 1998, Menzies & Kourteva, 2000, Abul-Milh *et al.*, 2001, Bantel *et al.*, 2001, Esen *et al.*, 2001, Mannering *et al.*, 2002, Popov *et al.*, 2002a, Haslinger *et al.*, 2003, Schmeck *et al.*, 2004, Carrero *et al.*, 2004b, Jain *et al.*, 2007, Cervantes *et al.*, 2008, Parra *et al.*, 2008, Tattoli *et al.*, 2008). Since the apoptosis output clearly depends on the aforementioned parameters, and the investigated mutations may affect these primarily, we think that most scientific literature on the

role of specific bacterial factors in apoptosis is marred by serious experimental flaws and should be interpreted with caution.

We, therefore, decided, as a first step in our work on *Listeria* and apoptosis, to very carefully establish the experimental conditions to monitor and accurately measure apoptosis in cells infected by an intracellularly proliferating pathogen. With the aid of a mathematician, we developed an apoptosis index *AI* that incorporates two key variables with a clear potential impact on the apoptosis output, *i.e.* the total number of bacteria present in the monolayer and the percentage of infected cells.

A limitation to the application of the *AI* is that it is not really possible to estimate the relative apoptogenic potential of two species unless we know how the apoptosis rate of infected cells depends on the number of bacteria in the cells. This is referred to as β, a variable that describes how the number of bacteria affects the apoptosis rate and which has a profound impact on the *AI* value (see equation on p. 145). β can be = 0 (apoptosis rate assumed to be independent from the number of intracellular bacteria), = 1 (apoptosis increases linearly with the number of bacteria), = 2 (apoptosis increases quadratically), *etc*. To decide what assumption is closer to the real situation, we carried out experiments in which we semi-quantitatively assessed the number of bacteria present in apoptotic and non-apoptotic cells. We observed that while apoptotic cells were always associated with bacteria, a significant number of non-apoptotic cells were also infected, albeit with lower bacterial numbers. From our data we concluded that, whilst bacteria need to be present for apoptosis, a strict correlation does not exist between the total number of bacteria in the monolayer and the percentage of apoptosis. In other words, most likely $\beta = 0$ and, therefore, the *AI* depends mainly on the percentage of infected cells.

Another conclusion is that since β (how the rate of apoptosis B^{β} depends on the number of bacteria B; see p. 145 and Appendix II) has a strong influence on the *AI* calculations (see table 3.3), it is, therefore, also important to try to estimate the rate of change of the percentage of apoptotic cells. This can only be achieved with at least two measurements of the net (above background) percentage of apoptotic cells

a. Therefore, a more accurate method for determining the *AI* would be to incorporate into the equation the values for two time points, t_1 and t_2, as follows:

$$AI = \frac{a_{t_2} - a_{t_1}}{(t_2 - t_1) b_{t_2}^{\beta} c_{t_2}^{1-\beta}}$$

Our data indicate that at early time points, like $t = 4$, the percentage of net apoptotic cells does not differ significantly from background values due to the presence of insufficient no. of bacteria in the monolayer. Based on our experience, the ideal dual time points for *AI* calculation would be between 10 and 12 h for t_1 and 18 to 20 h for t_2. Future work will address this question and will establish the optimal working protocol for accurately determining the apoptosis potential of pathogenic *Listeria* using the two-time point *AI* equation.

When applying the *AI* equation with $\beta = 0$ to our data, it appears that *L. ivanovii* would be at least twice more apoptogenic than *L. monocytogenes*. A possible reason is that *L. ivanovii*-infected cells contain significantly more bacteria than those infected by *L. monocytogenes*. Thus, the presence of excess pathogenic *Listeria* (and corresponding secreted products) in the host cell cytosol seems to promote programmed cell death. This could be linked to the reduced cell-to-cell spread capacity observed for *L. ivanovii* (60% that of *L. monocytogenes*; figure 3.2.12), which may lead to overcrowding of the cytosol due to the incapacity of the bacteria to move to neighbouring cells after replication.

We tested whether host cell bacterial overcrowding determines an increase in the apoptosis rate by carrying out infection experiments with a Δ*actA* mutant and its parent *L. monocytogenes* strain. Bacteria lacking ActA do not spread to neighbouring cells and accumulate in the initially invaded cell, forming large perinuclear microcolonies after multiplication in the cytosol (Domann *et al.*, 1992, Kocks *et al.*, 1992). Indeed, our data confirmed that the cells infected with Δ*actA* tend to contain more bacteria (figure 3.2.14). Apoptotic cells in the Δ*actA*-infected monolayers also contained significantly more bacteria than the apoptotic cells infected with the cell-

to-cell-proficient bacteria. However, according to the *AI* calculations, the Δ*actA* mutant did not differ from the parent strain in apoptogenic activity. Thus, overcrowding in itself does not seem to explain the greater apoptogenic activity of *L. ivanovii* compared to *L. monocytogenes*, implying that other species-specific differences or factors are possibly involved.

The methods and approaches developed in this chapter should be helpful in determining whether such pro-apoptotic factors indeed do exist in *L. ivanovii*, and in examining the possible role of SmcL in ceramide signalling and apoptosis in *L. ivanovii*-infected MDBK cells.

4 CONCLUSIONS AND PERSPECTIVES

4.1 CONCLUSIONS

The experimental work described in this thesis has led to the following conclusions:

(i) We developed a robust methodology to measure PrfA-dependent gene expression by RT-QPCR that provides accurate and reproducible transcription data in *L. monocytogenes*. The technique uses the lactate dehydrogenase gene *ldh* as housekeeping reference gene for normalization. We found that this gene is constitutively expressed in most conditions relevant to analysis of PrfA regulation, including intracellular conditions. The *rpoB* gene, encoding the β subunit of the RNA polymerase, also shows a stable and constitutive pattern of expression suitable for PrfA-dependent gene regulation analysis; this gene can be used alternatively to -or in conjunction with- *ldh* as housekeeping reference gene for transcription data normalization.

(ii) The synthetic adsorbent resin Amberlite^{TM} XAD-4 leads to an activation of PrfA-dependent genes comparable to that observed with activated charcoal. However, in contrast to charcoal, the presence of the resin in the culture is not required. Pre-treatment of the medium, with subsequent removal of Amberlite^{TM} XAD-4, leads to virulence gene activation levels similar to those observed when the medium incorporates the resin during bacterial growth. Amberlite^{TM} XAD-4 did not affect bacterial growth and a σ^B stress response was not involved in the virulence gene activation, indicating that the effect is most likely related to chemical signalling rather than to a stress response indirectly affecting PrfA. Thus, the resin seems to exert its effect by adsorbing a chemical component of the medium with PrfA repressor activity. This conclusion does not support the notion that the gene activation effect is due to the sequestration of a *Listeria*-derived quorum-sensing PrfA autorepressor substance.

(iii) The levels of PrfA-dependent gene activation in wild-type *L. monocytogenes* with Amberlite^{TM} XAD-4 were clearly below those observed in HeLa cells, suggesting that the intracellular activation of the PrfA system does not only involve de-repression but an additional positive regulation pathway. A *prfA** mutation lifts the medium-associated repression, indicating that the constitutively activated PrfA* protein is not sensitive to the medium-derived chemical repressor signal.

(iv) We identified in the PrfA N-terminal domain a solvent-exposed cavity at an equivalent position to that of the cAMP-binding site of the structurally related enterobacterial Crp regulator. We examined the function of this pocket by structure-based site-directed mutagenesis. Our results provide strong experimental support to the notion that PrfA is allosterically activated within host cells via a putative ligand-binding pocket in the jelly-roll β-barrel that forms the N-terminal domain of the protein monomer.

(v) We described and characterized three new spontaneous loss-of-function mutations in PrfA, A129T in the αC helix and E173G in the HTH motif, identified as PrfA*^{G145S}-supressor mutations, and C229Y in the C-terminal extension, which is always present together with the G145S substitution in *L. monocytogenes* phylogenetic division II spontaneous *prfA** mutants. A129T and E173G caused total loss of activity in PrfA, even when in "on" (PrfA*) conformation, by directly affecting dimerization and DNA-binding, respectively; C229Y alone totally inactivated PrfA but only partially suppressed the PrfA* phenotype conferred by the G145S mutation. Our data highlight the critical importance for PrfA function of the central inter-subunit αC helix, the HTH motif, and the C-terminal wedge unique to the listerial regulator among the Crp family of bacterial transcription factors.

(vi) We clarified several key aspects of carbon source regulation of *L. monocytogenes* virulence genes. (a) Hexose phosphates do not repress PrfA-dependent expression, this only occurs with PTS-transported sugars. (b) A PrfA* protein ("on" conformation) does not render *L. monocytogenes* insensitive to sugar-mediated virulence gene regulation; repression is still observable but with higher

final output levels that are proportional to the intrinsic activity of the PrfA protein. (c) The intensity of the repression varies depending on the sugar utilized and may depend on the number of potential PTS permeases involved in sugar uptake. Our observations suggest a clear interconnection between the PrfA and carbon catabolite repression systems in *L. monocytogenes*.

(vii) We demonstrate that the unusual phenotype reported for *L. monocytogenes* strain NCTC 7973 in response to sugars, with a differential response to glucose and cellobiose, previously assumed to reflect the existence of independent repression mechanisms for the two carbohydrates, is due to the attenuation effect of the double C229Y mutation on PrfA*^{G145S}. Depending on the gene expression analysis technique used and its corresponding signal saturation threshold, the attenuated activity of the double PrfA*$^{G145S/C229Y}$ may lead to the wrong interpretation that one sugar represses (cellobiose), whereas the other (glucose) not.

(viii) Contrary to what was initially thought, the constitutively hyperactive PrfA*^{G145S} mutant form is sensitive to PTS sugar-mediated repression. Although final expression levels remained still high, sugars clearly repressed the transcription of PrfA-dependent genes in *prfA** bacteria. This suggests that the carbon source-mediated repression pathway represents a level of regulation that is superimposed to that of the PrfA allosteric activation pathway.

(ix) Contradicting previous reports by other groups, our data do not support that the stress mediator σ^B plays a major role in host cell invasion by *L. monocytogenes*. The Δ*sigB* mutation had no obvious influence on invasion or *inlAB* expression, except for a small decrease only observable in the *prfA*^{WT} background in *in vitro* conditions, not in the *prfA**^{G145S} background mimicking the *in vivo* PrfA regulation status. We question the biological significance of these effects, as they are observed in an already much reduced invasive phenotype that corresponds to a PrfA activation status only seen *in vitro* and not *in vivo* during infection.

(x) Consistent with the lack of effect of σ^B on *L. monocytogenes* invasiveness and *inlAB* expression, growth in acidic conditions did not seem to trigger a stress response leading to an enhancement in the internalization rate.

(xi) We confirm previous observations from our laboratory that *L. monocytogenes* invasiveness is strictly dependent on the central virulence gene regulator, PrfA. We showed that PrfA is essential for the expression of the *L. monocytogenes* invasion locus *inlAB* and the ability of *L. monocytogenes* to invade host cells. Like other members of the PrfA regulon, the *inlAB* locus was expressed only weakly in extracellular conditions, whereas it was strongly induced during intracellular infection, to levels similar to those observed in *prfA** bacteria.

(xii) Our work with Δ*sigB* mutants in two *L. monocytogenes* serotypes, 1/2a and 4b, indicate that there are strain-specific differences regarding the protective role of σ^B against environmental stresses. Our data are consistent with previous observations by other groups suggesting that σ^B does not play a significant role in the stress response of *L. monocytogenes* strains belonging to phylogenetic division I. There appear also to be qualitative differences in the protective role of σ^B within a same strain depending on the type of stress.

(xiii) We have identified that the quantitative data published in the scientific literature about apoptosis in bacterial infections are frequently flawed by methodological errors. They do not take into account that the percentage of apoptotic cells in an infected population may be affected by the invasiveness, intracellular proliferation and spread capacities of the bacteria. Key variables, such as the actual total number of bacteria in the monolayer, or the percentage of infected cells, are not taken into account when quantifying apoptosis. As a first step in our work programme on *Listeria*-induced apoptosis, we addressed these problems and developed, with the aid of a mathematician, an Apoptosis Index (*AI*) equation that incorporates the major parameters that may influence the outcome variable. The application of this *AI* in pilot experiments conducted with the ruminant pathogen *L.*

ivanovii showed that this species is more apoptogenic than *L. monocytogenes* for MDBK bovine epithelial cells.

(xiv) Detailed microscopical examinations of infected MDBK monolayers led us to conclude that the presence of pathogenic *Listeria* within host cells is associated with the occurrence of apoptosis. However, a strict correlation did not exist between the total number of bacteria in the monolayer and the percentage of apoptotic cells, indicating that both variables are not linearly correlated. A significant number of infected cells did not undergo apoptosis, reflecting the possible existence of host cell subpopulations differing in susceptibility to *Listeria*-induced apoptosis, or a time-bacterial load exposure threshold effect.

(xv) Despite the significant differences in number of intracellular bacteria within infected cells between a Δ*actA* mutant (unable to spread to neighbouring cells and which, therefore, accumulates in the invaded cell after replication) and its wild-type parental *L. monocytogenes*, the application of the *AI* indicated that the two strains did not differ in apoptogenic activity. Thus, overcrowding in itself does not seem to result in increased levels of apoptosis, possibly reflecting the existence of a bacterial input threshold for triggering cell death in an infected cell.

4.2 FUTURE DIRECTIONS

Future directions of the research based on the findings and work reported in this thesis are:

(a) Continuation of the search for the presence of the medium-derived PrfA repressor signal will be greatly facilitated by the use of the chemically defined medium IMM and the synthetic resin Amberlite^{TM} XAD-4. The chemical signal adsorbed by the resin can be selectively eluted through monitoring of its repressor activity, and its

nature determined using standard analytical chemistry procedures. Once the identity of the repressor is determined, biochemical and structural studies of its mode of action can be undertaken.

(b) The identification of the N-terminal putative binding pocket is a major breakthrough for understanding the allosteric nature of PrfA and how the activity of the central regulator of listerial virulence is modulated. The shape and physicochemical characteristics of the pocket suggest that it could bind a relatively hydrophobic, elongated molecule with an aromatic head and aliphatic tail. Future work will aim at the identification of the putative PrfA-activating ligand and use this knowledge in the development of inactive analogues that could serve as potent *Listeria* anti-infectives.

(c) Future work will also focus on the detailed structural characterization of the spontaneous PrfA^{-} mutations identified in this thesis, which will allow us to gain a better understanding of the structure-function of the listerial virulence regulator. Understanding the reason for the selective advantage conferred by the second C229Y mutation in the phylogenetic division II spontaneous *prfA*^{*G145S} mutants will provide insight into basic aspects of listerial physiology and the impact of the PrfA regulatory network on *L. monocytogenes* fitness and evolution.

(d) It will also be interesting to investigate the differential role of σ^{B} in the stress response of *L. monocytogenes* serotypes, in particular the apparent lack of impact of this alternative sigma factor on stress tolerance and virulence in serotype 4b.

(e) The methods and approaches developed in this thesis for the determination of apoptosis will be very helpful in the research programme on SmcL, ceramide and programmed cell death. Future work will focus on the refinement and further testing of the *AI* equation for determination of the apoptogenic activity of *Listeria* strains (and eventually other bacterial pathogens). The role of SmcL in the modulation of apoptosis and other cell responses will also constitute a major area of research in our laboratory.

5 MATERIALS AND METHODS

5.1 MICROBIOLOGICAL TECHNIQUES

5.1.1 BACTERIAL STRAINS, CULTURE CONDITIONS AND CHEMICALS

Bacterial strains used in this study are listed in table 5.1. *Listeria* spp. and *E.coli* strains were routinely cultured in Brain Heart Infusion (BHI) (BD, Laboratories–Beckton, Dickinson and Co.) and Luria–Bertani (LB) (Pronadisa S.A., Spain) media, respectively. Bacteria were grown in aerobic conditions at 37ºC, (Memmert UM-800/400 Universal Incubators; Shwabach, Germany) with or without continuous shaking at 200 rpm (Inmersa 4230 Refrigerated Incubators. New Brusnwick Scientific; New Jersey, USA). To obtain solid media, 1.6% of bacteriological agar (Oxoid, Nº1; Hampshire, England) was added to the broth media. The base medium was supplemented with appropriate antibiotics when required. Chemicals and antibiotics were purchased from Sigma-Aldrich Co. (Dorset, UK) unless otherwise stated.

5.1.2 PREPARATION OF BACTERIAL INOCULA

Bacterial cultures grown overnight were inoculated 1:100 in 200 ml BHI broth (or BHI broth acidified with HCl to pH = 5.5 for Δ*sigB* mutant experimental purposes; see section 3.1.2), incubated at 37°C with shaking (200 rpm) until mid-exponential phase (OD_{600} = 1.0 - 1.2). Bacteria were collected by centrifugation (5,836 x *g* for 10 min. at 4˚C using 6K15 Sigma Lab Centrifuge), washed three times in ice-cold PBS (phosphate-buffered saline, pH = 7.4), resuspended in 4 ml of ice-cold 20% glycerol PBS v/v solution, aliquoted into vials (100 μl portions) and stored at -80°C until use. The number of bacteria present in the frozen stocks was determined by thawing three aliquots and calculating the average CFU / ml by plate counting on BHI agar. For inoculation purposes, aliquots were thawed, washed twice

in PBS and resuspended in 900 μl of PBS. Inocula of *Listeria* with a pPL2 plasmid integrated into the chromosome were prepared as described above, but cultured in BHI broth supplemented with 7.5 μg / ml chloramphenicol.

5.1.3 PREPARATION OF IMM BROTH

IMM (Improved Minimal Medium) is a chemically defined medium, which was prepared according to the formulation described by Phan-Thanh and Gormon, (1997) (table 5.2). Different components of this medium were either stored at 4°C or frozen at -20°C when appropriate. Ready IMM was stored at 4°C for a period no longer than 2 weeks and protected from light. Sugar source such as glucose, glucose-1-phosphate (G-1-P) or cellobiose (Sigma) was added at an appropriate final concentration. For experimental purposes described in section 3.1.1.4.2.3, the concentration of phosphates was decreased (from 1,642 mM to 25 mM) and the IMM medium was buffered with 100 ml of 1 M 3-(N-morpholino)propanesulfonic acid (MOPS) (pH = 7.03) (Sigma).

5.1.4 BACTERIAL GROWTH MEASUREMENTS AND GROWTH CURVES

An overnight culture of *Listeria* spp. was inoculated (1:100) into BHI or IMM broth and incubated at 37˚C, with shaking (200 rpm). For manual growth curves (figure 3.1.5), flasks with 30 ml broth were used. The OD_{600} was determined using a spectrophotometer (model mentioned above) after inoculation (t = 0) and at one-hour intervals. Uninoculated BHI or IMM was used as blank. Growth data of figures 3.1.30, 3.1.2.5 and 3.1.2.6 were obtained using an automated microplate reader machine (FluoStar OPTIMA, BMG Labtech) at the same optical density (measures taken every 30 min.).

5.1.5 BACTERIAL CULTURES FOR RT-QPCR EXPRESSION ANALYSES

Stationary phase overnight bacterial cultures were diluted 1:100 in 30 ml of BHI medium or IMM (Improved Minimal Medium) (Phan-Thanh & Gormon, 1997), supplemented with appropriate concentration of antibiotics if necessary, or with 1% Amberlite™ XAD-4 (Sigma) before sterilizing of the media, to achieve PrfA activation *in vitro*. For some experiments (see section 3.1.1.2), a pre-treated IMM medium was obtained by incubating IMM with 1% Amberlite™ XAD-4 at 37°C for 24 h, and, then, the amberlite particles were removed by filtration through 0.2 μm pore size membrane. Bacteria were grown in 100 ml flasks with shaking at 200 rpm at 37°C. The OD_{600} was measured for each culture using the Ultrospec 3300 pro UV/Visible spectrophotometer (Amersham Biosciences). At the initial and middle exponential phase (OD_{600} ~ 0.3 and OD_{600} ~ 1, respectively), 0.5 ml of medium containing *L. monocytogenes* cells were transferred into 1.5 ml microcentrifuge tube and chilled on ice immediately. Collected samples were kept for further expression analysis by RT-QPCR. In parallel, aliquots of bacterial cultures were diluted and plated on BHI agar plates to determine the number of bacteria (CFU).

5.1.6 MEASUREMENT OF HAEMOLYSIN AND PHOSPHOLIPASE ACTIVITY

Strains were regularly checked for PrfA activity using as reporters the strictly PrfA-dependent genes *hly* and *plcB*, encoding the LLO cytolysin, and the broad substrate-range phospholipase/lecithinase, respectively (Vazquez-Boland *et al.*, 1992). Semi-quantitative determination of Hly and PlcB activity was carried out by streaking *L. monocytogenes* onto 5% sheep-blood agar (SBA) plates (BioMerieux; Marcy l'Etoile, France) or egg yolk agar (EYA) BHI plates, respectively. EYA plates were prepared by adding 5% v/v of egg yolk suspension (a fresh egg yolk in 100 ml of sterile saline solution) to BHI agar. The egg yolk agar plates, either with or

without the supplementation of activated charcoal (0.5% v/w, Merck), were incubated at 37°C for 48 - 72 h. Determination of the activity was based on the diameter of the halos developed around colonies.

5.1.7 PREPARATION OF ELECTROCOMPETENT *E. COLI*

An overnight culture of *E. coli* was inoculated in LB-broth (1:100) and grown until OD_{600} = 0.6. Then, the culture was centrifuged at 5,836 x *g* for 10 min. at 4˚C (6K15 Sigma Lab Centrifuge). The pellet was resuspended in 100 ml ice-cold destilled water and centrifuged as previously. After a second wash with the same conditions, bacterial cells were resuspended in 20 ml of 10% glycerol and Milli-Q water, and centrifuged as previously. Finally, the pellet was resuspended in 400 μl of ice-cold, 10% glycerol solution and 20 μl aliquots in microtubes were stored at -80˚C (U410 Ultra Low Temperature Freezer; New Brunswick Scientific, Hertfordshire, UK).

5.1.8 ELECTROCOMPETENT *LISTERIA* CELLS

Listeria were grown overnight in 5 ml BHI supplemented with 0.5 M sucrose. The culture was diluted 1:100 in BHI broth containing 0.5 M sucrose and incubated at 37˚C with vigorous shaking (200 rpm) until reaching OD_{600} value of 0.2. Then, penicillin G (10 μg / ml) was added and the culture was incubated for further 2 h in the same conditions. After this time, bacteria were transferred to sterile, ice-cold centrifuge tubes and spun at 5,836 x *g* for 10 min. at 4°C (6K15 Sigma Lab Centrifuge). Cells were washed three times with ice-cold transformation buffer prepared by mixing 0.5 M sucrose, 1 mM HEPES in Milli-Q water (pH = 7.0) and the pellet was resuspended in 500 μl of ice-cold transformation buffer containing 10% v/v glycerol. Aliquots of 50 μl were quickly dispensed into chilled, sterile microfuge tubes and immediately stored at -80˚C (U410 Ultra Low Temperature Freezer; New Brunswick Scientific, Hertfordshire, UK) until use.

5.1.9 LYSIS OF *LISTERIA* CELLS FOR STANDARD PCR

Bacteria were resusupended in 50 µl of buffer for PCR 1x (prepared by mixing 5 µl of Biotools buffer 10x and 45 µl of sterile Milli-Q water). After vortexing the sample, 5 µl of lysozime (100 mg / ml) was added. After mixing thoroughly, the sample was incubated at 37˚C for 1 h. Then, 1.2 µl of Proteinase K (20 mg / ml) was added. The sample was vortexed and incubated for 1 h at 55˚C and later for 15 min. at 100˚C. 3 µl of the suspension was taken to prepare the PCR reaction (final volume 50 µl).

5.2 MOLECULAR BIOLOGY TECHNIQUES

5.2.1 DNA TECHNIQUES AND SEQUENCE ANALYSES

Extraction of genomic DNA from bacteria was carried according to Ausubel *et al*. (2002) with modifications (Ausubel *et al.*, 2002). A 10 ml overnight culture of *Listeria* spp. was centrifuged at 3,864 x *g* for 10 min. (3K30C Lab Centrifuge, Sigma; Harz, Germany). The pellet was re-suspended in 576 µl of TE buffer (10 mM Tris-HCl, 1 mM EDTA pH = 8), and 3 µl of 100 mg / ml lysozyme was added. The mixture was incubated at 37°C for 1 h and stirred every 10 min.. After this time, 3 µl of 20 mg / ml proteinase K and 30 µl of 10% SDS (sodium dodecyl sulphate) were added and the suspension was incubated for another hour at 37°C with stirring every 10 min.. Then, 170 µl of 5 M NaCl were added and the suspension was mixed thoroughly (to resuspend the salt added). Afterwards, 5 µl of 0.5 mg / ml RNAse (Qiagen, Crawley, West Sussex, UK) and 80 µl of CTAB/NaCl solution (10% CTAB - hexadecyltrimethyl ammonium bromide in 0.7 M NaCl) were added and the suspension was incubated for 30 min. at 65 °C. After cooling to room temperature, 750 µl of phenol/chloroform/isoamyl alcohol was added, the suspension mixed and spun for 10 min. at maximum speed on a benchtop centrifuge (MiniSpin Plus bench

Centrifuge, Eppendorf; Cambridge, UK). The aqueous phase (~ 600 µl) was transferred to a fresh tube and an equal volume of chloroform was added. After mixing thoroughly, the suspension was centrifuged for 10 min. at maximum speed, at room temperature. The aqueous phase (~ 450 µl) was transferred to a new tube and mixed with 0.6 volume of isopropanol to precipitate the nucleic acids. The tube was shaken back and forth until DNA became visible. After centrifugation (5 min. at 6,000 × *g*, at room temperature), the supernatant of the suspension was carefully removed. The remaining pellet of DNA was washed with 70% ethanol to eliminate residual CTAB and centrifuged again (5 min., 6,000 × *g*, room temperature). The supernatant was discarded and the pellet was air-dried and re-suspended in 100 µl of sterile Milli-Q water (double-distilled).

The oligonucleotides used during this study are listed in table 5.3 and were purchased from Metabion (Martinsried, Germany) or Sigma (UK). The genome sequence of *L. monocytogenes* strain P14 (sequenced by our laboratory using the facility in the School of Biological Sciences, University of Edinburgh) or the genome sequence of *L. monocytogenes* F2365 (Nelson *et al.*, 2004), served as the basis for designing the primers.

Taq DNA polymerase (Biotools; Madrid, Spain) was used to carry out polymerase chain reaction (PCR), *PfuTurbo*® DNA polymerase and the *PfuUltra* II fusion HS DNA polymerase (both from Stratagene [CA, United States]) were used when high-fidelity PCR was required. Restriction enzymes were obtained from Promega (Southampton, UK) and New England Biolabs (Herts, UK). All enzymes were used according to the manufacturer's instructions.

PCRs were carried out using Minicycler (M.J. Research, Inc; Massachusetts, USA) and MasterCycler Gradient (Eppendorf; Hamburg, Germany) thermal cyclers. General parameters used were as follows: 1) 5 min. of initial denaturation at 95˚C, 2) 30 cycles of amplification involving i) 30-60 sec. of denaturation at 94˚C, ii) 30-60 sec. of oligonucleotide hybridization at the appropriate temperature (calculated according to the general formula T=[2˚(A+T)+4˚(G+C)]) and iii) elongation at 72˚C

for 1 min. per 1 Kb amplified, and 3) 10 min. of final elongation at 72˚C. A volume of 50 μl per reaction was used to carry out the PCR with 10 to 100 ng of template, 10 mM dNTPs (Biotools; Madrid, Spain), 10 μM of each oligonucleotide, an appropriate amount of reaction buffer and DNA polymerase enzyme.

For routine analysis, the PCR products were visualized on 1% agarose gels (Pronadisa; Madrid, Spain) by running a gel electrophoresis in a Mini-Sub® Cell GT, with a PowerPac Basic Power Supply Kit (Bio-Rad Laboratories, Ltd., UK). For cloning purposes, the PCR products were used directly, or after purification from 0.7% megabase certified agarose gel (Bio-Rad Laboratories, Ltd., UK) with QIAquick Gel Extraction Kit (Qiagen, Crawley, West Sussex, UK), as recommended by the manufacturer.

Quantity and purity of the DNA extracted was assessed either by using Nanodrop® Spectrophotometer ND-1000 (ThermoScientific, USA) or by measuring the absorbance of the solution at 260 and 280 nm wavelengths (Ultrospec 3300 pro UV/Visible spectrophotometer; Amersham Biosciences). In order to increase the purity of the DNA, samples were purified with the QIAquick PCR Purification Kit (Qiagen, Crawley, West Sussex, UK). DNA samples with an A260/A280 absorbance ratio lower than 1.75 - 1.80 were discarded. DNA samples were sent to Agowa genomics services (Gesellschaft für molekularbiologische Technologie mbH, Berlin, Germany) or submitted to the GenePool (University of Edinburgh, UK) for sequencing. Sequences and chromatograms were analyzed using FinchTV (Geospiza) and DNA strider 1.2 softwares. Alignment of nucleotides and protein sequences was carried out using the multiple sequence alignment programmes ClustalW (http://www.ebi.ac.uk/Tools/clustalw2/index.html) and the Basic Local Alignment Search Tool (Blast) (http://blast.ncbi.nlm.nih.gov/Blast.cgi). Chemicals were purchased from Sigma-Aldrich Co. (Dorset, UK) unless otherwise stated.

5.2.2 RNA ISOLATION FOR RT-QPCR

An aliquot of 0.5 ml BHI containing exponentially growing *Listeria* cells or 0.5 ml of PBS containing *Listeria* infected mammalian cells were added to 1 ml of RNAprotect bacteria reagent (Qiagen, Crawley, West Sussex, UK) and mixed immediately by vortexing for 5 sec.. The mixture was incubated for 5 min. at room temperature and subsequently centrifuged at 5,000 × *g* for 10 min. at 4 °C (3K30C Lab Centrifuge) and stored at -80˚C until use. The pellet was thawed on ice and resuspended in the Buffer RA1 (Macherey-Nagel, Düren, Germany) containing 1:100 β-mercaptoethanol (Sigma) and transferred to a blue-cap tube containing Lysing Matrix B (Q-Biogen). Samples were processed in the FastPrep® Instrument (Q-Biogen) at a setting of 6.0 during 40 sec. and centrifuged at 12,000 × *g* for 5 min. at 4ºC (3K30C Lab Centrifuge). The supernatant was transferred to a new microcentrifuge tube and an equal volume of 70% ethanol (Sigma; prepared in autoclaved 0.01% diethylpyrocarbonate [DEPC] water) was added and mixed well by pipetting. The nucleic acid solution was purified using the Nucleospin RNA II kit (Macherey-Nagel). The resulting 50 µl elute was treated with 10 U of DNase I (RQ1 RNase-free DNase I, Promega, UK) for 30 min. at 37ºC. Subsequently, the total RNA solution was purified in a second round using the kit Nucleospin RNA II (Macherey-Nagel) and finally eluted in 50 µl of RNase- and DNase-free water.

5.2.3 cDNA SYNTHESIS

RNA was reverse transcribed using the Improm-II reverse system (Promega, UK) in a 20 µl reaction mix including 1× Improm II reaction buffer, 1.5 mM Mg^{2+}, 0.5 mM dNTPs, 100 µM random hexamers (Eurogentec, Belgium), 5 µl of RNA template and 1 µl Improm-II reverse transcriptase. Before reverse transcription, RNA was denatured for 5 min. at 65ºC followed by cooling on ice. The reverse transcription conditions were: 25ºC for 5 min., 42ºC for 1 h, and inactivation by heating for 15 min. at 70ºC. All cDNAs were diluted 1:10 in nuclease-free water before being used as a PCR template for RT-QPCR.

5.2.4 EXPRESSION ANALYSES BY RT-QPCR

The assays were performed in a 20 µl reaction volume containing 1× PCR TaqMan® buffer II (Applied Biosystems, UK), 6 mM $MgCl_2$, 200 µM dNTP (Promega and Biotools), 300 nM primers (Metabion, see table 5.3), specified concentration of the probe (100 nM or 150 nM, Applied Biosystems, see table 5.3), 1 U of AmpliTaq Gold® DNA polymerase (Applied Biosystems, UK) and 5 µl of the target solution. Reactions were run on an iCycler 2.0 (BioRad, UK) and StepOnePlus™ Real-Time PCR System (Applied Biosystems, UK) using the following program: 10 min. at 95ºC and 40 cycles of 15 sec. at 95ºC and 1 min. at 60ºC. Assays were analyzed using the iCycler IQ Optical System Software v3.0a (BioRad, UK) and StepOne Software v2.0 (Applied Biosystems, UK), respectively.

To determine the absolute starting number of each specific cDNA molecules present in the samples, standard curves were created using *Listeria* genomic DNA. Genomic DNA isolated from overnight culture of wild-type *Listeria* were serially diluted to final concentrations equivalent to approximately 3×10^5, 3×10^4, 3×10^3 and 3×10^2 genomic-equivalent per reaction, and used in triplicate for building the standard regression curve, which was used in each RT-QPCR run.

The number of transcripts was calculated from threshold cycle (C_T) values of cDNA preparations after extrapolation from a standard regression curve of cycle C_T values plotted against *L. monocytogenes* P14 genomic DNA standards of known concentration (a comparative threshold method). Negative amplification results were considered for those reactions with C_T value of 40 or above. All reactions were performed by duplicate.

Expression data were normalized by dividing the number of transcripts for the target gene by the number of transcripts for the *L. monocytogenes* housekeeping

gene *ldh* (encoding lactate dehydrogenase) and/or *rpoB* (encoding the β subunit of RNA polymerase).

5.2.5 PLASMID EXTRACTION AND TRANSFORMATION BY HIGH-VOLTAGE ELECTROPORATION

Plasmids used in this thesis are listed in table 5.4. Extraction of plasmids from *E. coli* was carried out using the BIO 101® Systems RPM® SPIN MIDI, (QBiogene; La Jolla, USA) or QIAprep® Spin Miniprep Kit (Qiagen, Crawley, West Sussex, UK), according to manufacturer's instructions. The electrocompetent bacteria were thawn on ice and mixed with 10 ng / μl of plasmid (2-4 μl). The mix was transferred into a previously chilled, 2 mm electroporation cuvettes (Biorad, UK) and kept on ice for 3-4 minutes. After electroporation (with following settings: voltage = 2500 V, capacitance = 25 μF, resistance = 200 Ω for *E.coli* or 2900 V, 25 μF, 100 Ω for *Listeria* spp.) using GenePulserXcell electroporator (Biorad, UK), 250 μl of LB broth or 500 μl of BHI broth with 0.5 M sucrose, respectively, was quickly added to the bacterial cells. The contents of the cuvettes was transferred into microfuge tubes and incubated at 37˚C, with shaking at 200 rpm for 1 h. After this time, transformed competent cells were transferred onto BHI agar plates containing appropriate antibiotic and incubated at 37˚C until the appearance of single bacterial colonies.

5.2.6 SITE-DIRECTED MUTAGENESIS OF *PRFA* GENE

Complementation plasmids pPL2*prfA*^{WT} and pPL2*prfA**, carrying the wild-type *prfA* and the *prfA** gene, respectively, were constructed. The *prfA* gene, including its regulatory regions, of *L. monocytogenes* P14 and P14A, was amplified by PCR using oligonucleotides MR2*Sal*I and MR10*Sal*I (both carrying *Sal*I restriction sites), purified and cloned into pTOPO T-vector (Invitrogen, UK) to give pTOPO*prfA* and pTOPO*prfA**, respectively. After transforming into *E. coli*, the

plasmid was extracted and sequenced. The *prfA* and *prfA** inserts were released by restriction with *Sal*I (2 h at 37°C), purified and transferred to the site-specific phage integration vector, pPL2 (Lauer *et al.*, 2002), (the ligation time was 17 h at 16°C), giving pPL2*prfA* and pPL2*prfA**, respectively. Both of these complementation plasmids were used in subsequent steps to construct pPL2$prfA^{A129T}$ and pPL2$prfA^{*A129T}$, respectively. A point mutation (GCC→ACC) was introduced resulting in an amino acid substitution (Ala→Thr) in codon 129 of the *prfA* and *prfA** (Gly145Ser) allele carried by pPL2*prfA* and pPL2*prfA**, respectively.

Site-directed mutagenesis was carried out by overlap extension (Ho *et al.*, 1989) using oligonucleotides: Ala129Thrforward and Ala129Thrreverse, which carried the point mutation (in capital letters in table 5.3). Firstly, two fragments of *prfA* (or *prfA**) gene, including its regulatory regions, were amplified by PCR using oligonucleotides: MR2*Sal*I - Ala129Thrreverse and Ala129Thrforward - MR10*Sal*I. Both fragments were purified, mixed together by pipetting and, then, amplified by PCR using oligonucleotides: MR2*Sal*I - MR10*Sal*I. The amplified insert, which carried the desired mutation, was purified, cloned into pTOPO T-vector and sequenced. The insert was, then, released by restriction with *Sal*I (2 h at 37°C), purified and ligated into pPL2 vector (with the same conditions as described above) giving pPL2$prfA^{A129T}$ and pPL2$prfA^{*A129T}$, respectively. The complementation plasmids, pPL2*prfA*, pPL2*prfA**, pPL2$prfA^{A129T}$ and pPL2$prfA^{*A129T}$ were introduced into *E. coli* by electroporation, extracted, sequenced and introduced into *L. monocytogenes* Δ*prfA** knock-out mutant by electroporation. The transformants were selected on BHI-chloramphenicol (7.5 μg / ml) agar plates.

Other complementation plasmids carrying *prfA* mutant genes (table 5.4) were constructed using similar technique to the one described above. The complementation plasmids pPL2*prfA* and pPL2*prfA** were constructed again using oligonucleotides MR2*Kpn*I and MR10*Spe*I. Site-directed mutagenesis into the *prfA* gene was performed by overlap extension strategy involving two flanking sequences using two outside primers (MR2*Kpn*I, MR10*Spe*I) as well as the corresponding internal primers harbouring the relevant mutations (forward, reverse). The two

intermediate products with terminal complementarity formed a new template DNA used for the recombinant PCR (MR2*Kpn*I + MR10*Spe*I), which was digested by *Kpn*I and *Spe*I, and cloned in the integrative plasmid vector pPL2, digested by the same enzymes. The *prfA* mutant genes were under the control of the P*prfA*1 and P*prfA*2 promoters (Mengaud *et al.*, 1991, Freitag *et al.*, 1993). Selected plasmids were checked by digestion and sequencing and, then, electroporated into *L. monocytogenes* Δ*prfA**. Transformants were selected on chloramphenicol containing plates. Oligonucleotides used to generate the mutants are listed in table 5.3.

5.2.7 CONSTRUCTION OF Δ*SIGB* IN-FRAME DELETION MUTANTS IN *LISTERIA*

In order to construct in-frame deletion mutants in *L. monocytogenes* 4b, a homologous recombination technique was used as previously described in Dominguez-Bernal *et al.* (2006), with modifications. *E.coli*(pLSV101Δ*sigB*) strain (DH10b) was a gift from Prof. W. Goebel (Biocenter, Microbiology; University of Würzburg, Germany). Plasmidic DNA from the *E.coli*(pLSV101Δ*sigB*) was introduced by electroporation into the wild-type *L. monocytogenes* P14 and *L. monocytogenes prfA** (P14A) for construction of Δ*sigB* mutants or into *L. monocytogenes* P14AΔ*prfA* for construction of a P14AΔ*prfA*Δ*sigB* mutant. The transformants were incubated at 30˚C on BHI plates supplemented with 5 μg / ml of erythromycin (ery), presence of plasmid was confirmed by PCR. A positive clone was chosen and grown over-day at 30˚C in 10 ml BHI-ery 5 μg / ml broth. Then, the culture was diluted 1:100 into fresh BHI-ery 5 μg / ml broth and grown at 37˚C overnight. The next day, bacteria were subcultured, as previously, into the fresh broth and grown at 42˚C (to inhibit the plasmid replication) for 7 h. The bacteria were subcultured once again into fresh BHI-ery broth and grown overnight at 37˚C. Dilutions of this culture were plated onto BHI-ery agar plates and incubated at 37˚C until the appearance of bacterial colonies. The integration of plasmids into the chromosome of the first recombinant bacteria was confirmed using PCR (with following PCR conditions: 1) 95˚C for 5 min., 2) 94˚C for 1 min., 3) 55˚C for 1 min.,

4) 68˚C for 2 min., 5) repeat steps 2-4 30 times, 6) 68˚C for 10 min., 7) hold at 4˚C) with oligonucleotides: sigBF-plsv1B and sigBR-plsv1C (table 5.3). The first recombinant was re-isolated on BHI-ery agar plates and blood agar plates to check purity. To select the second event of recombination that leads to the mutant strain (or revertant strain to the wild-type genotype), the chosen clone was grown over-day in BHI broth without antibiotic selection at 37˚C, and subsequently subcultured every 12 h for the next couple of days under the same conditions. Each day, a sample was plated on BHI agar and incubated at 37˚C until colonies appeared. Bacterial clones were streaked on BHI agar plates with and without antibiotic selection (by replica plating) and incubated at 37˚C. Erythromycin-sensitive bacterial colonies were checked for the presence of deletion in *sigB* gene by PCR using chromosomal primers (sigBF and sigBR), designed in the flanking sequence of the recombination regions inserted into pLSV101 vector.

5.2.8 CONSTRUCTION OF EGDΔ*PLCAB*(PPL2) AND EGDΔ*PLCAB*(PPL2*SMCL*) MUTANTS.

Listeria monocytogenes EGDΔ*plcAB* strain was a gift from Prof. J. Kreft (Biocenter, Microbiology; University of Würzburg, Germany). EGDΔ*plcAB*(pPL2) strain was obtained by electroporating the pPL2 plasmid (Lauer *et al.*, 2002) into electrocompetent EGDΔ*plcAB*. To obtain EGDΔ*plcAB*(pPL2*smcL*) strain, the *smcL* gene, including its regulatory regions, of *L. ivanovii* ATCC 19119 was amplified by PCR using oligonucleotides: smcL-XmaI (forward) and smcL-SalI (reverse) (table 5.3), purified, digested by *Xma*I and *Sal*I and cloned into the integrative plasmid vector pPL2 (previously digested by the same restriction enzymes). pPL2*smcL* plasmid was checked by PCR and sequencing and finally electroporated into *L. monocytogenes* EGDΔ*plcAB*. Transformants were selected on chloramphenicol (7.5 μg / ml) containing BHI plates. Correct insertion of the plasmid into the chromosome of *Listeria* was checked by PCR using primers NC16 and PL95 (table 5.3).

5.3 BIOCHEMICAL TECHNIQUES

5.3.1 RECOMBINANT PRFA PROTEIN PRODUCTION AND PURIFICATION

The *prfA* alleles were amplified by PCR using the oligonucleotide pair prfAH1-P14 and prfAH2-P14 (table 5.3), which contain respectively the *Nde*I and *Sal*I restriction sites, and the corresponding pPL2 plasmid as a template. The resulting *prfA*-containing DNA fragments were digested by *Nde*I and *Sal*I restriction enzymes and cloned in the pET28a plasmid (Novagen) digested by the same restriction enzymes. The resulting *prfA* genes were cloned in frame with a His-tag in N-terminal extremity and electroporated in *E. coli* Bl21DE$_3$ (Invitrogen) for the overproduction of the recombinant PrfA proteins. Host bacteria were grown at 37°C in 500 ml of LB medium containing kanamycin (50 μg / ml) until OD_{600} = 0.8, and the protein expression was induced by adding 1 mM of IPTG. After 3 h, the induced bacteria were pelleted and resuspended in 500 μl of lysis buffer (50 mM NaH_2PO_4, NaCl 300 mM, 20 mM imidazole) containing protease inhibitor cocktail (Roche). After addition of lysozyme 1 mg / ml, the bacteria were incubated 30 min. on ice and lysed (using Lysing Matrix B; Q-Biogen) three times by FastPrep® Instrument (Q-Biogen) for 30 sec. at a setting of 6.5. The cell debris was removed by centrifugation at 10,000 x *g* for 20 min. at 4°C (3K30C Lab Centrifuge). Recombinant PrfA proteins were purified from the bacterial soluble extract by column affinity chromatography using a HiTrap IMAC FF nickel column in an AKTA system (GE Healthcare), according to the manufacturer's instructions. The eluted fractions were analyzed by SDS-PAGE with Coomassie blue staining. The fractions containing PrfA were collected and preserved at -20°C in glycerol 20%.

5.3.2 ANALYTICAL ULTRACENTRIFUGATION (AUC)

Equilibrium sedimentation experiments were carried out at the Department of Biochemistry of the University of Cambridge with help from Zbigniew Pietras using a Beckman Optima XL-I ultracentrifuge (Beckman Coulter UK Ltd.). The purified PrfA proteins stock was buffer exchanged into 10 mM HEPES pH = 7.4, 150 mM NaCl, 3 mM EDTA, 1 mM TCEP and 10% glycerol. The concentration of each sample was quantified by Nanodrop® Spectrophotometer ND-1000 (ThermoScientific, USA). A 400 µl of samples in the range of OD_{280} = 0.8 - 1.0 were centrifuged at 60,000 rpm (Beckman Optima XL-I ultracentrifuge) for 3 h at 22°C. Data were analyzed with the Sedfit Analysis Software v1180. The average protein molecular mass was determined for each sample.

5.3.3 FLUORESCENCE-BASED PROTEIN THERMAL STABILITY ASSAY

Assays were performed at the Department of Biochemistry of the University of Cambridge with help from Zbigniew Pietras using an IQ5 96-well format real-time PCR instrument (Bio-Rad) over a temperature range starting at 25°C and ranging up to 95°C with a heating rate of 0.5°C / min.. Assay samples of 25 µl consisted of 3.5 µg of each PrfA variant, and 5 µl of 12.5X Sypro Orange solution (Invitrogen) diluted 1:400 in the protein buffer. Excitation and emission wavelengths of SYPRO Orange are 470 nm and 570 nm, respectively. Protein thermal unfolding curves were monitored through closed-circuit device camera detection of changes in fluorescence for the SYPRO Orange environmentally sensitive dye (Pantoliano *et al.*, 2001). The inflection point of the melting transition from folded and unfolded states (melting temperarature, T_m) was determined from the first derivative of the plot of fluorescence intensities (Lo *et al.*, 2004).

5.3.4 SURFACE PLASMON RESONANCE

The DNA-binding affinity of purified PrfA proteins was determined by SPR at the Biophysical Characterization facility (Centre for Translational and Chemical Biology) of Edinburgh University using a Biacore biosensor system T100 (Biacore, GE Healthcare). Biotinylated oligonucleotides (40 bp) containing the PrfA box of *plcA* or *actA* promoters in a central position (table 5.3) were immobilized to a streptavidin-coated sensor chip (SA Chip, Amersham-Pharmacia Biotech). To create double-stranded DNA, saturating amounts of non-biotinylated complementary DNA was flowed over the chip. Binding assays were performed at 25ºC in 10 mM HEPES pH = 7.4, 150 mM NaCl, 3 mM EDTA, 0.005% v/v P20 surfactant (HBS-EP buffer, Biacore Life Sciences) containing 1mM tris(2-carboxyethyl)phosphine. PrfA proteins were injected at concentrations ranging from 0.3 nM to 6 μM at a flow rate of 75 μl / min.. DNA binding was measured for 240 sec. until binding approached a steady state, followed by dissociation for another 120 sec. and surface regeneration with 0.1% SDS 3 mM EDTA for 60 sec. at 100 μl / min.. The reference signal (oligonucleotide-free streptavidin-coated cell) was subtracted from each sensorgram and the resulting curves were aligned to a common baseline. Some experiments included a flow cell coated with a random 40-mer oligonucleotide, and no significant binding was detected. For kinetic constants and binding affinity determinations, the 1:1 Langmuir binding model was selected as fitting model in the Biacore T100 Evaluation software. The fits showed chi-square values between 1 and 10.

5.3.5 STRUCTURAL ANALYSES AND MODELLING

Theoretical models of the structures of PrfA mutants were obtained using MODELLER (Sali & Blundell, 1993), which generates protein structures by satisfaction of spatial restraints with simultaneous optimization of CHARMm energies, conjugate gradients and molecular dynamics with simulated annealing. Comparative models were validated with PROCHEK (Laskowski *et al.*, 1993), WHAT_CHECK (Hooft *et al.*, 1996), VERIFY3D (Luthy *et al.*, 1992), and JOY

(Mizuguchi *et al.*, 1998). The crystal structure of $PrfA^{WT}$ at 2.7Å resolution (pdb entry: 2BEO, [Eiting *et al.*, 2005]) was used as template for modeling the structures of the PrfA mutants. The interactions of the new side chains with surrounding residues, and the accessible surface areas (ASA), gap volumes and gap volume indexes were calculated from the models of the PrfA mutants to infer possible changes in the relative position of the two protomers of the dimeric PrfA structure. Dimer interface surfaces were calculated as variation of the ASAs on complexation (Jones & Thornton, 1996). Gap volumes between the two chains of the PrfA dimer was calculated using the program SURFNET (Laskowski, 1995). Interface ASA, gap volume and gap volume index values were obtained from the server PROTORP (http://www.bioinformatics.sussex.ac.uk/protorp/) (Reynolds *et al.*, 2009). Electrostatic interactions between charged residues, and contact atoms and type of interactions, were identified using ELECINT and CONTACTS in-house programs (Núñez Miguel, R., unpublished data). Coordinate superimposition of proteins was carried out using the program MNYFIT (Sutcliffe *et al.*, 1987). The graphical program MacPyMOL (DeLano Scientific LLC, http://www.pymol.org) was used for visualization of protein structures.

5.4 CELL-BASED TECHNIQUES

5.4.1 MAMMALIAN CELL CULTURES

The human cervix epithelial cell line -HeLa- (CCL–2™) and Madin-Darby Bovine Kidney -MDBK- (CCL-22™) epithelial-like cells were obtained from the ATCC repository. L929 (mouse fibroblasts derived from normal subcutaneous areolar and adipose tissue) cell line was a gift from Prof. T. Chakraborty's laboratory (Justus-Liebig-University, Institute of Medical Microbiology, Germany). All cell lines were routinely cultured in 25 or 75 cm^2 plastic flasks (Costar®-Corning; New York, USA) and grown at 37°C in HeraCell incubators (Heraeus; Hanau, Germany) under 5% CO_2 atmosphere in Dulbecco's modified Eagle's medium (DMEM, Gibco

BRL) supplemented with 10% heat-inactivated foetal bovine serum (FBS, BioWhittaker, Cambrex Co.), 2 mM L-glutamine (BioWhittaker, Cambrex Co.) and 25mM glucose. All cell culture manipulations were carried in a HeraSafe class II laminar flow cabinet (Heraeus). Cell lines were regularly inspected using an inverted light microscope (DM IL, Leica Microsystems GmbH; Wetzlar, Germany). Aliquots of low-passage cell lines were prepared in a medium supplemented with 20% FBS and 10% dimethyl sulfoxide (DMSO, Sigma) and kept at -80˚C (U410 Ultra Low Temperature Freezer; New Brunswick Scientific, Hertfordshire, UK) or at -196˚C in liquid nitrogen for short- and long-term storage, respectively.

5.4.2 CELL VIABILITY DETERMINATION

Trypan blue dye exclusion method was used to determine the cell viability. Cell monolayers grown in 24-well plates, 6-well plates or 60 x 15 mm tissue culture dishes (TPP, Switzerland) were washed twice with Dulbecco's phosphate-buffered saline (DPBS; BioWhittaker, Cambrex Co.) and incubated with 100 µl, 200 µl or 300 µl trypsin-EDTA (BioWhittaker, Cambrex Co.), respectively until detachment. To neutralise the trypsin, DMEM was added appropriately up to 1 ml. 50 µl aliquot was diluted 1:2 in trypan blue and viable cells (unstained) were counted using a Thoma's chamber after 5 min. incubation at room temperature.

5.4.3 CELL INVASION AND INTRACELLULAR PROLIFERATION ASSAYS

As far as invasion and proliferation assays (or bacterial intracellular growth assay) were concerned, both techniques involved similar initial steps of the procedure. Both HeLa and MDBK cells were cultured in a 24-well plate (Costar®-Corning; New York, USA) at 37°C under 5% CO_2 in DMEM medium containing 10% foetal bovine serum (FBS; BioWhittaker) until 80% confluence (for detecting the bacterial apoptosis through fluorescent microscopy, additional 24-well plate [Costar®-Corning; New York, USA] with MDBK cells was prepared containing a

slide cover in each well). Bacteria were added to cells at appropriate multiplicity of infection (MOI). Infected monolayers were centrifuged immediately for 3 min. at 145 x *g* (4K15C Sigma Lab Centrifuge) at room temperature and incubated for 30 or 40 min. (for *L. ivanovii* and *L. monocytogenes*, respectively) at 37°C in 5% CO_2 atmosphere. Cell monolayers were washed twice with DPBS to remove non-adherent bacteria, and incubated during 1 hour in DMEM containing 100 μg / ml gentamicin (Sigma) to kill extracellular bacteria. Cell monolayers were, then, washed twice with PBS, lysed by incubation with 1% Triton X-100 (Sigma) for 3 min., eluted in 400 μl of PBS (final volume = 500 μl) and, then, appropriately diluted. The lysates were plated for bacterial counting on BHI agar. Invasion was determined 1 h after gentamicin addition ($t = 0$). For proliferation assay, immediately after $t = 0$ the cell culture medium was changed to contain 10 μg / ml gentamicin and at the specified time points the cells were washed, lysed, as indicated above and the number of CFU determined. For apoptosis determination experiments, at specific time points, the coverslips from additional 24-well plate were also taken out from each well and treated as described in section 5.4.7. Each assay was performed in at least duplicate (or triplicate) for each experiment. The number of intracellular bacteria was calculated as the percentage of the bacteria inoculated that were internalized, according to the formula:

$$\%\ \text{INVASION} = \frac{\text{No. intracellular CFUs}}{\text{No. inoculated CFUs}} \times 100$$

5.4.4 INTRACELLULAR INFECTIONS FOR RT-QPCR EXPRESSION ANALYSES

HeLa cells were grown to 90% confluence in 60 x 15 mm tissue culture dishes (TPP, Switzerland) and infected with an appropriate MOI for each strain (ranging from 20:1 to 150:1 depending on the invasiveness of the strain to obtain similar amounts of intracellular bacteria at the sampling time point). The cell

monolayers were processed as described in the previous section 5.4.3. After 6 h of infection the gentamicin containing medium was removed and cells were washed, detached from the culture dishes by adding 700 μl of PBS and sweeping with a cell lifter (Fisher Scientific). The suspension was transferred into a 1.5 ml microcentrifuge tube and placed immediately on ice. The suspension was used for RNA isolation (500 μl) and for determination of intracellular number of bacteria (100 μl).

5.4.5 PLAQUE ASSAY

Plaque assays were carried out as described by Sun *et al.* (1990), with modifications (Sun *et al.*, 1990). L929 cell line was grown at 37ºC in 5% CO_2 in a 6-well plate (Costar) in RPMI (Roswell Park Memorial Institute; BioWhittaker, Cambrex Co.) supplemented with 10% FBS (BioWhittaker, Cambrex Co.) and 2 mM L-glutamine (BioWhittaker, Cambrex Co.) until 100% confluence. For characterization of *prfA* mutants, frozen bacterial inocula (prepared as described in section 5.1.2) were used to infect a monolayer of L929 cells at appropriate MOI (ranging from 0.005:1 to 2:1, to obtain equal distribution of single plaques). After 1 h incubation at 37°C in 5% CO_2 atmosphere, cell monolayers were washed twice with 1 ml of DPBS and 2 ml of fresh RPMI medium (containing 10 % FBS, 2 mM L-glutamine), supplemented with 50 μg / ml of gentamicin was added to kill extracellular bacteria. Cells were incubated for 1 h in the same conditions as above, after that washed 3 times with 1 ml of DPBS. Each cell monolayer was overlaid with 1.5 ml of agar solution prepared by mixing equal volumes of RPMI (with 10 % FBS, 2 mM L-glutamine, and 5 μg / ml of gentamicin) and 2% cell culture agar (Sigma) and incubated under cell culture conditions for up to 5 days for plaque formation. On the third day, RPMI medium containing appropriate concentration of antibiotic was added to each well to avoid the agar to dry out. For plaque visualization, each well was overlaid with 10% neutral red solution (Sigma) in DPBS and incubated for 2 h at 37°C in 5% CO_2 atmosphere.

The plaque assay technique used to determine cell-to-cell spread in section 3.2.2.2.2 was slightly different. Overnight bacterial culture grown in BHI broth was diluted in 1:50 in BHI and finally grown to OD_{600} = 1. One ml of bacterial suspension was centrifuged at 1,100 x *g* (Eppendorf MiniSpin 5452, Eppendorf AG, UK) for 3 min. and washed twice in 1 ml of RPMI medium. The bacterial suspension was diluted in 1:10,000 and 5 µl were added into the wells. Infected cells were incubated for 2 h under cell culture conditions. The next steps are the same as described above (with exception of 30 min. incubation time with the antibiotic instead of 1 h). After 3 days of incubation, plaques were visualized as described above.

Images of the plates were taken using an Arcus II scanner (Agfa; Mortsel, Belgium). The two perpendicular axes of a minimum of 20 plaques per strain were measured by appropriately amplifying digital images of the plates (x200), using Adobe Photoshop CS3 Standard software (Adobe Photoshop CS3 Standard, USA).

5.4.6 APOPTOSIS DETERMINATIONS BY FLOW CYTOFLUOROMETRY

Apoptosis was quantified by flow cytofluorometry using Annexin V-FITC staining (Beckman Coulter, UK). MDBK cells were seeded on 6-well plate (Costar) 10-12 h before infection with 3 x 10^5 cells per well (1.5 x 10^5 cells / ml). Cell monolayers were infected as described in section 5.4.3. At the specific time points, infected monolayers were washed twice with DPBS and treated for 3 min. at 37°C in 5% CO_2 atmosphere with 400 µl of Trypsin-EDTA solution (BioWhittaker). The detached cell suspension was brought up to 2 ml with 1,600 µl of DMEM (supplemented with 10% FBS) and split into two 1 ml aliquots, one for apoptosis determination and another for bacteria counting. For determination of apoptosis, the cells were spun at 155 x *g* (Sigma 3K30C centrifuge) at 4°C during 5 min., washed once in 5 ml ice-cold binding buffer (10 mM HEPES, 140 mM NaCl, 2.5 mM $CaCl_2$) and spun again. The supernatant was removed until ~300 µl were left and 1 µl of

Annexin V-FITC solution and 5 µl of propidium iodide (PI) were added to each sample and incubated during 15 min. on ice. Cells were washed and resuspended in approximately 1 ml of cold binding buffer and analyzed in an argon-ion flow cytometer (Epics® XL-MCL, Coulter), recording 15,000 events per sample. Annexin V-FITC and PI are absorbed at 488 nm and 536 nm, respectively, giving green (520 nm) and red (617 nm) emissions, respectively. Data were analyzed to obtain the percentage of fluorescing cells using uninfected cells as controls by System II Software v.3.0. Cells treated with 200 nM staurosporine (Sigma) for 3-4 h were used as positive control. Untreated cells were used as a negative control. To determine the CFU, the cells were lysed with 1% Triton X-100 (Sigma) in PBS and the lysates were plated for bacterial counting on BHI agar.

5.4.7 MICROSCOPICAL TECHNIQUE FOR APOPTOSIS

Coverslips with monolayer of infected eukaryotic cells (see section 5.4.3) were washed by immersing them 10 times in a beaker containing PBS, dried on a tissue paper and fixed by treating with 1.5 ml of 2% paraformaldehyde (Sigma) in 12-well plates. They were stored at 4°C until use. Prior to staining, the coverslips were washed by immersing them 10 times in a beaker containing either binding buffer (for staining with Annexin V-FITC) or PBS (for staining with Hoechst), dried on a tissue paper and put in wells of 12-well plate (Costar). Cells attached to the coverslip surface were stained with 200 µl of Annexin V-FITC (Beckman Coulter) at a concentration of 25 µg /ml and/or Hoechst no. 33258 (Sigma) at a concentration of 1 µg / ml and kept in the dark for 10 min.. After this time, the cells were washed as described before and dried on a tissue paper (keeping away from the light). The coverslips were mounted upside down onto a slide using a mounting solution (Vectashield®, Vector Laboratories, Inc.) and fixed to the slide by surrounding with a layer of a nail polish, thus, avoiding the movement of coverslips during microscopic examination, drying out of the preparation and preventing air trapping between the coverslip and the slide. The coverslips were examined under an inverted fluorescence microscope (Leica DMIRE2) and images were captured and processed using OpenLab software (Improvision, USA). Changes in phosphatidylserine asymmetry in

apoptotic cells were detected by the binding of Annexin V-FITC (bright green fluorescence), Hoechst, which is absorbed at 360 nm with emission at 465 nm enabled to visualize chromatin aggregation fluorescing bright blue.

5.5 STATISTICAL ANALYSES

Statistical analyses were carried out using two-tailed unpaired Student's *t*-test with Microsoft Office Excel software.

Table 5.1: Bacterial strains used in this thesis.

Strain	Other designations[a]	Collection no.[b]	Description	Source (reference)
L. monocytogenes				
P14	*prfA*^{WT}	PAM 14	Wild-type strain of serovar 4b, clinical isolate	Our laboratory (Ripio *et al*., 1996; 1997a)
P14A	*prfA**^{G145S}	PAM 50	*prfA** derivative of strain P14	Our laboratory (Ripio *et al*., 1996; 1997a)
P14AΔ*prfA*	Δ*prfA*	PAM 373	In-frame *prfA* deletion mutant of P14A	Our laboratory (Vega *et al*., 2004)
Δ*prfA** (pPL2)	vector	PAM 3293	Δ*prfA** complemented with pPL2 vector	Our laboratory [c]
Δ*prfA** (pPL2*prfA*^{WT})	*prfA*^{WT}	PAM 3294	Δ*prfA** complemented with pPL2*prfA*^{WT}	Our laboratory [c]
Δ*prfA** (pPL2*prfA**^{G145S})	*prfA**^{G145S}	PAM 3295	Δ*prfA** complemented with pPL2*prfA**^{G145S}	Our laboratory [c]
Δ*prfA** (pPL2*prfA*^{V80L})	V80L	PAM 3296	Δ*prfA** complemented with pPL2*prfA*^{V80L}	Our laboratory [c]
Δ*prfA** (pPL2*prfA*^{S71L})	S71L	PAM 3297	Δ*prfA** complemented with pPL2*prfA*^{S71L}	Our laboratory [c]
Δ*prfA** (pPL2*prfA**^{S71L})	S71L*	PAM 3298	Δ*prfA** complemented with pPL2*prfA**^{S71L}	Our laboratory [c]
Δ*prfA** (pPL2*prfA*^{L48F})	L48F	PAM 3299	Δ*prfA** complemented with pPL2*prfA*^{L48F}	Our laboratory [c]
Δ*prfA** (pPL2*prfA**^{L48F})	L48F*	PAM 3300	Δ*prfA** complemented with pPL2*prfA**^{L48F}	Our laboratory [c]
Δ*prfA** (pPL2*prfA*^{Y63W})	Y63W	PAM 3301	Δ*prfA** complemented with pPL2*prfA*^{Y63W}	Our laboratory [c]
Δ*prfA** (pPL2*prfA**^{Y63W})	Y63W*	PAM 3302	Δ*prfA** complemented with pPL2*prfA**^{Y63W}	Our laboratory [c]
Δ*prfA** (pPL2*prfA*^{I69W})	I69W	PAM 3303	Δ*prfA** complemented with pPL2*prfA*^{I69W}	Our laboratory [c]
Δ*prfA** (pPL2*prfA*^{E36Q})	E36Q	PAM 3304	Δ*prfA** complemented with pPL2*prfA*^{E36Q}	Our laboratory [c]
Δ*prfA** (pPL2*prfA*^{E36R})	E36R	PAM 3305	Δ*prfA** complemented with pPL2*prfA*^{E36R}	Our laboratory [c]
Δ*prfA** (pPL2*prfA*^{F29M})	F29M	PAM 3306	Δ*prfA** complemented with pPL2*prfA*^{F29M}	Our laboratory [c]
Δ*prfA** (pPL2*prfA*^{L120V})	L120V	PAM 3307	Δ*prfA** complemented with pPL2*prfA*^{L120V}	Our laboratory [c]
Δ*prfA** (pPL2*prfA*^{E173G})	E173G	PAM 3313	Δ*prfA** complemented with pPL2*prfA*^{E173G}	Our laboratory [c]
Δ*prfA** (pPL2*prfA**^{E173G})	E173G*	PAM 3314	Δ*prfA** complemented with pPL2*prfA**^{E173G}	Our laboratory [c]
Δ*prfA** (pPL2*prfA*^{C229Y})	C229Y	PAM 3315	Δ*prfA** complemented with pPL2*prfA*^{C229Y}	Our laboratory [c]
Δ*prfA** (pPL2*prfA**^{C229Y})	C229Y*	PAM 3316	Δ*prfA** complemented with pPL2*prfA**^{C229Y}	Our laboratory [c]
Δ*prfA** (pPL2*prfA*^{A129T})	A129T	PAM 3317	Δ*prfA** complemented with pPL2*prfA*^{A129T}	Our laboratory [d]
Δ*prfA** (pPL2*prfA**^{A129T})	A129T*	PAM 3318	Δ*prfA** complemented with pPL2*prfA**^{A129T}	Our laboratory [d]

Table 5.1: Bacterial strains used in this thesis (continued).

Strain	Other designations[a]	Collection no.[b]	Description	Source (reference)
P14AΔ*actA*	Δ*actA*	PAM 185	In-frame *actA* deletion mutant of P14A	Our laboratory (Suarez *et al*., 2001)
P14Δ*sigB*		PAM 3187	In-frame *sigB* deletion mutant of P14	Our laboratory[d]
P14AΔ*sigB*		PAM 3185	In-frame *sigB* deletion mutant of P14A	Our laboratory[d]
P14A$^{prfA\text{A129T}}$		PAM 3184	In-frame *sigB* deletion mutant of P14A with a naturally occurring point mutation A129T in *prfA*	Our laboratory[d]
EGDe		PAM 3120	Wild-type strain of serovar 1/2a	Glaser *et al*. (2001)
EGDeΔ*sigB*		PAM 3121	In-frame *sigB* deletion mutant of EGDe	Stritzker *et al.* (2005)
EGDeΔ*prfA*		PAM 225	In-frame *prfA* deletion mutant of EGDe	Böckmann *et al.* (1996)
EGDΔ*plcAB*		PAM 648	In-frame *plcA* and *plcB* deletion mutant of EGD (referred as WL-106)	Hauf *et al.* (1997)
EGDΔ*plcAB(*pPL2)		PAM 3097	EGDΔ*plcAB* complemented with pPL2 vector	Our laboratory[d]
EGDΔ*plcAB(*pPL2*smcL*)		PAM 3096	EGDΔ*plcAB* complemented with pPL2*smcL*	Our laboratory[e]
L. ivanovii				
ATCC 19119		PAM 424	Special Listeria Culture Collection strain 2379, (serovar 5) (referred as ATCC 19119)	Institut fur Hygiene und Mikrobiologie, University of Würzburg, Federal Republic of Germany)
E.coli				
Bl21DE$_3$		PAM 3484	*E. coli* strain	Invitrogen
Bl21DE$_3$ (pET28a)		PAM 3485	*E. coli* complemented with pET28a vector	Our laboratory
Bl21DE$_3$ (pET28a*prfA*^{WT})		PAM 3486	*E. coli* complemented with pET28a*prfA*^{WT}	Dr. Mark Banfield (University of Newcastle)
Bl21DE$_3$ (pET28a*prfA**)		PAM 3487	*E. coli* complemented with pET28a*prfA**	Our laboratory[c]
Bl21DE$_3$ (pET28a*prfA*^{V80L})		PAM 3488	*E. coli* complemented with pET28a*prfA*^{V80L}	Our laboratory[c]
Bl21DE$_3$ (pET28a*prfA*^{S71L})		PAM 3489	*E. coli* complemented with pET28a*prfA*^{S71L}	Our laboratory[c]
Bl21DE$_3$ (pET28a*prfA**^{S71L})		PAM 3490	*E. coli* complemented with pET28a*prfA**^{S71L}	Our laboratory[c]
Bl21DE$_3$ (pET28a*prfA*^{L48F})		PAM 3491	*E. coli* complemented with pET28a*prfA*^{L48F}	Our laboratory[c]
Bl21DE$_3$ (pET28a*prfA**^{L48F})		PAM 3492	*E. coli* complemented with pET28a*prfA**^{L48F}	Our laboratory[c]

Table 5.1: Bacterial strains used in this thesis (continued).

Strain	Other designations[a]	Collection no.[b]	Description	Source (reference)
Bl21DE$_3$ (pET28a*prfA*^{Y63W})		PAM 3493	*E. coli* complemented with pET28a*prfA*^{Y63W}	Our laboratory[c]
Bl21DE$_3$ (pET28a*prfA**^{Y63W})		PAM 3494	*E. coli* complemented with pET28a*prfA**^{Y63W}	Our laboratory[c]
Bl21DE$_3$ (pET28a*prfA*^{I69W})		PAM 3495	*E. coli* complemented with pET28a*prfA*^{I69W}	Our laboratory[c]
Bl21DE$_3$ (pET28a*prfA*^{E36Q})		PAM 3496	*E. coli* complemented with pET28a*prfA*^{E36Q}	Our laboratory[c]
Bl21DE$_3$ (pET28a*prfA*^{E36R})		PAM 3497	*E. coli* complemented with pET28a*prfA*^{E36R}	Our laboratory[c]
Bl21DE$_3$ (pET28a*prfA*^{F29M})		PAM 3498	*E. coli* complemented with pET28a*prfA*^{F29M}	Our laboratory[c]
Bl21DE$_3$ (pET28a*prfA*^{L120V})		PAM 3499	*E. coli* complemented with pET28a*prfA*^{L120V}	Our laboratory[c]
Bl21DE$_3$ (pET28a*prfA*^{E173G})		PAM 3505	*E. coli* complemented with pET28a*prfA*^{E173G}	Our laboratory[c]
Bl21DE$_3$ (pET28a*prfA**^{E173G})		PAM 3506	*E. coli* complemented with pET28a*prfA**^{E173G}	Our laboratory[c]
Bl21DE$_3$ (pET28a*prfA*^{C229Y})		PAM 3507	*E. coli* complemented with pET28a*prfA*^{C229Y}	Our laboratory[c]
Bl21DE$_3$ (pET28a*prfA**^{C229Y})		PAM 3508	*E. coli* complemented with pET28a*prfA**^{C229Y}	Our laboratory[c]
Bl21DE$_3$ (pET28a*prfA*^{A129T})		PAM 3509	*E. coli* complemented with pET28a*prfA*^{A129T}	Our laboratory[c]
Bl21DE$_3$ (pET28a*prfA**^{A129T})		PAM 3510	*E. coli* complemented with pET28a*prfA**^{A129T}	Our laboratory[c]
DH10b (pLSV101Δ*sigB*)		PAM 3123	*E.coli* complemented with mutagenesis plasmid pLSV101Δ*sigB*	Stritzker *et al.* (2005)
DH5-α		PAM 3511	Cloning host strain	Our laboratory
TOP10			Cloning host strain	Invitrogen

[a] - Some strains were on occasions referred to in the text by their genotype / relevant mutation
[b]- PAM refers to our internal central isolate / recombinant strain collection
[c, d, e] - These strains were constructed in collaboration for the projects described in this work ([c], Dr. Caroline Deshayes; [d], Magdalena Bielecka; [e], Dr. Mariela Scortti)

Table 5.2: Components of the chemically defined medium (IMM).

Compound	Amount per litre
KH_2PO_4	6,56 g
Na_2HPO_4* 7 H_2O	30,96 g
$MgSO_4$ * 7 H_2O	0,41 g
Ferric citrate	88 mg
L – Glutamine	0,6 g
L – Leucine	0,1 g
DL – Isoleucine	0,1 g
DL – Valinie	0,1 g
DL – Methionine	0,1 g
L – Arginine HCl	0,1 g
L – Cysteine HCl	0,1 g
L – Histidine HCl	0,1 g
L – Tryptophan	0,1 g
L – Phenylalanine	0,1 g
Adenine	2,5 mg
Biotin	0,5 mg
Riboflavine	5 mg
Thiamine HCl	1 mg
Pyridoxal HCl	1 mg
Para – aminobenzoic acid	1 mg
Calcium panthothenate	1 mg
Nicotinamide	1 mg
Thioctic acid (α – lipoic acid)	5 µg

Table 5.3: Oligonucleotides used in this thesis.
Capital letters indicate the mutated codons, italisized capitals indicate a restriction site, underlined capitals indicate the position of a PrfA box.

Name	5'-3' sequence	Purpose	Restriction site	Modification
F29Mforward F29Mreverse	aacttattATGaaccaatggga tcccattggttCATaataagtt	Mutagenesis Phe29Met of PrfA		
E36Qforward E36Qreverse	atccacaaCAAtattgtatttt aaaatacaataTTGttgtggat	Mutagenesis Gly36Gln of PrfA		
E36Rforward E36Rreverse	atccacaaAGAtattgtatttt aaaatacaataTCTttgtggat	Mutagenesis Gly36Arg of PrfA		
L48Fforward L48Freverse	tatcacaaagTTTacgagtatt aatactcgtAAActttgtgata	Mutagenesis Leu48Phe of PrfA		
Y63Wforward Y63Wreverse	ttacaatacTGGaaaggggctt aagccccttCCAgtattgtaa	Mutagenesis Tyr63Trp of PrfA		
I69Wforward I69Wreverse	gctttcgttTGGatgtctggct agccagacatCCAaacgaaagc	Mutagenesis Ile69Trp of PrfA		
S71Lforward S71Lreverse	cgttataatgTTAggctttatt aataaagccTAAcattataacg	Mutagenesis Ser71Leu of PrfA		
V80Lforward V80Lreverse	agaaacatcgTTAggctattat ataatagccTAAcgatgtttct	Mutagenesis Val80Leu of PrfA		
L120Vforward L120Vreverse	tccaaaccGTTcaaaaacaagt acttgtttttgAACggtttgga	Mutagenesis Leu120Val of PrfA		
A129Tforward A129Treverse	caagtttcatacagcctaACCaaatttaatg cattaaatttGGTtaggctgtatgaaacttg	Mutagenesis Ala129Thr of PrfA		
E173Gforward E173Greverse	caatgcagGGCttaggctattc gaatagcctaaGCCctgcattg	Mutagenesis Glu173Gly of PrfA		
C229Yforward C229Yreverse	tatttagcaTATcctgctacttg caagtagcaggATAtgctaaata	Mutagenesis Cys229Tyr of PrfA		

Table 5.3: Oligonucleotides used in this thesis (continued).

Name	5'-3' sequence	Purpose	Restriction site	Modification
MR2SalI (forward) MR10SalI (reverse)	*GTCGAC*caactaacatatattattcct *GTCGAC*cttggcgaagcaatcgttcgc	Amplification of *prfA* for pPL2	*SalI* *SalI*	
MR2KpnI (forward) MR10SpeI (reverse)	ctag*GGTACC*caactaacatatattattcct ctagA*CTAGT*cttggtgaagcaatcgtacgc	Amplification of *prfA* for pPL2	*KpnI* *SpeI*	
prfAH1-P14 prfAH2-P14	atga*CATATG*aacgctcaagcagaag ga*GTCGAC*attgagacatcctgtttt	Ampilfication of *prfA* for pET28a	*NdeI* *SalI*	
Promo28plcA-P14 Promo40plcA-P14 Promo40actA-P14 Random Promo28plcAREV Promo40plcAREV Promo40actAREV RandomREV	ttatcgtcgTTAACAaaTGTTAAtgcc tgtccctttatcgtcgTTAACAaaTGTTAAtgcctcgaca ggtcggagttaactgaTTAACAaaTGTTAGagaaaactta atgtatctatgtatgcagatgttcaatacgtcaagctatt ggcaTTAACAttTGTTAAcgacgataa tgtcgaggcaTTAACAttTGTTAAcgacgataaagggaca taagttttctCTAACAttTGTTAAtcagttaactccgacc aatagcttgacgtattgaacatctgcatacatagatacat	Biacore experiments		5'biotin-TEG 5'biotin-TEG 5'biotin-TEG 5'biotin-TEG
lmoldh-491F (forward) lmoldh-555R (reverse) lmoldh-P (probe)	atgctcgtaacgtccatggtt gctccatgctgggaattctg FAM-catccttggcgaacacggcga-BHQ	RT-QPCR experiments		
rpoB1-QF (forward) rpoB1-QR (reverse) rpoB1-P (probe)	tggttcttagatgaagggctacgt acccgcaaaatcctcaattg FAM-aatatcgcggaacatct –BHQ			
actA38F (forward) actA109R (reverse) actA64p (probe)	aagaaattgatcgcctagctgatt gtaaaaaacccgcatttcttgagt FAM-tttcctgttcctctatctct-MGB-NFQ			
inlA1-204F (forward) inlA1-294R (reverse) inlA1-239P (probe)	aataagtgatataactccacttgggattt cgccaatgtgcctatatcttttaact FAM-accatttaaggataattcgtccaaat–MGB–NFQ			

Table 5.3: Oligonucleotides used in this thesis (continued).

Name	5'-3' sequence	Purpose	Restriction site	Modification
inlB4b-QF (forward) inlB4b-QR (reverse) inlB4b-P (probe)	ccagggaatgcagtttgga tggtagacggaaagcttgttca FAM-aatacagctggcgcaac–MGB–NFQ	RT-QPCR experiments		
plcA-11F (forward) plcA-99R (reverse) plcA-P (probe)	caggtacacatgatacgatgagctataa gtacaatgacatcgtttgtgtttgag FAM–agtggtttggttaatgtcc–MGB–NFQ			
Random	NNN-NNN			
sigBF (forward) sigBR (reverse) pLSV1-B pLSV1-C	attatcaggaattgcaagtcgcg cgcgagaaagaacaagtccatc gatgtgctgcaaggcgat ccttcgacagtcatcatata	*sigB* deletion mutants construction check		
smcL-XmaI (forward) smcL-SalI (reverse)	tcccc*CCCGGG*ctttgtttccaaactcatgt acgc*GTCGAC*gatacttttagctttcacacg	Amplification of *smcL* for pPL2	*XmaI* *SalI*	
NC16 (forward) PL95 (reverse)	gtcaaaacatacgctcttatc acataatcagtccaaagtagatgc	integration of pPL2 into *Listeria* chromosome check		

Table 5.4: Plasmids used in this thesis.

Plasmid	Description	Source (reference)
pPL2	site-specific phage integration vector, derivative of pPL1 vector	Lauer *et al.* (2002)
pPL2*prfA*^{WT}	pPL2 inserted with the wild-type *prfA* allele from P14	Our laboratory[a]
pPL2*prfA**^{G145S}	pPL2 inserted with the *prfA**^{G145S} allele from P14A	Our laboratory[a]
pPL2*prfA*^{V80L}	pPL2 inserted with the *prfA* allele with a point mutation Val80Leu	Our laboratory[b]
pPL2*prfA*^{S71L}	pPL2 inserted with the *prfA* allele with a point mutation Ser71Leu	Our laboratory[b]
pPL2*prfA**^{S71L}	pPL2 inserted with the *prfA**^{G145S} allele with a point mutation Ser71Leu	Our laboratory[b]
pPL2*prfA*^{L48F}	pPL2 inserted with the *prfA* allele with a point mutation Leu48Phe	Our laboratory[b]
pPL2*prfA**^{L48F}	pPL2 inserted with the *prfA**^{G145S} allele with a point mutation Leu48Phe	Our laboratory[b]
pPL2*prfA*^{Y63W}	pPL2 inserted with the *prfA* allele with a point mutation Tyr63Trp	Our laboratory[b]
pPL2*prfA**^{Y63W}	pPL2 inserted with the *prfA**^{G145S} allele with a point mutation Tyr63Trp	Our laboratory[b]
pPL2*prfA*^{I69W}	pPL2 inserted with the *prfA* allele with a point mutation Ile69Trp	Our laboratory[b]
pPL2*prfA*^{E36Q}	pPL2 inserted with the *prfA* allele with a point mutation Glu36Gln	Our laboratory[b]
pPL2*prfA*^{E36R}	pPL2 inserted with the *prfA* allele with a point mutation Glu36Arg	Our laboratory[b]
pPL2*prfA*^{F29M}	pPL2 inserted with the *prfA* allele with a point mutation Phe29Met	Our laboratory[b]
pPL2*prfA*^{L120V}	pPL2 inserted with the *prfA* allele with a point mutation Leu120Val	Our laboratory[b]
pPL2*prfA*^{E173G}	pPL2 inserted with the *prfA* allele with a point mutation Glu173Gly	Our laboratory[b]
pPL2*prfA**^{E173G}	pPL2 inserted with the *prfA**^{G145S} allele with a point mutation Glu173Gly	Our laboratory[b]
pPL2*prfA*^{C229Y}	pPL2 inserted with the *prfA* allele with a point mutation Cys229Tyr	Our laboratory[b]
pPL2*prfA**^{C229Y}	pPL2 inserted with the *prfA**^{G145S} allele with a point mutation Cys229Tyr	Our laboratory[b]
pPL2*prfA*^{A129T}	pPL2 inserted with the *prfA* allele with a point mutation Ala129Thr	Our laboratory[a]
pPL2*prfA**^{A129T}	pPL2 inserted with the *prfA**^{G145S} allele with a point mutation Ala129Thr	Our laboratory[a]
pPL2*smcL*	pPL2 inserted with the *smcL* allele from *L. ivanovii* ATCC 19119	Our laboratory[c]
pET28a	His-tag vector	Novagen
pET28a*prfA*^{WT}	pET28a inserted with the wild-type *prfA* allele from P14	Our laboratory[b]
pET28a*prfA**^{G145S}	pET28a inserted with the *prfA**^{G145S} allele from P14A	Our laboratory[b]

Table 5.4: Plasmids used in this thesis (continued).

Plasmid	Description	Source (reference)
pET28a*prfA*^{V80L}	pET28a inserted with the *prfA* allele with a point mutation Val80Leu	Our laboratory[b]
pET28a*prfA*^{S71L}	pET28a inserted with the *prfA* allele with a point mutation Ser71Leu	Our laboratory[b]
pET28a*prfA**^{S71L}	pET28a inserted with the *prfA**^{G145S} allele with a point mutation Ser71Leu	Our laboratory[b]
pET28a*prfA*^{L48F}	pET28a inserted with the *prfA* allele with a point mutation Leu48Phe	Our laboratory[b]
pET28a*prfA**^{L48F}	pET28a inserted with the *prfA**^{G145S} allele with a point mutation Leu48Phe	Our laboratory[b]
pET28a*prfA*^{Y63W}	pET28a inserted with the *prfA* allele with a point mutation Tyr63Trp	Our laboratory[b]
pET28a*prfA**^{Y63W}	pET28a inserted with the *prfA**^{G145S} allele with a point mutation Tyr63Trp	Our laboratory[b]
pET28a*prfA*^{I69W}	pET28a inserted with the *prfA* allele with a point mutation Ile69Trp	Our laboratory[b]
pET28a*prfA*^{E36Q}	pET28a inserted with the *prfA* allele with a point mutation Glu36Gln	Our laboratory[b]
pET28a*prfA*^{E36R}	pET28a inserted with the *prfA* allele with a point mutation Glu36Arg	Our laboratory[b]
pET28a*prfA*^{F29M}	pET28a inserted with the *prfA* allele with a point mutation Phe29Met	Our laboratory[b]
pET28a*prfA*^{L120V}	pET28a inserted with the *prfA* allele with a point mutation Leu120Val	Our laboratory[b]
pET28a*prfA*^{E173G}	pET28a inserted with the *prfA* allele with a point mutation Glu173Gly	Our laboratory[b]
pET28a*prfA**^{E173G}	pET28a inserted with the *prfA**^{G145S} allele with a point mutation Glu173Gly	Our laboratory[b]
pET28a*prfA*^{C229Y}	pET28a inserted with the *prfA* allele with a point mutation Cys229Tyr	Our laboratory[b]
pET28a*prfA**^{C229Y}	pET28a inserted with the *prfA**^{G145S} allele with a point mutation Cys229Tyr	Our laboratory[b]
pET28a*prfA*^{A129T}	pET28a inserted with the *prfA* allele with a point mutation Ala129Thr	Our laboratory[b]
pET28a*prfA**^{A129T}	pET28a inserted with the *prfA**^{G145S} allele with a point mutation Ala129Thr	Our laboratory[b]
pLSV101Δ*sigB*	Mutagenesis plasmid, derivative of pLSV1 vector, inserted with the Δ*sigB* recombination fragment	Stritzker *et al.* (2005)
pH*smcL*	pHPS9 inserted with the *L. ivanovii* ATCC 19119 *smcL* gene	Gonzalez-Zorn *et al.* (1999)

[a, b, c] - These plasmids were constructed in collaboration for the projects described in this work ([a], Magdalena Bielecka; [b], Dr. Caroline Deshayes; [c], Dr. Mariela Scortti)

6 REFERENCES

Abram, F., E. Starr, K. A. G. Karatzas, K. Matlawska-Wasowska, A. Boyd, M. Wiedmann, K. J. Boor, D. Connally & C. P. O'Byrne, (2008b) Identification of components of the sigma B regulon in *Listeria monocytogenes* that contribute to acid and salt tolerance. *Appl. Environ. Microbiol.*

Abram, F., W. L. Su, M. Wiedmann, K. J. Boor, P. Coote, C. Botting, K. A. Karatzas & C. P. O'Byrne, (2008a) Proteomic analyses of a *Listeria monocytogenes* mutant lacking sigma B identify new components of the sigma B regulon and highlight a role for sigma B in the utilization of glycerol. *Applied and environmental microbiology* **74**: 594-604.

Abu-Zant, A., M. Santic, M. Molmeret, S. Jones, J. Helbig & Y. Abu Kwaik, (2005) Incomplete activation of macrophage apoptosis during intracellular replication of *Legionella pneumophila*. *Infection and immunity* **73**: 5339-5349.

Abul-Milh, M., Y. Wu, B. Lau, C. A. Lingwood & D. Barnett Foster, (2001) Induction of epithelial cell death including apoptosis by enteropathogenic *Escherichia coli* expressing bundle-forming pili. *Infection and immunity* **69**: 7356-7364.

Andrieu-Abadie, N. & T. Levade, (2002) Sphingomyelin hydrolysis during apoptosis. *Biochimica et biophysica acta* **1585**: 126-134.

Anonymous, (2003) Recent trends in listeriosis in the UK. *A report. Microbiological Safety Division, Food Standards Agency*.

Anonymous, (2005) Preliminary FoodNet data on the incidence of infection with pathogens transmitted commonly through food--10 sites, United States, 2004. *Mmwr* **54**: 352-356.

Arous, S., C. Buchrieser, P. Folio, P. Glaser, A. Namane, M. Hebraud & Y. Hechard, (2004) Global analysis of gene expression in an *rpoN* mutant of *Listeria monocytogenes*. *Microbiology (Reading, England)* **150**: 1581-1590.

Arvidson, S. & K. Tegmark, (2001) Regulation of virulence determinants in *Staphylococcus aureus*. *Int J Med Microbiol* **291**: 159-170.

Ausubel, F. M., R. Brent, R. E. Kingston, D. D. Moore, J. G. Seidman, J. A. Smith & K. Struhl, (2002) *Current Protocols in Molecular Biology. Ed. John Wiley and Sons Inc., N. Y.*

Autio, T., S. Hielm, M. Miettinen, A. M. Sjoberg, K. Aarnisalo, J. Bjorkroth, T. Mattila-Sandholm & H. Korkeala, (1999) Sources of *Listeria monocytogenes* contamination in a cold-smoked rainbow trout processing plant detected by pulsed-field gel electrophoresis typing. *Applied and environmental microbiology* **65**: 150-155.

Avery, S. M. & S. Buncic, (1997) Differences in pathogenicity for chick embryos and growth kinetics at 37 degrees C between clinical and meat isolates of *Listeria monocytogenes* previously stored at 4 degrees C. *International journal of food microbiology* **34**: 319-327.

Bantel, H., B. Sinha, W. Domschke, G. Peters, K. Schulze-Osthoff & R. U. Janicke, (2001) alpha-Toxin is a mediator of *Staphylococcus aureus*-induced cell death and activates caspases via the intrinsic death pathway independently of death receptor signaling. *The Journal of cell biology* **155**: 637-648.

Barsig, J. & S. H. Kaufmann, (1997) The mechanism of cell death in *Listeria monocytogenes*-infected murine macrophages is distinct from apoptosis. *Infection and immunity* **65**: 4075-4081.

Becker, L. A., M. S. Cetin, R. W. Hutkins & A. K. Benson, (1998) Identification of the gene encoding the alternative sigma factor sigma B from *Listeria monocytogenes* and its role in osmotolerance. *Journal of bacteriology* **180**: 4547-4554.

Becker, L. A., S. N. Evans, R. W. Hutkins & A. K. Benson, (2000) Role of sigma(B) in adaptation of *Listeria monocytogenes* to growth at low temperature. *Journal of bacteriology* **182**: 7083-7087.

Behari, J. & P. Youngman, (1998a) A homolog of CcpA mediates catabolite control in *Listeria monocytogenes* but not carbon source regulation of virulence genes. *Journal of bacteriology* **180**: 6316-6324.

Behari, J. & P. Youngman, (1998b) Regulation of *hly* expression in *Listeria monocytogenes* by carbon sources and pH occurs through separate mechanisms mediated by PrfA. *Infection and immunity* **66**: 3635-3642.

Behnia, M., K. A. Robertson & W. J. Martin, 2nd, (2000) Lung infections: role of apoptosis in host defense and pathogenesis of disease. *Chest* **117**: 1771-1777.

Belmokhtar, C. A., J. Hillion & E. Segal-Bendirdjian, (2001) Staurosporine induces apoptosis through both caspase-dependent and caspase-independent mechanisms. *Oncogene* **20**: 3354-3362.

Berman, H. M., L. F. Ten Eyck, D. S. Goodsell, N. M. Haste, A. Kornev & S. S. Taylor, (2005) The cAMP binding domain: an ancient signaling module. *Proceedings of the National Academy of Sciences of the United States of America* **102**: 45-50.

Bielecki, J., P. Youngman, P. Connelly & D. A. Portnoy, (1990) *Bacillus subtilis* expressing a haemolysin gene from *Listeria monocytogenes* can grow in mammalian cells. *Nature* **345**: 175-176.

Bifrare, Y. D., C. Gianinazzi, H. Imboden, S. L. Leib & M. G. Tauber, (2003) Bacterial meningitis causes two distinct forms of cellular damage in the hippocampal dentate gyrus in infant rats. *Hippocampus* **13**: 481-488.

Birbes, H., S. El Bawab, Y. A. Hannun & L. M. Obeid, (2001) Selective hydrolysis of a mitochondrial pool of sphingomyelin induces apoptosis. *Faseb J* **15**: 2669-2679.

Bischoff, M., P. Dunman, J. Kormanec, D. Macapagal, E. Murphy, W. Mounts, B. Berger-Bachi & S. Projan, (2004) Microarray-based analysis of the *Staphylococcus aureus* sigma B regulon. *Journal of bacteriology* **186**: 4085-4099.

Bischoff, M., J. M. Entenza & P. Giachino, (2001) Influence of a functional *sigB* operon on the global regulators *sar* and *agr* in *Staphylococcus aureus*. *Journal of bacteriology* **183**: 5171-5179.

Boerlin, P., J. Rocourt, F. Grimont, P. A. D. Grimont, J. C. & J. C. Piffaretti, (1992) *Listeria ivanovii*, subsp. *londoniensis* subsp. nov. *Int. J . Syst. Bacteriol.* **42**: 69-73.

Bohne, J., H. Kestler, C. Uebele, Z. Sokolovic & W. Goebel, (1996) Differential regulation of the virulence genes of *Listeria monocytogenes* by the transcriptional activator PrfA. *Molecular microbiology* **20**: 1189-1198.

Bortner, C. D., N. B. Oldenburg & J. A. Cidlowski, (1995) The role of DNA fragmentation in apoptosis. *Trends in cell biology* **5**: 21-26.

Bortolussi, R., (2008) Listeriosis: a primer. *Cmaj* **179**: 795-797.

Braun, J. S., J. E. Sublett, D. Freyer, T. J. Mitchell, J. L. Cleveland, E. I. Tuomanen & J. R. Weber, (2002) Pneumococcal pneumolysin and H(2)O(2) mediate brain cell apoptosis during meningitis. *The Journal of clinical investigation* **109**: 19-27.

Brehm, K., M. T. Ripio, J. Kreft & J. A. Vazquez-Boland, (1999) The *bvr* locus of *Listeria monocytogenes* mediates virulence gene repression by beta-glucosides. *Journal of bacteriology* **181**: 5024-5032.

Brody, M. S. & C. W. Price, (1998) *Bacillus licheniformis sigB* operon encoding the general stress transcription factor sigma B. *Gene* **212**: 111-118.

Bubert, A., Z. Sokolovic, S. K. Chun, L. Papatheodorou, A. Simm & W. Goebel, (1999) Differential expression of *Listeria monocytogenes* virulence genes in mammalian host cells. *Mol Gen Genet* **261**: 323-336.

Buncic, S., S. M. Avery, J. Rocourt & M. Dimitrijevic, (2001) Can food-related environmental factors induce different behaviour in two key serovars, 4b and 1/2a, of *Listeria monocytogenes*? *International journal of food microbiology* **65**: 201-212.

Bustin, S. A., (2000) Absolute quantification of mRNA using real-time reverse transcription polymerase chain reaction assays. *Journal of molecular endocrinology* **25**: 169-193.

Bustin, S. A. & T. Nolan, (2004) Pitfalls of quantitative real-time reverse-transcription polymerase chain reaction. *J Biomol Tech* **15**: 155-166.

Butcher, B. G. & J. D. Helmann, (2006) Identification of *Bacillus subtilis sigma*-dependent genes that provide intrinsic resistance to antimicrobial compounds produced by *Bacilli*. *Molecular microbiology* **60**: 765-782.

Camilli, A., H. Goldfine & D. A. Portnoy, (1991) *Listeria monocytogenes* mutants lacking phosphatidylinositol-specific phospholipase C are avirulent. *The Journal of experimental medicine* **173**: 751-754.

Camilli, A., L. G. Tilney & D. A. Portnoy, (1993) Dual roles of *plcA* in *Listeria monocytogenes* pathogenesis. *Molecular microbiology* **8**: 143-157.

Carpinteiro, A., C. Dumitru, M. Schenck & E. Gulbins, (2008) Ceramide-induced cell death in malignant cells. *Cancer letters* **264**: 1-10.

Carrero, J. A., B. Calderon & E. R. Unanue, (2004a) Listeriolysin O from *Listeria monocytogenes* is a lymphocyte apoptogenic molecule. *J Immunol* **172**: 4866-4874.

Carrero, J. A., B. Calderon & E. R. Unanue, (2004b) Type I interferon sensitizes lymphocytes to apoptosis and reduces resistance to *Listeria* infection. *The Journal of experimental medicine* **200**: 535-540.

Carrero, J. A., B. Calderon & E. R. Unanue, (2006) Lymphocytes are detrimental during the early innate immune response against *Listeria monocytogenes*. *The Journal of experimental medicine* **203**: 933-940.

Carrero, J. A., B. Calderon, H. Vivanco-Cid & E. R. Unanue, (2009) Recombinant *Listeria monocytogenes* expressing a cell wall-associated listeriolysin O is weakly virulent but immunogenic. *Infection and immunity* **77**: 4371-4382.

Carrero, J. A. & E. R. Unanue, (2006) Lymphocyte apoptosis as an immune subversion strategy of microbial pathogens. *Trends in immunology* **27**: 497-503.

Carrero, J. A., H. Vivanco-Cid & E. R. Unanue, (2008) Granzymes drive a rapid listeriolysin O-induced T cell apoptosis. *J Immunol* **181**: 1365-1374.

Castedo, M., K. Ferri, T. Roumier, D. Metivier, N. Zamzami & G. Kroemer, (2002) Quantitation of mitochondrial alterations associated with apoptosis. *Journal of immunological methods* **265**: 39-47.

Cervantes, J., T. Nagata, M. Uchijima, K. Shibata & Y. Koide, (2008) Intracytosolic *Listeria monocytogenes* induces cell death through caspase-1 activation in murine macrophages. *Cellular microbiology* **10**: 41-52.

Cetin, M. S., C. Zhang, R. W. Hutkins & A. K. Benson, (2004) Regulation of transcription of compatible solute transporters by the general stress sigma factor, sigma B, in *Listeria monocytogenes*. *Journal of bacteriology* **186**: 794-802.

Chae, H. J., J. S. Kang, J. O. Byun, K. S. Han, D. U. Kim, S. M. Oh, H. M. Kim, S. W. Chae & H. R. Kim, (2000) Molecular mechanism of staurosporine-induced apoptosis in osteoblasts. *Pharmacol Res* **42**: 373-381.

Chakraborty, T., M. Leimeister-Wachter, E. Domann, M. Hartl, W. Goebel, T. Nichterlein & S. Notermans, (1992) Coordinate regulation of virulence genes in *Listeria monocytogenes* requires the product of the *prfA* gene. *Journal of bacteriology* **174**: 568-574.

Chan, Y. C., S. Raengpradub, K. J. Boor & M. Wiedmann, (2007a) Microarray-based characterization of the *Listeria monocytogenes* cold regulon in log- and stationary-phase cells. *Applied and environmental microbiology* **73**: 6484-6498.

Chatterjee, S. S., H. Hossain, S. Otten, C. Kuenne, K. Kuchmina, S. Machata, E. Domann, T. Chakraborty & T. Hain, (2006) Intracellular gene expression profile of *Listeria monocytogenes*. *Infection and immunity* **74**: 1323-1338.

Chaturongakul, S. & K. J. Boor, (2004) RsbT and RsbV contribute to sigma B-dependent survival under environmental, energy, and intracellular stress conditions in *Listeria monocytogenes*. *Applied and environmental microbiology* **70**: 5349-5356.

Chaturongakul, S. & K. J. Boor, (2006) Sigma B activation under environmental and energy stress conditions in *Listeria monocytogenes*. *Applied and environmental microbiology* **72**: 5197-5203.

Chaturongakul, S., S. Raengpradub, M. Wiedmann & K. J. Boor, (2008) Modulation of stress and virulence in *Listeria monocytogenes*. *Trends in microbiology* **16**: 388-396.

Chen, Y. & A. Zychlinsky, (1994) Apoptosis induced by bacterial pathogens. *Microbial pathogenesis* **17**: 203-212.

Cheng, X., L. Kovac & J. C. Lee, (1995) Probing the mechanism of CRP activation by site-directed mutagenesis: the role of serine 128 in the allosteric pathway of cAMP receptor protein activation. *Biochemistry* **34**: 10816-10826.

Chico-Calero, I., M. Suarez, B. Gonzalez-Zorn, M. Scortti, J. Slaghuis, W. Goebel & J. A. Vazquez-Boland, (2002) Hpt, a bacterial homolog of the microsomal glucose- 6-phosphate translocase, mediates rapid intracellular proliferation in *Listeria*. *Proceedings of the National Academy of Sciences of the United States of America* **99**: 431-436.

Chowdhury, I., B. Tharakan & G. K. Bhat, (2006) Current concepts in apoptosis: the physiological suicide program revisited. *Cellular & molecular biology letters* **11**: 506-525.

Christiansen, J. K., M. H. Larsen, H. Ingmer, L. Sogaard-Andersen & B. H. Kallipolitis, (2004) The RNA-binding protein Hfq of *Listeria monocytogenes*: role in stress tolerance and virulence. *Journal of bacteriology* **186**: 3355-3362.

Clarke, C. J. & Y. A. Hannun, (2006) Neutral sphingomyelinases and nSMase2: bridging the gaps. *Biochimica et biophysica acta* **1758**: 1893-1901.

Cohen, P., M. Bouaboula, M. Bellis, V. Baron, O. Jbilo, C. Poinot-Chazel, S. Galiegue, E. H. Hadibi & P. Casellas, (2000) Monitoring cellular responses to *Listeria monocytogenes* with oligonucleotide arrays. *The Journal of biological chemistry* **275**: 11181-11190.

Collins, M. D., S. Wallbanks, D. J. Lane, J. Shah, R. Nietupski, J. Smida, M. Dorsch & E. Stackebrandt, (1991) Phylogenetic analysis of the genus *Listeria* based on reverse transcriptase sequencing of 16S rRNA. *International journal of systematic bacteriology* **41**: 240-246.

Corr, S., C. Hill & C. G. Gahan, (2006) An *in vitro* cell-culture model demonstrates internalin- and hemolysin-independent translocation of *Listeria monocytogenes* across M cells. *Microbial pathogenesis* **41**: 241-250.

Corr, S. C. & L. A. O'Neill, (2009) *Listeria monocytogenes* infection in the face of innate immunity. *Cellular microbiology*.

Cossart, P., (2000a) Actin-based motility of pathogens: the Arp2/3 complex is a central player. *Cellular microbiology* **2**: 195-205.

Cossart, P., J. Pizarro-Cerda & M. Lecuit, (2003) Invasion of mammalian cells by *Listeria monocytogenes*: functional mimicry to subvert cellular functions. *Trends in cell biology* **13**: 23-31.

Cossart, P. & A. Toledo-Arana, (2008) *Listeria monocytogenes*, a unique model in infection biology: an overview. *Microbes and infection / Institut Pasteur* **10**: 1041-1050.

Cotter, P. D., L. A. Draper, E. M. Lawton, K. M. Daly, D. S. Groeger, P. G. Casey, R. P. Ross & C. Hill, (2008) Listeriolysin S, a novel peptide haemolysin associated with a subset of lineage I *Listeria monocytogenes*. *PLoS pathogens* **4**: e1000144.

Cotter, P. D., S. Ryan, C. G. Gahan & C. Hill, (2005) Presence of GadD1 glutamate decarboxylase in selected *Listeria monocytogenes* strains is associated with an ability to grow at low pH. *Applied and environmental microbiology* **71**: 2832-2839.

Danelishvili, L., J. McGarvey, Y. J. Li & L. E. Bermudez, (2003) *Mycobacterium tuberculosis* infection causes different levels of apoptosis and necrosis in human macrophages and alveolar epithelial cells. *Cellular microbiology* **5**: 649-660.

Dao, D. N., L. Kremer, Y. Guerardel, A. Molano, W. R. Jacobs, Jr., S. A. Porcelli & V. Briken, (2004) *Mycobacterium tuberculosis* lipomannan induces apoptosis and interleukin-12 production in macrophages. *Infection and immunity* **72**: 2067-2074.

de Valk, H., C. Jacquet, V. Goulet, V. Vaillant, A. Perra, F. Simon, J. C. Desenclos & P. Martin, (2005) Surveillance of *Listeria* infections in Europe. *Euro Surveill* **10**: 251-255.

DeLeo, F. R., (2004) Modulation of phagocyte apoptosis by bacterial pathogens. *Apoptosis* **9**: 399-413.

Diller, T. C., Madhusudan, N. H. Xuong & S. S. Taylor, (2001) Molecular basis for regulatory subunit diversity in cAMP-dependent protein kinase: crystal structure of the type II beta regulatory subunit. *Structure* **9**: 73-82.

Dockrell, D. H., (2001) Apoptotic cell death in the pathogenesis of infectious diseases. *The Journal of infection* **42**: 227-234.

Domann, E., J. Wehland, M. Rohde, S. Pistor, M. Hartl, W. Goebel, M. Leimeister-Wachter, M. Wuenscher & T. Chakraborty, (1992) A novel bacterial virulence gene in *Listeria monocytogenes* required for host cell microfilament interaction with homology to the proline-rich region of vinculin. *The EMBO journal* **11**: 1981-1990.

Dominguez-Bernal, G., S. Muller-Altrock, B. Gonzalez-Zorn, M. Scortti, P. Herrmann, H. J. Monzo, L. Lacharme, J. Kreft & J. A. Vazquez-Boland, (2006) A spontaneous genomic deletion in *Listeria ivanovii* identifies LIPI-2, a species-specific pathogenicity island encoding sphingomyelinase and numerous internalins. *Molecular microbiology* **59**: 415-432.

Doumith, M., C. Cazalet, N. Simoes, L. Frangeul, C. Jacquet, F. Kunst, P. Martin, P. Cossart, P. Glaser & C. Buchrieser, (2004) New aspects regarding evolution and virulence of *Listeria monocytogenes* revealed by comparative genomics and DNA arrays. *Infection and immunity* **72**: 1072-1083.

Dramsi, S., I. Biswas, E. Maguin, L. Braun, P. Mastroeni & P. Cossart, (1995) Entry of *Listeria monocytogenes* into hepatocytes requires expression of *inlB*, a surface protein of the internalin multigene family. *Molecular microbiology* **16**: 251-261.

Drevets, D. A., R. T. Sawyer, T. A. Potter & P. A. Campbell, (1995) *Listeria monocytogenes* infects human endothelial cells by two distinct mechanisms. *Infection and immunity* **63**: 4268-4276.

Duche, O., F. Tremoulet, P. Glaser & J. Labadie, (2002) Salt stress proteins induced in *Listeria monocytogenes*. *Applied and environmental microbiology* **68**: 1491-1498.

Dussurget, O., D. Cabanes, P. Dehoux, M. Lecuit, C. Buchrieser, P. Glaser & P. Cossart, (2002) *Listeria monocytogenes* bile salt hydrolase is a PrfA-regulated virulence factor involved in the intestinal and hepatic phases of listeriosis. *Molecular microbiology* **45**: 1095-1106.

Dussurget, O., J. Pizarro-Cerda & P. Cossart, (2004) Molecular determinants of *Listeria monocytogenes* virulence. *Annual review of microbiology* **58**: 587-610.

Eiting, M., G. Hageluken, W. D. Schubert & D. W. Heinz, (2005) The mutation G145S in PrfA, a key virulence regulator of *Listeria monocytogenes*, increases DNA-binding affinity by stabilizing the HTH motif. *Molecular microbiology* **56**: 433-446.

Engelbrecht, F., G. Dominguez-Bernal, J. Hess, C. Dickneite, L. Greiffenberg, R. Lampidis, D. Raffelsbauer, J. J. Daniels, J. Kreft, S. H. Kaufmann, J. A. Vazquez-Boland & W. Goebel, (1998) A novel PrfA-regulated chromosomal locus, which is specific for *Listeria ivanovii*, encodes two small, secreted internalins and contributes to virulence in mice. *Molecular microbiology* **30**: 405-417.

Ericsson, U. B., B. M. Hallberg, G. T. Detitta, N. Dekker & P. Nordlund, (2006) Thermofluor-based high-throughput stability optimization of proteins for structural studies. *Analytical biochemistry* **357**: 289-298.

Ermolaeva, S., S. Novella, Y. Vega, M. T. Ripio, M. Scortti & J. A. Vazquez-Boland, (2004) Negative control of *Listeria monocytogenes* virulence genes by a diffusible autorepressor. *Molecular microbiology* **52**: 601-611.

Esen, M., B. Schreiner, V. Jendrossek, F. Lang, K. Fassbender, H. Grassme & E. Gulbins, (2001) Mechanisms of *Staphylococcus aureus* induced apoptosis of human endothelial cells. *Apoptosis* **6**: 431-439.

Farber, J. M. & P. I. Peterkin, (1991) *Listeria monocytogenes,* a food-borne pathogen. *Microbiological reviews* **55**: 476-511.

Fenlon, D. R., (1999) *Listeria monocytogenes* in the natural environment. *In E. T. Ryser and E. H. Marth (ed.), Listeria, listeriosis and food safety, second ed. Marcel Dekker Inc., New York, N. Y.*: 21-37.

Ferreira, A., C. P. O'Byrne & K. J. Boor, (2001) Role of sigma(B) in heat, ethanol, acid, and oxidative stress resistance and during carbon starvation in *Listeria monocytogenes*. *Applied and environmental microbiology* **67**: 4454-4457.

Ferreira, A., D. Sue, C. P. O'Byrne & K. J. Boor, (2003) Role of *Listeria monocytogenes* sigma(B) in survival of lethal acidic conditions and in the acquired acid tolerance response. *Applied and environmental microbiology* **69**: 2692-2698.

Fettucciari, K., I. Fetriconi, R. Mannucci, I. Nicoletti, A. Bartoli, S. Coaccioli & P. Marconi, (2006) Group B *Streptococcus* induces macrophage apoptosis by calpain activation. *J Immunol* **176**: 7542-7556.

Fettucciari, K., E. Rosati, L. Scaringi, P. Cornacchione, G. Migliorati, R. Sabatini, I. Fetriconi, R. Rossi & P. Marconi, (2000) Group B *Streptococcus* induces apoptosis in macrophages. *J Immunol* **165**: 3923-3933.

Fiorentini, C., L. Falzano, S. Travaglione & A. Fabbri, (2003) Hijacking Rho GTPases by protein toxins and apoptosis: molecular strategies of pathogenic bacteria. *Cell death and differentiation* **10**: 147-152.

Fraser, K. R. & C. P. O'Byrne, (2002) Osmoprotection by carnitine in a *Listeria monocytogenes* mutant lacking the OpuC transporter: evidence for a low affinity carnitine uptake system. *FEMS microbiology letters* **211**: 189-194.

Fraser, K. R., D. Sue, M. Wiedmann, K. Boor & C. P. O'Byrne, (2003) Role of sigma B in regulating the compatible solute uptake systems of *Listeria monocytogenes:* osmotic induction of *opuC* is sigma B dependent. *Applied and environmental microbiology* **69**: 2015-2022.

Freitag, N. E., G. C. Port & M. D. Miner, (2009) *Listeria monocytogenes* - from saprophyte to intracellular pathogen. *Nature reviews* **7**: 623-628.

Freitag, N. E. & D. A. Portnoy, (1994) Dual promoters of the *Listeria monocytogenes prfA* transcriptional activator appear essential *in vitro* but are redundant *in vivo*. *Molecular microbiology* **12**: 845-853.

Freitag, N. E., L. Rong & D. A. Portnoy, (1993) Regulation of the *prfA* transcriptional activator of *Listeria monocytogenes*: multiple promoter elements contribute to intracellular growth and cell-to-cell spread. *Infection and immunity* **61**: 2537-2544.

Gahan, C. G. & C. Hill, (2005) Gastrointestinal phase of *Listeria monocytogenes* infection. *Journal of applied microbiology* **98**: 1345-1353.

Gandhi, M. & M. L. Chikindas, (2007) *Listeria*: A foodborne pathogen that knows how to survive. *International journal of food microbiology* **113**: 1-15.

Gao, L. & Y. Abu Kwaik, (2000) Hijacking of apoptotic pathways by bacterial pathogens. *Microbes and infection / Institut Pasteur* **2**: 1705-1719.

Garges, S. & S. Adhya, (1988) Cyclic AMP-induced conformational change of cyclic AMP receptor protein (CRP): intragenic suppressors of cyclic AMP-independent CRP mutations. *Journal of bacteriology* **170**: 1417-1422.

Garner, M. R., B. L. Njaa, M. Wiedmann & K. J. Boor, (2006) Sigma B contributes to *Listeria monocytogenes* gastrointestinal infection but not to systemic spread in the guinea pig infection model. *Infection and immunity* **74**: 876-886.

Geoffroy, C., J. L. Gaillard, J. E. Alouf & P. Berche, (1987) Purification, characterization, and toxicity of the sulfhydryl-activated hemolysin listeriolysin O from *Listeria monocytogenes*. *Infection and immunity* **55**: 1641-1646.

Gibson, U. E., C. A. Heid & P. M. Williams, (1996) A novel method for real time quantitative RT-PCR. *Genome research* **6**: 995-1001.

Gilot, P., A. Genicot & P. Andre, (1996) Serotyping and esterase typing for analysis of *Listeria monocytogenes* populations recovered from foodstuffs and from human patients with listeriosis in Belgium. *Journal of clinical microbiology* **34**: 1007-1010.

Glaser, P., L. Frangeul, C. Buchrieser, C. Rusniok, A. Amend, F. Baquero, P. Berche, H. Bloecker, P. Brandt, T. Chakraborty, A. Charbit, F. Chetouani, E. Couve, A. de Daruvar, P. Dehoux, E. Domann, G. Dominguez-Bernal, E. Duchaud, L. Durant, O. Dussurget, K. D. Entian, H. Fsihi, F. Garcia-del Portillo, P. Garrido, L. Gautier, W. Goebel, N. Gomez-Lopez, T. Hain, J. Hauf, D. Jackson, L. M. Jones, U. Kaerst, J. Kreft, M. Kuhn, F. Kunst, G. Kurapkat, E. Madueno, A. Maitournam, J. M. Vicente, E. Ng, H. Nedjari, G. Nordsiek, S. Novella, B. de Pablos, J. C. Perez-Diaz, R. Purcell, B. Remmel, M. Rose, T. Schlueter, N. Simoes, A. Tierrez, J. A. Vazquez-Boland, H. Voss, J. Wehland & P. Cossart, (2001) Comparative genomics of *Listeria* species. *Science (New York, N.Y* **294**: 849-852.

Goebel, W., J. Kreft & R. Bockmann, (2000) Regulation of virulence genes in pathogenic *Listeria*. *In V. A. Fischetti, et al. (ed.), Gram-positive pathogens. American Society for Microbiology, Washington, D. C.*: 499-506.

Goni, F. M. & A. Alonso, (2002) Sphingomyelinases: enzymology and membrane activity. *FEBS letters* **531**: 38-46.

Gonzalez-Pastor, J. E., E. C. Hobbs & R. Losick, (2003) Cannibalism by sporulating bacteria. *Science (New York, N.Y* **301**: 510-513.

Gonzalez-Zorn, B., G. Dominguez-Bernal, M. Suarez, M. T. Ripio, Y. Vega, S. Novella, A. Rodriguez, I. Chico, A. Tierrez & J. A. Vazquez-Boland, (2000) SmcL, a novel membrane-damaging virulence factor in *Listeria*. *Int J Med Microbiol* **290**: 369-374.

Gonzalez-Zorn, B., G. Dominguez-Bernal, M. Suarez, M. T. Ripio, Y. Vega, S. Novella & J. A. Vazquez-Boland, (1999) The *smcL* gene of *Listeria ivanovii* encodes a sphingomyelinase C that mediates bacterial escape from the phagocytic vacuole. *Molecular microbiology* **33**: 510-523.

Gouet, P., E. Courcelle, D. I. Stuart & F. Metoz, (1999) ESPript: analysis of multiple sequence alignments in PostScript. *Bioinformatics (Oxford, England)* **15**: 305-308.

Gouin, E., P. Dehoux, J. Mengaud, C. Kocks & P. Cossart, (1995) *iactA* of *Listeria ivanovii*, although distantly related to *Listeria monocytogenes actA*, restores actin tail formation in an *L. monocytogenes actA* mutant. *Infection and immunity* **63**: 2729-2737.

Goulet, V., H. de Valk, O. Pierre, F. Stainer, J. Rocourt, V. Vaillant, C. Jacquet & J. C. Desenclos, (2001) Effect of prevention measures on incidence of human listeriosis, France, 1987-1997. *Emerging infectious diseases* **7**: 983-989.

Goulet, V., C. Hedberg, A. Le Monnier & H. de Valk, (2008) Increasing incidence of listeriosis in France and other European countries. *Emerging infectious diseases* **14**: 734-740.

Grassme, H., V. Jendrossek & E. Gulbins, (2001) Molecular mechanisms of bacteria induced apoptosis. *Apoptosis* **6**: 441-445.

Grassme, H., V. Jendrossek, A. Riehle, G. von Kurthy, J. Berger, H. Schwarz, M. Weller, R. Kolesnick & E. Gulbins, (2003) Host defense against *Pseudomonas aeruginosa* requires ceramide-rich membrane rafts. *Nature medicine* **9**: 322-330.

Gravany, R., (1999) Incidence and control of *Listeria* in food-processing facilities. *In E. T. Ryser and E. H. Marth (ed.), Listeria, listeriosis and food safety, second ed. Marcel Dekker Inc., New York, N. Y.*: 657-709.

Graves, L. M., L. O. Helsel, A. G. Steigerwalt, R. E. Morey, M. I. Daneshvar, S. E. Roof, R. H. Orsi, E. D. Fortes, S. R. Milillo, H. C. den Bakker, M. Wiedmann, B. Swaminathan & B. D. Sauders, (2009) *Listeria marthii* sp. nov., isolated from the natural environment, Finger Lakes National Forest. *International journal of systematic and evolutionary microbiology*.

Gray, M. J., N. E. Freitag & K. J. Boor, (2006) How the bacterial pathogen *Listeria monocytogenes* mediates the switch from environmental Dr. Jekyll to pathogenic Mr. Hyde. *Infection and immunity* **74**: 2505-2512.

Gray, M. J., R. N. Zadoks, E. D. Fortes, B. Dogan, S. Cai, Y. Chen, V. N. Scott, D. E. Gombas, K. J. Boor & M. Wiedmann, (2004) *Listeria monocytogenes* isolates from foods and humans form distinct but overlapping populations. *Applied and environmental microbiology* **70**: 5833-5841.

Green, J., C. Scott & J. R. Guest, (2001) Functional versatility in the CRP-FNR superfamily of transcription factors: FNR and FLP. *Advances in microbial physiology* **44**: 1-34.

Griner, E. M. & M. G. Kazanietz, (2007) Protein kinase C and other diacylglycerol effectors in cancer. *Nat Rev Cancer* **7**: 281-294.

Grundling, A., L. S. Burrack, H. G. Bouwer & D. E. Higgins, (2004) *Listeria monocytogenes* regulates flagellar motility gene expression through MogR, a transcriptional repressor required for virulence. *Proceedings of the National Academy of Sciences of the United States of America* **101**: 12318-12323.

Guillet, C., O. Join-Lambert, A. L. Monnier, A. Leclercq, F. Mechai, M. F. Mamzer-Bruneel, M. K. Bielecka, M. Scortti, O. Disson, P. Berche, J. Vazquez-Boland, O. Lortholary & M. Lecuit, (2010) Human listeriosis caused by *Listeria ivanovii*. *Emerging infectious diseases* **16**: 136-138.

Gulbins, E., (2003) Regulation of death receptor signaling and apoptosis by ceramide. *Pharmacol Res* **47**: 393-399.

Gulbins, E., A. Jekle, K. Ferlinz, H. Grassme & F. Lang, (2000) Physiology of apoptosis. *American journal of physiology* **279**: F605-615.

Guzman, C. A., E. Domann, M. Rohde, D. Bruder, A. Darji, S. Weiss, J. Wehland, T. Chakraborty & K. N. Timmis, (1996) Apoptosis of mouse dendritic cells is triggered by listeriolysin, the major virulence determinant of *Listeria monocytogenes*. *Molecular microbiology* **20**: 119-126.

Hain, T., H. Hossain, S. S. Chatterjee, S. Machata, U. Volk, S. Wagner, B. Brors, S. Haas, C. T. Kuenne, A. Billion, S. Otten, J. Pane-Farre, S. Engelmann & T. Chakraborty, (2008) Temporal transcriptomic analysis of the *Listeria monocytogenes* EGD-e sigma B regulon. *BMC microbiology* **8**: 20.

Haldenwang, W. G. & R. Losick, (1979) A modified RNA polymerase transcribes a cloned gene under sporulation control in *Bacillus subtilis*. *Nature* **282**: 256-260.

Haldenwang, W. G. & R. Losick, (1980) Novel RNA polymerase sigma factor from *Bacillus subtilis*. *Proceedings of the National Academy of Sciences of the United States of America* **77**: 7000-7004.

Hamon, M., H. Bierne & P. Cossart, (2006) *Listeria monocytogenes*: a multifaceted model. *Nature reviews* **4**: 423-434.

Hannun, Y. A. & C. Luberto, (2000) Ceramide in the eukaryotic stress response. *Trends in cell biology* **10**: 73-80.

Hannun, Y. A. & L. M. Obeid, (2002) The Ceramide-centric universe of lipid-mediated cell regulation: stress encounters of the lipid kind. *The Journal of biological chemistry* **277**: 25847-25850.

Harman, J. G., (2001) Allosteric regulation of the cAMP receptor protein. *Biochimica et biophysica acta* **1547**: 1-17.

Haslinger, B., K. Strangfeld, G. Peters, K. Schulze-Osthoff & B. Sinha, (2003) *Staphylococcus aureus* alpha-toxin induces apoptosis in peripheral blood mononuclear cells: role of endogenous tumour necrosis factor-alpha and the mitochondrial death pathway. *Cellular microbiology* **5**: 729-741.

Haslinger-Loffler, B., B. C. Kahl, M. Grundmeier, K. Strangfeld, B. Wagner, U. Fischer, A. L. Cheung, G. Peters, K. Schulze-Osthoff & B. Sinha, (2005) Multiple virulence factors are required for *Staphylococcus aureus*-induced apoptosis in endothelial cells. *Cellular microbiology* **7**: 1087-1097.

Hasnain, S. E., R. Begum, K. V. Ramaiah, S. Sahdev, E. M. Shajil, T. K. Taneja, M. Mohan, M. Athar, N. K. Sah & M. Krishnaveni, (2003) Host-pathogen interactions during apoptosis. *Journal of biosciences* **28**: 349-358.

Hecker, M., J. Pane-Farre & U. Volker, (2007) SigB-dependent general stress response in *Bacillus subtilis* and related gram-positive bacteria. *Annual review of microbiology* **61**: 215-236.

Heid, C. A., J. Stevens, K. J. Livak & P. M. Williams, (1996) Real time quantitative PCR. *Genome research* **6**: 986-994.

Held, M., A. Schmid, H. P. Kohler, W. Suske, B. Witholt & M. G. Wubbolts, (1999) An integrated process for the production of toxic catechols from toxic phenols based on a designer biocatalyst. *Biotechnology and bioengineering* **62**: 641-648.

Herler, M., A. Bubert, M. Goetz, Y. Vega, J. A. Vazquez-Boland & W. Goebel, (2001) Positive selection of mutations leading to loss or reduction of transcriptional activity of PrfA, the central regulator of *Listeria monocytogenes* virulence. *Journal of bacteriology* **183**: 5562-5570.

Herro, R., S. Poncet, P. Cossart, C. Buchrieser, E. Gouin, P. Glaser & J. Deutscher, (2005) How seryl-phosphorylated HPr inhibits PrfA, a transcription activator of *Listeria monocytogenes* virulence genes. *Journal of molecular microbiology and biotechnology* **9**: 224-234.

Ho, S. N., H. D. Hunt, R. M. Horton, J. K. Pullen & L. R. Pease, (1989) Site-directed mutagenesis by overlap extension using the polymerase chain reaction. *Gene* **77**: 51-59.

Hooft, R. W., G. Vriend, C. Sander & E. E. Abola, (1996) Errors in protein structures. *Nature* **381**: 272.

Hsu, L. C., J. M. Park, K. Zhang, J. L. Luo, S. Maeda, R. J. Kaufman, L. Eckmann, D. G. Guiney & M. Karin, (2004) The protein kinase PKR is required for macrophage apoptosis after activation of Toll-like receptor 4. *Nature* **428**: 341-345.

Huang, Y., M. J. Lemieux, J. Song, M. Auer & D. N. Wang, (2003) Structure and mechanism of the glycerol-3-phosphate transporter from *Escherichia coli*. *Science (New York, N.Y* **301**: 616-620.

Hueffer, K. & J. E. Galan, (2004) *Salmonella*-induced macrophage death: multiple mechanisms, different outcomes. *Cellular microbiology* **6**: 1019-1025.

Huggett, J., K. Dheda, S. Bustin & A. Zumla, (2005) Real-time RT-PCR normalisation; strategies and considerations. *Genes and immunity* **6**: 279-284.

Ireton, K. & P. Cossart, (1997) Host-pathogen interactions during entry and actin-based movement of *Listeria monocytogenes*. *Annual review of genetics* **31**: 113-138.

Jain, M., S. Kumar, R. Upadhyay, P. Lal, A. Tiwari, U. C. Ghoshal & B. Mittal, (2007) Influence of apoptosis (BCL2, FAS), cell cycle (CCND1) and growth factor (EGF, EGFR) genetic polymorphisms on survival outcome: an exploratory study in squamous cell esophageal cancer. *Cancer biology & therapy* **6**: 1553-1558.

Jeffers, G. T., J. L. Bruce, P. L. McDonough, J. Scarlett, K. J. Boor & M. Wiedmann, (2001) Comparative genetic characterization of *Listeria monocytogenes* isolates from human and animal listeriosis cases. *Microbiology (Reading, England)* **147**: 1095-1104.

Jensen, V. B., J. T. Harty & B. D. Jones, (1998) Interactions of the invasive pathogens *Salmonella typhimurium*, *Listeria monocytogenes*, and *Shigella flexneri* with M cells and murine Peyer's patches. *Infection and immunity* **66**: 3758-3766.

Johansson, J., P. Mandin, A. Renzoni, C. Chiaruttini, M. Springer & P. Cossart, (2002) An RNA thermosensor controls expression of virulence genes in *Listeria monocytogenes*. *Cell* **110**: 551-561.

Jones, D., (1991) Foodborne listeriosis *In: Waites, W. M. Arbuthnott, J., (Eds.) Foodborne illness. Edward Arnold, London, UK*: 68-76.

Jones, D. & H. P. R. Seeliger, (1983) Designation of a New Type Strain for *Listeria monocytogenes.* Request for an Opinion. *International Journal od Systematic Bacteriology*: 429.

Jones, S. & J. M. Thornton, (1996) Principles of protein-protein interactions. *Proceedings of the National Academy of Sciences of the United States of America* **93**: 13-20.

Joseph, B., K. Przybilla, C. Stuhler, K. Schauer, J. Slaghuis, T. M. Fuchs & W. Goebel, (2006) Identification of *Listeria monocytogenes* genes contributing to intracellular replication by expression profiling and mutant screening. *Journal of bacteriology* **188**: 556-568.

Kadner, R. J., C. A. Webber & M. D. Island, (1993) The family of organo-phosphate transport proteins includes a transmembrane regulatory protein. *Journal of bioenergetics and biomembranes* **25**: 637-645.

Kannan, N., J. Wu, G. S. Anand, S. Yooseph, A. F. Neuwald, J. C. Venter & S. S. Taylor, (2007) Evolution of allostery in the cyclic nucleotide binding module. *Genome biology* **8**: R264.

Karge, W. H., 3rd, E. J. Schaefer & J. M. Ordovas, (1998) Quantification of mRNA by polymerase chain reaction (PCR) using an internal standard and a nonradioactive detection method. *Methods in molecular biology (Clifton, N.J* **110**: 43-61.

Karunasagar, I., R. Lampidis, W. Goebel & J. Kreft, (1997) Complementation of *Listeria seeligeri* with the *plcA-prfA* genes from *L. monocytogenes* activates transcription of seeligerolysin and leads to bacterial escape from the phagosome of infected mammalian cells. *FEMS microbiology letters* **146**: 303-310.

Kathariou, S. & L. Pine, (1991) The type strain(s) of *Listeria monocytogenes*: a source of continuing difficulties. *International journal of systematic bacteriology* **41**: 328-330.

Kazmierczak, M. J., S. C. Mithoe, K. J. Boor & M. Wiedmann, (2003) *Listeria monocytogenes* sigma B regulates stress response and virulence functions. *Journal of bacteriology* **185**: 5722-5734.

Kazmierczak, M. J., M. Wiedmann & K. J. Boor, (2005) Alternative sigma factors and their roles in bacterial virulence. *Microbiol Mol Biol Rev* **69**: 527-543.

Kazmierczak, M. J., M. Wiedmann & K. J. Boor, (2006) Contributions of *Listeria monocytogenes* sigma B and PrfA to expression of virulence and stress response genes during extra- and intracellular growth. *Microbiology (Reading, England)* **152**: 1827-1838.

Kerr, J. F., A. H. Wyllie & A. R. Currie, (1972) Apoptosis: a basic biological phenomenon with wide-ranging implications in tissue kinetics. *British journal of cancer* **26**: 239-257.

Kim, H., K. J. Boor & H. Marquis, (2004) *Listeria monocytogenes* sigma B contributes to invasion of human intestinal epithelial cells. *Infection and immunity* **72**: 7374-7378.

Kim, H., H. Marquis & K. J. Boor, (2005) Sigma B contributes to *Listeria monocytogenes* invasion by controlling expression of *inlA* and *inlB*. *Microbiology (Reading, England)* **151**: 3215-3222.

Kobayashi, S. D., K. R. Braughton, A. R. Whitney, J. M. Voyich, T. G. Schwan, J. M. Musser & F. R. DeLeo, (2003) Bacterial pathogens modulate an apoptosis differentiation program in human neutrophils. *Proceedings of the National Academy of Sciences of the United States of America* **100**: 10948-10953.

Kocks, C., E. Gouin, M. Tabouret, P. Berche, H. Ohayon & P. Cossart, (1992) *L. monocytogenes*-induced actin assembly requires the *actA* gene product, a surface protein. *Cell* **68**: 521-531.

Kohler, C., S. Orrenius & B. Zhivotovsky, (2002) Evaluation of caspase activity in apoptotic cells. *Journal of immunological methods* **265**: 97-110.

Kolb, A., S. Busby, H. Buc, S. Garges & S. Adhya, (1993) Transcriptional regulation by cAMP and its receptor protein. *Annual review of biochemistry* **62**: 749-795.

Kolesnick, R. N. & M. Kronke, (1998) Regulation of ceramide production and apoptosis. *Annual review of physiology* **60**: 643-665.

Koopman, G., C. P. Reutelingsperger, G. A. Kuijten, R. M. Keehnen, S. T. Pals & M. H. van Oers, (1994) Annexin V for flow cytometric detection of phosphatidylserine expression on B cells undergoing apoptosis. *Blood* **84**: 1415-1420.

Kornev, A. P., S. S. Taylor & L. F. Ten Eyck, (2008) A generalized allosteric mechanism for cis-regulated cyclic nucleotide binding domains. *PLoS computational biology* **4**: e1000056.

Kreft, J., M. Dumbsky & S. Theiss, (1995) The actin-polymerization protein from *Listeria ivanovii* is a large repeat protein which shows only limited amino acid sequence homology to ActA from *Listeria monocytogenes*. *FEMS microbiology letters* **132**: 181-182.

Kreft, J. & J. A. Vazquez-Boland, (2001) Regulation of virulence genes in *Listeria*. *Int J Med Microbiol* **291**: 145-157.

Kuhn, M. & W. Goebel, (2000) Internalization of *Listeria monocytogenes* by nonprofessional and professional phagocytes. *Sub-cellular biochemistry* **33**: 411-436.

Kuo, C. F., J. J. Wu, P. J. Tsai, F. J. Kao, H. Y. Lei, M. T. Lin & Y. S. Lin, (1999) Streptococcal pyrogenic exotoxin B induces apoptosis and reduces phagocytic activity in U937 cells. *Infection and immunity* **67**: 126-130.

Lalic-Multhaler, M., J. Bohne & W. Goebel, (2001) *In vitro* transcription of PrfA-dependent and -independent genes of *Listeria monocytogenes*. *Molecular microbiology* **42**: 111-120.

Laskowski, R. A., (1995) SURFNET: a program for visualizing molecular surfaces, cavities, and intermolecular interactions. *Journal of molecular graphics* **13**: 323-330, 307-328.

Laskowski, R. A., M. W. MacArthur, D. S. Moss & J. M. Thornton, (1993) PROCHECK: a program to check the stereochemical quality of protein structures. *J Appl Cryst* **26**: 283-291.

Lauer, P., M. Y. Chow, M. J. Loessner, D. A. Portnoy & R. Calendar, (2002) Construction, characterization, and use of two *Listeria monocytogenes* site-specific phage integration vectors. *Journal of bacteriology* **184**: 4177-4186.

Lebowitz, J., M. S. Lewis & P. Schuck, (2002) Modern analytical ultracentrifugation in protein science: a tutorial review. *Protein Sci* **11**: 2067-2079.

Leclercq, A., D. Clermont, C. Bizet, P. A. Grimont, A. Le Fleche-Mateos, S. M. Roche, C. Buchrieser, V. Cadet-Daniel, A. Le Monnier, M. Lecuit & F. Allerberger, (2009) *Listeria rocourtiae* sp. nov. *International journal of systematic and evolutionary microbiology*.

Lecoeur, H., (2002) Nuclear apoptosis detection by flow cytometry: influence of endogenous endonucleases. *Experimental cell research* **277**: 1-14.

Lecuit, M., (2007) Human listeriosis and animal models. *Microbes and infection / Institut Pasteur* **9**: 1216-1225.

Lecuit, M., S. Dramsi, C. Gottardi, M. Fedor-Chaiken, B. Gumbiner & P. Cossart, (1999) A single amino acid in E-cadherin responsible for host specificity towards the human pathogen *Listeria monocytogenes*. *The EMBO journal* **18**: 3956-3963.

Lecuit, M., S. Vandormael-Pournin, J. Lefort, M. Huerre, P. Gounon, C. Dupuy, C. Babinet & P. Cossart, (2001) A transgenic model for listeriosis: role of internalin in crossing the intestinal barrier. *Science (New York, N.Y* **292**: 1722-1725.

Lee, E. J., J. Glasgow, S. F. Leu, A. O. Belduz & J. G. Harman, (1994) Mutagenesis of the cyclic AMP receptor protein of *Escherichia coli*: targeting positions 83, 127 and 128 of the cyclic nucleotide binding pocket. *Nucleic acids research* **22**: 2894-2901.

Lee, J., H. G. Remold, M. H. Ieong & H. Kornfeld, (2006) Macrophage apoptosis in response to high intracellular burden of *Mycobacterium tuberculosis* is mediated by a novel caspase-independent pathway. *J Immunol* **176**: 4267-4274.

Leighton, I., D. R. Threlfall & C. L. Oakley, (1975) Phospholipase C activity in culture filtrates from *Listeria monocytogenes*. *In M. Woodbine (ed.), Problems of listeriosis. Leicester University Press, Leicester, England*: 239-241.

Lemieux, M. J., Y. Huang & D. N. Wang, (2004) The structural basis of substrate translocation by the *Escherichia coli* glycerol-3-phosphate transporter: a member of the major facilitator superfamily. *Current opinion in structural biology* **14**: 405-412.

Lemon, K. P., N. E. Freitag & R. Kolter, (2010) The virulence regulator PrfA promotes biofilm formation by *Listeria monocytogenes*. *Journal of bacteriology*.

Leu, S. F., C. H. Baker, E. J. Lee & J. G. Harman, (1999) Position 127 amino acid substitutions affect the formation of CRP:cAMP:lacP complexes but not CRP:cAMP:RNA polymerase complexes at lacP. *Biochemistry* **38**: 6222-6230.

Levade, T., S. Malagarie-Cazenave, V. Gouaze, B. Segui, C. Tardy, S. Betito, N. Andrieu-Abadie & O. Cuvillier, (2002) Ceramide in apoptosis: a revisited role. *Neurochemical research* **27**: 601-607.

Li, P., D. Nijhawan, I. Budihardjo, S. M. Srinivasula, M. Ahmad, E. S. Alnemri & X. Wang, (1997) Cytochrome c and dATP-dependent formation of Apaf-1/caspase-9 complex initiates an apoptotic protease cascade. *Cell* **91**: 479-489.

Lin, C. F., C. L. Chen & Y. S. Lin, (2006) Ceramide in apoptotic signaling and anticancer therapy. *Current medicinal chemistry* **13**: 1609-1616.

Lingnau, A., E. Domann, M. Hudel, M. Bock, T. Nichterlein, J. Wehland & T. Chakraborty, (1995) Expression of the *Listeria monocytogenes* EGD *inlA* and *inlB* genes, whose products mediate bacterial entry into tissue culture cell

lines, by PrfA-dependent and -independent mechanisms. *Infection and immunity* **63**: 3896-3903.

Liu, D., (2006a) Identification, subtyping and virulence determination of *Listeria monocytogenes*, an important foodborne pathogen. *Journal of medical microbiology* **55**: 645-659.

Liu, D., M. L. Lawrence, L. Gorski, R. E. Mandrell, A. J. Ainsworth & F. W. Austin, (2006b) *Listeria monocytogenes* serotype 4b strains belonging to lineages I and III possess distinct molecular features. *Journal of clinical microbiology* **44**: 214-217.

Liu, S., J. E. Graham, L. Bigelow, P. D. Morse, 2nd & B. J. Wilkinson, (2002) Identification of *Listeria monocytogenes* genes expressed in response to growth at low temperature. *Applied and environmental microbiology* **68**: 1697-1705.

Lo, M. C., A. Aulabaugh, G. Jin, R. Cowling, J. Bard, M. Malamas & G. Ellestad, (2004) Evaluation of fluorescence-based thermal shift assays for hit identification in drug discovery. *Analytical biochemistry* **332**: 153-159.

Luberto, C., J. M. Kraveka & Y. A. Hannun, (2002) Ceramide regulation of apoptosis versus differentiation: a walk on a fine line. Lessons from neurobiology. *Neurochemical research* **27**: 609-617.

Luthy, R., J. U. Bowie & D. Eisenberg, (1992) Assessment of protein models with three-dimensional profiles. *Nature* **356**: 83-85.

Lynch, M., J. Painter, R. Woodruff & C. Braden, (2006) Surveillance for foodborne-disease outbreaks--United States, 1998-2002. *MMWR Surveill Summ* **55**: 1-42.

Mannering, S. I., J. Zhong & C. Cheers, (2002) T-cell activation, proliferation and apoptosis in primary *Listeria monocytogenes* infection. *Immunology* **106**: 87-95.

Maria, S. S., B. C. Vidal & M. L. Mello, (2000) Image analysis of DNA fragmentation and loss in V79 cells under apoptosis. *Gen. Mol. Biol.* **23**: 109-112.

Marr, A. K., B. Joseph, S. Mertins, R. Ecke, S. Muller-Altrock & W. Goebel, (2006) Overexpression of PrfA leads to growth inhibition of *Listeria monocytogenes* in glucose-containing culture media by interfering with glucose uptake. *Journal of bacteriology* **188**: 3887-3901.

Marriott, H. M., F. Ali, R. C. Read, T. J. Mitchell, M. K. Whyte & D. H. Dockrell, (2004) Nitric oxide levels regulate macrophage commitment to apoptosis or necrosis during pneumococcal infection. *Faseb J* **18**: 1126-1128.

Mauder, N., R. Ecke, S. Mertins, D. I. Loeffler, G. Seidel, M. Sprehe, W. Hillen, W. Goebel & S. Muller-Altrock, (2006) Species-specific differences in the activity of PrfA, the key regulator of listerial virulence genes. *Journal of bacteriology* **188**: 7941-7956.

McCarthy, S. A., (1990) *Listeria* in the environment. *In A. J. Miller, J. L. Smith and G. A. Somkuti (ed.), Foodborne listeriosis. Elsevier, New York, N. Y.*: 25-29.

McGann, P., S. Raengpradub, R. Ivanek, M. Wiedmann & K. J. Boor, (2008) Differential regulation of *Listeria monocytogenes* internalin and internalin-like genes by Sigma B and PrfA as revealed by subgenomic microarray analyses. *Foodborne pathogens and disease* **5**: 417-435.

McGann, P., M. Wiedmann & K. J. Boor, (2007) The alternative sigma factor sigma B and the virulence gene regulator PrfA both regulate transcription of *Listeria monocytogenes* internalins. *Applied and environmental microbiology* **73**: 2919-2930.

McLauchlin, J., (1987) *Listeria monocytogenes*, recent advances in the taxonomy and epidemiology of listeriosis in humans. *The Journal of applied bacteriology* **63**: 1-11.

Menaker, R. J., P. J. Ceponis & N. L. Jones, (2004) *Helicobacter pylori* induces apoptosis of macrophages in association with alterations in the mitochondrial pathway. *Infection and immunity* **72**: 2889-2898.

Mengaud, J., S. Dramsi, E. Gouin, J. A. Vazquez-Boland, G. Milon & P. Cossart, (1991) Pleiotropic control of *Listeria monocytogenes* virulence factors by a gene that is autoregulated. *Molecular microbiology* **5**: 2273-2283.

Menzies, B. E. & I. Kourteva, (2000) *Staphylococcus aureus* alpha-toxin induces apoptosis in endothelial cells. *FEMS immunology and medical microbiology* **29**: 39-45.

Miguel, R. N., (2004) Sequence patterns derived from the automated prediction of functional residues in structurally-aligned homologous protein families. *Bioinformatics (Oxford, England)* **20**: 2380-2389.

Milenbachs, A. A., D. P. Brown, M. Moors & P. Youngman, (1997) Carbon-source regulation of virulence gene expression in *Listeria monocytogenes*. *Molecular microbiology* **23**: 1075-1085.

Milenbachs Lukowiak, A., K. J. Mueller, N. E. Freitag & P. Youngman, (2004) Deregulation of *Listeria monocytogenes* virulence gene expression by two distinct and semi-independent pathways. *Microbiology (Reading, England)* **150**: 321-333.

Milohanic, E., P. Glaser, J. Y. Coppee, L. Frangeul, Y. Vega, J. A. Vazquez-Boland, F. Kunst, P. Cossart & C. Buchrieser, (2003) Transcriptome analysis of *Listeria monocytogenes* identifies three groups of genes differently regulated by PrfA. *Molecular microbiology* **47**: 1613-1625.

Miner, M. D., G. C. Port & N. E. Freitag, (2008b) Functional impact of mutational activation on the *Listeria monocytogenes* central virulence regulator PrfA. *Microbiology (Reading, England)* **154**: 3579-3589.

Mizuguchi, K., C. M. Deane, T. L. Blundell, M. S. Johnson & J. P. Overington, (1998) JOY: protein sequence-structure representation and analysis. *Bioinformatics (Oxford, England)* **14**: 617-623.

Monk, I. R., C. G. Gahan & C. Hill, (2008) Tools for functional postgenomic analysis of *Listeria monocytogenes*. *Applied and environmental microbiology* **74**: 3921-3934.

Moorhead, S. M. & G. A. Dykes, (2003) The role of the *sigB* gene in the general stress response of *Listeria monocytogenes* varies between a strain of serotype 1/2a and a strain of serotype 4c. *Current microbiology* **46**: 461-466.

Moorhead, S. M. & G. A. Dykes, (2004) Influence of the *sigB* gene on the cold stress survival and subsequent recovery of two *Listeria monocytogenes* serotypes. *International journal of food microbiology* **91**: 63-72.

Moors, M. A., B. Levitt, P. Youngman & D. A. Portnoy, (1999) Expression of listeriolysin O and ActA by intracellular and extracellular *Listeria monocytogenes*. *Infection and immunity* **67**: 131-139.

Mostowy, S. & P. Cossart, (2009) Cytoskeleton rearrangements during *Listeria* infection: clathrin and septins as new players in the game. *Cell motility and the cytoskeleton* **66**: 816-823.

Murray, E. G. D., R. A. Webb & S. M. B. R., (1926) A disease of rabbits characterized by a large mononuclear leukocytosis, caused by a hitherto undescribed bacillus *Bacterium monocytogenes*. *j. Pathol. Bacteriol.* **29**: 407-439.

Nadon, C. A., B. M. Bowen, M. Wiedmann & K. J. Boor, (2002) Sigma B contributes to PrfA-mediated virulence in *Listeria monocytogenes*. *Infection and immunity* **70**: 3948-3952.

Nakagawa, I., M. Nakata, S. Kawabata & S. Hamada, (2004) Transcriptome analysis and gene expression profiles of early apoptosis-related genes in *Streptococcus pyogenes*-infected epithelial cells. *Cellular microbiology* **6**: 939-952.

Navarre, W. W. & A. Zychlinsky, (2000) Pathogen-induced apoptosis of macrophages: a common end for different pathogenic strategies. *Cellular microbiology* **2**: 265-273.

Navas, J., B. Gonzalez-Zorn, N. Ladron, P. Garrido & J. A. Vazquez-Boland, (2001) Identification and mutagenesis by allelic exchange of choE, encoding a cholesterol oxidase from the intracellular pathogen *Rhodococcus equi*. *Journal of bacteriology* **183**: 4796-4805.

Nelson, K. E., D. E. Fouts, E. F. Mongodin, J. Ravel, R. T. DeBoy, J. F. Kolonay, D. A. Rasko, S. V. Angiuoli, S. R. Gill, I. T. Paulsen, J. Peterson, O. White, W. C. Nelson, W. Nierman, M. J. Beanan, L. M. Brinkac, S. C. Daugherty, R. J. Dodson, A. S. Durkin, R. Madupu, D. H. Haft, J. Selengut, S. Van Aken, H. Khouri, N. Fedorova, H. Forberger, B. Tran, S. Kathariou, L. D. Wonderling, G. A. Uhlich, D. O. Bayles, J. B. Luchansky & C. M. Fraser, (2004) Whole genome comparisons of serotype 4b and 1/2a strains of the food-borne pathogen *Listeria monocytogenes* reveal new insights into the core genome components of this species. *Nucleic acids research* **32**: 2386-2395.

Nicoletti, I., G. Migliorati, M. C. Pagliacci, F. Grignani & C. Riccardi, (1991) A rapid and simple method for measuring thymocyte apoptosis by propidium iodide staining and flow cytometry. *Journal of immunological methods* **139**: 271-279.

Nordlie, R. C., J. D. Foster & A. J. Lange, (1999) Regulation of glucose production by the liver. *Annual review of nutrition* **19**: 379-406.

Nyflet, A., (1929) Etilogie de la mononucleose infectieuse. *C. R. Soc. Biol.* **101**: 590-591.

O'Byrne, C. P. & I. R. Booth, (2002) Osmoregulation and its importance to food-borne microorganisms. *International journal of food microbiology* **74**: 203-216.

Ogawa, M. & C. Sasakawa, (2006) Intracellular survival of *Shigella*. *Cellular microbiology* **8**: 177-184.

Ojcius, D. M., P. Souque, J. L. Perfettini & A. Dautry-Varsat, (1998) Apoptosis of epithelial cells and macrophages due to infection with the obligate intracellular pathogen *Chlamydia psittaci*. *J Immunol* **161**: 4220-4226.

Ojeniyi, B., H. C. Wegener, N. E. Jensen & M. Bisgaard, (1996) *Listeria monocytogenes* in poultry and poultry products: epidemiological

investigations in seven Danish abattoirs. *The Journal of applied bacteriology* **80**: 395-401.

Okada, Y., N. Okada, S. Makino, H. Asakura, S. Yamamoto & S. Igimi, (2006) The *sigma* factor RpoN (Sigma54) is involved in osmotolerance in *Listeria monocytogenes*. *FEMS microbiology letters* **263**: 54-60.

Ollinger, J., M. Wiedmann & K. J. Boor, (2008) Sigma B- and PrfA-dependent transcription of genes previously classified as putative constituents of the *Listeria monocytogenes* PrfA regulon. *Foodborne pathogens and disease* **5**: 281-293.

Openshaw, A. E., P. R. Race, H. J. Monzo, J. A. Vazquez-Boland & M. J. Banfield, (2005) Crystal structure of SmcL, a bacterial neutral sphingomyelinase C from *Listeria*. *The Journal of biological chemistry* **280**: 35011-35017.

Pallardy, M., M. Perrin-Wolff & A. Biola, (1997) Cellular stress and apoptosis. *Toxicology in vitro* **11**: 573-578

Palmer, M. E., M. Wiedmann & K. J. Boor, (2009) sigma(B) and sigma(L) Contribute to *Listeria monocytogenes* 10403S Response to the Antimicrobial Peptides SdpC and Nisin. *Foodborne pathogens and disease*.

Pantoliano, M. W., E. C. Petrella, J. D. Kwasnoski, V. S. Lobanov, J. Myslik, E. Graf, T. Carver, E. Asel, B. A. Springer, P. Lane & F. R. Salemme, (2001) High-density miniaturized thermal shift assays as a general strategy for drug discovery. *J Biomol Screen* **6**: 429-440.

Parida, S. K., E. Domann, M. Rohde, S. Muller, A. Darji, T. Hain, J. Wehland & T. Chakraborty, (1998) Internalin B is essential for adhesion and mediates the invasion of *Listeria monocytogenes* into human endothelial cells. *Molecular microbiology* **28**: 81-93.

Park, S. F., (1994) The repression of listeriolysin O expression in *Listeria monocytogenes* by the phenolic beta-D-glucoside, arbutin. *Letters in applied microbiology* **19**: 258-260.

Park, S. F. & R. G. Kroll, (1993) Expression of listeriolysin and phosphatidylinositol-specific phospholipase C is repressed by the plant-derived molecule cellobiose in *Listeria monocytogenes*. *Molecular microbiology* **8**: 653-661.

Parra, M. C., F. Baquero & J. C. Perez-Diaz, (2008) The role of apoptosis in *Listeria monocytogenes* neural infection: listeriolysin O interaction with neuroblastoma Neuro-2a cells. *Infect Genet Evol* **8**: 59-67.

Passner, J. M., S. C. Schultz & T. A. Steitz, (2000) Modeling the cAMP-induced allosteric transition using the crystal structure of CAP-cAMP at 2.1 A resolution. *Journal of molecular biology* **304**: 847-859.

Petersohn, A., M. Brigulla, S. Haas, J. D. Hoheisel, U. Volker & M. Hecker, (2001) Global analysis of the general stress response of *Bacillus subtilis*. *Journal of bacteriology* **183**: 5617-5631.

Petrek, M., M. Otyepka, P. Banas, P. Kosinova, J. Koca & J. Damborsky, (2006) CAVER: a new tool to explore routes from protein clefts, pockets and cavities. *BMC bioinformatics* **7**: 316.

Pettus, B. J., C. E. Chalfant & Y. A. Hannun, (2002) Ceramide in apoptosis: an overview and current perspectives. *Biochimica et biophysica acta* **1585**: 114-125.

Phan-Thanh, L. & T. Gormon, (1997) A chemically defined minimal medium for the optimal culture of *Listeria*. *International journal of food microbiology* **35**: 91-95.

Piffaretti, J. C., H. Kressebuch, M. Aeschbacher, J. Bille, E. Bannerman, J. M. Musser, R. K. Selander & J. Rocourt, (1989) Genetic characterization of clones of the bacterium *Listeria monocytogenes* causing epidemic disease. *Proceedings of the National Academy of Sciences of the United States of America* **86**: 3818-3822.

Pirie, J. H. H., (1940) *Listeria*: change of name for a genus of bacteria. *Nature* **154**: 264.

Popov, S. G., R. Villasmil, J. Bernardi, E. Grene, J. Cardwell, T. Popova, A. Wu, D. Alibek, C. Bailey & K. Alibek, (2002b) Effect of *Bacillus anthracis* lethal toxin on human peripheral blood mononuclear cells. *FEBS letters* **527**: 211-215.

Popov, S. G., R. Villasmil, J. Bernardi, E. Grene, J. Cardwell, A. Wu, D. Alibek, C. Bailey & K. Alibek, (2002a) Lethal toxin of *Bacillus anthracis* causes apoptosis of macrophages. *Biochemical and biophysical research communications* **293**: 349-355.

Popovych, N., S. R. Tzeng, M. Tonelli, R. H. Ebright & C. G. Kalodimos, (2009) Structural basis for cAMP-mediated allosteric control of the catabolite activator protein. *Proceedings of the National Academy of Sciences of the United States of America* **106**: 6927-6932.

Portnoy, D. A., V. Auerbuch & I. J. Glomski, (2002) The cell biology of *Listeria monocytogenes* infection: the intersection of bacterial pathogenesis and cell-mediated immunity. *The Journal of cell biology* **158**: 409-414.

Poyart, C., E. Abachin, I. Razafimanantsoa & P. Berche, (1993) The zinc metalloprotease of *Listeria monocytogenes* is required for maturation of phosphatidylcholine phospholipase C: direct evidence obtained by gene complementation. *Infection and immunity* **61**: 1576-1580.

Pron, B., C. Boumaila, F. Jaubert, P. Berche, G. Milon, F. Geissmann & J. L. Gaillard, (2001) Dendritic cells are early cellular targets of *Listeria monocytogenes* after intestinal delivery and are involved in bacterial spread in the host. *Cellular microbiology* **3**: 331-340.

Racz, P., K. Tenner & E. Mero, (1972) Experimental *Listeria* enteritis. I. An electron microscopic study of the epithelial phase in experimental *Listeria* infection. *Laboratory investigation; a journal of technical methods and pathology* **26**: 694-700.

Radonic, A., S. Thulke, I. M. Mackay, O. Landt, W. Siegert & A. Nitsche, (2004) Guideline to reference gene selection for quantitative real-time PCR. *Biochemical and biophysical research communications* **313**: 856-862.

Raengpradub, S., M. Wiedmann & K. J. Boor, (2008) Comparative analysis of the sigma B-dependent stress responses in *Listeria monocytogenes* and *Listeria innocua* strains exposed to selected stress conditions. *Applied and environmental microbiology* **74**: 158-171.

Raffray, M. & G. M. Cohen, (1997) Apoptosis and necrosis in toxicology: a continuum or distinct modes of cell death? *Pharmacology & therapeutics* **75**: 153-177.

Rajabian, T., B. Gavicherla, M. Heisig, S. Muller-Altrock, W. Goebel, S. D. Gray-Owen & K. Ireton, (2009) The bacterial virulence factor InlC perturbs apical cell junctions and promotes cell-to-cell spread of *Listeria*. *Nature cell biology* **11**: 1212-1218.

Ramaswamy, V., V. M. Cresence, J. S. Rejitha, M. U. Lekshmi, K. S. Dharsana, S. P. Prasad & H. M. Vijila, (2007) *Listeria*--review of epidemiology and pathogenesis. *Journal of microbiology, immunology, and infection = Wei mian yu gan ran za zhi* **40**: 4-13.

Rauch, M., Q. Luo, S. Muller-Altrock & W. Goebel, (2005) SigB-dependent *in vitro* transcription of *prfA* and some newly identified genes of *Listeria monocytogenes* whose expression is affected by PrfA *in vivo*. *Journal of bacteriology* **187**: 800-804.

Ray, K., B. Marteyn, P. J. Sansonetti & C. M. Tang, (2009) Life on the inside: the intracellular lifestyle of cytosolic bacteria. *Nature reviews* **7**: 333-340.

Reddy, M. C., S. K. Palaninathan, J. B. Bruning, C. Thurman, D. Smith & J. C. Sacchettini, (2009) Structural insights into the mechanism of the allosteric transitions of *Mycobacterium tuberculosis* cAMP receptor protein. *The Journal of biological chemistry* **284**: 36581-36591.

Rehmann, H., A. Wittinghofer & J. L. Bos, (2007) Capturing cyclic nucleotides in action: snapshots from crystallographic studies. *Nat Rev Mol Cell Biol* **8**: 63-73.

Renzoni, A., P. Cossart & S. Dramsi, (1999) PrfA, the transcriptional activator of virulence genes, is upregulated during interaction of *Listeria monocytogenes* with mammalian cells and in eukaryotic cell extracts. *Molecular microbiology* **34**: 552-561.

Reynolds, C., D. Damerell & S. Jones, (2009) ProtorP: a protein-protein interaction analysis server. *Bioinformatics (Oxford, England)* **25**: 413-414.

Ripio, M. T., K. Brehm, M. Lara, M. Suarez & J. A. Vazquez-Boland, (1997b) Glucose-1-phosphate utilization by *Listeria monocytogenes* is PrfA dependent and coordinately expressed with virulence factors. *Journal of bacteriology* **179**: 7174-7180.

Ripio, M. T., G. Dominguez-Bernal, M. Lara, M. Suarez & J. A. Vazquez-Boland, (1997a) A Gly145Ser substitution in the transcriptional activator PrfA causes constitutive overexpression of virulence factors in *Listeria monocytogenes*. *Journal of bacteriology* **179**: 1533-1540.

Ripio, M. T., G. Dominguez-Bernal, M. Suarez, K. Brehm, P. Berche & J. A. Vazquez-Boland, (1996) Transcriptional activation of virulence genes in wild-type strains of *Listeria monocytogenes* in response to a change in the extracellular medium composition. *Research in microbiology* **147**: 371-384.

Ripio, M. T., C. Geoffroy, G. Dominguez, J. E. Alouf & J. A. Vazquez-Boland, (1995) The sulphydryl-activated cytolysin and a sphingomyelinase C are the major membrane-damaging factors involved in cooperative (CAMP-like) haemolysis of *Listeria* spp. *Research in microbiology* **146**: 303-313.

Roberts, A., Y. Chan & M. Wiedmann, (2005) Definition of genetically distinct attenuation mechanisms in naturally virulence-attenuated *Listeria monocytogenes* by comparative cell culture and molecular characterization. *Applied and environmental microbiology* **71**: 3900-3910.

Roberts, A. J. & M. Wiedmann, (2003) Pathogen, host and environmental factors contributing to the pathogenesis of listeriosis. *Cell Mol Life Sci* **60**: 904-918.

Robichon, D., E. Gouin, M. Debarbouille, P. Cossart, Y. Cenatiempo & Y. Hechard, (1997) The *rpoN* (sigma 54) gene from *Listeria monocytogenes* is involved in resistance to mesentericin Y105, an antibacterial peptide from *Leuconostoc mesenteroides*. *Journal of bacteriology* **179**: 7591-7594.

Roche, S. M., P. Gracieux, E. Milohanic, I. Albert, I. Virlogeux-Payant, S. Temoin, O. Grepinet, A. Kerouanton, C. Jacquet, P. Cossart & P. Velge, (2005) Investigation of specific substitutions in virulence genes characterizing phenotypic groups of low-virulence field strains of *Listeria monocytogenes*. *Applied and environmental microbiology* **71**: 6039-6048.

Rocourt, J., (1989) Species of the genus *Listeria*. *Acta microbiologica Hungarica* **36**: 285-288.

Rocourt, J., (1999) The genus *Listeria* and *Listeria monocytogenes*: phylogenetic position, taxonomy and identification. *In E. T. Ryser and E. H. Marth (ed.), Listeria, listeriosis and food safety, second ed. Marcel Dekker Inc., New York, N. Y.*: 1-20.

Rocourt, J. & H. P. Seeliger, (1985) [Distribution of species of the genus *Listeria*]. *Zentralblatt fur Bakteriologie, Mikrobiologie, und Hygiene* **259**: 317-330.

Rogers, H. W., M. P. Callery, B. Deck & E. R. Unanue, (1996) *Listeria monocytogenes* induces apoptosis of infected hepatocytes. *J Immunol* **156**: 679-684.

Ruckdeschel, K., A. Roggenkamp, V. Lafont, P. Mangeat, J. Heesemann & B. Rouot, (1997) Interaction of *Yersinia enterocolitica* with macrophages leads to macrophage cell death through apoptosis. *Infection and immunity* **65**: 4813-4821.

Ryan, E. M., C. G. Gahan & C. Hill, (2008) A significant role for Sigma B in the detergent stress response of *Listeria monocytogenes*. *Letters in applied microbiology* **46**: 148-154.

Ryser, E. T., (1999) Foodborne listeriosis. *In E. T. Ryser and E. H. Marth (ed.), Listeria, listeriosis and food safety, second ed. Marcel Dekker Inc., New York, N. Y.*: 299-358.

Sali, A. & T. L. Blundell, (1993) Comparative protein modelling by satisfaction of spatial restraints. *Journal of molecular biology* **234**: 779-815.

Schmeck, B., R. Gross, P. D. N'Guessan, A. C. Hocke, S. Hammerschmidt, T. J. Mitchell, S. Rosseau, N. Suttorp & S. Hippenstiel, (2004) *Streptococcus pneumoniae*-induced caspase 6-dependent apoptosis in lung epithelium. *Infection and immunity* **72**: 4940-4947.

Schuchat, A., B. Swaminathan & C. V. Broome, (1991) Epidemiology of human listeriosis. *Clinical microbiology reviews* **4**: 169-183.

Schwab, U., B. Bowen, C. Nadon, M. Wiedmann & K. J. Boor, (2005) The *Listeria monocytogenes prfA*P2 promoter is regulated by sigma B in a growth phase dependent manner. *FEMS microbiology letters* **245**: 329-336.

Schwartz, B., C. A. Ciesielski, C. V. Broome, S. Gaventa, G. R. Brown, B. G. Gellin, A. W. Hightower & L. Mascola, (1988) Association of sporadic listeriosis with consumption of uncooked hot dogs and undercooked chicken. *Lancet* **2**: 779-782.

Scorrano, L. & S. J. Korsmeyer, (2003) Mechanisms of cytochrome c release by proapoptotic BCL-2 family members. *Biochemical and biophysical research communications* **304**: 437-444.

Scortti, M., H. J. Monzo, L. Lacharme-Lora, D. A. Lewis & J. A. Vazquez-Boland, (2007) The PrfA virulence regulon. *Microbes and infection / Institut Pasteur* **9**: 1196-1207.

Seeliger, H. P. R. & D. Jones, (1986) Genus *Listeria* Pirie 1940. *In: Sneath, P.H.A., Mair, N. S., Sharpe, M. E. and Holt, J. G. (eds.) Bergey's Manual of Systematic Bacteriology. Williams and Wilkins Co., Baltimore, USA* **2**: 1235-1245.

Seeliger, H. P. R., J. Rocourt, A. Schrettenbrunner, P. A. D. Grimont & D. Jones, (1984) *Listeria ivanovii* sp. nov. . *Int. J. Syst. Bacteriol.* **34**: 336-337.

Senn, M. M., P. Giachino, D. Homerova, A. Steinhuber, J. Strassner, J. Kormanec, U. Fluckiger, B. Berger-Bachi & M. Bischoff, (2005) Molecular analysis and organization of the sigma B operon in *Staphylococcus aureus*. *Journal of bacteriology* **187**: 8006-8019.

Severino, P., O. Dussurget, R. Z. Vencio, E. Dumas, P. Garrido, G. Padilla, P. Piveteau, J. P. Lemaitre, F. Kunst, P. Glaser & C. Buchrieser, (2007) Comparative transcriptome analysis of *Listeria monocytogenes* strains of the two major lineages reveals differences in virulence, cell wall, and stress response. *Applied and environmental microbiology* **73**: 6078-6088.

Sheehan, B., A. Klarsfeld, R. Ebright & P. Cossart, (1996) A single substitution in the putative helix-turn-helix motif of the pleiotropic activator PrfA attenuates *Listeria monocytogenes* virulence. *Molecular microbiology* **20**: 785-797.

Sheehan, B., A. Klarsfeld, T. Msadek & P. Cossart, (1995) Differential activation of virulence gene expression by PrfA, the *Listeria monocytogenes* virulence regulator. *Journal of bacteriology* **177**: 6469-6476.

Shetron-Rama, L. M., H. Marquis, H. G. Bouwer & N. E. Freitag, (2002) Intracellular induction of *Listeria monocytogenes actA* expression. *Infection and immunity* **70**: 1087-1096.

Skoble, J., V. Auerbuch, E. D. Goley, M. D. Welch & D. A. Portnoy, (2001) Pivotal role of VASP in Arp2/3 complex-mediated actin nucleation, actin branch-formation, and *Listeria monocytogenes* motility. *The Journal of cell biology* **155**: 89-100.

Sleator, R. D., H. H. Wemekamp-Kamphuis, C. G. Gahan, T. Abee & C. Hill, (2005) A PrfA-regulated bile exclusion system (BilE) is a novel virulence factor in *Listeria monocytogenes*. *Molecular microbiology* **55**: 1183-1195.

Sleator, R. D., J. Wouters, C. G. Gahan, T. Abee & C. Hill, (2001) Analysis of the role of OpuC, an osmolyte transport system, in salt tolerance and virulence potential of *Listeria monocytogenes*. *Applied and environmental microbiology* **67**: 2692-2698.

Stritzker, J., C. Schoen & W. Goebel, (2005) Enhanced synthesis of internalin A in *aro* mutants of *Listeria monocytogenes* indicates posttranscriptional control of the *inlAB* mRNA. *Journal of bacteriology* **187**: 2836-2845.

Suarez, M., B. Gonzalez-Zorn, Y. Vega, I. Chico-Calero & J. A. Vazquez-Boland, (2001) A role for ActA in epithelial cell invasion by *Listeria monocytogenes*. *Cellular microbiology* **3**: 853-864.

Sue, D., K. J. Boor & M. Wiedmann, (2003) Sigma (B)-dependent expression patterns of compatible solute transporter genes *opuCA* and *lmo1421* and the conjugated bile salt hydrolase gene bsh in *Listeria monocytogenes*. *Microbiology (Reading, England)* **149**: 3247-3256.

Sue, D., D. Fink, M. Wiedmann & K. J. Boor, (2004) SigmaB-dependent gene induction and expression in *Listeria monocytogenes* during osmotic and acid stress conditions simulating the intestinal environment. *Microbiology (Reading, England)* **150**: 3843-3855.

Sun, A. N., A. Camilli & D. A. Portnoy, (1990) Isolation of *Listeria monocytogenes* small-plaque mutants defective for intracellular growth and cell-to-cell spread. *Infection and immunity* **58**: 3770-3778.

Sutcliffe, M. J., I. Haneef, D. Carney & T. L. Blundell, (1987) Knowledge based modelling of homologous proteins, Part I: Three-dimensional frameworks derived from the simultaneous superposition of multiple structures. *Protein engineering* **1**: 377-384.

Swaminathan, B. & P. Gerner-Smidt, (2007) The epidemiology of human listeriosis. *Microbes and infection / Institut Pasteur* **9**: 1236-1243.

Tamura, F., R. Nakagawa, T. Akuta, S. Okamoto, S. Hamada, H. Maeda, S. Kawabata & T. Akaike, (2004) Proapoptotic effect of proteolytic activation of matrix metalloproteinases by *Streptococcus pyogenes* thiol proteinase (*Streptococcus* pyrogenic exotoxin B). *Infection and immunity* **72**: 4836-4847.

Tasara, T. & R. Stephan, (2007) Evaluation of housekeeping genes in *Listeria monocytogenes* as potential internal control references for normalizing mRNA expression levels in stress adaptation models using real-time PCR. *FEMS microbiology letters* **269**: 265-272.

Tattoli, I., L. Lembo-Fazio, G. Nigro, L. A. Carneiro, E. Ferraro, G. Rossi, M. C. Martino, M. E. de Stefano, F. Cecconi, S. E. Girardin, D. J. Philpott & M. L. Bernardini, (2008) Intracellular bacteriolysis triggers a massive apoptotic cell death in *Shigella*-infected epithelial cells. *Microbes and infection / Institut Pasteur* **10**: 1114-1123.

Tilney, L. G. & D. A. Portnoy, (1989) Actin filaments and the growth, movement, and spread of the intracellular bacterial parasite, *Listeria monocytogenes*. *The Journal of cell biology* **109**: 1597-1608.

Toledo-Arana, A., O. Dussurget, G. Nikitas, N. Sesto, H. Guet-Revillet, D. Balestrino, E. Loh, J. Gripenland, T. Tiensuu, K. Vaitkevicius, M. Barthelemy, M. Vergassola, M. A. Nahori, G. Soubigou, B. Regnault, J. Y. Coppee, M. Lecuit, J. Johansson & P. Cossart, (2009) The *Listeria* transcriptional landscape from saprophytism to virulence. *Nature* **459**: 950-956.

Tomlinson, S. R., Y. Tutar & J. G. Harman, (2003) Interaction of CRP L124 with cAMP affects CRP cAMP binding constants, cAMP binding cooperativity, and CRP allostery. *Biochemistry* **42**: 3759-3765.

Tsai, P. J., Y. S. Lin, C. F. Kuo, H. Y. Lei & J. J. Wu, (1999) Group A *Streptococcus* induces apoptosis in human epithelial cells. *Infection and immunity* **67**: 4334-4339.

Ulett, G. C. & E. E. Adderson, (2006) Regulation of Apoptosis by Gram-Positive Bacteria: Mechanistic Diversity and Consequences for Immunity. *Current immunology reviews* **2**: 119-141.

Ulett, G. C., J. F. Bohnsack, J. Armstrong & E. E. Adderson, (2003) Beta-hemolysin-independent induction of apoptosis of macrophages infected with serotype III group B *Streptococcus*. *The Journal of infectious diseases* **188**: 1049-1053.

Valenti, P., R. Greco, G. Pitari, P. Rossi, M. Ajello, G. Melino & G. Antonini, (1999) Apoptosis of Caco-2 intestinal cells invaded by *Listeria monocytogenes*: protective effect of lactoferrin. *Experimental cell research* **250**: 197-202.

Vallender, E. J. & B. T. Lahn, (2006) A primate-specific acceleration in the evolution of the caspase-dependent apoptosis pathway. *Human molecular genetics* **15**: 3034-3040.

van Engeland, M., L. J. Nieland, F. C. Ramaekers, B. Schutte & C. P. Reutelingsperger, (1998) Annexin V-affinity assay: a review on an apoptosis detection system based on phosphatidylserine exposure. *Cytometry* **31**: 1-9.

van Schaik, W., M. H. Tempelaars, M. H. Zwietering, W. M. de Vos & T. Abee, (2005) Analysis of the role of RsbV, RsbW, and RsbY in regulating {sigma} B activity in *Bacillus cereus*. *Journal of bacteriology* **187**: 5846-5851.

Vazquez-Boland, J. A., L. Dominguez, E. F. Rodriguez-Ferri, J. F. Fernandez-Garayzabal & G. Suarez, (1989) Preliminary evidence that different domains are involved in cytolytic activity and receptor (cholesterol) binding in listeriolysin O, the *Listeria monocytogenes* thiol-activated toxin. *FEMS microbiology letters* **53**: 95-99.

Vazquez-Boland, J. A., G. Dominguez-Bernal, B. Gonzalez-Zorn, J. Kreft & W. Goebel, (2001b) Pathogenicity islands and virulence evolution in *Listeria*. *Microbes and infection / Institut Pasteur* **3**: 571-584.

Vazquez-Boland, J. A., C. Kocks, S. Dramsi, H. Ohayon, C. Geoffroy, J. Mengaud & P. Cossart, (1992) Nucleotide sequence of the lecithinase operon of *Listeria monocytogenes* and possible role of lecithinase in cell-to-cell spread. *Infection and immunity* **60**: 219-230.

Vazquez-Boland, J. A., M. Kuhn, P. Berche, T. Chakraborty, G. Dominguez-Bernal, W. Goebel, B. Gonzalez-Zorn, J. Wehland & J. Kreft, (2001a) *Listeria* pathogenesis and molecular virulence determinants. *Clinical microbiology reviews* **14**: 584-640.

Vega, Y., C. Dickneite, M. T. Ripio, R. Bockmann, B. Gonzalez-Zorn, S. Novella, G. Dominguez-Bernal, W. Goebel & J. A. Vazquez-Boland, (1998) Functional similarities between the *Listeria monocytogenes* virulence regulator PrfA and cyclic AMP receptor protein: the PrfA* (Gly145Ser) mutation increases binding affinity for target DNA. *Journal of bacteriology* **180**: 6655-6660.

Vega, Y., M. Rauch, M. J. Banfield, S. Ermolaeva, M. Scortti, W. Goebel & J. A. Vazquez-Boland, (2004) New *Listeria monocytogenes prfA** mutants, transcriptional properties of PrfA* proteins and structure-function of the virulence regulator PrfA. *Molecular microbiology* **52**: 1553-1565.

Vermes, I., C. Haanen & C. Reutelingsperger, (2000) Flow cytometry of apoptotic cell death. *Journal of immunological methods* **243**: 167-190.

Vitale, M., L. Zamai, G. Mazzotti, A. Cataldi & E. Falcieri, (1993) Differential kinetics of propidium iodide uptake in apoptotic and necrotic thymocytes. *Histochemistry* **100**: 223-229.

Watkins, J. & K. P. Sleath, (1981) Isolation and enumeration of *Listeria monocytogenes* from Sewage, Sewage Sludge and River Water. *The Journal of applied bacteriology* **50**: 1-9.

Weber, I. T., G. L. Gilliland, J. G. Harman & A. Peterkofsky, (1987a) Crystal structure of a cyclic AMP-independent mutant of catabolite gene activator protein. *The Journal of biological chemistry* **262**: 5630-5636.

Weinrauch, Y. & A. Zychlinsky, (1999) The induction of apoptosis by bacterial pathogens. *Annual review of microbiology* **53**: 155-187.

Weis, J. & H. P. Seeliger, (1975) Incidence of *Listeria monocytogenes* in nature. *Applied microbiology* **30**: 29-32.

Weiss, D. S. & A. Zychlinsky, (2002) Methods for studying bacteria-induced host cell death. *Methods in Microbiology; in book: Molecular cellular microbiology; edited by Sansonetti, P. and Zychlinsky, A., Academic Press Inc, San Diego, 2002* **31**: 439-460.

Welshimer, H. J. & J. Donker-Voet, (1971) *Listeria monocytogenes* in nature. *Applied microbiology* **21**: 516-519.

Wemekamp-Kamphuis, H. H., J. A. Wouters, P. P. de Leeuw, T. Hain, T. Chakraborty & T. Abee, (2004) Identification of sigma factor sigma B-controlled genes and their impact on acid stress, high hydrostatic pressure, and freeze survival in *Listeria monocytogenes* EGD-e. *Applied and environmental microbiology* **70**: 3457-3466.

Wiedmann, M., T. J. Arvik, R. J. Hurley & K. J. Boor, (1998) General stress transcription factor sigma B and its role in acid tolerance and virulence of *Listeria monocytogenes*. *Journal of bacteriology* **180**: 3650-3656.

Wiedmann, M., J. L. Bruce, C. Keating, A. E. Johnson, P. L. McDonough & C. A. Batt, (1997) Ribotypes and virulence gene polymorphisms suggest three distinct *Listeria monocytogenes* lineages with differences in pathogenic potential. *Infection and immunity* **65**: 2707-2716.

Williams, J. R., C. Thayyullathil & N. E. Freitag, (2000) Sequence variations within PrfA DNA binding sites and effects on *Listeria monocytogenes* virulence gene expression. *Journal of bacteriology* **182**: 837-841.

Winau, F., S. H. Kaufmann & U. E. Schaible, (2004) Apoptosis paves the detour path for CD8 T cell activation against intracellular bacteria. *Cellular microbiology* **6**: 599-607.

Wyllie, A. H., G. J. Beattie & A. D. Hargreaves, (1981) Chromatin changes in apoptosis. *The Histochemical journal* **13**: 681-692.

Zalevsky, J., I. Grigorova & R. D. Mullins, (2001) Activation of the Arp2/3 complex by the *Listeria* acta protein. ActA binds two actin monomers and three subunits of the Arp2/3 complex. *The Journal of biological chemistry* **276**: 3468-3475.

Zhang, B. F., F. F. Peng, J. Z. Zhang & D. C. Wu, (2003) Staurosporine induces apoptosis in NG108-15 cells. *Acta pharmacologica Sinica* **24**: 663-669.

Zhang, Y., A. T. Ting, K. B. Marcu & J. B. Bliska, (2005) Inhibition of MAPK and NF-kappa B pathways is necessary for rapid apoptosis in macrophages infected with *Yersinia*. *J Immunol* **174**: 7939-7949.

Zhang, Y. X., Y. Geng, J. W. Yang, X. K. Guo & G. P. Zhao, (2008) Cytotoxic activity and probable apoptotic effect of Sph2, a sphigomyelinase hemolysin from *Leptospira interrogans* strain Lai. *BMB reports* **41**: 119-125.

Zychlinsky, A., M. C. Prevost & P. J. Sansonetti, (1992) *Shigella flexneri* induces apoptosis in infected macrophages. *Nature* **358**: 167-169.

7 APPENDICES

7.1 APPENDIX I

Guillet, C., Join-Lambert, O., Monnier, A. L., Leclercq, A., Mechai, F., Mamzer-Bruneel, M.F., Bielecka, M. K., Scortti, M., Disson, O., Berche, P., Vazquez-Boland, J., Lortholary, O., and Lecuit, M.

Human listeriosis caused by *Listeria ivanovii.*

Emerging Infectious Diseases, 2010 January; 16 (1): 136-138.

7.2 APPENDIX II

Derivation of Apoptosis Index (*AI*):

(Developed by Dr. Nick Savill, Centre for Infectious Diseases and Immunity, Infection & Evolution, University of Edinburgh)

Glossary of variables

Variable	Description
N	total number of cells
A	net number of apoptotic cells (after subtraction of spontaneous apoptosis)
C	number of infected cells
B	average number of bacteria per infected cell
$a = {}^{100A}/_{N}$	net % apoptotic cells (after subtraction of spontaneous apoptosis)
$c = {}^{100C}/_{N}$	% infected cells
$b = BC$	total number of intracellular bacteria
α	apoptosis rate per bacterium
β	determines how the number of bacteria in a cell affects apoptosis rate
AI	apoptosis index

To establish an index describing the occurrence of apoptosis it is important to consider the factors that influence the outcome variable. The number (or percentage) of apoptotic cells observed after a certain time depends on how quickly bacteria invade host cells, grow in the cell monolayer, and cause apoptosis. To determine the apoptogenic potential of a specific bacterial species it is important to know how the rate of apoptosis depends on the number of bacteria (B) in an infected cell. This rate may be independent of the number of bacteria, or may rise linearly, quadratically, or exponentially, or even show threshold behaviour. If the apoptosis rate goes as B^{β}, $\beta = 0$ means that the apoptosis rate is independent, $\beta = 1$ that the relationship is linear, *etc*.

The rate of change of the net number of apoptotic cells (${}^{dA}/_{dt}$) is proportional to the number of infected cells (C) times the apoptosis rate (B^{β}):

$$\frac{dA}{dt} \propto B^{\beta} C \qquad (1)$$

To rewrite this equation in terms of percentages of cells rather than numbers of cells (as we have measured apoptosis in percentages), both sides are multiplied by $^{100}/_{N}$:

$$\frac{100}{N}\frac{dA}{dt} \propto \frac{100}{N} B^{\beta} C \tag{2}$$

$$\frac{d{}^{100A}/_{N}}{dt} \propto B^{\beta} \frac{100C}{N} \tag{3}$$

$$\frac{da}{dt} \propto B^{\beta} c \tag{4}$$

Let us call the constant of proportionality α, therefore:

$$\frac{da}{dt} = \alpha B^{\beta} c \tag{5}$$

By, definition, $^{1}/(\alpha B^{\beta})$ is the half-life of infected cells containing B bacteria. If $B = 1$ (*i.e.* one bacterium per cell), then, $^{1}/\alpha$ is the half-life of infected cells containing a single bacterium. α is, therefore, a measure of the apoptogenic potential of a bacterial species; the bigger α is, the shorter the half-life of infected cells and the faster these cells become apoptotic. α is independent of the species' growth and invasion rates.

Because B may not be known, it can be removed from Equation 5. This can be done considering that the number of intracellular bacteria (b) equals the average number of bacteria per infected cell (B) times the number of infected cells (C):

$$b = BC \tag{6}$$

Mulitply both sides by $^{100}/_{N}$:

$$\frac{100b}{N} = B\frac{100C}{N} \tag{7}$$

$$\frac{100b}{N} = Bc \tag{8}$$

therefore:

$$B = \frac{100b}{Nc} \tag{9}$$

substituting (9) into Equation 5:

$$\frac{da}{dt} = \alpha\left(\frac{100b}{cN}\right)^{\beta} c \tag{10}$$

Since N (the total number of cells) is not different across experiments, we can subsume it (and 100) into α. Let us call $\alpha(^{100}/_{N})^{\beta}$ the apoptotic index (AI), therefore:

$$\frac{da}{dt} = AI\left(\frac{b}{c}\right)^{\beta} c \tag{11}$$

which can be written as:

$$\frac{da}{dt} = AIb^{\beta}c^{1-\beta} \tag{12}$$

We can, therefore, find AI from Equation 12 as follows:

$$AI = \frac{da/dt}{b^{\beta}c^{1-\beta}} \tag{13}$$

To estimate the apoptotic index we need to estimate the slope of apoptotic cell growth curve ($^{da}/_{dt}$). According to Equation 5, the growth of a is dependent on c and B, which are both changing in time. Therefore, the form of a is unlikely to be simple (*e.g.* linear, exponential), but we can approximate it.

If we assume that the rate of growth of apoptotic cells is linear from the start of the experiment (which may not be true), then, the slope is constant over time. Let a_t be the % apoptotic cells at time t, then:

$$\left.\frac{da}{dt}\right|_{t} = \frac{a_t}{t} \tag{14}$$

(The vertical line indicates that the slope is calculated at a specific time t rather than general time). Substituting this into Equation 13 gives the apoptotic index (method #1):

$$AI = \frac{a_t}{tb_t^{\beta}c_t^{1-\beta}} \tag{15}$$

where b_t and c_t are the number of intracellular bacteria and the % infected cells at time t, respectively, and β determines how the number of bacteria in a cell affects apoptosis rate.

A more accurate method would be, however, to measure a at two time points, t_1 and t_2, and assume linear growth between these two times. Then $^{da}/_{dt}$ at time t_2 is:

$$\left.\frac{da}{dt}\right|_{t_2} = \frac{a_{t_2} - a_{t_1}}{t_2 - t_1} \tag{16}$$

Substituting this into Equation 13 gives the apoptotic index (method #2):

$$AI = \frac{a_{t_2} - a_{t_1}}{(t_2 - t_1) b_{t_2}^{\beta} c_{t_2}^{1-\beta}} \tag{17}$$

Potential problems and additional assumptions

The first problem is that the AI changes as β changes (can be $\beta = 0$ if apoptosis rate is independent of the number of bacteria per cell, $\beta = 1$ if the relationship is linear, $\beta = 2$ if the relationship is quadratic, *etc*.). The second problem is that the two methods of approximating $^{da}/_{dt}$ can give different conclusions, particularly when β is in the range 0.5 to 1. It is, therefore, important to accurately estimate the rate of change of % of a. Therefore, it is not possible to estimate the relative apoptogenic potential of two species unless it is known how the apoptosis rate of infected cells depends on the number of bacteria in cells. Moreover, for simplicity it has been assumed that the apoptosis rate goes as B^{β}, but it could be more complicated than this. For example, apoptosis rate could increase sharply when the number of bacteria pass a threshold, or apoptosis rate saturates at high bacterial loads.

The following assumptions have been also considered in the analyses. One is that the probability of an infected cell (with a fixed number of bacteria) becoming apoptotic is constant in time. The implications of this are that the lifespan of infected cells is exponentially distributed and that cells can become apoptotic immediately upon infection. Another assumption is that the number of apoptotic cells that have died (disappeared) is negligible at the time points sampled. Finally, the background rate of apoptosis of uninfected cells is unaffected by the presence of infected cells.